



**Development of Bioplastics : Cassava Starch Grafted  
Polystyrene and Effect of Additives in Gluten**

**Kaewta Kaewtatip**

**A Thesis Submitted in Fulfillment of the Requirements  
for the Degree of Doctor of Philosophy in  
Polymer Science and Technology  
Prince of Songkla University  
2010**

**Copyright of Prince of Songkla University**

**Thesis Title**                      Development of Bioplastics : Cassava Starch Grafted Polystyrene and  
Effect of Additives in Gluten  
**Author**                                Miss Kaewta Kaewtatip  
**Major Program**                    Polymer Science and Technology

---

**Major Advisor :**

.....  
(Assoc. Prof. Dr.Varaporn Tanrattanakul)

**Examining Committee:**

.....Chairperson  
(Asst. Prof. Dr.Chiraphon Chaibundit)

.....  
(Assoc. Prof. Dr.Varaporn Tanrattanakul)

.....  
(Assoc. Prof. Dr.Ittipol Jangchud)

.....  
(Assoc. Prof. Dr.Ratana Rujiravanit)

.....  
(Dr.Watchanida Chinpa)

The Graduate School, Prince of Songkla University, has approved this thesis as fulfillment of the requirements for the Doctor of Philosophy Degree in Polymer Science and Technology

.....  
(Assoc. Prof. Dr.Krerchai Thongnoo)  
Dean of Graduate School

ชื่อวิทยานิพนธ์	การพัฒนาพลาสติกชีวภาพ : กราฟท์โคพอลิเมอร์ระหว่างแป้งมันสำปะหลังและพอลิสไตรีนและผลของสารเติมแต่งในกัญเตน
ผู้เขียน	นางสาวแก้วตา แก้วตาทิพย์
สาขาวิชา	วิทยาศาสตร์และเทคโนโลยีพอลิเมอร์
ปีการศึกษา	2552

### บทคัดย่อ

วิทยานิพนธ์นี้มีวัตถุประสงค์เพื่อเป็นแนวทางในการพัฒนาพลาสติกชีวภาพที่เตรียมจากแป้ง และผลิตภัณฑ์ที่เป็นผลพลอยได้จากอุตสาหกรรมแป้ง ซึ่งก็คือ กัญเตนแป้งสาลี ดังนั้น วิทยานิพนธ์นี้จึงประกอบด้วยงานวิจัยที่แบ่งเป็น 2 ตอน คือ การเตรียมกราฟท์โคพอลิเมอร์ของแป้งมันสำปะหลังกับพอลิสไตรีน และการตรวจสอบสมบัติของสารตัวเติมที่มีอิทธิพลต่อการเกิดการเชื่อมโยงโมเลกุลของโปรตีนในพลาสติกชีวภาพที่เตรียมจากกัญเตนแป้งสาลี

กราฟท์โคพอลิเมอร์ของแป้งมันสำปะหลังกับพอลิสไตรีนถูกเตรียมผ่านปฏิกิริยาฟรีเรดิคอล พอลิเมอไรเซชัน โดยใช้เทคนิคพอลิเมอไรเซชันแบบแขวนลอยและไม่ใช้สารลดแรงตึงผิว ในตัวกลางที่เป็นน้ำภายใต้บรรยากาศไนโตรเจน ใช้โพแทสเซียมเปอร์ซัลเฟตเป็นสารริเริ่มโครงสร้างทางเคมี สันฐานวิทยา ปริมาณผลึก อุณหภูมิสลายตัวทางความร้อน และพฤติกรรมทางความร้อนของกราฟท์โคพอลิเมอร์ของแป้งมันสำปะหลังกับพอลิสไตรีนตรวจสอบโดยใช้ฟูเรียร์ทรานสฟอร์มอินฟราเรดสเปกโตรสโคปี กล้องจุลทรรศน์อิเล็กตรอนแบบส่องกราด เอ็กซ์เรดิฟลักซ์เทอร์โมกราวิเมตริกอะนาไลซิส และดีพีเพอเรนเชียลสแกนนิ่งคาลอริเมตรี ตามลำดับ พบว่าลักษณะตัวอย่างที่สังเคราะห์ได้ก่อนการทำการสกัดด้วยเทคนิคชอกเลก จะปรากฏเม็ดขนาดไมครอนของพอลิสไตรีนบนผิวของเม็ดแป้ง แต่หลังจากทำการสกัดด้วยเทคนิคชอกเลกจะมีแผ่นรูพรุนของพอลิสไตรีนปรากฏบนผิวของเม็ดแป้ง ซึ่งเป็นการยืนยันว่าไฮโดรพอลิสไตรีนได้ถูกสกัดออกไปหลังจากการทำการสกัดด้วยเทคนิคชอกเลก ผลที่ได้จากการวิเคราะห์ด้วยเทคนิคฟูเรียร์ทรานสฟอร์มอินฟราเรดสเปกโตรสโคปียืนยันการเกิดกราฟท์โคพอลิเมอร์ระหว่างแป้งมันสำปะหลังกับพอลิสไตรีน ปริมาณผลึกของกราฟท์โคพอลิเมอร์ไม่มีความแตกต่างอย่างมีนัยสำคัญเมื่อเปรียบเทียบกับปริมาณผลึกของแป้งมันสำปะหลัง จากการตรวจสอบอิทธิพลของอัตราส่วนระหว่างแป้งมันสำปะหลังกับสไตรีนมอนอเมอร์ ปริมาณของโพแทสเซียมเปอร์ซัลเฟต อุณหภูมิ และเวลาที่ใช้ในการทำปฏิกิริยาที่มีผลต่อเปอร์เซ็นต์การกราฟท์ พบว่าเปอร์เซ็นต์การกราฟท์ที่มากที่สุดในการทดลองนี้คือ 31.47 เปอร์เซ็นต์ ภายใต้สภาวะดังต่อไปนี้ อัตราส่วนระหว่างแป้งมันสำปะหลังกับสไตรีนมอนอเมอร์เท่ากับ 25 ต่อ 75 และมีปริมาณของโพแทสเซียมเปอร์ซัลเฟตเท่ากับ 0.4 กรัม ใช้อุณหภูมิ 50 องศาเซลเซียส ใน

เวลา 2 ชั่วโมง การศึกษานี้แสดงให้เห็นว่าพอลิซิสไตรีนสามารถเกิดกราฟท์โคพอลิเมอร์ไรเซชันบนเม็ดแป้งโดยใช้สารลดแรงตึงผิว และไม่เกิดเจลลาที่ไนท์ของเม็ดแป้ง กราฟท์โคพอลิเมอร์ที่มีเปอร์เซ็นต์การกราฟท์เท่ากับ 21.81 เปอร์เซ็นต์ ถูกนำไปผสมกับแป้งมันสำปะหลังที่อัตราส่วนต่างๆ โดยใช้กลีเซอรอลและน้ำเป็นพลาสติกไซเซออร์ พบว่าเมื่อกราฟท์โคพอลิเมอร์มีอัตราส่วนน้อยกว่า 40 เปอร์เซ็นต์ ตัวอย่างที่เตรียมได้จะเกิดการหดตัว และเมื่อกราฟท์โคพอลิเมอร์มีอัตราส่วน 40 ถึง 60 เปอร์เซ็นต์ การหดตัวของตัวอย่างไม่เกิดขึ้น แสดงว่ากราฟท์โคพอลิเมอร์เพิ่มความเสถียรของโครงสร้างของพอลิเมอร์ผสมที่เตรียมได้ อย่างไรก็ตามเมื่อกราฟท์โคพอลิเมอร์ของแป้งมันสำปะหลังกับพอลิซิสไตรีนมีอัตราส่วนมากกว่า 60 เปอร์เซ็นต์ ตัวอย่างที่เตรียมได้จะมีความเปราะและผิวหน้าของตัวอย่างมีความเหนียวมาก ซึ่งเป็นผลจากการเกิดดีพลาสติกไซเซชันของกลีเซอรอล จากเหตุผลที่กล่าวมาทำให้ไม่สามารถทดสอบสมบัติการทนต่อแรงดึงของตัวอย่างได้

ได้ศึกษาการเกิดการเชื่อมโยงโมเลกุลของโปรตีนในกลูเตนผ่านปฏิกิริยาเคมีระหว่างกราฟท์ลิกนินและกลูเตนแป้งสาลี และศึกษาปฏิกิริยาเคมีที่เกิดจากหมู่ฟังก์ชันที่แตกต่างกันของลิกนิน โดยเปรียบเทียบอิทธิพลของกราฟท์ลิกนินกับเอสเทอร์ลิกนินและสารตัวเติมอื่นๆ ที่มีโมเลกุลขนาดเล็กและมีหมู่ฟังก์ชันที่แตกต่างกัน (เช่น พันธะคู่คอนจูเกต หมู่ไฮดรอกซิล หมู่เอสเทอร์ หมู่แอลดีไฮด์ หมู่คาร์บอกซิล และหมู่เอโทเมททอกซี) สารโมเลกุลเล็กเหล่านี้เป็นโครงสร้างพื้นฐานที่ประกอบอยู่ในโครงสร้างพอลิฟีนอลิกของกราฟท์ลิกนิน เอสเทอร์ลิกนินเตรียมผ่านปฏิกิริยาเอสเทอร์ฟิเคชันของหมู่ไฮดรอกซิลในกราฟท์ลิกนิน โครงสร้างทางเคมีและสัณฐานวิทยาของเอสเทอร์ลิกนิน ถูกตรวจสอบด้วยฟูเรียรทรานสฟอร์มอินฟราเรดสเปกโตรสโคปีและกล้องจุลทรรศน์อิเล็กตรอนแบบส่องกราด ตามลำดับ ทำการผสมกลูเตนแป้งสาลีกับกลีเซอรอล และสารตัวเติมในเครื่องผสมแบบปิด โดยทำการบันทึกค่าทอร์กและอุณหภูมิระหว่างการผสม ตัวอย่างที่ได้จากการผสมจะถูกนำมาให้ความร้อนด้วยกระบวนการอัดที่อุณหภูมิ 100 องศาเซลเซียส เป็นเวลา 10 นาที หลังจากนั้นนำตัวอย่างไปทดสอบเพื่อหาค่าโปรตีนที่ละลายได้ในสารละลายโซเดียมโอดีเดคิลซัลเฟตด้วยเทคนิคเคลดาล เพื่อใช้ในการระบุปริมาณการเกิดการเชื่อมโยงโมเลกุลของโปรตีนในกลูเตน ซึ่งจะเกี่ยวข้องกับความสามารถในการเป็นสารจับอนุมูลอิสระของสารตัวเติมแต่ละชนิด สารตัวเติมที่ประกอบด้วยหมู่ไฮดรอกซิลในโครงสร้างแสดงสมบัติเป็นพลาสติกไซเซออร์ แต่กราฟท์ลิกนินและเอสเทอร์ลิกนินไม่แสดงสมบัติเป็นพลาสติกไซเซออร์ เพราะทั้งกราฟท์ลิกนิน และเอสเทอร์ลิกนินมีโครงสร้างขนาดใหญ่ และมีความเป็นขั้วต่ำสมบัติการจับอนุมูลอิสระของกราฟท์ลิกนินเกิดจากการมีหมู่ฟังก์ชันทางเคมีที่แตกต่างกันภายในโครงสร้าง โดยโครงสร้างฟีนอลและพันธะคอนจูเกตในกราฟท์ลิกนินสามารถจับอนุมูลอิสระและสามารถทำปฏิกิริยากับไทโอเลตไอออนที่เกิดขึ้นระหว่างการให้แรงเฉือนแก่กลูเตนแป้งสาลี

<b>Thesis title</b>	Development of Bioplastics : Cassava Starch Grafted Polystyrene and Effect of Additives in Gluten
<b>Author</b>	Miss Kaewta Kaewtatip
<b>Major Program</b>	Polymer Science and Technology
<b>Academic Year</b>	2009

### **Abstract**

This thesis is focused on the development of new bioplastics made from starch and its by-product which was wheat gluten. This thesis has two parts, i.e., the preparation of cassava starch grafted with a polystyrene copolymer (PS-g-starch copolymer) and investigation of additives that affect the crosslinking of wheat gluten-based bioplastics.

A PS-g-starch copolymer was synthesized via free-radical polymerization using the suspension polymerization technique, without any surfactant, in an aqueous medium under a nitrogen gas atmosphere. Potassium persulfate (PPS) was used as an initiator. The chemical structure, morphology, degree of crystallinity, thermal decomposition temperatures and thermal behavior of the PS-g-starch copolymer were investigated using fourier transform infrared spectroscopy (FTIR), scanning electron microscopy (SEM), X-ray diffraction (XRD), thermal gravimetric analysis (TGA) and differential scanning calorimetry (DSC). Before Soxhlet extraction, PS spherical microbeads were observed on the surfaces of starch granules. Porous patches of PS were present on starch granules after Soxhlet extraction. This confirmed that homopolystyrene was removed by Soxhlet extraction. The FTIR spectra also confirmed the presence of the PS-g-starch copolymer. The degree of crystallinity of the PS-g-starch copolymer was not changed from that of the cassava starch. The effects of starch:styrene monomer ratios, amounts of PPS, reaction times and reaction temperature on the percentage of grafting (G (%)), were investigated. The maximum G (%) was determined to be 32.80% under the optimized conditions when the starch:styrene monomer ratio, the amount of PPS, the reaction temperature and the reaction time was 25:75, 0.4 g, 50 °C and 2 h, respectively. This study demonstrated

the capability of polymerization of polystyrene onto the granular starch in the absence of emulsifier and the synthesis of a graft copolymer without the starch being gelatinized. The PS-g-starch copolymer at  $G (\%) = 21.80\%$  was subsequently mixed with cassava starch in various proportions in a mixer by using glycerol and water as plasticizers. It was found that the samples shrank when the amount of PS-g-starch was lower than 40%. When the PS-g-cassava starch copolymer content was 40% - 60%, the shrinkage of samples disappeared showing that the PS-g-cassava starch copolymer can enhance dimensional stability. However, the samples were very brittle and their surfaces were very sticky when the PS-g-cassava starch copolymer content was higher than 60%. From that result, it was difficult to measure the tensile properties. This can be attributed to the deplasticization effect.

In Part II, chemical interactions between Kraft lignin (KL) and wheat gluten were investigated by determining the extent of crosslinking in the protein to KL. To clarify the role of different chemical functions found in lignin, the effect of KL was compared with esterified lignin (EL) and with a series of simple aromatic and phenolic structures with different functionalities (i.e. conjugated double bonds, hydroxyl, ester, aldehyde, carboxyl and ortho-methoxy groups). EL was produced via the esterification reaction of the KL hydroxyl groups. The chemical structure and morphology of EL was investigated by using FTIR and SEM, respectively. Wheat gluten was mixed with glycerol and additives in an internal mixer. Torque and temperature were recorded during the mixing. The thermal treatment was performed by using compression molding at 100 °C for 10 min. The soluble protein content in the sodium dodecyl sulfate (SDS) solution was determined by using the Kjeldahl method to identify the protein crosslinking that was related to the radical scavenging capability of each additive. The additives that consisted of hydroxyl groups demonstrated the plasticizing properties. However, KL and EL did not act as plasticizers because they have very large structures and a low polarity. The radical scavenging properties of KL were due to the different functional chemical groups found on KL. The phenol structures and the conjugated double bonds were able to trap the free radicals and interact with the thiolate anions produced from wheat gluten under the shearing forces.

## Acknowledgements

The completion of this thesis would be impossible without the help of many people, whom I would like to thank.

I express my deep gratitude and sincere appreciation to my advisor, Associate Professor Dr. Varaporn Tanrattanakul for valuable advice, the scientific opportunity, particularly her excellent teaching, assistance and all the help throughout this thesis.

I would like to thank Assistant Professor Dr. Chiraphon Chaibundit, Dr. Watchanida Chinpa, Associate Professor Dr. Ittipol Jangchud and Associate Professor Dr. Ratana Rujiravanit for serving on the thesis committees.

I would like to thank Professor Dr. Stephane Guilbert for his kindness and financial support to do the research at Agropolymers Engineering and Emerging Technologies Research Unit, Montpellier SupAgro, INRA, France. I also would like to thank Assistant Professor Dr. Paul Menut for his help, tireless assistance and suggestion about wheat gluten and lignin knowledge. Thanks to Dr. Marie-Helene Morel and Dr. Remi Aubergne for their useful advice.

My sincere thank to Prof. Jaroslava Budinski-Simendic and her family for their kindness and help in Serbia. I would like to thank Prof. Katalin Meszaros Szecsenyi and Prof. Dr. Ljubica Dokic for their valuable advice and support in Novi Sad University, Serbia. I also wish to thank my best friend in Serbia, Jelena Pavlicevic and her family for their kindness.

I am deeply indebted to Faculty of Science and Graduate School in Prince of Sonhkla University for the scholarship. I also thank Agropolymers Engineering and Emerging Technologies Research Unit, Montpellier SupAgro, INRA, France and Novi Sad University, Serbia for the grant during my visit in France and Serbia, respectively.

I am very grateful to staffs of Polymer Science Program, Faculty of Science and Graduate School, Prince of Sonhkla University, Thailand; Agropolymers Engineering and Emerging Technologies Research Unit, Montpellier SupAgro, INRA, France and Department of Material Engineering, Faculty of Technology and Faculty of Science, Novi Sad University, Serbia.

Thanks to my friends whose names are not mentioned here for their encouragements. Special thanks to my best friend, Dr. Apon Numnuam for all the support and encouragement.

Finally, I would like to extend my appreciation to my father and my mother for their valuable suggestion, endless love, understanding and confidence in me and thanks to my brothers and my sister for their love and encouragement.

**Kaewta Kaewtatip**



## Preface

The purposes of this thesis were to modify and develop the bioplastics that made from starch and its by-product. Therefore, this thesis composed of two parts.

The first part is related to starch-based polymers produced by modifying the starch molecule using chemical method via graft copolymerization. Starch-based bioplastics have some limitations such as poor long-term stability, poor mechanical properties, a strong ability to absorb water and the difficulty in processing. A starch grafted copolymer was one example of the use of a chemical method to improve the physical and chemical properties of starch-based bioplastics. As this method is regarded as a powerful technique to modify properties. We prepared cassava starch grafted with polystyrene (PS) (PS-g-starch copolymer) via a suspension polymerization method using potassium persulfate (PPS) as an initiator.

The second part describes the modification and properties of bioplastics made from wheat gluten by a physical method. Wheat gluten is a plant protein often a by-product of wheat starch fabrication and the food processing industry. Wheat gluten has advantages because it is renewable, biodegradable and has suitable properties for use as a plastic. However, the effect of shearing forces during processing and thermal treatment causes the protein aggregation (crosslinking) that affects the quality of the final product. Therefore, we investigated the use additives that can control the aggregation of wheat gluten protein. These were composed of Kraft lignin (KL), Esterified lignin (EL) and other additives that presented the different functional groups (i.e. conjugated double bonds, hydroxyls, aldehydes, carboxyl and ortho-methoxy groups). EL was carried out via the esterification reaction of KL hydroxyl groups.

This thesis demonstrates how to improve the quality of bioplastic products to help to solve the worldwide environmental pollution problems caused by plastic waste materials.

## Contents

	<b>Page</b>
List of Tables	xvi
List of Figures	xvii
Part I	
Chapter 1: Introduction	1
1.1 Background and rationale	1
1.2 Objectives of the research	3
1.3 Benefits	3
Chapter 2: Literature Review	4
2.1 Biodegradable polymers	4
2.2 Starch	5
2.2.1 Amylose	6
2.2.2 Amylopectin	6
2.2.3 Starch granules	9
2.2.4 Crystalline structure	11
2.2.5 Gelatinization	13
2.2.6 Retrogradation	14
2.3 Copolymer	14
2.3.1 Random copolymer	15
2.3.2 Alternating copolymer	15
2.3.3 Block copolymer	15
2.3.4 Graft copolymer	15
2.4 Starch graft copolymer	16
2.4.1 Chemical initiation	17
2.4.1.1 Thermal decomposition initiator	17

## Contents (Continued)

	<b>Page</b>
2.4.1.2 Redox initiation	18
(i) Potassium persulfate (PPS)	19
(ii) Ceric ammonium nitrate	20
2.4.2 Irradiation initiation	21
2.5 Suspension polymerization	23
2.6 Polystyrene (PS)	23
Chapter 3: Experimental	25
3.1 Materials	25
3.2 Experimental Procedure	25
3.2.1 Preparation of cassava starch grafted with polystyrene (PS-g-starch copolymer)	25
3.2.1.1 Graft copolymerization process	25
3.2.1.2 Soxhlet extraction	26
3.2.2 Preparation of PS by the suspension polymerization technique	26
3.2.3 Effects of reaction parameters	27
3.2.3.1 The amount of cassava starch, styrene monomer and reaction temperature	27
3.2.3.2 The PPS content	27
3.2.3.3 The reaction time	28
3.2.4 Preparation of PS-g-cassava starch copolymer /cassava starch blend	28
3.3 Characterization of PS-g-starch copolymer and PS-g-cassava starch copolymer/cassava starch blend	28
3.3.1 Determination of percentage of grafting (G (%))	28
3.3.2 Determination of grafting efficiency (GE (%))	29

## Contents (Continued)

	<b>Page</b>
3.3.3 Fourier transform infrared analysis	29
3.3.4 Morphological analysis	29
3.3.5 Thermogravimetric analysis	29
3.3.6 Differential scanning calorimetry analysis	30
3.3.7 X-ray diffraction analysis	30
3.3.8 Shrinkage determinations	31
Chapter 4: Results and Discussion	33
4.1 Suspension polymerization of polystyrene	33
4.2 Effects of reaction parameters	34
4.2.1 Cassava starch:styrene monomer ratios and reaction temperature	34
4.2.2 The amount of PPS	37
4.2.3 The reaction time	38
4.2.4 Mechanisms of grafting between polystyrene and cassava starch	41
4.3 Characterization of graft copolymer	42
4.3.1 Fourier transform infrared analysis	42
4.3.2 Morphological analysis	44
4.3.3 Thermogravimetric analysis	48
4.3.4 Differential scanning calorimetry analysis (DSC)	54
4.3.5 X-ray diffraction analysis	57
4.3.6 The efficiency of Soxhlet extraction	58
4.4 PS-g-cassava starch copolymer/cassava starch blend	59
Chapter 5: Conclusions	65

## Contents (Continued)

	<b>Page</b>
Part II	
Chapter 6: Introduction	66
6.1 Background and rationale	66
6.2 Objectives of the research	69
6.3 Benefits	69
Chapter 7: Literature Review	70
7.1 Gluten	70
7.1.1 Gliadin	72
7.1.2 Glutenin	72
7.1.3 Wheat gluten based materials	74
(i) Films made from wheat gluten	75
(ii) Other bioplastics made from wheat gluten	75
7.2 Lignocellulosic materials of plant cell walls	76
7.2.1 Cellulose	77
7.2.2 Hemicellulose	77
7.2.3 Lignin	77
7.2.3.1 The Lignin properties and applications	81
7.3 Kjeldahl method	82
(i) Digestion	83
(ii) Distillation	83
(iii) Titration	84
Chapter 8: Experimental	85
8.1 Materials	85
8.2 Esterification on Kraft lignin	85
8.3 Sample preparation	85

## Contents (Continued)

	<b>Page</b>
8.4 Thermal treatment	86
8.5 Gluten protein extraction	86
8.6 Characterization	87
8.6.1 Kjeldahl method	87
(i) Digestion	87
(ii) Distillation	87
(iii) Titration	87
8.6.2 Morphological analysis	89
8.6.3 Fourier transform infrared analysis	89
 Chapter 9: Results and Discussion	 92
9.1 Kraft lignin (KL) esterification	92
9.2 Materials processing	95
(i) The wheat gluten reference	95
(ii) Effect of glycerol	96
(iii) Effect of KL and EL	97
(iv) Effect of other additives	97
9.3 Protein solubility during processing	103
9.4 Protein solubility after mixing and thermomolding	105
 Chapter 10: Conclusions	 113
 <b>References</b>	 <b>115</b>
<b>Appendices</b>	<b>138</b>
<b>Appendix A Rheology of native cassava starch, ester starch     and oxidized starch</b>	<b>139</b>

## Contents (Continued)

	<b>Page</b>
<b>Appendix B Surface morphology of native cassava starch, ester starch and oxidized starch</b>	145
<b>Appendix C Effect of glycerol content on storage modulus, loss modulus and tan delta of wheat gluten</b>	149
<b>Appendix D Publication</b>	152
<b>Appendix E Manuscript 2</b>	162
<b>Vitae</b>	194

## List of Tables

<b>Table</b>	<b>Page</b>
2.1 Approximate amylose and amylopectin content of common starches (Thomas and Atwell, 1997).	5
2.2 Characteristics of amylose and amylopectin (Thomas and Atwell, 1999).	9
2.3 Starch granule characteristics (Eliasson, 2000).	10
3.1 The amount of starch, styrene monomer and reaction temperature.	27
4.1 FTIR assignment of cassava starch and polystyrene	43
4.2 Appearance of the starch-based plastics as affected by plasticizer type and concentration (The ratios of PS-g-cassava starch copolymer (GS):cassava starch (CS) = 50:50).	61
4.3 Composition and appearance of the starch-based plastics as affected by amount of PS-g-starch copolymer and cassava starch (glycerol (45 phr) and water (10 phr)).	62
4.4 Shrinkage (%) for PS-g-starch copolymer/cassava starch blends (65% RH)	63
7.1 Amino acid unit of gliadine and glutenine in gluten (Kunanopparat, 2008).	71
7.2 Cellulose, hemicellulose and lignin content of various plant (McGinnis and Shafizaden, 1991).	76
7.3 Kjeldahl factor of various proteins (Merrill and Watt, 1973).	84
8.1 Structure and molecular weight of all additives.	90



## List of Figures

Figure	Page
2.1 Categorization of biodegradable polymers (Averous and Boquillon, 2004).	4
2.2 The structure of amylose showing $\alpha$ -1,4-linkage (a), $\alpha$ -1,6-linkage and D-glucopyranose unit (b) and helical structure (c) (Bettelheim and March, 1990; Thomas and Atwell, 1999).	7
2.3 The structure of amylopectin (Steinbuchel and Rhee, 2005).	8
2.4 The cluster model of amylopectin (Manners, 1989).	8
2.5 The organization of amylose and amylopectin in starch granule (Thomas and Atwell, 1999).	10
2.6 Scanning electron micrographs of (a) cassava starch, (b) potato starch, (c) rice starch and (d) corn starch (Kiatkamjornwong et al., 2006; Uttapap et al., 2008).	11
2.7 Structure of starch granule with alternating amorphous and semi-crystalline zones constituting the growth rings (Donald et al., 1997).	12
2.8 X-ray diffraction pattern of A, B and Vh type of starch (Bulemon et al., 1998).	13
2.9 Influence of hydrothermic processing on physical characteristics of starch granule (Eliasson, 2000).	14
2.10 The simplest structure of copolymers containing A and B repeating units: random copolymer (a), alternating copolymer (b), block copolymer (c) and graft copolymer (d).	16
2.11 Dissociation of (a) BPO and (b) AIBN (Young and Lovell, 1991; Fried, 2003).	18
2.12 The mechanism of PMMA-g-sago starch copolymer, where AGU-OH is sago starch and $R^\bullet$ is free radical species (Qudsieh et al., 2004).	20

## List of Figures (Continued)

Figure	Page
2.13 The mechanism of PMMA-g-sago starch copolymer by using ceric ammonium nitrate as an initiator (Qudsieh et al., 2001).	21
2.14 Manufacture of styrene monomer (Ulrich, 1993).	24
3.1 Crystalline and non-crystalline regions (Shujun et al., 2005).	31
4.1 SEM micrographs of PS spherical microbeads.	33
4.2 DSC thermogram second-heating of PS spherical microbeads.	34
4.3 Effect of cassava starch:styrene monomer ratios on the G (%) and GE (%) at different the reaction temperature; (a) 30°C, (b) 40°C, (c) 50°C and (d) 60°C.	36
4.4 Effect of PPS content on the G (%) and GE (%) of samples polymerized at 50°C for 2 h with 100 g of water, 2.5 g of cassava starch and 7.5 g of styrene monomer.	38
4.5 Effect of reaction time on G (%) and GE (%) of samples polymerized at 50°C with 100 g of water, 2.5 g of cassava starch, 7.5 g of styrene monomer and 0.4 g of PPS.	39
4.6 SEM micrographs of the PS-g-cassava starch copolymer before Soxhlet extraction at different reaction time (G (%) = 9.57%); (a) 15 min, (b) 30 min, 1 h ((c) and (d)) and 2 h ((e) and (f)).	40
4.7 Mechanisms of grafting between polystyrene and cassava starch.	42
4.8 FTIR spectrum of cassava starch (a), PS (b), PS-g-cassava starch copolymer before Soxhlet extraction (c) and PS-g-cassava starch copolymer after Soxhlet extraction with G (%) = 22.80% (d).	44
4.9 SEM micrograph of the cassava starch.	45
4.10 SEM micrographs of the PS-g-cassava starch copolymer with G (%) = 22.80% at the reaction time for 2 h before Soxhlet extraction.	46

## List of Figures (Continued)

Figure	Page
4.11 SEM micrographs of the PS-g-cassava starch copolymer with G (%) = 22.80% at the reaction time for 2 h after Soxhlet extraction.	47 48
4.12 SEM micrographs of the PS-g-cassava starch copolymer (after Soxhlet extraction); G (%) = 14.00% ((a) and (b)) and G (%) = 32.80% ((c) and (d)).	
4.13 TGA and DTG thermograms of cassava starch.	49
4.14 TGA and DTG thermograms of PS.	50
4.15 TGA and DTG thermograms of PS-g-cassava starch copolymer before (a) and after Soxhlet extraction (b) with G (%) = 22.80%.	51
4.16 TGA and DTG thermograms of PS-g-cassava starch copolymer after Soxhlet extraction with G (%) = 14.00% (a), 22.80% (b) and 32.80% (c).	53
4.17 DSC thermogram from the first heating scan of cassava starch (a), PS-g-cassava starch copolymer after Soxhlet extraction with G (%) = 14.00% (b), 22.80% (c), 32.80% (d) and PS (e).	55
4.18 DSC thermogram from the second heating scan of cassava starch.	55
4.19 DSC thermogram from the second heating scan of PS.	56
4.20 DSC thermogram from the second heating scan of PS-g-cassava starch copolymer before Soxhlet extraction with G (%) = 22.80% (a), PS-g-cassava starch copolymer after Soxhlet extraction with G (%) = 14.00% (b), 22.80% (c) and 32.80% (d).	57
4.21 XRD pattern of the cassava starch and the PS-g-cassava starch copolymer after Soxhlet extraction with G (%) = 22.80%.	58
4.22 FTIR spectrum of virgin cassava starch (a) and the product of the starch and PS blend after Soxhlet extraction (b).	59
4.23 XRD patterns of the cassava starch, PS-g-cassava starch copolymer and the PS-g-cassava starch/cassava starch blend.	64

## List of Figures (Continued)

Figure	Page
7.1 The structure of glutamine, praline and cystine (Walsh, 2002).	71
7.2 Radical (a) and (b) nucleophilic exchange mechanism between a thiyl and a disulfide bond (Walsh, 2002; Auvergne et al., 2008; Kunanopparat, 2008).	73
7.3 Cellulose, hemicellulose and lignin in cell walls (Charles and Bin, 2009).	78
7.4 Cellulose structure (Ouellette, 1998).	79
7.5 Hemicellulose structure (Kunanopparat, 2008).	79
7.6 The main primary monolignols of lignin (Kunanopparat, 2008).	79
7.7 Lignin structure (Nimz, 1974). (Note that the structure of Kraft lignin is slightly different due to the Kraft processing).	80
7.8 Trapping and stabilization of radicals by lignin (Barclay et al., 1997).	81
9.1 Mechanism of Kraft lignin esterification.	92
9.2 SEM micrographs of (a) Kraft lignin and (b) Esterified lignin.	93
9.3 The FTIR spectrum of the Kraft lignin and Esterified lignin.	94
9.4 Torque and temperature evolution of controlled wheat gluten (glycerol 30%)	96
9.5 Effect of glycerol content on torque and temperature evolution of wheat gluten; controlled wheat gluten (glycerol 30%) ( $\diamond$ ), 31% ( $\circ$ ), 35% ( $\times$ ) and 40% ( $\triangle$ ).	96
9.6 Effect of KL content on torque and temperature evolution of wheat gluten; controlled wheat gluten ( $\diamond$ ), 1% ( $\circ$ ), 5% ( $\times$ ) and 10% ( $\triangle$ ).	98
9.7 Effect of ML content on torque and temperature evolution of wheat gluten; controlled wheat gluten ( $\diamond$ ), 1% ( $\circ$ ), 5% ( $\times$ ) and 10% ( $\triangle$ ).	98

## List of Figures (Continued)

Figure	Page
9.8 Effect of vanillin content on torque and temperature evolution of wheat gluten; controlled wheat gluten (◇), 1% (○), 5% (×) and 10% (△).	99
9.9 Effect of ferulic acid content on torque and temperature evolution of wheat gluten; controlled wheat gluten (◇), 1% (○), 5% (×) and 10% (△).	99
9.10 Effect of coumaric acid content on torque and temperature evolution of wheat gluten; controlled wheat gluten (◇), 1% (○), 5% (×) and 10% (△).	100
9.11 Effect of guaiacol content on torque and temperature evolution of wheat gluten; controlled wheat gluten (◇), 1% (○), 5% (×) and 10% (△).	100
9.12 Effect of cinnamyl alcohol content on torque and temperature evolution of wheat gluten; controlled wheat gluten (◇), 1% (○), 5% (×) and 10% (△).	101
9.13 Effect of cinnamaldehyde content on torque and temperature evolution of wheat gluten; controlled wheat gluten (◇), 1% (○), 5% (×) and 10% (△).	101
9.14 Effect of <i>trans</i> -anethole content on torque and temperature evolution of wheat gluten; controlled wheat gluten (◇), 1% (○), 5% (×) and 10% (△).	102
9.15 The repetition of torque evolution of wheat gluten with cinnamaldehyde 10%.	102
9.16 The repetition of torque evolution of wheat gluten with <i>trans</i> -anethole 10%.	103

## List of Figures (Continued)

Figure	Page
9.17 Effect of additives on the SDS-soluble protein content of wheat gluten after mixing (without thermal treatment): glycerol (◇, —), KL (○, ---), EL (○, —), guaiacol (□, —), vanillin (◇, ---), <i>trans</i> -anethole (▽, —), ferulic acid (△, ---), coumaric acid (△, —), cinnamaldehyde (⊞, —), cinnamyl alcohol (♣, —); controlled wheat gluten (glycerol 30%) (■) and un-plasticize wheat gluten (●).	104
9.18 Effect of KL (○, ---), EL (○, —), guaiacol (□, —) and glycerol (◇, —) on the insoluble protein content of wheat gluten after thermalmolding; controlled wheat gluten (■) and un-plasticize wheat gluten (●).	106
9.19 Effect of phenolic compounds on the insoluble protein content of wheat gluten after thermalmolding; controlled wheat gluten (■), un-plasticize wheat gluten (●), guaiacol (□, —), vanillin (◇, ---) and ferulic acid (△, ---).	107
9.20 The structure of intramolecular hydrogen bond in guaiacol.	108
9.21 The resonance structures of phenoxide ion (a) and phenol (b) (Brown and Foote, 2002).	108
9.22 Possible resonance structures of ferulic acid phenoxy radical (Butterfield et al., 2002).	109
9.23 Nucleophilic addition reaction (Michael reaction) (Dewick, 2006).	109
9.24 Example of radical reaction (a) and nucleophilic addition reaction (b) of ferulic acid with cysteine functions.	111

## List of Figures (Continued)

Figure	Page
9.25 Effect of aromatics compounds containing conjugated double bonds on the insoluble protein content of wheat gluten after thermalmolding; controlled wheat gluten (■), un-plasticize wheat gluten (●), ferulic acid (△, ---), coumaric acid (△, —), cinnamaldehyde (⊞, —), cinnamyl alcohol (⊟, —) and <i>trans</i> -anethole (▽, —).	112

## CHAPTER 1

### INTRODUCTION

#### 1.1 Background and rationale

Synthetic plastics are major materials in daily life. Because of their durable properties, ease of production, convenience and cheapness, synthetic plastics are ideal materials for a large number of applications. Plastics find uses as containers, packaging materials for the fast food, picnic tableware and agricultural films or in combination with other materials as part of transportation vehicles, computers, tools, etc. The significant increase in plastic waste has become a worldwide environmental problem. This results in accumulation of synthetic plastics in nature as a consequence of their excellent mechanical properties as well as their resistance to chemicals, weather and biodegradability.

As a result, it is recognized that one solution to this plastic waste problem is to produce and use biodegradable polymers. Some biodegradable polymers include polycaprolactone, poly(lactic acid) and bacterial polyesters such as polyhydroxybutyrate (PHB) and polyhydroxyvalerate (PHV). However, they are not widely used because of their high production costs. In contrast, starch has been considered to be a good candidate for preparing biodegradable products because it is inexpensive, abundant, biodegradable, has versatile uses and is a readily available and renewable agricultural resource (Athawale and Lele, 1998; Qudsieh et al., 2004; Chen et al., 2005; Don et al., 2006; Yin et al., 2008).

Useful starch-based plastic materials can be prepared using common thermoplastic processing such as vacuum thermoforming and compression molding (Soest and Borger, 1996; Soest et al., 1996; Averous and Fringant, 2001; Souza and Andrade, 2002; Roz et al., 2006; Corradini et al., 2007; Orts et al., 2007; Wang and Huang, 2007). However, starch-based materials have some drawbacks including their poor long-term stability, poor mechanical properties, the strong ability to absorb water and the difficulties in processing (Averous et al., 2000; Averous and Fringant, 2001; Sacak and Celik, 2002; de Graaf et al., 2003; Mano et al., 2003; Chen et al., 2005; Corradini et al., 2007). Chemical modification of starch via free radical graft



copolymerization with vinyl monomers is one of the most effective methods for improving the properties of starch (Wurzburg, 1987; Athawale and Lele, 1998; Sacak and Celik, 2002; Chen et al., 2005). The initiation of free radical graft copolymerization begins when free radicals generated on the starch molecules react with vinyl monomers. The free radicals can be obtained by two methods which are chemical and irradiation initiation. The graft copolymerization of vinyl monomers (i.e., methyl methacrylate, methacrylonitrile, styrene, acrylonitrile, acrylamide and methyl acrylate) with various starches has been achieved with various types of chemical initiation, including benzoyl peroxide (BPO) (Pimpan and Thothong, 2006), 2,2'-azobis(isobutyronitrile) (AIBN) (Suat, 2001; Sacak and Celik, 2002; Brockway and Moser, 2003; Brockway and Seaberg, 2003), potassium persulfate (PPS) (Khalil et al., 1993; Taghizadeh and Mafakhery, 2001; Cho and Lee, 2002; Fang et al., 2005) and ceric ammonium nitrate (Silong et al., 2000; Athawale and Lele, 2000; Qudsieh et al., 2001; Janarthanan et al., 2003; Don et al., 2006). Moreover, there have been many research groups that have prepared various types of starch grafted with vinyl monomers by using  $\gamma$ -rays from a  $^{60}\text{Co}$ -source. (Fanta et al., 1975; Henderson and Rudin, 1981; Lyer et al., 1990; Kiatkamjornwong et al., 1999; Kiatkamjornwong et al., 2000; Geresh et al., 2002; Fang et al., 2004; Fang et al., 2005).

However, there have been fewer reports of starch grafted with polystyrene (PS). Trimnell and coworkers (2003) reported that thiolated starch grafted with PS was carried out using hydrogen peroxide as the initiator. The acryloylated potato starch grafted with polystyrene was prepared by using PPS in aqueous solution (Fang et al., 2005). Gelatinized sago starch grafted with polystyrene was produced using ceric ammonium nitrate as a redox initiator (Janarthanan et al., 2003). Starch grafted with polystyrene prepared by  $\gamma$ -ray irradiation was reported by Fanta and coworkers (1975), Henderson and coworker (1981) and Kiatkamjornwong and coworkers (1999). However, it is difficult to prepare starch grafted with PS by free radical initiation (Cho and Lee, 2002). There have been no reports of starch grafted with PS via suspension polymerization using PPS as the initiator. Cho and Lee (2002) reported that corn starch granules grafted with PS could occur via an emulsion polymerization method using PPS as an initiator, sodium dodecylbenzenesulfonate as an emulsifier and tetraethylthiuram disulfide as a chain transfer agent. They suggested that the

starch graft copolymerization did not occur without the emulsifier because it is difficult to prepare PS by using a water-soluble initiator. For starch graft copolymerization, it is better to employ a water-soluble initiator because water is the medium that provides the starch slurry. In this thesis, cassava starch grafted with PS (PS-g-starch copolymer) was prepared via suspension polymerization using PPS as an initiator in aqueous medium.

### **1.2 Objectives of the research**

1. To synthesize the PS-g-starch copolymer via a suspension polymerization method using PPS as an initiator.
2. To determine the most suitable conditions for the graft copolymerization reaction referred to in 1.
3. To investigate the properties of the PS-g-starch copolymer derived from 1.

### **1.3 Benefits**

It was expected that the PS-g-starch can be used directly as the compatibilizer for PS/starch blends and for use as a biodegradable plastic. Moreover, it could increase the value of agriculture products and reduce the accumulation of plastic waste.

## CHAPTER 2

### LITERATURE REVIEW

#### 2.1 Biodegradable polymers

Biodegradable polymers consist of four families each obtained from renewable resources and fossil origin (Figure 2.1). Polysaccharides (e.g., starch, cellulose and chitin) and protein (e.g., gluten, zein and casein) are agro-polymers. Starch is deposited in granules in plants (see section 2.2). Gluten is a composite of the proteins gliadin and glutenin (see Chapter 7). Some polymers are obtained from micro-organisms such as polyhydroxy-alkanoates (PHAs). They are synthesized by several bacterial species and are accumulated as energy and/or carbon storage materials. Poly(lactic acid) (PLA) is a biodegradable polymer obtained by biotechnology. It can be produced from lactic acid a fermentation product from crops (e.g., maize or other starch-rich substances like maize, sugar or wheat). Biodegradable polymers can also be obtained from petrochemical processes such as polycaprolactone (PCL), polyesteramide (PEA) and aliphatic or aromatic copolyesters.

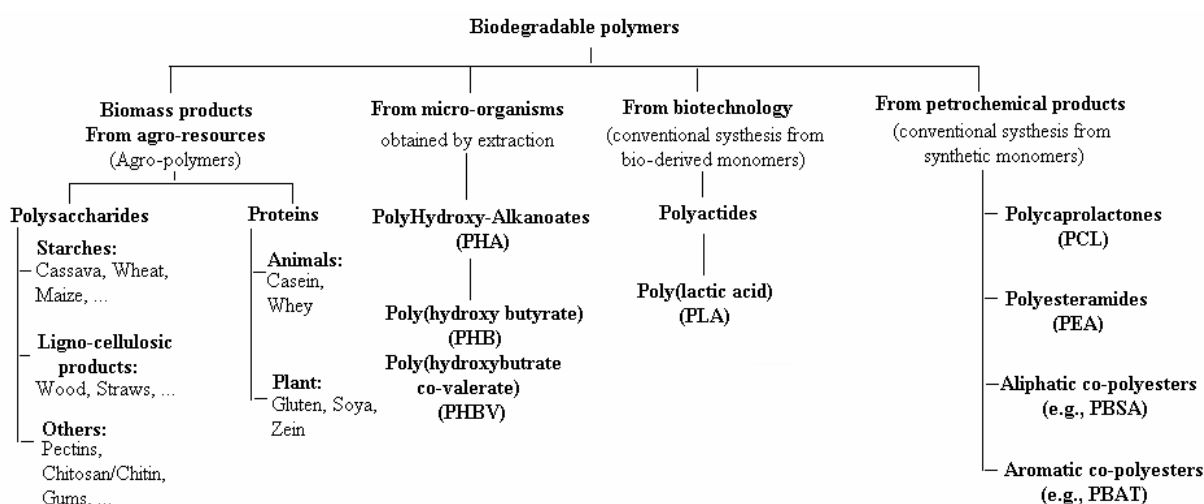


Figure 2.1 Categorization of biodegradable polymers (Averous and Boquillon, 2004).

## 2.2 Starch

Starch is a polysaccharide carbohydrate consisting of a large number of glucose units joined together by glycosidic bonds. Starch is produced by all green plants as an energy store and is a major food source for humans. Starch is derived from seeds, (e.g. wheat, corn, rice and barley), roots (e.g. potatoes and cassava) and legumes (e.g. peas, lentils, kidney beans and mung beans). Pure starch is a white, tasteless and odorless powder that is insoluble in cold water or alcohol (Eliasson, 2000). Starch consists of two types of molecules: the linear and helical *amylose* and the branched *amylopectin* (Bettelheim and March, 1990; Thomas and Atwell, 1999; Steinbuchel and Rhee, 2005). Depending on the plant, starch generally consists of 20 to 25% amylose and 75 to 80% amylopectin. The structural differences between these two polymers contribute to significant differences in starch properties and functionality (Eliasson, 2000; Steinbuchel and Rhee, 2005). The approximate amylose and amylopectin contents of several starches are presented in Table 2.1. The major physical and chemical properties of starch are gelatinization, retrogradation, solubility and water absorption power. These physical and chemical properties are influenced by the shape of the starch granule, molecular structure and botanical source of native starches from different vegetable sources (Whistler et al., 1984; Eliasson, 2000).

Table 2.1 Approximate amylose and amylopectin content of common starches  
(Thomas and Atwell, 1999)

Starch type	Amylose content (%)	Amylopectin content (%)
Waxy corn	< 1	> 99
High-amylose corn	55 – 70 (or higher)	30 – 45 (or lower)
Cassava	17	83
Potato	20	80
Wheat	25	75
Rice	19	81

### 2.2.1 Amylose

Amylose is considered to be an essentially linear polymer composed almost entirely of  $\alpha$ -1,4-linked D-glucopyranose (Figure 2.2) (Bettelheim and March, 1990; Ikan, 1991; Eliasson, 2000; Steinbuchel and Rhee, 2005). Less than 0.5% of the glucoses in amylose are in  $\alpha$ -1,6-linkage, resulting in a low degree of branching. Each chain of amylose is comprised of in the region of 200-700 glucoses residues per molecule which includes 9-20 branch points (Whistler et al., 1984; Thomas and Atwell, 1999; Steinbuchel and Rhee, 2005). The amylose chains display a natural twist giving a helical conformation (Figure 2.2 (c)). The formation of a helical complex between amylose and iodine gives rise to the typical deep blue color of starch dispersions stained with iodine and forms the basis for the quantitative determination of amylose content (Whistler et al., 1984; Thomas and Atwell, 1999). Amylose is able to form a gel and paste. This property is evident in the behavior of certain amylose-containing starches. Corn starch, wheat starch, rice starch and particularly high-amylose corn starch are usually considered gelling starches. A gel can be formed quite rapidly from the linear polymer amylose (Bettelheim and March, 1990; Thomas and Atwell, 1999; Eliasson, 2000).

### 2.2.2 Amylopectin

Amylopectin is a branched polymer that is much larger than amylose (Figure 2.3). It has a large influence on the properties of starch. Amylopectin is composed of  $\alpha$ -1,4-linked glucose segments connected by  $\alpha$ -1,6-linked branch points. Amylopectin has about 5% of its glucoses in  $\alpha$ -1,6-linkage (Ikan, 1991; Eliasson, 2000; Steinbuchel and Rhee, 2005). In recently, the cluster model is an acceptable model for amylopectin (Figure 2.4). The A chains are unbranched and are linked to the molecule through their reducing end-group, the B chains which are jointed to the molecule in the same way but carry one or more A chains and the C chain has the reducing end-group of the molecule (Eliasson, 2000; Noda et al., 2009).

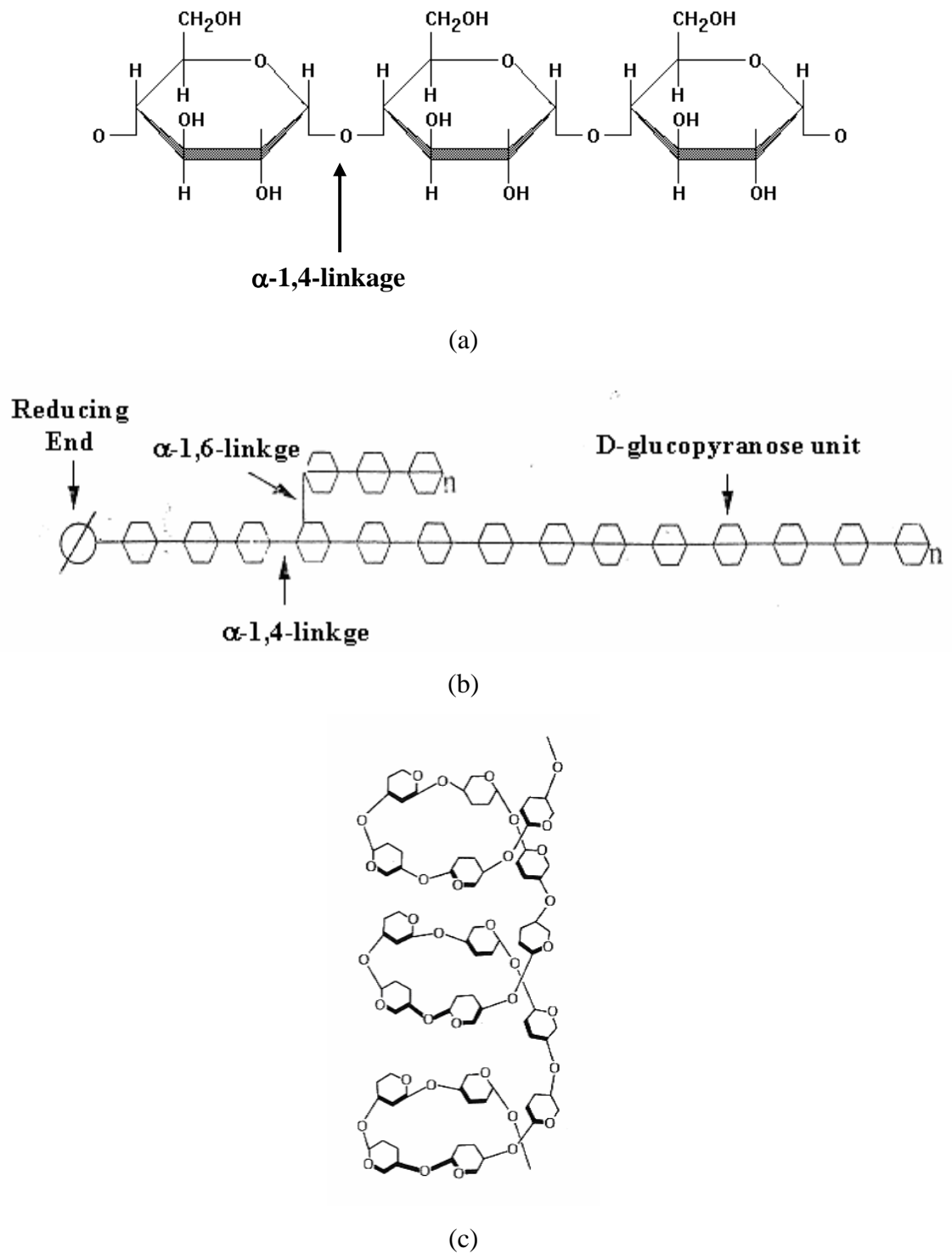


Figure 2.2 The structure of amylose showing  $\alpha$ -1,4-linkage (a),  $\alpha$ -1,6-linkage and D-glucopyranose unit (b) and helical structure (c) (Bettelheim and March, 1990; Thomas and Atwell, 1999).

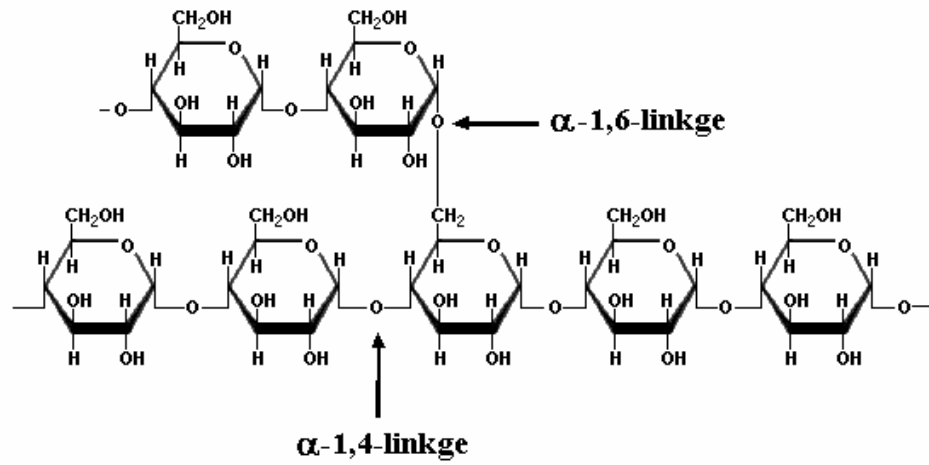


Figure 2.3 The structure of amylopectin (Steinbuechel and Rhee, 2005).

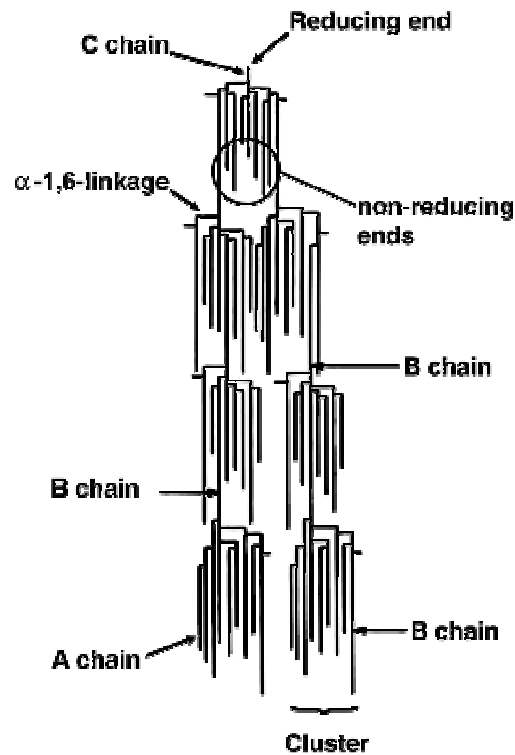


Figure 2.4 The cluster model of amylopectin (Manners, 1989).

Due to the highly branched nature of amylopectin, its properties differ from those of amylose. For example, the retrogradation and gel formation can either be delayed or prevented (Bettelheim and March, 1990; Thomas and Atwell, 1999; Eliasson, 2000). Moreover, iodine does not form a stable complex with amylopectin. Some important characteristics of amylose and amylopectin are displayed in Table 2.2.

Table 2.2 Characteristics of amylose and amylopectin (Thomas and Atwell, 1999)

Characteristic	Amylose	Amylopectin
Shape	Essentially linear	Branched
Linkage	$\alpha$ -1,4 (some $\alpha$ -1,6)	$\alpha$ -1,4 and $\alpha$ -1,6
Molecular weight	Typically < 0.5 million	50 -500 million
Gel formation	Firm	Non-gelling to soft
Color with iodine	Blue	Reddish brown

### 2.2.3 Starch granules

Amylose and amylopectin do not exist free in nature, but as components of discrete, semi-crystalline aggregates called starch granules (Figure 2.5). The size, shape and structure of these granules vary substantially among botanical sources, as presented in Table 2.3. The diameters of the granules generally range from less than 1  $\mu\text{m}$  to more than 100  $\mu\text{m}$ . The shape of starch granules can be regular (e.g., polygonal, spherical, ovoid or angular) or quite irregular depending on the content, structure and organization of the amylose and amylopectin molecules, the branching architecture of amylopectin and the degree of crystallinity (Lindeboom et al., 2004). The granules derived from tubers are larger than those from cereals. The starch granules are not broken and the cross polarization remains unchanged under dry heat conditions (Eliasson, 2000). The scanning electron microscope (SEM) is a valuable tool for the study of starch granules. Figure 2.6 demonstrates the SEM micrographs of various starch granules.



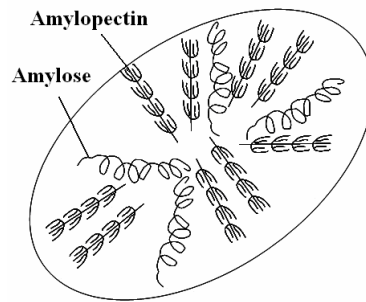


Figure 2.5 The organization of amylose and amylopectin in starch granule (Thomas and Atwell, 1999).

Table 2.3 Starch granule characteristics (Eliasson, 2000)

Starch	Type	Diameter ( $\mu\text{m}$ )	Morphology	Gelatinization temperature ( $^{\circ}\text{C}$ )
Maize <sup>*</sup>	Cereal	5-30	Round and Polygonal	62-72
Waxy maize	Cereal	5-30	Round and Polygonal	63-72
Cassava <sup>**</sup>	Root	4-35	Oval and Truncated “kettle drum”	62-73
Potato	Tuber	5-100	Oval and Spherical	59-68
Wheat	Cereal	1-45	Round and Lenticular	58-64
Rice	Cereal	3-8	Polygonal, Spherical and Compound granules	68-78
Sago	Pith	15-65	Oval and Truncated	69-74
High amylose maize	Cereal	5-30	Polygonal and Irregular elongated	63-92 <sup>***</sup>

<sup>\*</sup>Maize is also often referred to as “corn”, “dent corn” or “regular maize”.

<sup>\*\*</sup>Cassava is also often referred to as “tapioca” or “manioc”.

<sup>\*\*\*</sup>High amylose maize starches are not completely gelatinized in boiling water.

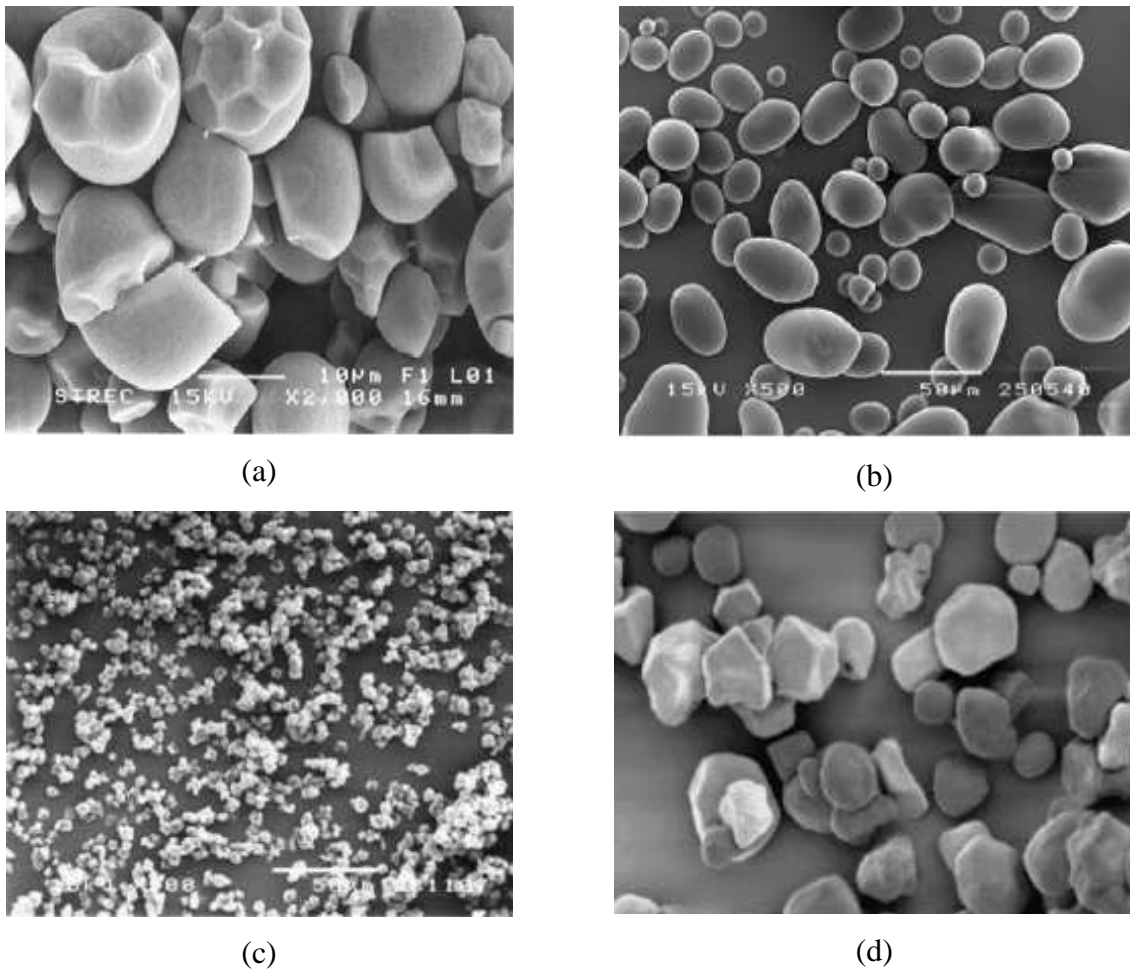


Figure 2.6 Scanning electron micrographs of (a) cassava starch, (b) potato starch, (c) rice starch and (d) corn starch (Kiatkamjornwong et al., 2006; Uttapap et al., 2008).

#### 2.2.4 Crystalline structure

The degree of crystallinity of native starch granules ranges from about 15% for high-amylose starches to about 45-50% for waxy starches. Multiple concentric layers of so-called growth rings of increasing diameter extend from the hilum (the center of growth) towards the surface of the granules (Figure 2.7). The growth rings are typically 120-400 nm in thickness (Steinbuchel and Rhee, 2005; Copeland et al., 2009). The concentric growth rings, in turn, contain alternating crystalline and amorphous regions of higher and lower density, respectively. Within the lamellae, the crystalline layers are considered to be formed mainly by the ordering of the amylopectin chains packed into a crystalline lattice. The linear chain within the

high molecular order region can form double helices and pack into a crystal structure, A, B, C and V types according to the type of starch as explained below. The amorphous layers contain the amylopectin branching points and free amylose in a disordered conformation (Steinbuechel and Rhee, 2005). X-ray diffraction patterns have been used to study the crystalline nature of starch. Native cereal starches such as wheat, corn and rice exhibit the A-crystalline pattern, tuber starches and amylose-rich starches present the B-crystalline pattern and pea and bean starches show the C-crystalline pattern which is a mixture of A-type and B-type. The difference between A-type and B-type is that the helices in the A-type are more compact than in the B-type (Steinbuechel and Rhee, 2005; Copeland et al., 2009). The V-type conformation is a result of amylose being complexed with substances such as aliphatic fatty acid, emulsifiers and long-chain alcohol (Cheetham and Tao, 1998; Thomas and Atwell, 1999; Noda et al., 2009). The V-type can be divided into two subtypes. They are Va (anhydrous) with peaks at  $13.2^\circ$  and  $20.6^\circ$  and Vh (hydrated) with peaks at  $12.6^\circ$  and  $19.4^\circ$  (Corradini et al., 2007). The X-ray diffraction pattern of A, B and Vh types of starch was displayed in Figure 2.8.

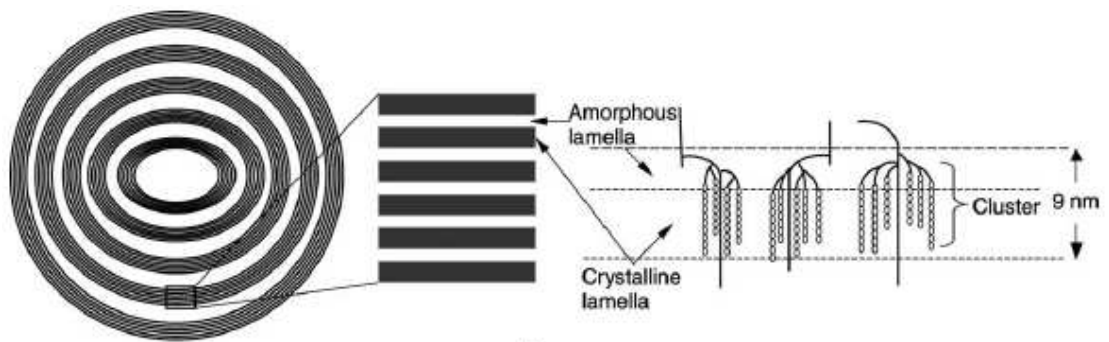


Figure 2.7 Structure of starch granule with alternating amorphous and semi-crystalline zones constituting the growth rings (Donald et al., 1997).

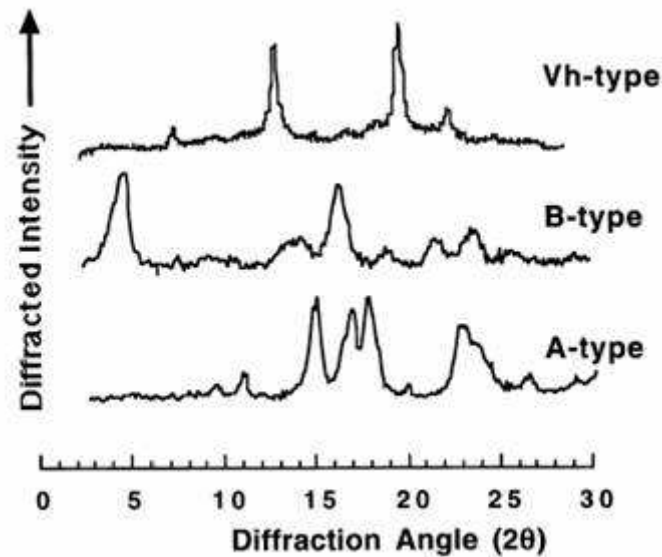


Figure 2.8 X-ray diffraction patterns of A, B and Vh type of starch (Bulemon et al., 1998).

### 2.2.5 Gelatinization

Gelatinization occurs when starch granules are heated in the presence of water, leading to the loss of crystalline order, swelling and leaching of amylose (Whistler et al., 1984; Steinbuchel and Rhee, 2005; Copeland et al., 2009). As the water is heated, water is absorbed into the starch granules which naturally begin to swell. As water absorption and heating continues, the starch granules burst and release amylose to the outside of the granules, causing less order in amylopectin and an increase in viscosity of the medium (Donald et al., 1998; Thomas and Atwell, 1999; Eliasson, 2000). The product that was obtained from this step is called a starch paste as shown in Figure 2.9 (Whistler et al., 1984). The paste viscosity reaches a maximum but some intact starch granules are still present. At this point, the starch is fully paste. The gelatinization temperature of most starches is between 50 °C and 80°C (Table 2.3). Many tools can be used to identify the gelatinization temperature, for example differential scanning calorimetry (DSC), X-ray scattering, light scattering, optical microscopy, thermo-mechanical analysis (TMA) and rapid visco analysis (RVA) (Eliasson, 2000; Steinbuchel and Rhee, 2005; Copeland et al., 2009).

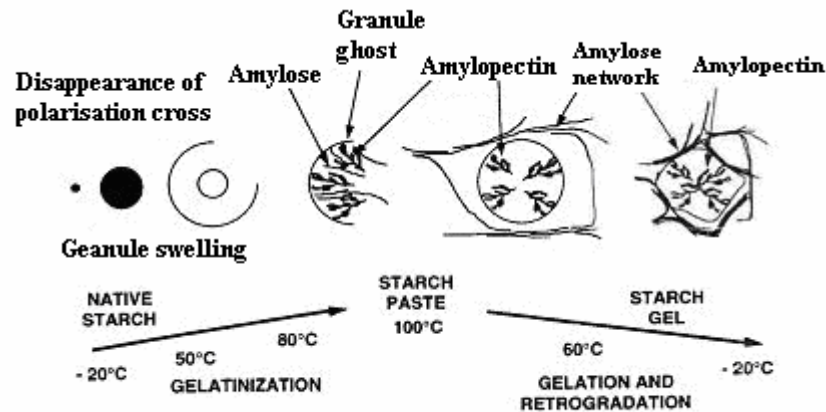


Figure 2.9 Influence of hydrothermic processing on the physical characteristics of starch granule (Eliasson, 2000).

### 2.2.6 Retrogradation

As the starch paste cools, the viscosity increases due to the amylose chains forming a cross-linked network. This process is referred to as “gelation” (Eliasson, 2000). A rearrangement between amylose chains occur. A three-dimensional network is rapidly constituted and the starch granules are ruptured. As amylose chains rearrange, hydrogen bonds between chains reappear and a novel crystalline structure is created; this is referred to as retrogradation. More amylose chains initially develop into more extensively ordered regions (Thomas and Atwell, 1999; Eliasson, 2000).

### 2.3 Copolymer

A copolymer is a polymer made from two or more different monomers. Any monomer must have at least two functional groups that can react or at least one double bond that can become a single bond when the corresponding residue has been incorporated into the polymer (Campbell, 1994; Kumar and Gupta, 1998). At the general level, there are several types of copolymers. Figure 2.10 shows the simplest structure of copolymers containing A and B repeating units.

### **2.3.1 Random copolymer**

The arrangement of random copolymer is presented in Figure 2.10 (a). The various repeat units occur randomly along the chain-link structure.

### **2.3.2 Alternating copolymer**

The regular copolymers contain a regular alternating sequence of two monomer units (Figure 2.10 (b)).

### **2.3.3 Block copolymer**

Block copolymers composed of a block of one monomer connected to a block of another (Figure 2. 10 (c)).

### **2.3.4 Graft copolymer**

Graft copolymers combining two long chains of different homopolymer. In their simplest structure they are composed of a main homopolymer chain (backbone) and a branch of the second homopolymer (Figure 2.10 (d)).

Graft copolymers can be performed by free radical polymerization. Graft copolymers often display properties that are characteristic of each homopolymer (O dian, 1991; Young and Lovell, 1991). Graft copolymers can be obtained by two general methods: (i) The formation of free radicals on molecules of the monomer was occurred by initiator. In this step, the side chains of monomers (branch) were obtained and it can be linked directly to the backbone. (ii) Initiators produce free radicals on the backbone directly, so, that they can react with monomers to yield the graft copolymer.

Both chemical (thermal decomposition initiator and redox initiator) and irradiation methods can be used to produce the free radicals of the graft copolymer (Allcock and Lampe, 1990; Fried, 2003; Pimpan and Thothong, 2006).

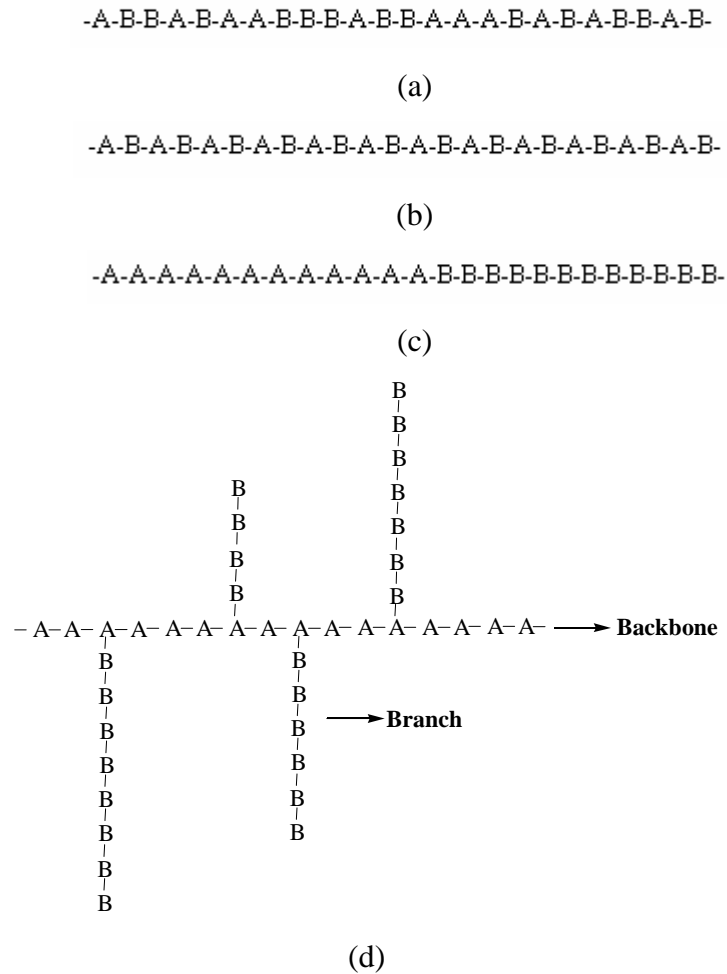


Figure 2.10 The simplest structure of copolymers containing A and B repeating units: random copolymer (a), alternating copolymer (b), block copolymer (c) and graft copolymer (d).

## 2.4 Starch graft copolymer

Starch itself is unsuitable for use as a plastic because it shows poor physical and mechanical properties. As a result, graft copolymerization of vinyl monomers onto starch by a free radical initiating system is an excellent method for improving starch properties (Qudsieh et al., 2001; Sacak and Celik, 2002). In this way, it is possible to modify the starch properties for example elasticity, sorbancy, ion exchange thermal resistance and resistance to microbiological attack. The initiation step of the graft copolymerization reaction begins when free radicals generated on starch molecules react with vinyl monomers. Irradiation and chemical initiation are general methods that have been used to generate the free radicals for the starch graft

copolymerization reaction. Many vinyl monomers were employed to prepared the graft copolymer with starch such as methyl methacrylate (Sacak and Celik, 2002; Brockwary and Moser, 2003; Brockwary and Seaberg, 2003), styrene (Pimpan and Thothong, 2006), acrylonitrile (Taghizadeh and Mafakhery, 2001; Trimmell, et al., 2003), acrylamide and methyl acrylate (Silong et al., 2000). These monomers can be prepared as graft copolymer with starch in a range of different forms e.g. granules, slurry, gelatinized and modified forms (Cho and Lee, 2002). Starch grafted with those polymers have potential uses for the agriculture industry, medical treatment, sanitation, compatibilizer, hydrogels, flocculants, ion exchangers, a biodegradable mulch film in agriculture, food packages and superabsorbents (Silong et al., 2000; Sacak and Celik, 2002; Don et al., 2006). A number of studies that have investigated the graft copolymers of vinyl monomers with starch using various initiators are further explained below.

## **2.4.1 Chemical initiation**

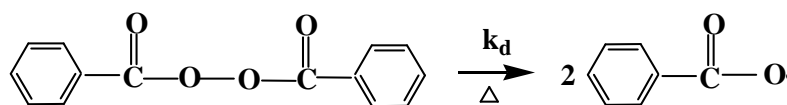
### **2.4.1.1 Thermal decomposition initiator**

Thermal decomposition of an initiator (I-I) is most widely used to produce the free radicals to initiate graft copolymer. This type of initiator is decomposed by the application of heat. It presents the two molecules of free radicals when the initiators were decomposed. The structure of thermal decomposition initiators include of -O-O- or -N=N- bonds. Example of thermal decomposition initiators are benzoyl peroxide (BPO) and 2,2'-azobis(isobutyronitrile) (AIBN). BPO decomposes by an initial cleavage of the oxygen-oxygen bond (Figure 2.11). AIBN decomposes thermally and provides two alkyl radicals and a nitrogen (Figure 2.11) (Allcock and Lampe, 1990; Odian, 1991).

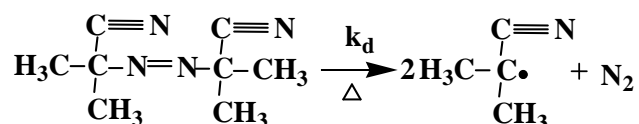
AIBN is commonly used at 50-70 °C and BPO is normally used at 80-85 °C. The percentage of grafting depends on the reaction parameters such as monomer concentration, reaction time and reaction temperature. BPO is more reactive than AIBN because the effect of resonance in AIBN structure reduces the efficiency of the free radical that generates the active sites on the backbone (Bhattacharya and Misra, 2004).



Recently, many researcher works have prepared starch graft copolymer by using this thermal decomposition initiator. AIBN was used as an initiator for preparation of starch grafted with 1-vinly 2-pyrrolidone (n-VP) (Suat, 2001) and methyl methacrylate (Sacak and Celik, 2002). Starch grafted with polyacrylonitrile and starch grafted with polymethyl methacrylate (PMMA-g-starch copolymer) by using AIBN as the initiator were prepared by Brockwary and Moser, 2003 and Brockwary and Seaberg, 2003, respectively. They found that polyacrylonitrile is more reactive with starch granule than PMMA. Trimnell and coworkers (2003) used hydrogen peroxide as an initiator to prepare the thiolated starch grafted with acrylonitrile, styrene, acrylamide, acrylic acid and dimethylaminoethyl methacrylate. Pimpan and Thothong (2006) successfully prepared a PMMA-g-cassava starch copolymer by using BPO as the initiator in an aqueous medium at 80 °C.



(a)



(b)

Figure 2.11 Dissociation of (a) BPO and (b) AIBN (Young and Lovell, 1991; Fried, 2003).

#### 2.4.1.2 Redox initiation

In this case free radicals were produced through redox reactions (oxidation-reduction reaction). The advantage of redox initiation is that free radical production occurs at reasonable rates over a very wide range of temperatures. Examples of redox initiators are potassium persulfate, manganic pyrophosphate,

potassium permanganate, ferrous ammonium sulfate-hydrogen peroxide and ceric ammonium nitrate. However, potassium persulfate and ceric ammonium nitrate have been extensively used as an initiator for starch graft copolymers.

**(i) Potassium persulfate (PPS)**

Hebeish and coworkers (1998) prepared starch grafted with polymethacrylic acid by using a potassium persulfate/sodium thiosulfate redox initiator system. Starch grafted with polyacrylamide (Khalil et al., 1993) and starch grafted with polyacrylonitrile (Taghizadeh and Mafakhery, 2001) were prepared by using the potassium persulfate redox system. A modified starch, acryloylated potato starch, was grafted with polystyrene using potassium persulfate in aqueous solution (Fang et al., 2005). Cho and Lee (2002) used an emulsion polymerization method in order to prepare corn starch grafted with polystyrene by using potassium persulfate as an initiator, sodium dodecylbenzenesulfonate as an emulsifier and tetraethylthiuram disulfide as a chain transfer agent. They proposed that the graft percent value had an attainable limit because the graft copolymerization reaction occurred at the surface of the starch particle. The maximum graft percent was obtained when the surface area of the starch particles were covered with polystyrene. Qudsieh and coworkers (2004) prepared a PMMA-g-sago starch copolymer by using potassium persulfate as a redox initiator. They presented the mechanism for forming the PMMA-g-sago starch copolymer as shown in Figure 2.12.

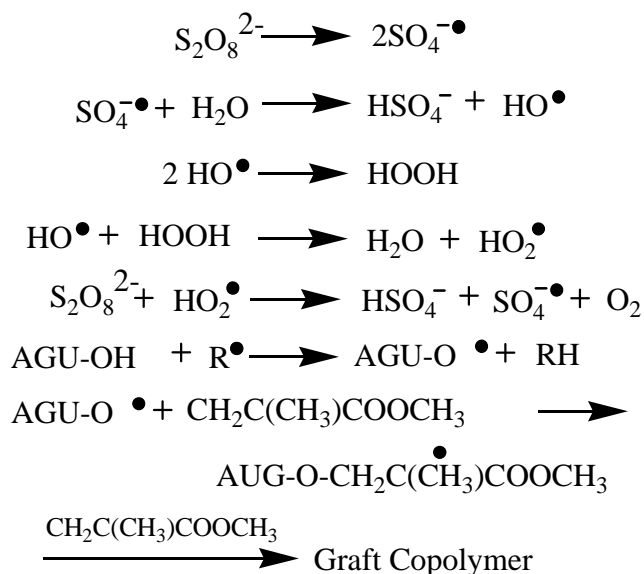


Figure 2.12 The mechanism of PMMA-g-sago starch copolymer, where AGU-OH is sago starch and  $\text{R}^{\bullet}$  is a free radical species (Qudsieh et al., 2004).

### (ii) Ceric ammonium nitrate

Sago starch grafted with polymethyl acrylate and sago starch grafted with polystyrene were prepared by using ceric ammonium nitrate as a redox initiator (Silong et al., 2000; Janarthanan et al., 2003). Preparation of maize starch grafted with polymethacrylonitrile, polyacrylamine, polymethacrylamine and polyacrylic acid was initiated by using ceric ammonium nitrate (Athawale and Lele, 2000). The modified starch, carboxymethyl starch, grafted with polyacrylamide was prepared by using ceric ammonium nitrate as an initiator (Cao et al., 2002). Ceric ammonium nitrate and PPS were used to prepare starch grafted with polyvinyl acetate (Don et al., 2006) and PMMA-g-starch copolymer (Qudsieh et al., 2001). They concluded that a higher percentage of grafting was obtained from the ceric ammonium nitrate initiated system under the same reaction condition. Figure 2.13 presents the mechanism of PMMA-g-sago starch copolymer using ceric ammonium nitrate as an initiator. In the first step, cerium ion attacked the starch molecules and obtained a starch-ceric complex. The  $\text{Ce}^{4+}$  ions in the complex are then reduced to a  $\text{Ce}^{3+}$  with the release of the protons. At that time, the free radicals are formed onto the starch backbone. The starch radicals react with monomers to initiate the graft copolymerization reaction.

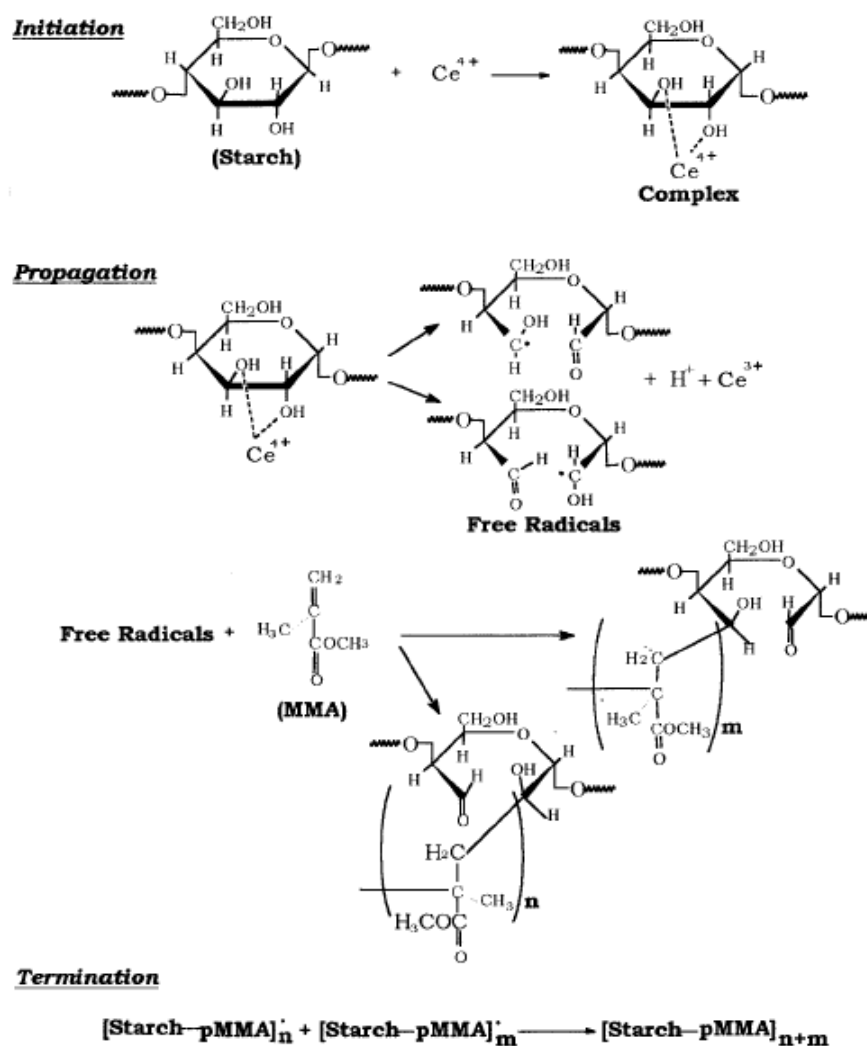


Figure 2.13 The mechanism of PMMA-g-sago starch copolymer by using ceric ammonium nitrate as an initiator (Qudsieh et al., 2001).

#### 2.4.2 Irradiation initiation

Free radical polymerization can also be obtained by irradiation of the monomer with high energy radiation such as X-rays,  $\gamma$ -rays,  $\alpha$ -particles, high energy electrons and protons (Allcock and Lampe, 1990). The advantages of this method are ease of grafting, high grafting efficiency and good properties of the resultant graft copolymers (Pimpan and Thothong, 2006). This method can produce free radicals in three different ways and these simple mechanisms are described below (Bhattacharya and Misra, 2004; Bucio et al., 2009).

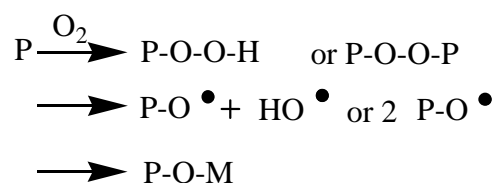
## (a) Pre-irradiation technique

The polymer backbone is first irradiated in vacuum or in the presence of an inert gas to form radicals.



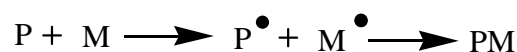
## (b) Peroxidation technique

The polymer backbone is irradiated first in the presence of air or oxygen to form hydroperoxides or diperoxides. Then, the polymer reacts with the monomer to initiate the graft copolymerization. The advantage of this method is that the intermediate peroxy products can be stored for long times before performing the grafting step.



## (c) Mutual irradiation technique

The polymer and the monomers are irradiated simultaneously, to produce free radicals and their subsequent addition.



Although it seems to have many advantages the disadvantages of the irradiation method are scission of the base polymer due to its direct irradiation, which can result in the formation of block copolymers, an expensive and hazardous method (Bhattacharya and Misra, 2004; Pimpan and Thothong, 2006).

The irradiation method can efficiently prepare starch grafted with various monomers. Polystyrene-g-starch copolymers were prepared by the technique of simultaneous irradiation by  $\gamma$ -rays from a  $^{60}\text{Co}$ -source (Fanta et al., 1975; Henderson

and Rudin, 1981; Kiatkamjornwong et al., 1999) in order to use as a part of styrene-based polymers (Kiatkamjornwong et al., 1999). Superabsorbent polymers, nanosuperabsorbent polymers and drug-delivery systems were prepared by using starch grafted with polyacrylic acid, polyacrylamide (Kiatkamjornwong et al., 2000; Fang et al., 2004; Fang et al., 2005), polyacrylonitrile (Lyer et al., 1990) and polymethyl acrylate (Geresh et al., 2002) through a gamma ray radiation method.

## **2.5 Suspension polymerization**

Polymerization of a monomer in a medium (i.e., water) overcomes many of the disadvantages of bulk and emulsion polymerization. The medium assists the heat transfer and acts as a diluent. The medium allows easier stirring, since the viscosity of the reaction mixture is decreased. Suspension polymerization (also referred to as bead or pearl polymerization) is carried out by suspending the monomer as droplets (50 – 500  $\mu\text{m}$  in diameter) in the medium. This is smaller than the monomer droplets obtained from emulsion polymerization. When the monomer droplets are small, it is easy to eliminate the solvent in the final step. Therefore, the products are very immaculate. The low viscosity of the reaction mixture and the high surface area of the dispersed droplets provide good heat transfer. Styrene, acrylic, methacrylic esters, vinyl chloride, vinyl acetate and tetrafluoroethylene are polymerized by the suspension method. Each monomer droplet in a suspension polymerization is considered to be a mini bulk polymerization system. The kinetics of polymerization within each droplet is the same as those for the corresponding bulk polymerization (Odian, 1991). Near the end of the polymerization, the particles harden and can then be recovered by filtration which is followed by a final washing step (Fried, 2003). These suspension polymerization reactions are sometimes (but not always) referred to as dispersion polymerization. The term microsuspension polymerization has also been used, especially when the monomer droplet sizes are 1  $\mu\text{m}$  or smaller (Odian, 1991).

## **2.6 Polystyrene (PS)**

Polystyrene is a vinyl polymer. Structurally, it is a long hydrocarbon chain, with a phenyl group attached to every other carbon atom. Polystyrene is prepared from the styrene monomer by free radical vinyl polymerization in bulk or suspension

with peroxides or trace oxygen as initiators (Fried, 2003). The styrene monomer is obtained from the reaction between benzene and ethylene (Figure 2.14) (Ulrich, 1993).

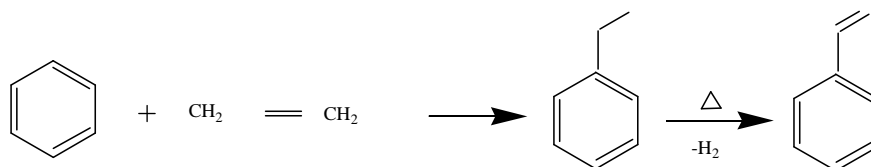


Figure 2.14 Manufacture of styrene monomer (Ulrich, 1993).

Polystyrene has a great chemical stability (towards acids, alkalis, etc.) and stability to water (Ulrich, 1993). However, polystyrene is especially susceptible to photooxidative degradation which results in brittleness and yellowing. Degradation is initiated by the phenyl group, which absorbs UV radiation from sunlight. This energy is transferred to other sites along the polymer chain, resulting in bond cleavage, radical formation and reaction with oxygen to form hydroperoxide and carbonyl groups (Fried, 2003).

Polystyrene has been used for many applications. Some common applications include containers, cups, dining utensils and toys. Expandable PS (EPS) is a closed-cell structure made from PS beads and a hydrocarbon propellant or blowing agent such as isopentane and butane. Impact modification of PS can be obtained through the incorporation of polybutadiene. For example, high-impact PS (HIPS) is produced by the emulsion polymerization of styrene in a polybutadiene or styrene-butadiene (SBR) latex. ABS was produced by blending latex emulsions of SAN and NBR (acrylonitrilebutadiene rubber) or by grafting styrene and acrylonitrile with polybutadiene in a form of latex (Ulrich, 1993; Fried, 2003).

## CHAPTER 3

### EXPERIMENTAL

#### 3.1 Materials

Cassava starch was kindly supplied by GSL General Starch Ltd., Thailand. The native cassava starch had standard specification as follows: maximum moisture content = 12.2%, maximum ash = 0.07%, fiber content = 0.1%, pH = 5.6, SO<sub>2</sub> content = 21.59 ppm, maximum viscosity = 630 Brabender units and sieve test = 99.61% after passing through 100 mesh. The starch was dried in an oven at 100°C for 48 h and kept in a desiccator before use. Styrene monomer was purchased from Fluka<sup>®</sup> and used after inhibitor was extracted with 5% sodium hydroxide aqueous solution and distilled water sequentially. The inhibitor-free styrene was dried with anhydrous calcium chloride and stored at 4 °C. Potassium persulfate (PPS), toluene and methanol were analytical or reagent grade and obtained from Fisher Chemical<sup>®</sup>.

#### 3.2 Experimental Procedure

##### 3.2.1 Preparation of cassava starch grafted with polystyrene (PS-g-starch copolymer)

###### 3.2.1.1 Graft copolymerization process

A mixture of dried starch and 100 ml of distilled water were stirred magnetically for 30 min under a N<sub>2</sub> atmosphere to make the homogeneous slurry at the reaction temperature. After adding PPS for 10 min, styrene monomer was added. The nitrogen atmosphere and agitation at 420 rpm of slurry were maintained throughout the experiment. After the reaction time was over, the PS-g-starch copolymer was precipitated by dropping into methanol. The precipitate was filtered and repeatedly washed with methanol. The precipitate was dried in an oven at 50 °C until a constant weight. To determine the optimum conditions for this graft copolymerization system, the reaction parameters, including the amount of PPS, cassava starch, styrene monomer, the reaction temperature and the reaction time were



varied. The amount of PPS used were 0.2, 0.4, 0.6, 0.8, 1.0 and 1.2 g, The amount of cassava starch used were 2.5, 5.0 and 7.5 g, The amount of styrene monomer used were 2.5, 5.0 and 7.5 g, the reaction times included 1, 2, 3, 4 and 5 h and the reaction temperature was varied between 30 and 60 °C.

### **3.2.1.2 Soxhlet extraction**

The homopolystyrene was removed by using the Soxhlet extraction process. The total dried product was weighed and then added into the thimble inserted in the Soxhlet extractor. Toluene was used as the solvent. The extraction was done at 120 °C for 10 h. The extracted solution was dropped into methanol which is a non-solvent of PS, if no precipitation was observed, complete extraction was confirmed. The PS-g-starch copolymer was dried in a vacuum oven at 60 °C until a constant weight and kept in the desiccator. The product was weighed to calculate the percentage of grafting, G (%) and the grafting efficiency, GE (%). The product prior to Soxhlet extraction was called the “non-extracted product”, and the product after extraction was called the “un-extractable product”.

A polymer blend of cassava starch and PS was prepared in order to attest the efficiency of the Soxhlet extraction process. The same extraction condition was applied to the polymer blend.

### **3.2.2 Preparation of PS by the suspension polymerization technique**

Styrene monomer (7.5 g), PPS (0.4 g) and distilled water (100 g) were mixed together and stirred at 420 rpm. The reaction time and temperature were 2 h and 50 °C, respectively. The mixture was precipitated in methanol. The precipitate was filtered and dried until a constant weight and kept in the desiccator.

### 3.2.3 Effects of reaction parameters

#### 3.2.3.1 The amount of cassava starch, styrene monomer and reaction temperature

The amount of cassava starch, styrene monomer and reaction temperature are shown in Table 3.1. The synthesis was carried out using a reaction time of 2 h and 0.2 g of PPS.

Table 3.1 The amount of starch, styrene monomer and reaction temperature

Starch (g)	Styrene monomer (g)	Temperature (°C)
2.5	7.5	30
2.5	7.5	40
2.5	7.5	50
2.5	7.5	60
5.0	5.0	30
5.0	5.0	40
5.0	5.0	50
5.0	5.0	60
7.5	2.5	30
7.5	2.5	40
7.5	2.5	50
7.5	2.5	60

#### 3.2.3.2 The PPS content

To investigate the effect of PPS, the PPS content was varied: 0.2, 0.4, 0.6, 0.8, 1.0 and 1.2 g. The synthesis was carried out using the reaction temperature of 50 °C, a reaction time of 2 h, 2.5 g of starch and 7.5 g of styrene monomer.

### 3.2.3.3 The reaction time

To determine an appropriate reaction time, the grafting reaction time was varied in the range of 1, 2, 3, 4 and 5 h. The synthesis was carried out using the reaction temperature at 50°C, 2.5 g of starch, 7.5 g of styrene monomer and 0.4 g of PPS.

### 3.2.4 Preparation of PS-g-starch copolymer /cassava starch blend

The blends were prepared by mixing the PS-g-starch copolymer (G (%) = 21.80%) and cassava starch ratios of 100:0, 90:10, 80:20, 70:30, 60:40, 50:50, 40:60, 30:70, 20:80, 10:90 and 0:100. The glycerol content was controlled at 25, 30, 35, 40 and 45 phr (parts per hundred of total weight of polymers) and the water content was controlled at 0, 5 and 10 phr (parts per hundred of total weight of polymers). Mixing was carried out in the mixer at room temperature for 10 min. The mixture was thermo-molded (12 cm × 10.5 cm × 0.4 mm) by using a compression molding machine, KT-7014 produced by Kao Tieh Ltd. (Taipei, Taiwan) at 160 °C for 10 min and a pressure of 100 kg/cm<sup>2</sup> was directly applied to the sample. The sheet sample was cooled to room temperature at about 65% RH and was stored under the same previous condition for 4 weeks then X-ray diffraction measurement were performed.

## 3.3 Characterization of PS-g-starch copolymer and PS-g-cassava starch copolymer/cassava starch blend

### 3.3.1 Determination of percentage of grafting (G (%))

The G (%) indicates the amount of the cassava starch granules grafted with PS and it can be determined based on equation (3.1) (Fang et al., 2005; Singh et al., 2006):

$$G(\%) = \frac{w_2 - w_1}{w_1} \times 100 \quad (3.1)$$

where  $w_1$  was the original weight of cassava starch and  $w_2$  was the weight of un-extractable products (after Soxhlet extraction).

### 3.3.2 Determination of grafting efficiency (GE (%))

The GE (%) described the capability of the monomer to graft onto the starch and it can be determined based on equation (3.2) (Singh et al., 2006; Fang et al., 2005):

$$Y(\%) = \frac{w_2 - w_1}{w_3} \times 100 \quad (3.2)$$

where  $w_1$  was the original weight of cassava starch,  $w_2$  was the weight of unextractable products (after Soxhlet extraction) and  $w_3$  was weight of the styrene monomer.

### 3.3.3 Fourier transform infrared analysis

The Fourier Transform Infrared Spectroscopy (FTIR) technique was performed by using BRUKER<sup>®</sup> EQUINOX 55 to characterize the chemical structure of the cassava starch, PS-g-starch copolymer, PS and polymer blend (cassava starch and PS). The dried powder samples were mixed with KBr and pressed into a disc form by hydraulic compression. The samples were scanned at a frequency range of 4000 - 400  $\text{cm}^{-1}$  with 128 consecutive scans in a 4  $\text{cm}^{-1}$  resolution.

### 3.3.4 Morphological analysis

A scanning electron microscope (JEOL<sup>®</sup> JSM-5800LV) was used to study the morphology of cassava starch, PS-g-starch copolymer and PS. The samples were first mounted on the brass stub with double sticky tape. Samples were then coated with a thin evaporated layer of gold in order to improve conductivity and prevent electron charging on the surface. The scanning electron microscopy was operated at 10 kV.

### 3.3.5 Thermogravimetric analysis

The thermal decomposition temperatures of cassava starch, PS-g-starch copolymer and PS were obtained using a PerkinElmer<sup>®</sup> TGA 7. Thermogravimetric analyzer (TGA) was operated at a heating rate of 10  $^{\circ}\text{C}/\text{min}$  from 50 to 950  $^{\circ}\text{C}$  under

a nitrogen atmosphere. Prior to the analysis, the samples were dried in a vacuum oven at 60 °C for 24 h.

### **3.3.6 Differential scanning calorimetry analysis**

The differential scanning calorimetry (PerkinElmer<sup>®</sup> DSC 7) was used to study the thermal properties of cassava starch, PS-g-starch copolymer and PS. The samples were initially heated using a heating rate of 5 °C/min from 25 to 180 °C in a nitrogen atmosphere and then cooling to 25 °C at a rate of 100 °C/min in order to ensure that there was no influence of thermal history and moisture. The samples were subsequently rescanned from 25 to 500 °C at a heating rate of 5 °C/min under a nitrogen atmosphere. Prior to the analysis, the samples were dried in a vacuum oven at 60 °C for 24 h.

### **3.3.7 X-ray diffraction analysis**

Wide angle X-ray diffraction (XRD) studies were carried out using a Phillips diffractometer (Model PW 1830) with copper as a target material. The voltage, the current and the wavelength of the X-ray source were 40 kV, 30 mA and 0.154060–0.154438 nm, respectively. The scanning regions of the diffraction angle  $2\theta$  were 5°-80° which covered all the significant diffraction peaks of starch crystallites.

The degree of crystallinity ( $X_c$ ) of the materials can be determined by analyzing the intensity of X-ray scattering which is most conveniently measured by means of a diffractometer and an example of a diffractometer trace is shown in Figure 3.1. The degree of crystallinity calculated from the ratio of the crystallized area to the total area (the crystallized area + the amorphous area) was quantitatively estimated using the equation (3.3) (O dian, 1991; Kumar and Gupta, 1998).

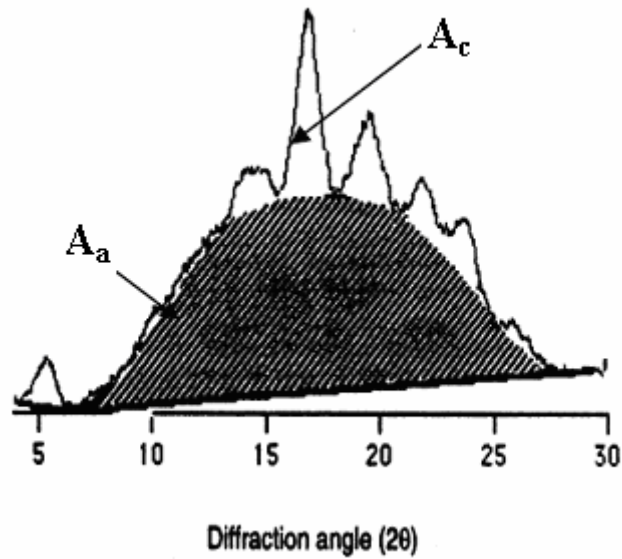


Figure 3.1 Crystalline and non-crystalline regions (Shujun et al., 2005).

$$X_c = A_c / (A_c + A_a) \quad (3.3)$$

where  $X_c$  is the degree of crystallinity,  $A_c$  is the crystallized area on the X-ray diffractogram and  $A_a$  is the amorphous area on the X-ray diffractogram.

In this thesis, the ratios of the crystallized area to the total area were obtained by cutting the relevant areas and weighing them (Campbell et al., 1989). The same measurements were made at room temperature three times by using the same paper density mass.

### 3.3.8 Shrinkage determinations

Shrinkage determinations were conducted after the samples were stored at room temperature (65%RH) for 4 weeks. Shrinkage can be determined based on equation (3.4) (Averous and Fringant, 2001; Averous et al., 2001):

$$\text{Shrinkage (\%)} = (1 - (L/L_0)) \times 100 \quad (3.4)$$

where L is the length of the dumbbell specimen after storage for 4 weeks and  $L_0$  is the initial length of the dumbbell specimen.

## CHAPTER 4

### RESULTS AND DISCUSSION

#### 4.1 Suspension polymerization of polystyrene

After the reaction time was over, the water phase changed from transparent to opaque and very fine particles of PS were present in the aqueous phase. Because of the stirring and the hydrophobic characteristics of the styrene monomer, monomer droplets were formed. Therefore, polymerization of PS had occurred in these droplets. The SEM micrographs in Figure 4.1 (a) exhibited the aggregation of the spherical microbeads of PS.

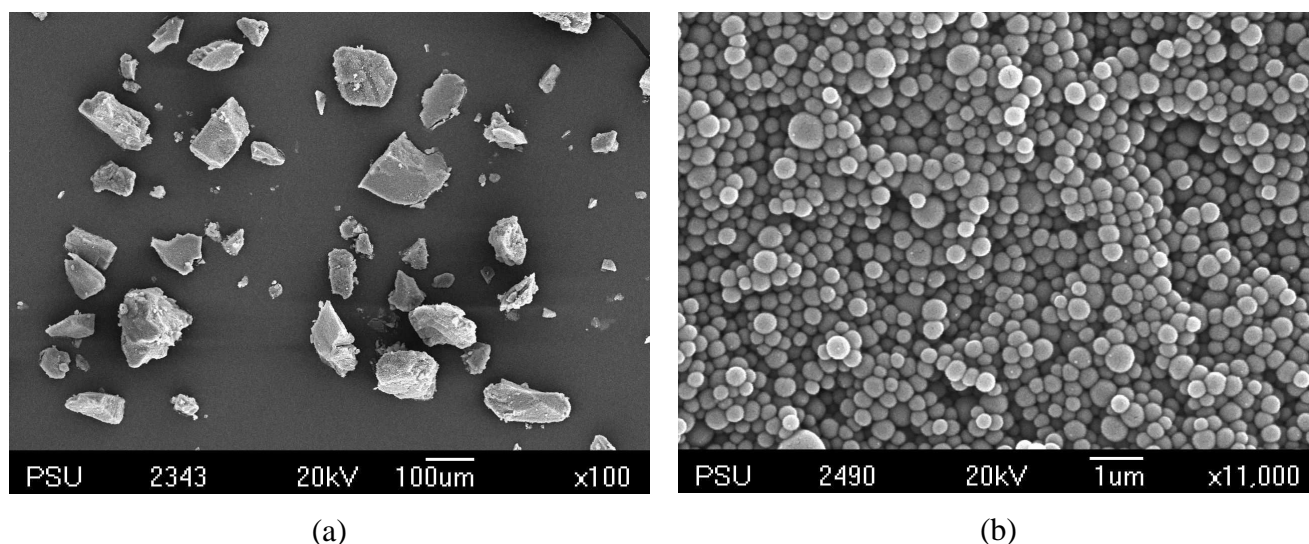


Figure 4.1 SEM micrographs of PS spherical microbeads.

The formation of the agglomerates can be explained by the fact that no surfactant was added to the polymerization system. Figure 4.1 (b) shows the spherical microbeads of PS which were smaller than 200 μm. The glass transition temperature ( $T_g$ ) of the PS spherical microbeads was 107.5 °C (Figure 4.2), a similar  $T_g$  of PS was found by Janarthanan and coworkers (2003). Therefore, it can be concluded that the suspension polymerization method was successful in preparing PS using potassium persulfate (PPS) as an initiator and water as the medium. As the results, indicate the



graft copolymerization between PS and cassava starch could occur using the present conditions.

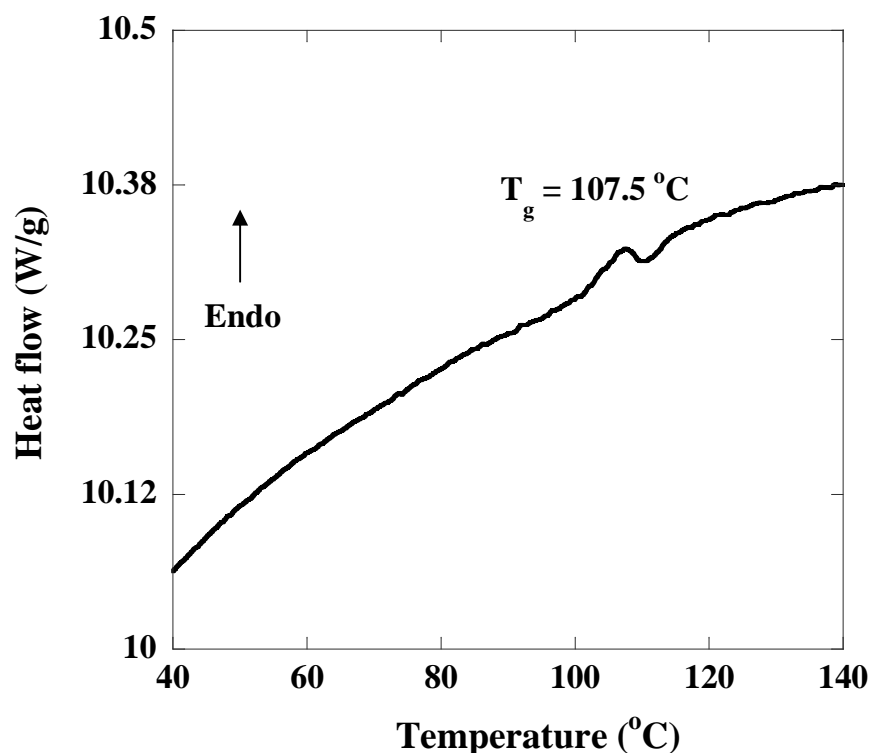


Figure 4.2 DSC thermogram second-heating of PS spherical microbeads.

## 4.2 Effects of reaction parameters

### 4.2.1 Cassava starch:styrene monomer ratios and reaction temperature

The effect of cassava starch:styrene monomer ratios and reaction temperature was studied and the grafting efficiency in terms of the percentage of grafting,  $G$  (%) and grafting efficiency,  $GE$  (%) were compared. The effect of cassava starch:styrene monomer ratios was investigated in three cases composed of 2.5:7.5, 5.0:5.0 and 7.5:2.5 and the reaction temperature was varied from 30°C to 60°C. The conditions of the reaction were 100 g of water, 0.2 g of PPS and the reaction time of 2 h was fixed for each set. The  $G$  (%) and  $GE$  (%) were calculated based on equation 3.1 and 3.2, respectively (see Chapter 3). The  $G$  (%) and  $GE$  (%) were not the same number because they are obtained from different equations and meanings.  $G$  (%) refers to the percentage of PS in the graft copolymer and  $GE$  (%) was used to describe

the capability of the monomer to graft onto the starch. Figure 4.3 presents the G (%) and GE (%) which were obtained from different cassava starch:styrene monomer ratios and reaction temperatures. The data showed that at the lowest reaction temperature (30 °C) the G (%) increased by increasing the amount of cassava starch but the G (%) was quite low. At the higher reaction temperatures (40 °C and 50 °C), the G (%) increased with decreasing amounts of cassava starch and the G (%) decreased when the amount of cassava starch increased. At the highest reaction temperature (60 °C) the G (%) significantly decreased. These results relate to the two parameters that were the rate of decomposition of initiator and the swelling of starch granules. Both parameters depended on the reaction temperature (Oadian, 1991; Copeland et al., 2009). The swelling of starch granules occurred when starch granules were heated in the presence of sufficient moisture. The starch granules absorbed water and swelled. Amylose molecules began to be released from the starch granules and the viscosity of the system increased (Whistler et al., 1984; Steinbuchel and Rhee, 2005; Copeland et al., 2009). This process was referred to as gelatinization. Cassava starch typically became gelatinization at 62-73 °C and this was the proposed gelatinization temperature (Eliasson, 2000) (see Chapter 2).

Although, the swelling of starch granules did not occur at 30°C because 30°C was lower than the gelatinization temperature but the G (%) was quite low because the rate of decomposition of initiator decreased when the reaction temperature was too low. Moreover, the G (%) decreased with increasing amounts of styrene monomer because the increasing monomer concentration accelerated the homopolymerization reaction rather than through grafting. The rate of decomposition of the initiator at the higher reaction temperatures (40 °C and 50 °C) was higher than that at 30 °C causing a significant increase in the G (%) when the amount of cassava starch was lower than the amount of the styrene monomer. The GE (%) tended to decrease when the amount of styrene monomer increased. This was because a higher amount of styrene monomer resulted in a higher production of both the PS-g-starch copolymer and the homopolystyrene.

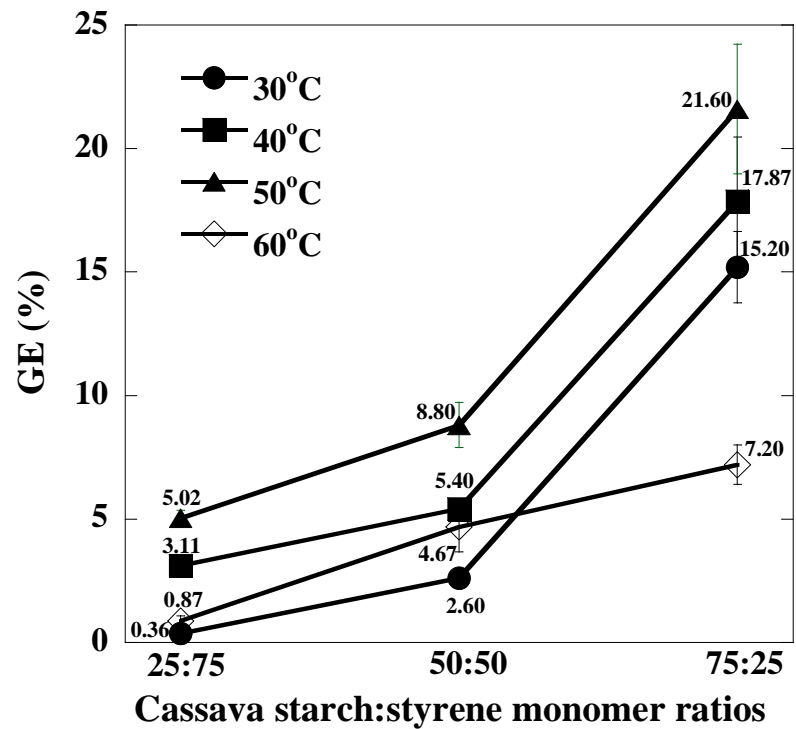
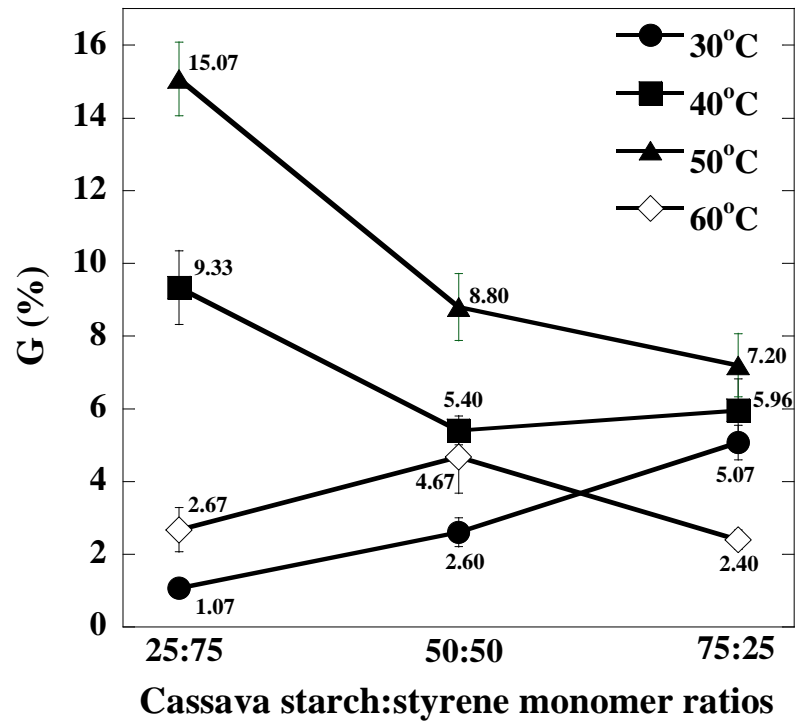


Figure 4.3 Effect of cassava starch:styrene monomer ratios on the G (%) and GE (%) at different reaction temperatures; (a) 30 °C, (b) 40 °C, (c) 50 °C and (d) 60 °C.

The G (%) decreased at the higher amount of cassava starch because when the reaction temperature was high, it had nearly reached the gelatinization temperature; therefore, starch granules began to swell. As a result, the viscosities of the systems increased so it was more difficult for all radical species to react with each other, thus reducing the potential for graft copolymerization (Athawale and Lele, 2000; Fang, et al., 2005; Pimpan and Thothong, 2006). Although, the rate of decomposition of PPS increased and the amount of cassava starch was low both the G (%) and GE (%) significantly decreased when the reaction temperature was 60 °C because the starch granules became extremely swollen. It was due to 60 °C being very close to the gelatinization temperature and the number of radicals available for grafting decreased with the increase of reaction temperature, so this combination with reduced monomer radicals resulted in a low graft yield.

It can be concluded that the maximum G (%) was 15.07 %, obtained when the reaction conditions were the reaction temperature of 50 °C and the ratio of cassava starch:styrene monomer was 25:75.

#### **4.2.2 The amount of PPS**

The PPS content was one of the factors to determine the extent of graft copolymerization. The amount of PPS was studied in the range of 0.2-1.2 g at a fixed amount of cassava starch (2.5 g), styrene monomer (7.5 g) and reaction time (2 h) at 50 °C in 100 g of water. The effect of the amount of PPS on the G (%) and GE (%) is presented in Figure 4.4. The G (%) and GE (%) increased after increasing the amount of PPS from 0.2 g to 0.4 g, as the G (%) increased from 15.07% to 31.47% and GE (%) increased from 5.02% to 10.49%, respectively. These phenomena could be explained by the fact that the increased amount of initiator produces greater numbers of oligomer chains due to the increased number of active radicals. (Fang et al., 2005; Pimpan and Thothong, 2006). As a result, the probability of graft initiation increased. When the amount of PPS was higher than 0.4 g, both the G (%) and GE (%) significantly decreased. It may be due to the opportunity for the styrene monomer to form PS oligomers and homopolystyrene increased (Silong et al., 2000; Qudsieh et al., 2004; Tiwari et al., 2006). However, both PS oligomers and PS could dissolve in toluene; therefore, they were removed by using the Soxhlet extraction process.

Moreover, when the amount of PPS increased the recombination of starch free radicals was more thermodynamically favorable than the formation the PS-g-cassava starch copolymer. Thus, it can be concluded that the optimum G (%), 31.47% and GE (%), 10.49% were obtained when the amount of the PPS was 0.4 g.

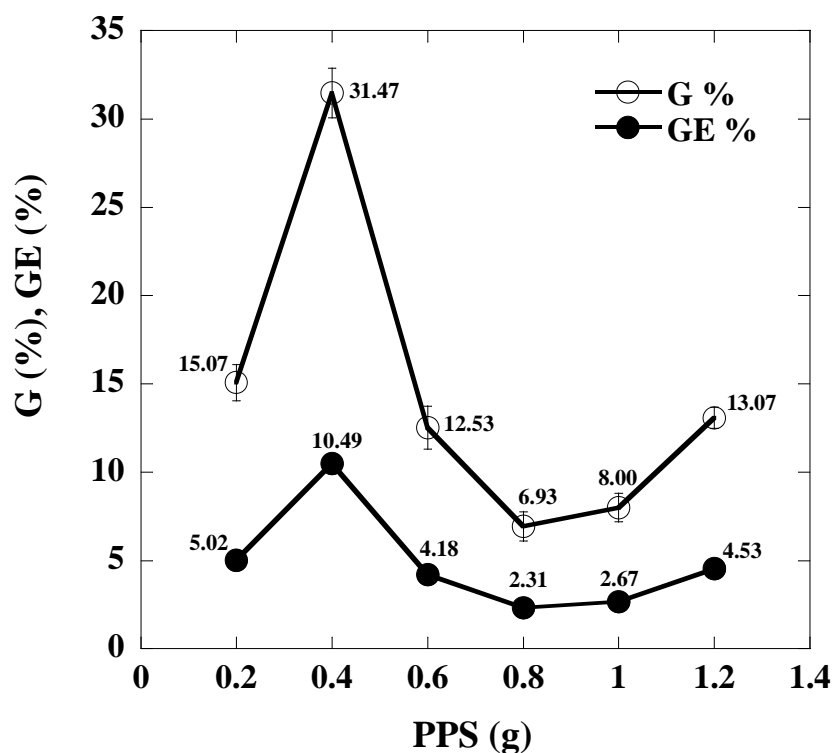


Figure 4.4 Effect of PPS content on the G (%) and GE (%) of samples polymerized at 50 °C for 2 h with 100 g of water, 2.5 g of cassava starch and 7.5 g of styrene monomer.

#### 4.2.3 The reaction time

The reaction time was the important parameter affecting the G (%) and GE (%). The reaction time was investigated in the range of 1-5 h at a fixed amount of cassava starch (2.5 g), styrene monomer (7.5 g) and PPS (0.4 g) at 50 °C in 100 g of water. Figure 4.5 shows the effect of the reaction time on the G (%) and GE (%). The G (%) and GE (%) presented a maximum at 2 h and subsequently decreased. The G (%) and GE (%) increased with increasing reaction time up to 2 h, as the G (%) increased from 21.07% to 31.47% and GE (%) increased from 7.02% to 10.49%,

respectively. A decrease of the G (%) and GE (%) after the maximum reaction time (2 h) was observed.

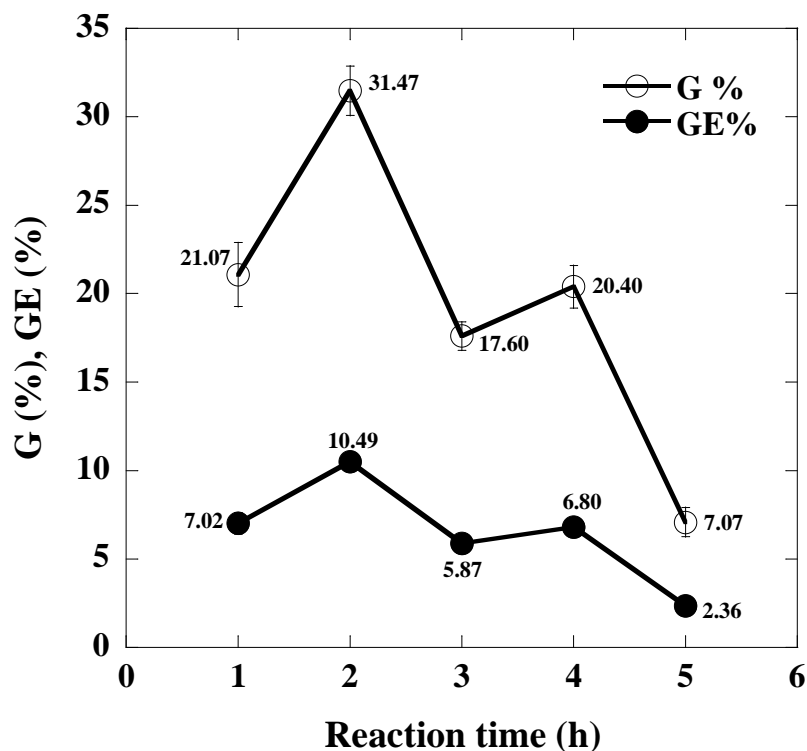


Figure 4.5 Effect of reaction time on G (%) and GE (%) of samples polymerized at 50°C with 100 g of water, 2.5 g of cassava starch, 7.5 g of styrene monomer and 0.4 g of PPS.

The G (%) and GE (%) exhibited a limit value because the graft copolymerization reaction occurred at the surface of the starch granules (Figures 4.6, 4.9, 4.10 and 4.11). The surface of the starch granules was covered with PS spherical microbeads completely at 2 h. Therefore, the optimum reaction time was 2 h. The grafting reaction did not complete at shorter reaction time (1 h). When the reaction time was too long (over 2 h), the G (%) and GE (%) decreased from 31.47% to 7.07% and from 10.49% to 2.36%, respectively. It may be due to degrafting after a certain time (Patra and Singh, 1994; Sangram Singh et al., 2004). The latter phenomenon occurred more easily than graft copolymerization reaction when the reaction time was increased from 2 h to 5 h.

Figure 4.6 shows the SEM micrographs of the PS-g-cassava starch copolymer before Soxhlet extraction at different reaction time with  $G (\%) = 9.57\%$ . Those samples were obtained from different reaction times including 15 min, 30 min, 1 h and 2 h. Figure 4.6 (a) shows the smooth surfaces of starch granules that were obtained from the reaction solution at the reaction time of 15 min. They looked similar to the starch granules of pure cassava starch (Figure 4.8) (see part 4.3.2), and indicate that the graft copolymerization reaction did not occur. The surfaces of starch granules were covered with the very fine PS spherical beads at the reaction time of 30 min (Figure 4.6 (b)). It shows that the PS spherical microbeads continuously increased as the reaction time increased (Figures 4.6 (c) and (d)). Many of the larger PS spherical microbeads covered the starch granules and there were some connections between starch granules that were most clearly seen at the reaction time of 2 h (Figure 4.6 (e) and (f)). From these results, it can be concluded that the graft copolymerization reaction occurred at the surface of the starch granules and the reaction time of 2 h was suitable for this graft copolymerization.

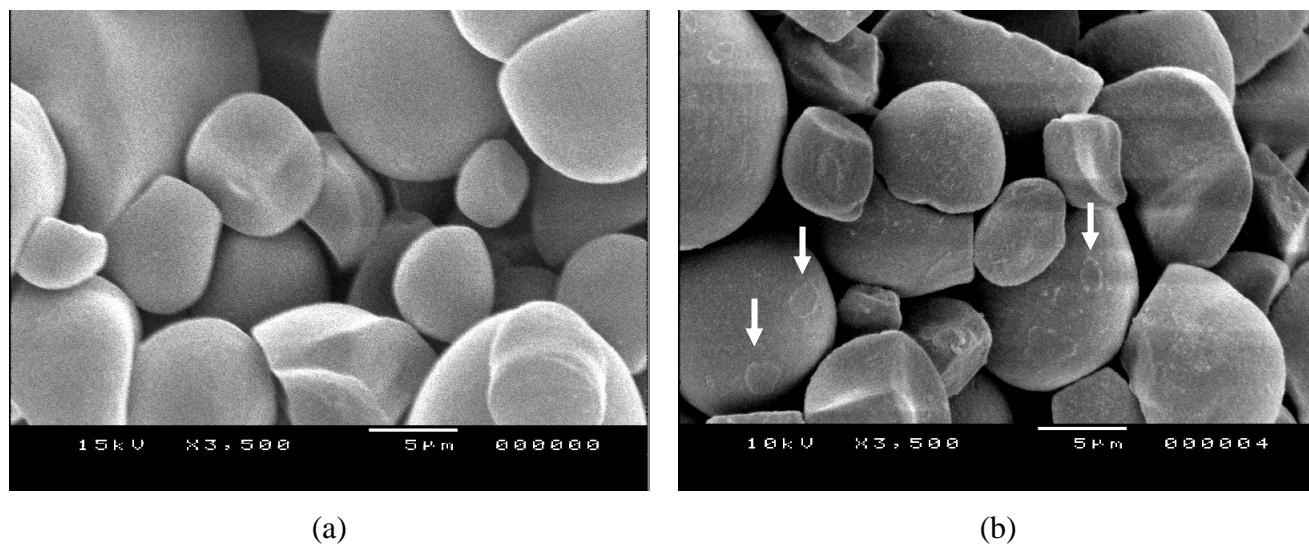
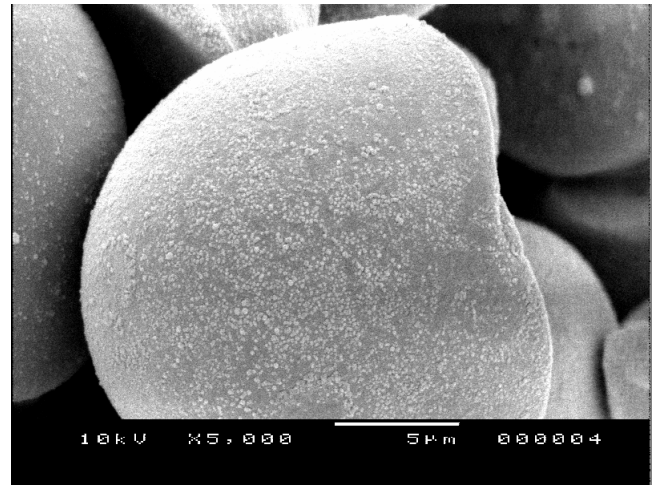


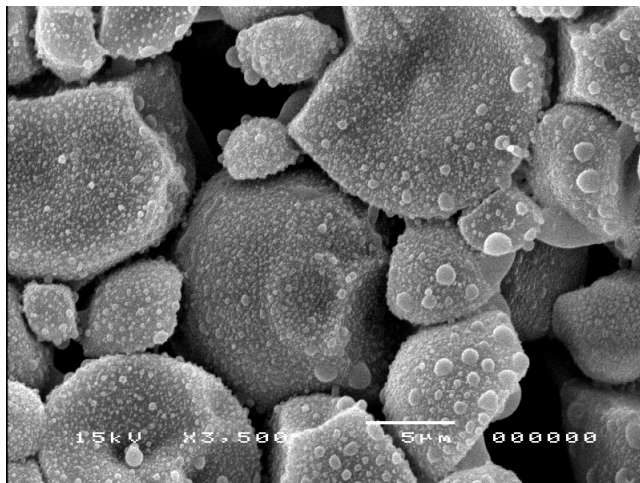
Figure 4.6 SEM micrographs of the PS-g-cassava starch copolymer before Soxhlet extraction at different reaction time ( $G (\%) = 9.57\%$ ); (a) 15 min, (b) 30 min, 1 h ((c) and (d)) and 2 h ((e) and (f)).



(c)



(d)



(e)



(f)

Figure 4.6 (cont.).

#### 4.2.4 Mechanisms of grafting between polystyrene and cassava starch

Figure 4.7 presents the most probable mechanisms for the graft copolymerization of styrene monomer onto the cassava starch granules by using PPS as an initiator. When an aqueous solution of persulfate is heated, it decomposes to yield a sulfate radical along with other free radical species. The grafting of PS onto the cassava starch granules could occur either via hydrogen abstraction or the homopolymerization of PS via free radical addition initiated by these radicals. Termination of the graft copolymerization is through a combination of two radicals.



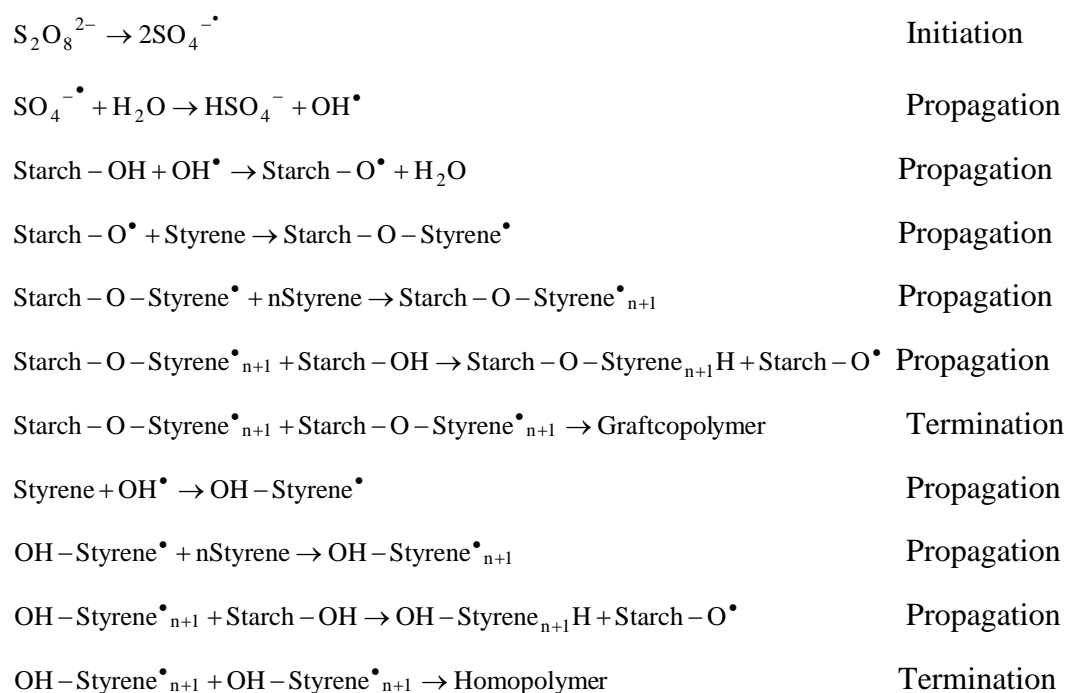


Figure 4.7 Mechanisms of grafting between polystyrene and cassava starch.

According to the mechanisms in Figure 4.7, the products obtained from the graft copolymerization were mostly a mixture of PS-g-starch copolymer and homopolystyrene, and this was confirmed by further characterization.

### 4.3 Characterization of the graft copolymer

#### 4.3.1 Fourier transform infrared analysis

Fourier transform infrared spectroscopy was used to investigate the chemical structure of cassava starch, PS and PS-g-cassava starch copolymer. FTIR assignment of starch and PS had been reported by many research groups (Athawale et al., 2000; Kiatkamjornwong et al., 2000; Janarthanan et al., 2003; Qudsieh et al., 2004; Fang et al., 2005; Meng et al., 2005; Pimpan and Thothong, 2006; Liao and Wu, 2009; Zaragoza-Contreras et al., 2009). The characteristic peaks of cassava starch and PS are described in Table 4.1. Figure 4.8 shows the FTIR spectra of cassava starch, PS and the PS-g-cassava starch copolymer.

Table 4.1 FTIR assignment of cassava starch and polystyrene

Wavenumber (cm <sup>-1</sup> )	Assignment
Cassava starch	
3600-3000	O-H stretching
2933 and 2881	C-H stretching of CH <sub>2</sub>
1190-950	C-O stretching
Polystyrene	
3100, 3000, 760 and 700	C-H stretching of aromatic ring
2920 and 2850	C-H stretching of CH <sub>2</sub>
1700-2000	overtones of the phenyl ring
1601, 1490 and 1450	C=C stretching of aromatic ring

However, the assignment of the peak of cassava starch at 1640-1650cm<sup>-1</sup> was not clear but was debatable as it had been reported in many articles. Ezekiel and coworkers (2007) commented on the bending mode of water at 1800-1600 cm<sup>-1</sup>, while the bending mode of O-H in starch was assigned at 1643 cm<sup>-1</sup> (Meng et al., 2005) and at 1650 cm<sup>-1</sup> (Athawale and Lele, 2000). The peak of the first overtone of OH bending appeared at 1653 cm<sup>-1</sup> (Sing et al., 2005). Mano and coworkers (2003) mentioned the  $\delta$ (OH) bend of absorbed water at 1640 cm<sup>-1</sup>. Furthermore, the wavenumber at 1650 cm<sup>-1</sup> was presented as a peak of the COC stretching (Lee et al., 2004). Nevertheless, this peak was not the main characteristic of starch. A little peak at 3444 cm<sup>-1</sup> that appeared in the PS spectrum may be due to the moisture content in the PS.

The FTIR spectra of a PS-g-cassava starch copolymer before and after Soxhlet extraction with a G (%) = 22.80% is presented in Figure 4.8 (c) and (d), respectively. The FTIR spectrum of the PS-g-cassava starch copolymer before Soxhlet extraction displayed the characteristic peaks of both cassava starch and PS (Figure 4.8 (c)) but all characteristics of the PS were the main peaks in this spectrum because this sample is composed of both grafted PS and homopolystyrene. After Soxhlet extraction, the characteristic peaks were similar to the characteristic peaks of both cassava starch and PS but the characteristic peaks of PS exhibited smaller intensities. This confirmed that homopolystyrene had been removed and only grafted

PS still appended on the starch backbone. From this result, it can be concluded that the PS-g-cassava starch copolymer had been obtained.

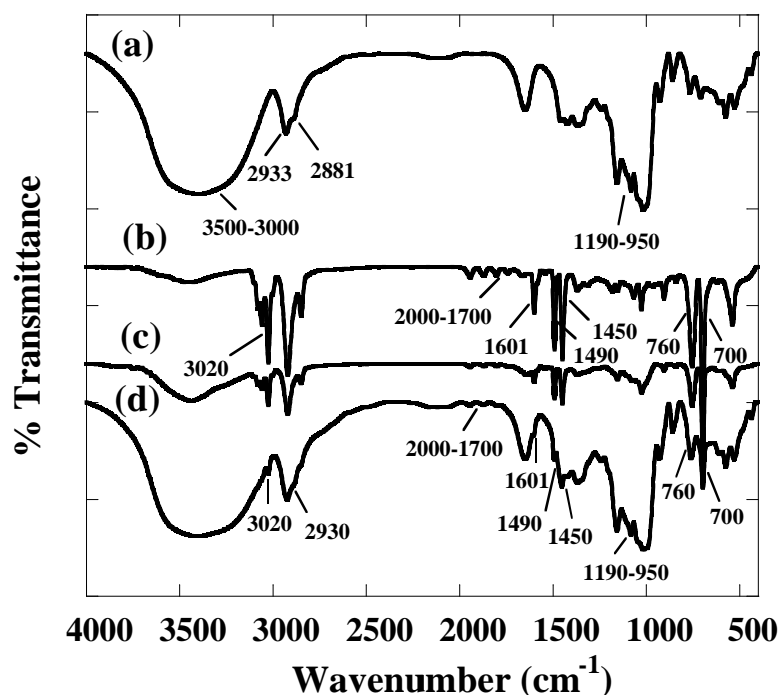


Figure 4.8 FTIR spectrum of cassava starch (a), PS (b), PS-g-cassava starch copolymer before Soxhlet extraction (c) and PS-g-cassava starch copolymer after Soxhlet extraction with  $G$  (%) = 22.80% (d).

#### 4.3.2 Morphological analysis

The surface appearance of cassava starch, PS and PS-g-cassava starch copolymers was observed by using SEM. The SEM micrographs of the spherical microbeads of PS are presented in Figure 4.1. Figure 4.9 had the SEM micrograph of pure cassava starch powder and clearly showed very smooth and compact surfaces. The granules of cassava starch varied in shape and size as some were round, others egg-shaped, cap-shaped or truncated “kettle drum” and the size was in the range of 4-35  $\mu\text{m}$ . A similar morphology has been detected by other authors (Whistler et al., 1984; Eliasson, 2000; Kiatkamjornwong et al., 2006; Wang et al., 2009).

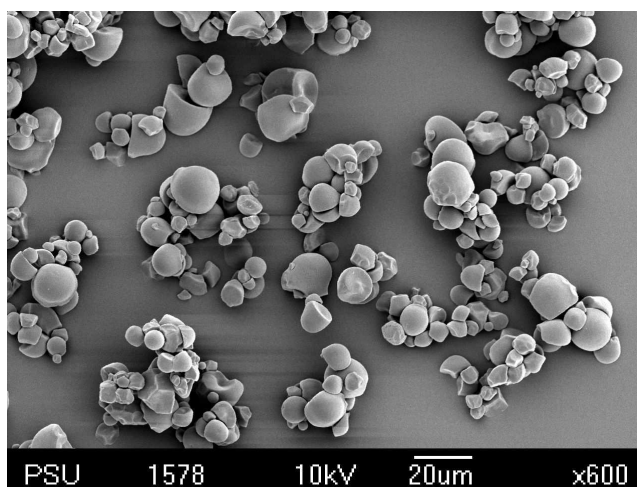
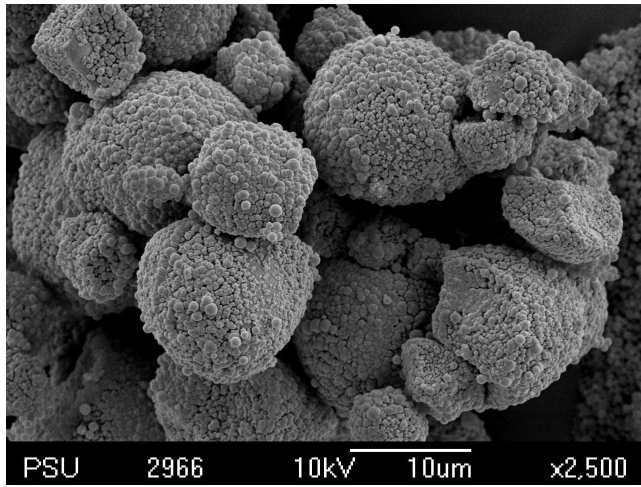


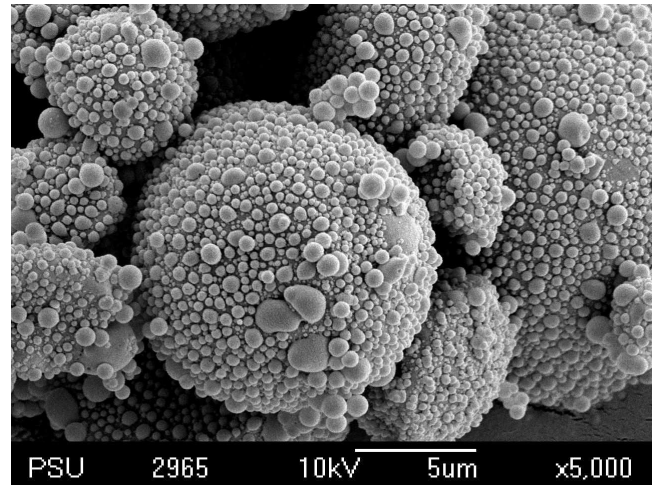
Figure 4.9 SEM micrograph of cassava starch.

SEM micrographs of the PS-g-cassava starch copolymers with a G (%) = 22.80% at the reaction time of 2 h before Soxhlet extraction are shown in Figure 4.10. After the graft copolymerization reaction, the surfaces of starch granules were covered with spherical beads of PS. The PS spherical microbeads adhered to both the surfaces of the starch granules and onto themselves. The SEM micrographs supported the hypothesis that the graft copolymerization reaction occurred at the surfaces of the starch granules. This can be confirmed from Figure 4.10 (d) that shows the fibrils of PS spherical microbeads embedded onto the surfaces of starch granules.

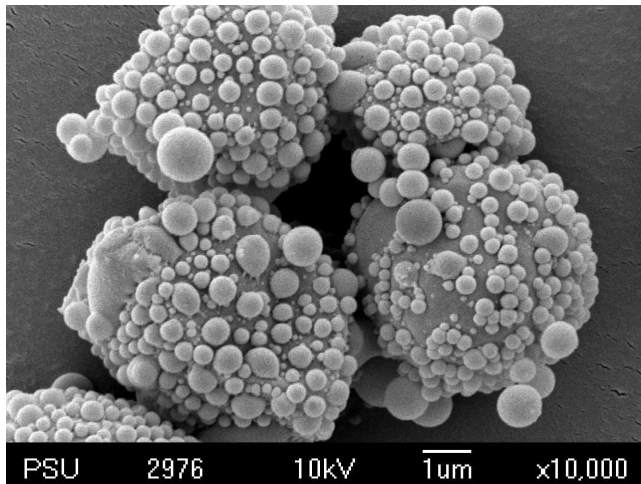
Figure 4.11 shows the PS-g-cassava starch copolymer after Soxhlet extraction. The PS spherical microbeads had disappeared but show that irregular crater-like shapes and the PS network had formed abundant pores linked between the starch granules. The holes on the PS network were formed from the PS spherical microbeads that had been dissolved by toluene during the Soxhlet extraction. From the SEM micrographs of the PS-g-cassava starch copolymer both before and after Soxhlet extraction (Figures 4.10 and 4.11), the starch granules still presented under the polymerization temperature of 50 °C, indicating that the gelatinized starch did not occur because the graft copolymerization reaction was carried out at lower temperature than the gelatinization temperature of cassava starch which was 62-73 °C (Eliasson, 2000).



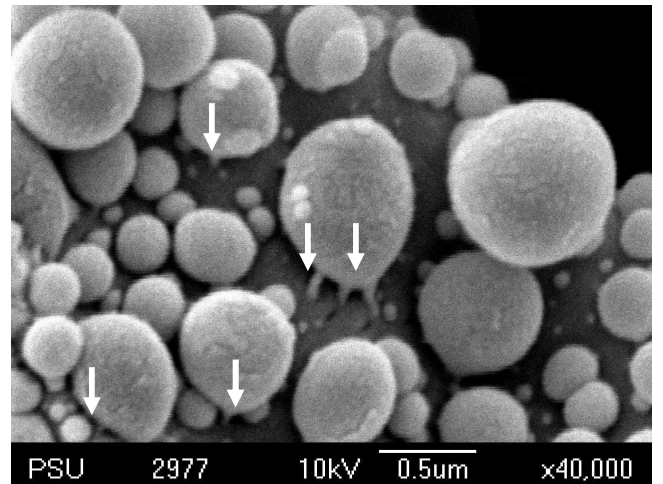
(a)



(b)



(c)



(d)

Figure 4.10 SEM micrographs of the PS-g-cassava starch copolymer with G (%) = 22.80% at the reaction time for 2 h before Soxhlet extraction.

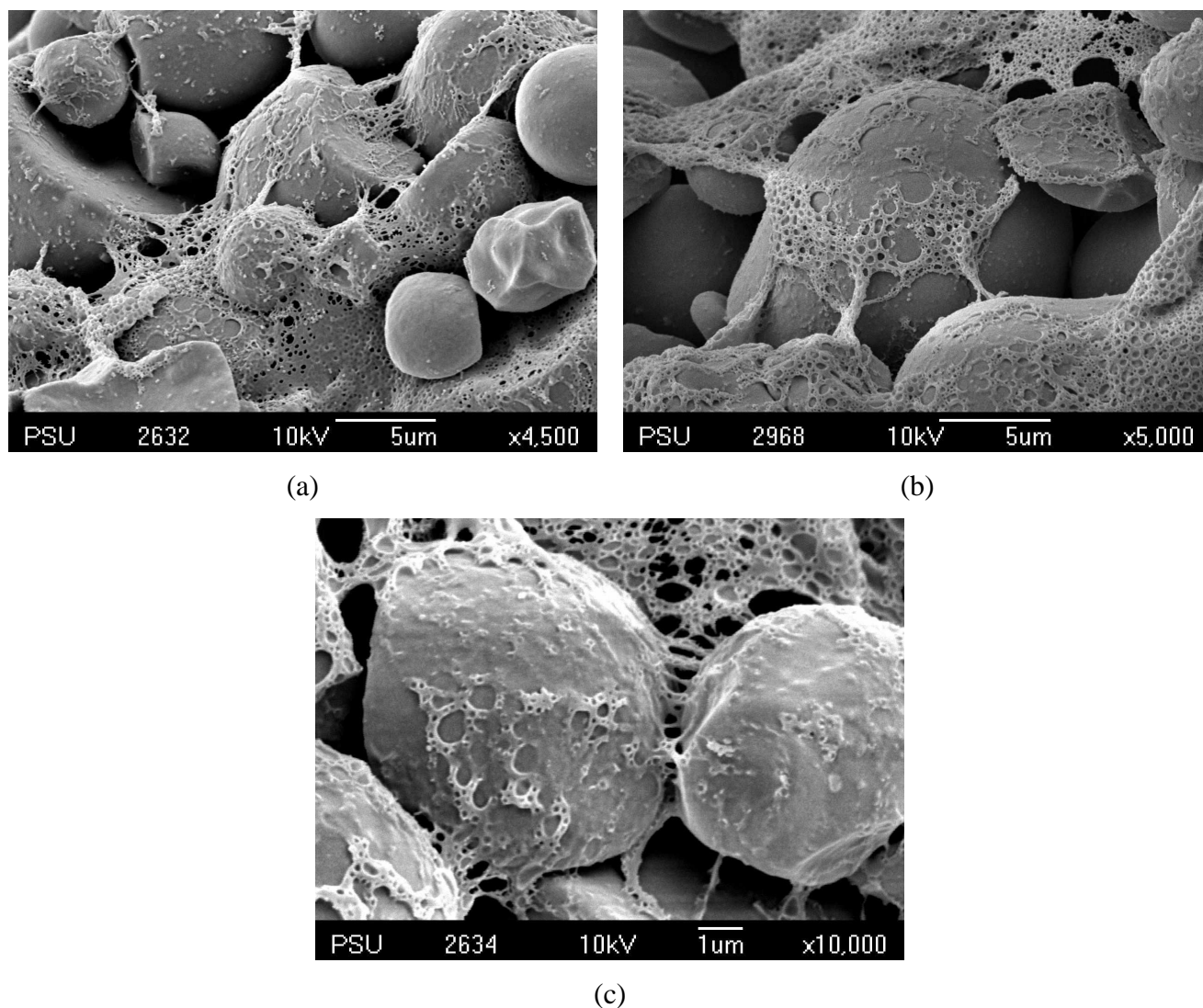


Figure 4.11 SEM micrographs of the PS-g-cassava starch copolymer with  $G (\%) = 22.80\%$  at the reaction time for 2 h after Soxhlet extraction.

SEM micrographs of the PS-g-cassava starch copolymer after Soxhlet extraction with a  $G (\%) = 14.00\%$  and  $32.80\%$  are shown in Figure 4.12. The morphology of the graft copolymer correlated to the value of the  $G (\%)$ . The PS network showed that abundant pores were still presented on the PS-g-cassava starch copolymer at the low  $G (\%)$  value (Figure 4.12 (a) and (b)). The highest  $G (\%)$  showed a denser graft copolymer (Figure 4.12 (c) and (d)).

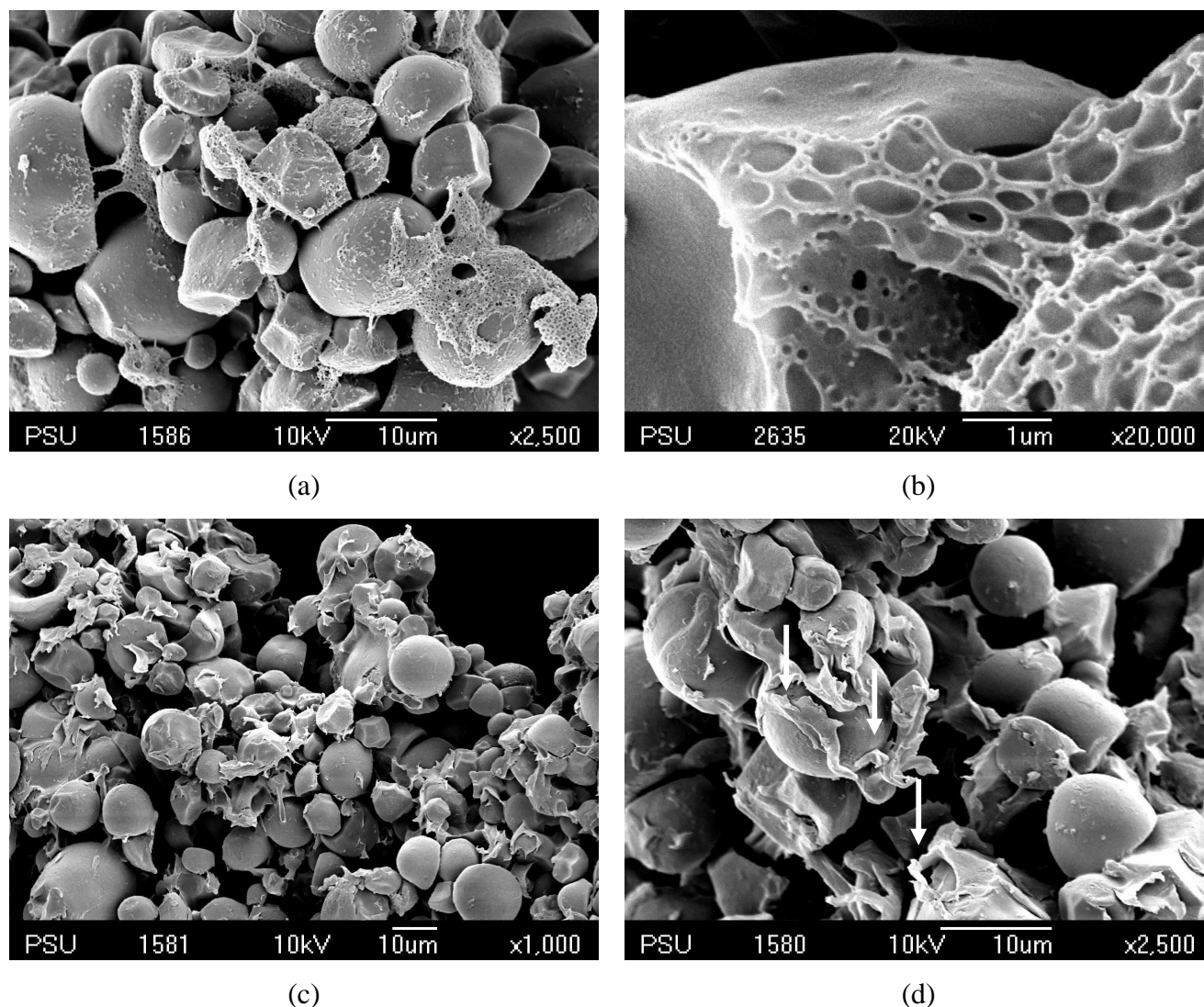


Figure 4.12 SEM micrographs of the PS-g-cassava starch copolymer (after Soxhlet extraction); G (%) = 14.00% ((a) and (b)) and G (%) = 32.80% ((c) and (d)).

### 4.3.3 Thermogravimetric analysis

TGA is a simple and accurate method to investigate the decomposition pattern and thermal stability of the polymers. Figures 4.13 – 4.16 displayed the TGA and derivative thermogravimetry (DTG) thermograms of cassava starch, PS and PS-g-cassava starch copolymer before and after Soxhlet extraction from different G (%). The TGA and DTG thermograms of cassava starch (Figure 4.13) showed the first weight loss, at around 100 °C. This was merely due to evaporation of absorbed moisture (Janarthanan et al., 2003; Kiatkamjornwong et al., 2006; Yin et al., 2008, Yu

et al., 2008). A significant weight loss that occurred in the second step in the temperature range of 275 – 360 °C could be attributed to the decomposition of the starch (Silong et al., 2000; Sacak and Celik, 2002; Janarthanan et al., 2003; Kiatkamjornwong et al., 2006). After thermal degradation, cassava starch provided 20% of ash.

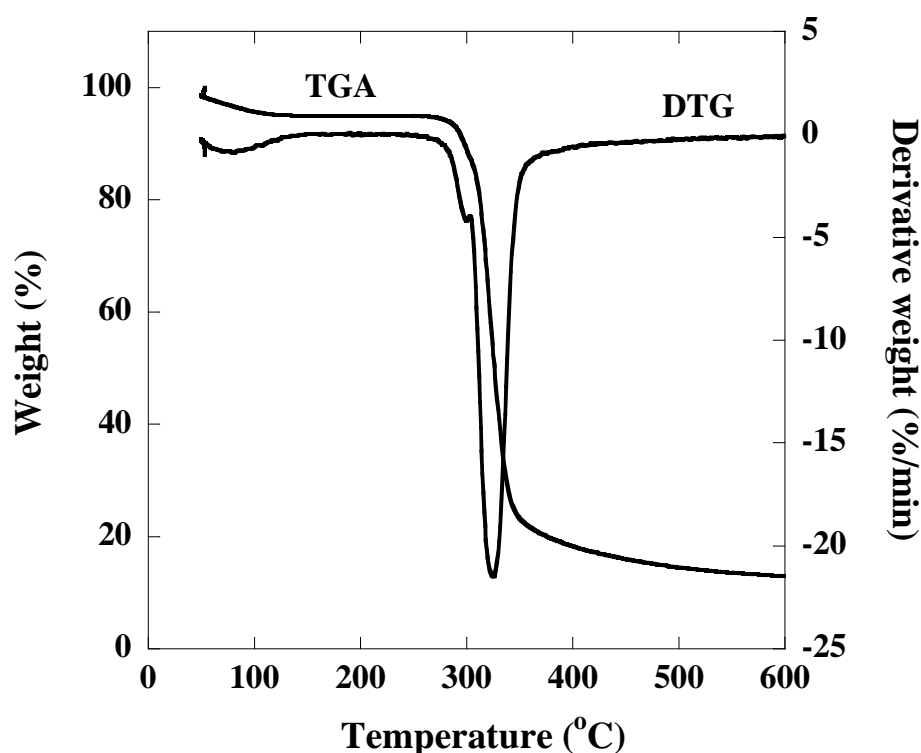


Figure 4.13 TGA and DTG thermograms of cassava starch.

Figure 4.14 presents the TGA and DTG thermograms of PS which show a weight loss from 360 – 465 °C. This was due to the decomposition of PS (Janarthanan et al., 2003; Kiatkamjornwong et al., 2006). Furthermore, PS showed very little ash ( $\approx 0\%$ ) after thermal degradation.



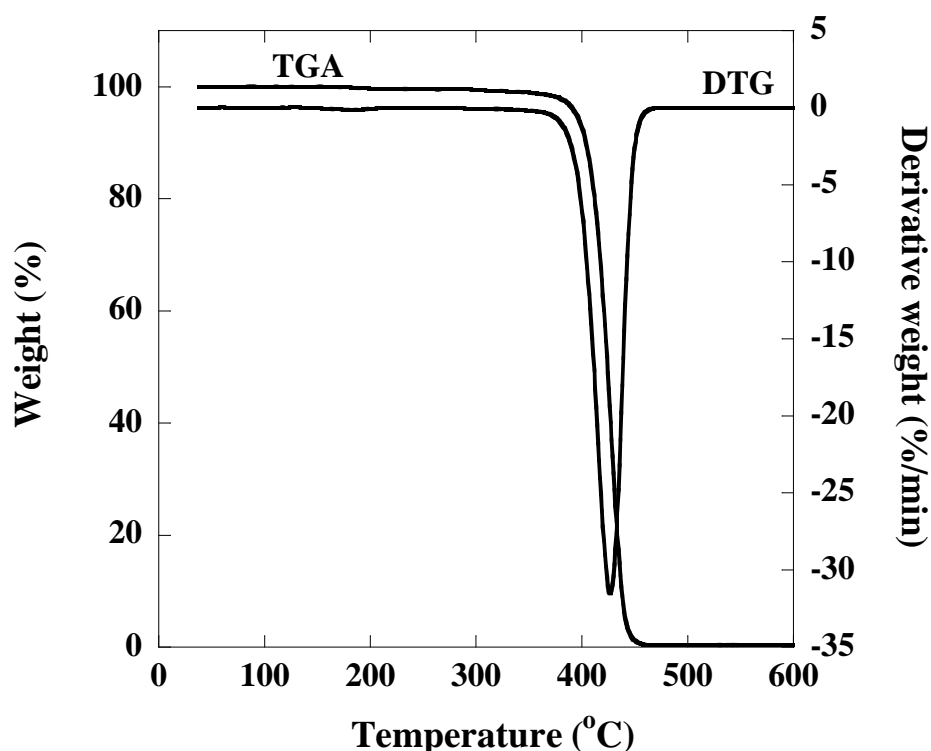


Figure 4.14 TGA and DTG thermograms of PS.

Figure 4.15 presents the TGA and DTG thermograms of PS-g-cassava starch copolymer before (a) and after Soxhlet extraction (b) with a  $G (\%) = 22.80\%$ . It can be seen that there were three steps of weight loss in both samples. First, the weight loss from 50 °C to 110 °C, that was assigned to water evaporation. The second step involved the decomposition of starch in the graft copolymer at the decomposition temperature of 280 – 340 °C. Finally, the weight loss in the range from 370 – 450 °C, that was due to the decomposition of PS in the graft copolymer. However, the quantity of percentage of the weight loss (Wight (%)) of starch and PS in the thermograms of both samples was different (Figure 4.15 (a) and (b)).

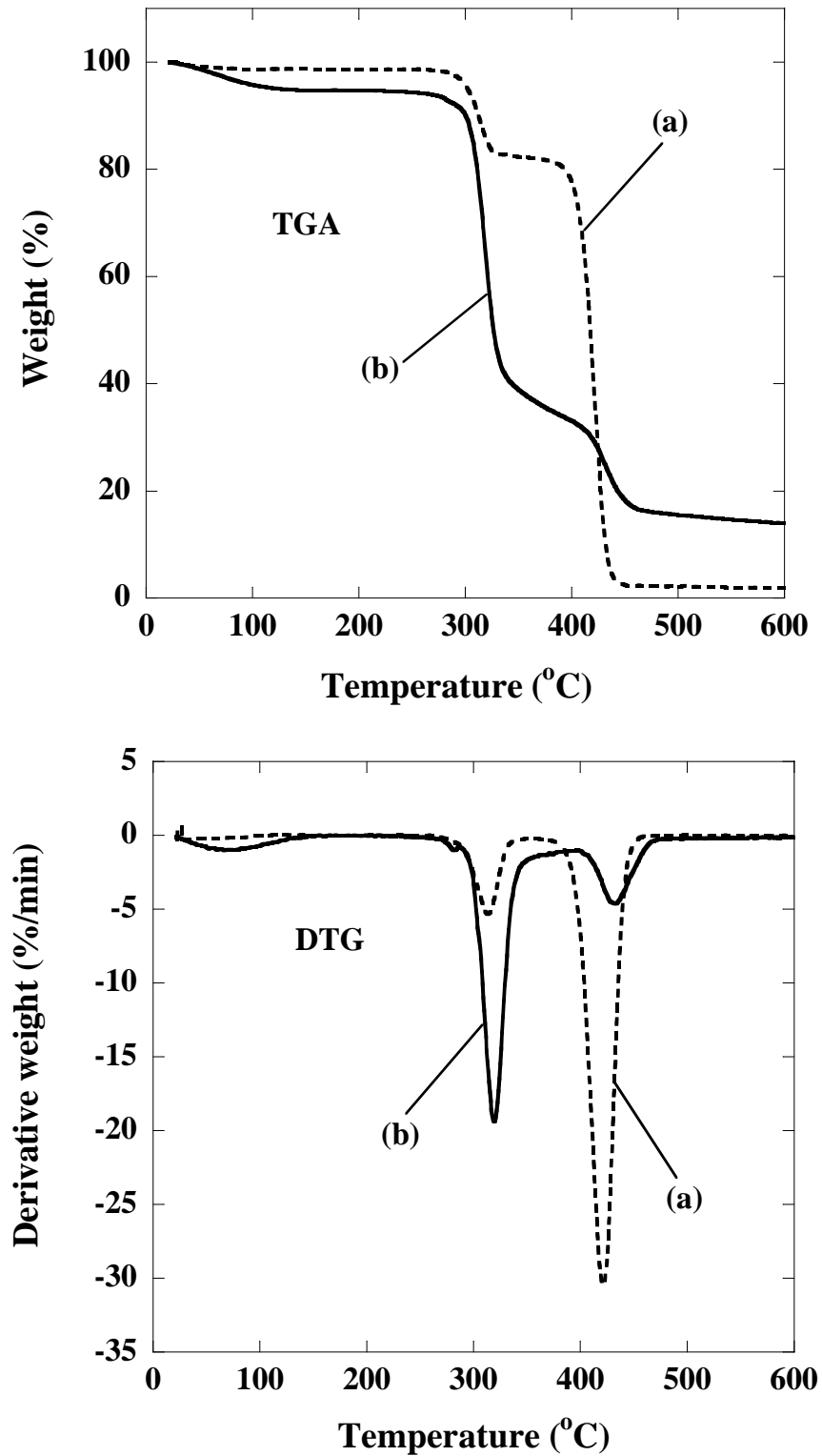


Figure 4.15 TGA and DTG thermograms of PS-g-cassava starch copolymer before (a) and after Soxhlet extraction (b) with G (%) = 22.80%.

The thermograms of the PS-g-cassava starch copolymer before Soxhlet extraction exhibited a higher quantity of percentage of the weight loss of PS than the thermograms of PS-g-cassava starch copolymer after Soxhlet extraction because the homopolystyrene had been removed after Soxhlet extraction. Therefore, the quantity of percentage of the weight loss of PS decreased after using Soxhlet extraction (Figure 4.15 (b)).

Figure 4.16 shows TGA and DTG thermograms of PS-g-cassava starch copolymer after Soxhlet extraction from different G (%) values including a G (%) = 14.00%, 22.80% and 32.80%. The three steps of weight loss were again obtained. The initial step of weight loss in the range of from 50 to about 100 °C, was a result of water evaporation. The second step is the weight loss from 280 – 350 °C and the third step is the weight loss from 380 – 470 °C which could be the decomposition of starch and PS in the graft copolymer, respectively. The homopolystyrene in all samples was completely extracted by the Soxhlet extraction process; therefore, the quantity of percentage of the weight loss of PS was lower than the quantity of percentage of the weight loss of starch. This confirmed that the PS-g-cassava starch copolymer had been obtained.

Furthermore, the different G (%) exhibited the different value of percentage of weight loss of a synthetic polymer grafted onto the starch backbone (Kiatkamjornwong et al., 2006; Yin et al., 2008). The value of percentage of weight loss of PS in the extracted sample with a G (%) = 14.00% was 8%. When the G (%) increased from 22.80% to 32.80%, the value of percentage of weight loss of PS increased from 17.5% to 20.5%, respectively (Figure 4.16). This result indicated that the extracted sample with a G (%) = 14.00% was degraded more rapidly than the extracted samples with a higher G (%) (22.80% and 32.80%).

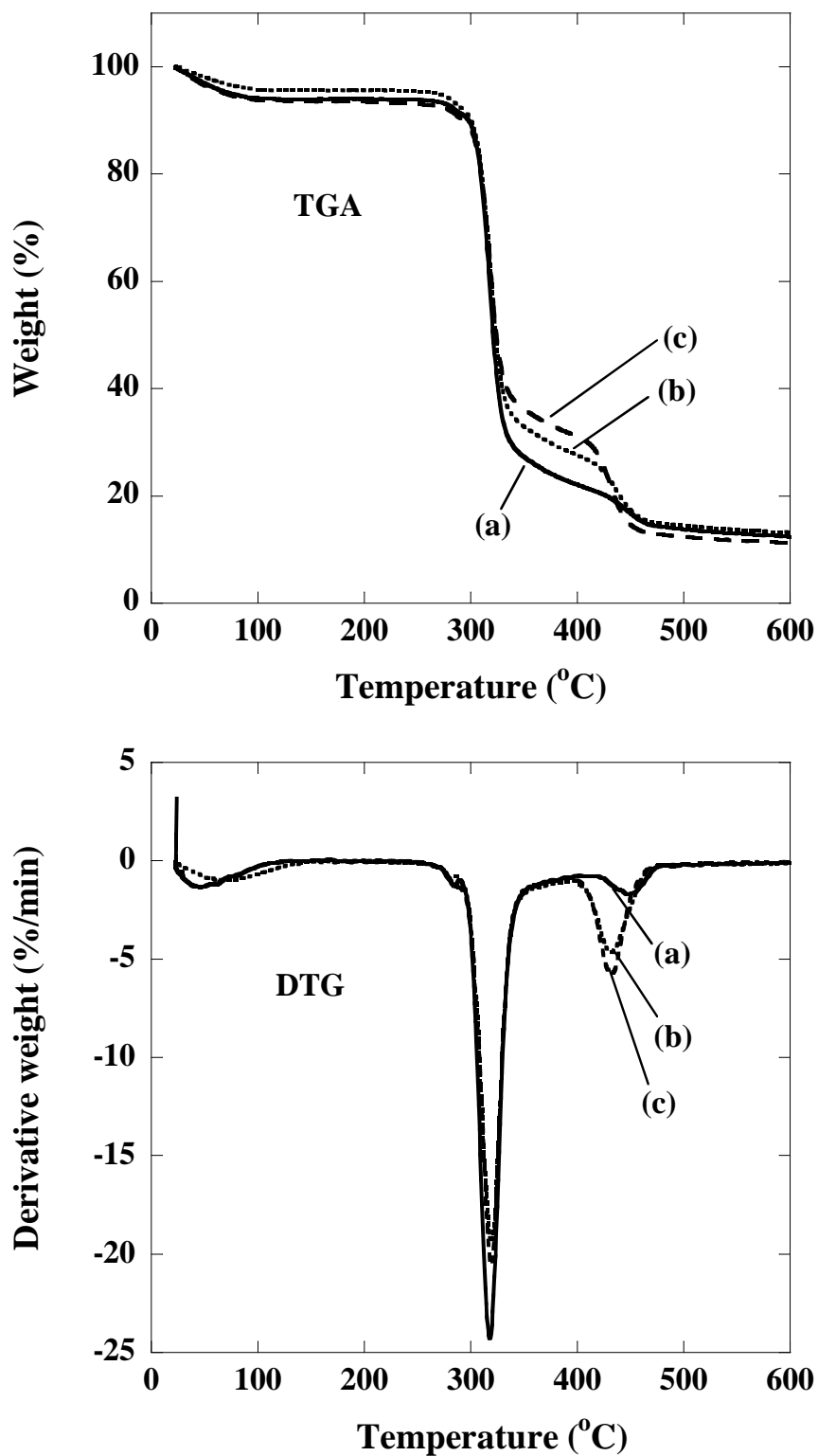


Figure 4.16 TGA and DTG thermograms of PS-g-cassava starch copolymer after Soxhlet extraction with  $G$  (%) = 14.00% (a), 22.80% (b) and 32.80% (c).

#### 4.3.4 Differential scanning calorimetry analysis (DSC)

DSC is an important tool used to explain the formation of graft copolymers. A DSC thermogram from the first heating scan of cassava starch, PS and PS-g-cassava starch copolymer after Soxhlet extraction from different G (%) values is presented in Figure 4.17. They show a broad endothermic peak at around 100°C. This peak was also observed by other authors. Mano and coworkers (2003) believed that a broad endothermic peak from room temperature up to a temperature of above 150°C may be due to water adsorption occurring above room temperature during the heating scan. The endothermic peak at 126.9°C was due to the melting of crystalline starch that had been formed between the water residue and the molecular chains of starch via hydrogen bondings (Meng et al., 2005). Hamdan and coworkers (2000) reported that the peak between 50 and 150°C was due to the melting of the amylopectin fraction. The additional stage observed at 144 °C was due to the loss of water contained in the starch sample (Rudink et al., 2005; Yin et al., 2008). The source of this peak is controversial and there is no conclusion. However, this peak was not apparent on the DSC thermogram from the second heating scan.

Figure 4.18 shows the DSC thermogram from the second heating scan of cassava starch. An exothermic reaction was detected at 275 °C and this correlated with its TGA and DTG thermograms, for the starting decomposition temperature of starch. The PS exhibited a heat flow change at 107.5 °C, and this corresponded to the  $T_g$  of PS (inserted in Figure 4.19) and the thermal oxidation at 400 °C (Figure 4.19) corresponding to its TGA and DTG thermograms.

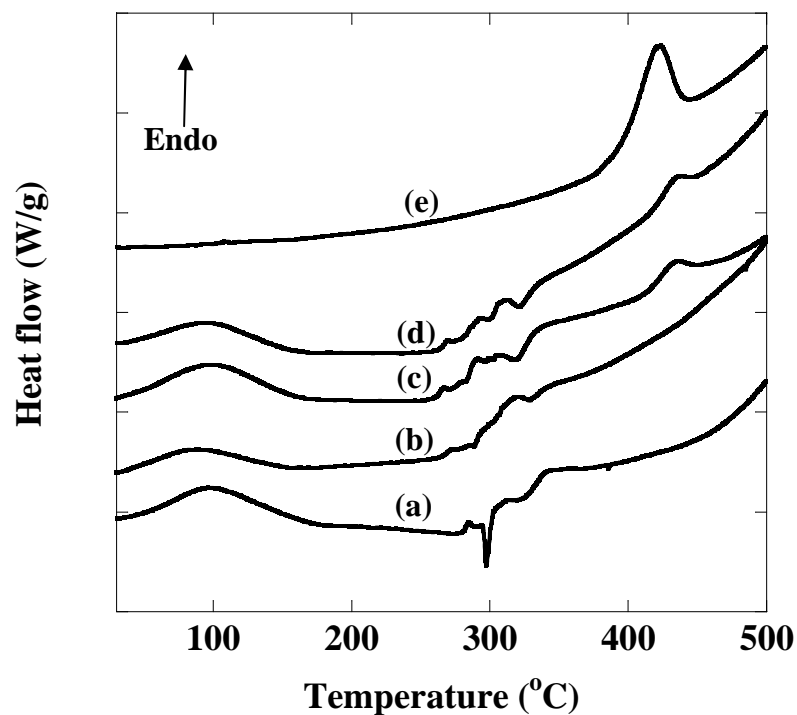


Figure 4.17 DSC thermograms from the first heating scan of cassava starch (a), PS-g-cassava starch copolymer after Soxhlet extraction with G (%) = 14.00% (b), 22.80% (c), 32.80% (d) and PS (e).

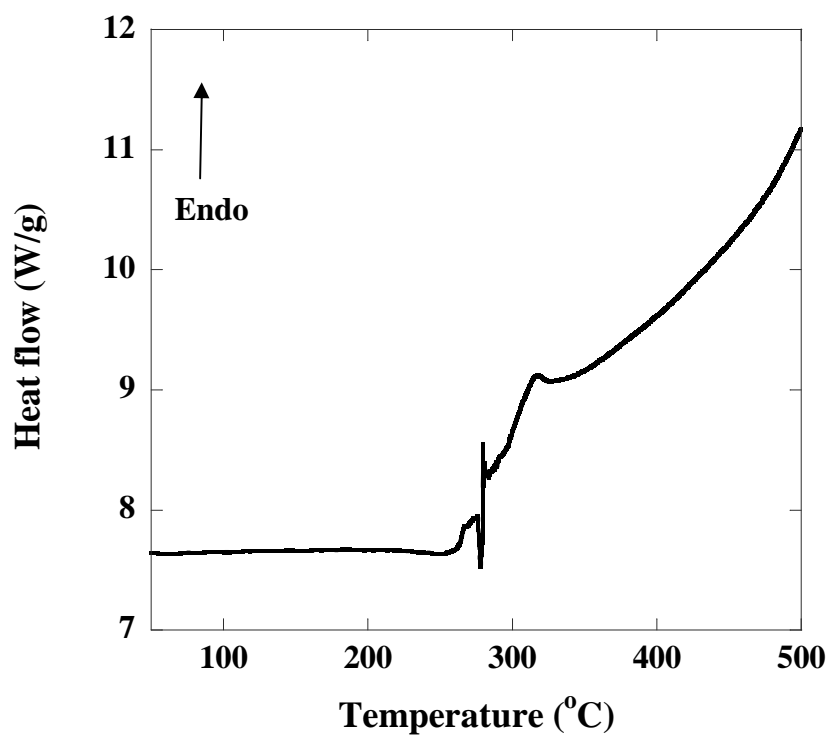


Figure 4.18 DSC thermogram from the second heating scan of cassava starch.

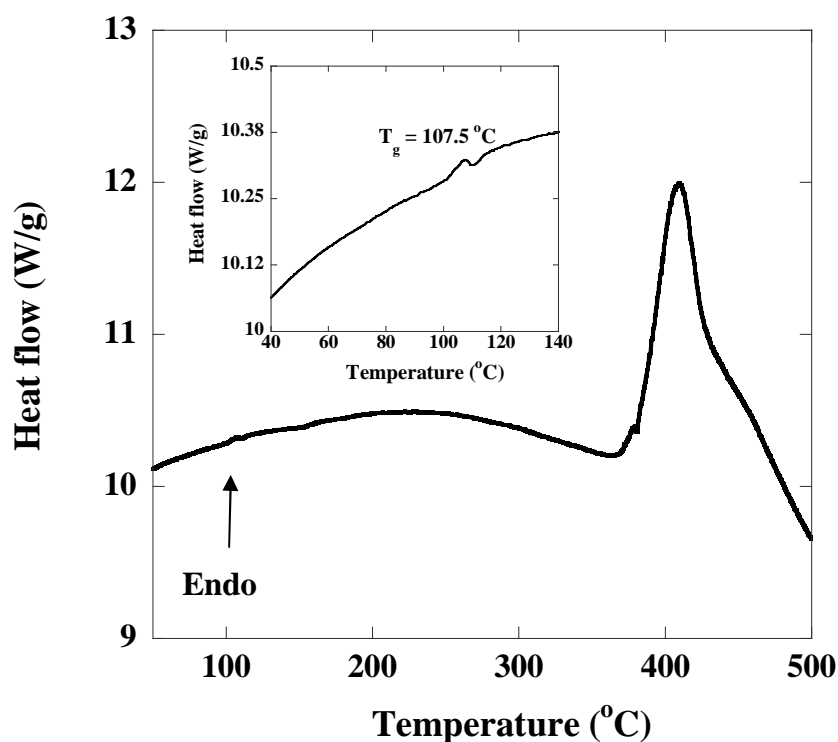


Figure 4.19 DSC thermogram from the second heating scan of PS.

The DSC thermogram from the second heating scan of PS-g-cassava starch copolymer before and after Soxhlet extraction is shown in Figure 4.20. The DSC thermogram of the PS-g-cassava starch copolymer before Soxhlet extraction with a G (%) = 22.80% (Figure 4.20 (a)) looked similar to the starch characteristic (Figure 4.18). The thermal oxidation of the starch phase in the samples after Soxhlet extraction occurred at a higher temperature ( $> 275$  °C) and the thermal oxidation peak of PS at about 400 °C was more clearly visible as the G (%) increased (Figure 4.20 (b)-(d)).

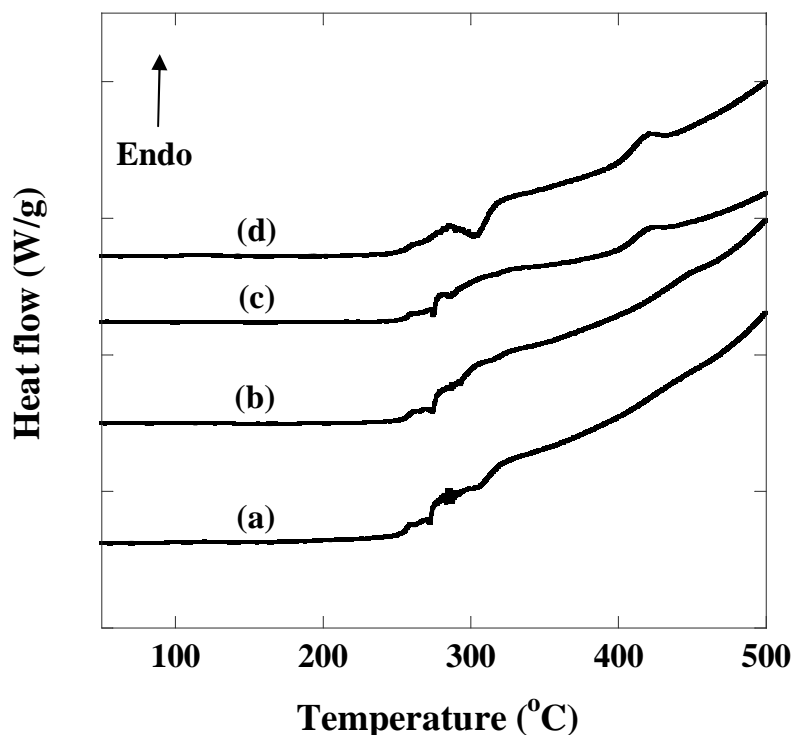


Figure 4.20 DSC thermograms from the second heating scan of PS-g-cassava starch copolymer before Soxhlet extraction with G (%) = 22.80% (a), PS-g-cassava starch copolymer after Soxhlet extraction with G (%) = 14.00% (b), 22.80% (c) and 32.80% (d).

#### 4.3.5 X-ray diffraction analysis

Starch granules were semi-crystalline in nature. The extent of crystallinity of native starch was determined by X-ray diffraction ranged from about 15% to 45% depending on the starch sources (Copeland et al., 2009). The crystallinity of cassava starch was about 38% (Steinbuchel and Rhee, 2005). The XRD pattern of the cassava starch and the PS-g-cassava starch copolymer after Soxhlet extraction with a G (%) = 22.80% are shown in Figure 4.21. The degree of crystallinity of the samples was quantitatively evaluated following the method previously explained in section 3.3.7. The XRD pattern of the extracted sample was similar to the XRD patterns of the cassava starch. The degree of crystallinity of the cassava starch and graft copolymer G (%) = 22.80% were in the same range which was 37% and 39%, respectively. Therefore, it obviously showed that the reaction conditions did not rupture the starch granules and this correlated with the results from SEM.



Undoubtedly, this was due to the polymerization reaction being carried out at a low reaction temperature that was lower than the gelatinization temperature of the cassava starch. If the system used gelatinized starch, then no crystal state could be observed.

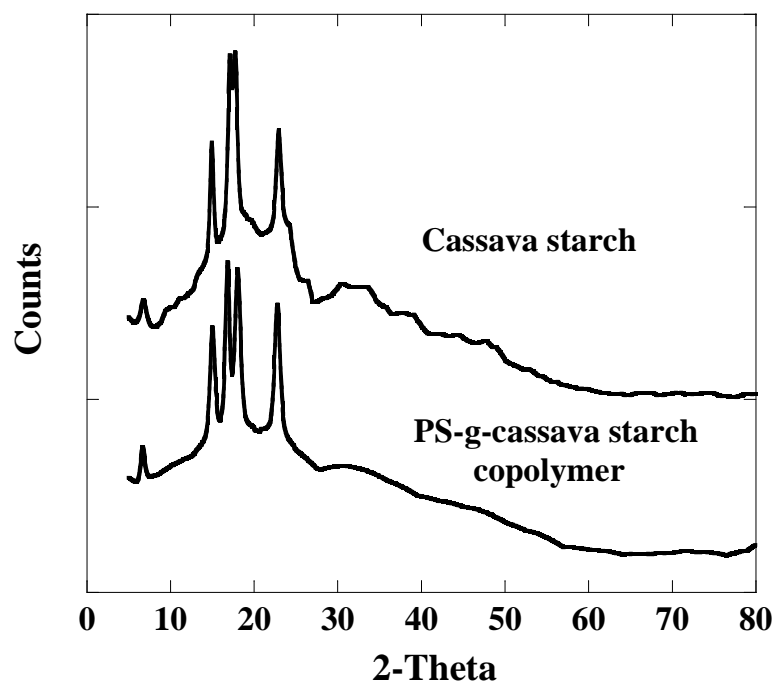


Figure 4.21 XRD pattern of the cassava starch and the PS-g-cassava starch copolymer after Soxhlet extraction with  $G (\%) = 22.80\%$ .

#### 4.3.6 The efficiency of Soxhlet extraction

The Soxhlet extraction was the important process used to remove the homopolystyrene that was obtained from the graft copolymerization reaction between cassava starch and the styrene monomer. Every extraction was checked by dropping the extracted solution into methanol which is a non-solvent of PS. If a precipitate did not occur, this confirmed that the extraction was complete. The polymer blend (cassava starch and PS blend) was prepared following the method described in Chapter 3 in order to check the efficiency of the Soxhlet extraction process. The FTIR spectrum of cassava starch and the polymer blend after Soxhlet extraction are displayed in Figure 4.22. The FTIR spectrum of the polymer blend after Soxhlet extraction (Figure 4.22 (b)) looked similar to the FTIR spectrum of virgin cassava starch (Figure 4.22 (a)). This indicated that PS had been completely removed from the

polymer blend. It confirmed that the homopolystyrene had been completely extracted by the Soxhlet extraction process and merely grafted PS still adjoined on the starch backbone. Therefore, the Soxhlet extraction process was efficient and reliable.

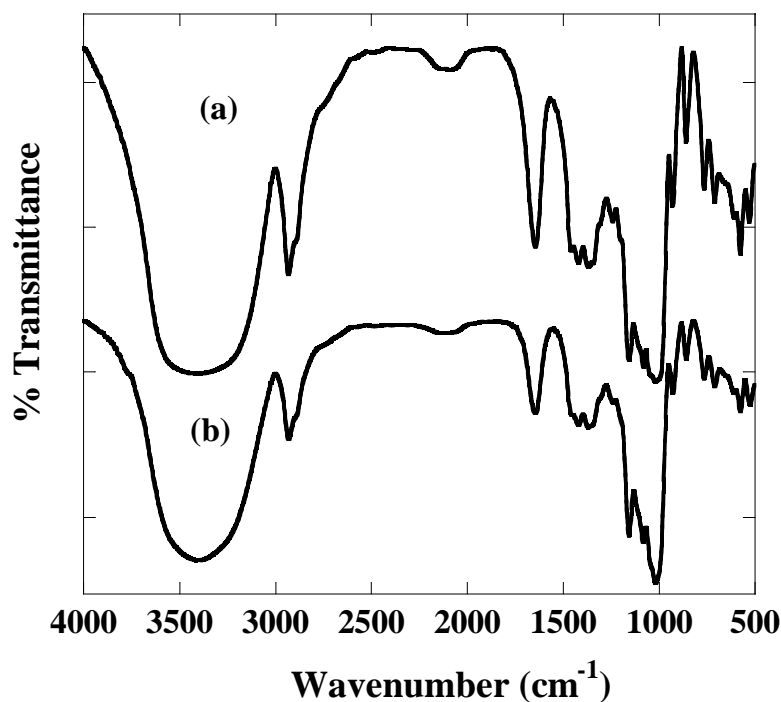


Figure 4.22 FTIR spectra of virgin cassava starch (a) and the product of the starch and PS blend after Soxhlet extraction (b).

#### 4.4 PS-g-cassava starch copolymer/cassava starch blend

Starch-based plastics have received more attention because of its availability and low price. However, starch-based plastics have the drawbacks that are their brittleness, poor mechanical properties, shrinkage and remarkable sensitivity to moisture content that limit its wide application. A plasticizer is required for preparing starch-based plastics because the plasticizer overcomes brittleness and avoids the cracking of the material during handling and storage. The addition of plasticizer reduces internal hydrogen bonding between the starch molecules while increasing its molecular volume (Laohakunjit and Noomhorm, 2004; Wang and Huang, 2007). Various plasticizers have been used for starch-based materials such as water, glycerol, sorbitol, sugars, ethanolamine, urea, citric acid, formamide and poly(ethylene glycol) (Laohakunjit and Noomhorm, 2004; Jiugao et al., 2005; Jiang et al., 2006; Yang et al.,

2006; Orts et al., 2007; Wang and Huang, 2007). Glycerol is a well known good plasticizer of starch-based materials because it provides good qualities is cheap and non-toxic. Blending with some other synthetic polymers is another way to improve the properties of starch-based plastics. In this study, starch-based plastics were prepared by blending cassava starch with PS-g-starch copolymer with a G (%) = 21.80%) using glycerol and water as plasticizers. The PS-g-cassava starch copolymer/cassava starch blends were prepared following the method described in Section 3.2.4.

Table 4.2 presents the appearance of starch-based plastics that made from a PS-g-starch copolymer of (G (%) = 21.80%)/cassava starch blend as affected by the plasticizer type and concentration. The samples were very brittle and heterogeneous at lower glycerol and water concentrations, whereas at very high concentrations, i.e. glycerol 45 phr (parts per hundred of total weight of polymers) and water 10 phr, the samples were very soft and homogeneous because of the better compatibility between cassava starch and the PS-g-starch copolymer.

Table 4.3 presents the composition and appearance of starch-based plastics that were made from a PS-g-starch copolymer of (G (%) = 21.80%)/cassava starch blends as affected by the amount of PS-g-starch copolymer and cassava starch (glycerol (45 phr) and water (10 phr) as plasticizer). Three different characteristics can be identified.

First, when the PS-g-cassava starch copolymer content were higher than 60%, the samples could not be handled and performed the tensile properties because they were extremely brittle and their surface were very sticky. This phenomenon is proposed to be called the deplasticizing effect which decreases the material processability (Shi et al., 2007). It may be due to cassava starch being hydrophilic and susceptible to compete for the glycerol and water absorption. When the amount of the PS-g-cassava starch copolymer increased, glycerol migrated to the surface of the samples and the water easily volatilized at the high temperatures during the compression molding because the absorption of glycerol and water took place with difficulty due to the PS being hydrophobic. Therefore, this phenomenon might be the cause of the sticky surface and brittleness of the sample

Table 4.2 Appearance of the starch-based plastics as affected by plasticizer type and concentration (The ratios of PS-g-cassava starch copolymer (GS):cassava starch (CS) = 50:50)

Plasticizer (phr)		Characteristic of compounds
Glycerol	Water	
25	0	Heterogeneous
	5	Heterogeneous
	10	Heterogeneous
30	0	Heterogeneous
	5	Heterogeneous
	10	Heterogeneous
35	0	Heterogeneous
	5	Heterogeneous
	10	Heterogeneous
40	0	Heterogeneous
	5	Heterogeneous
	10	Heterogeneous
45	0	Heterogeneous
	5	Heterogeneous
	10	Homogeneous

Second, when the PS-g-cassava starch copolymer content was 40% - 60%, the samples did not shrink. Shrinkage results at 65% RH are reported in Table 4.4. The PS-g-starch copolymer leads to a significant reduction of shrinkage. It can be considered to be a dimensional stability enhancement modifier. Moreover, the samples were less brittle and sticky when compared to higher amounts of PS-g-cassava starch copolymer. It is due to there being less influence on achieving the deplasticizing effect.

Finally, when the PS-g-cassava starch copolymer content was lower than 40%, the samples could not be monitored for their tensile properties because they shrank when exposed to relative humidity (RH) of about 65% (Table 4.4). This could be due

to the water acting as a plasticizer, but being volatilized rapidly at the high temperature used during the compression molding. When the samples were exposed to a higher relative humidity (%RH = 65%), starch absorbed sufficient water to reduce its  $T_g$ , and resulting in sample shrinkage (Patil and Fanat, 1995; Willett, 2008).

Table 4.3 Composition and appearance of the starch-based plastics as affected by the amount of PS-g-starch copolymer and cassava starch (glycerol (45 phr) and water (10 phr))

GS*:CS**	Characteristic of compounds	Visual and handling characteristics of samples
100:0	Homogeneous	Opaque, very brittle and very sticky
90:10	Heterogeneous	Opaque, very brittle and very sticky
80:20	Heterogeneous	Opaque, very brittle and very sticky
70:30	Heterogeneous	Opaque, very brittle and very sticky
60:40	Homogeneous	Opaque, less flexible and sticky
50:50	Homogeneous	Opaque, less flexible and sticky
40:60	Homogeneous	Opaque, less flexible and sticky
30:70	Homogeneous	Translucent, flexible and sticky
20:80	Homogeneous	Translucent and flexible
10:90	Homogeneous	Translucent and flexible
0:100	Homogeneous	Translucent and flexible

\*GS is PS-g-starch copolymer (G (%) = 21.80%).

\*\*CS is cassava starch.

X-ray diffraction was used to investigate the changes in crystallinity during the ageing of the PS-g-cassava starch/cassava starch blend. The XRD pattern of the original materials and the PS-g-cassava starch/cassava starch blends (conditioning in RH of 65% for 24 h and 4 weeks) are presented in Figure 4.23.

Table 4.4 Shrinkage (%) for PS-g-starch copolymer/cassava starch blends (65% RH)

GS:CS	Shrinkage (%)
60:40	0
50:50	0
40:60	0
30:70	1.04
20:80	2.61
10:90	3.39
0:100	7.80

The PS-g-cassava starch/cassava starch blend had XRD patterns that differed from the cassava starch granules and the PS-g-cassava starch copolymer. A complete change in the XRD pattern of the PS-g-cassava starch/cassava starch blend in relation to the original materials can be seen, confirming the disruption of the cassava starch granule. From Figure 4.23, when the ratios of GS:CS were 100:0 and 90:10, the intensity of the crystalline peak was higher and the ratios of GS:CS were 10:90 and 0:100 within 24 h due to the deplasticizing effect. The influence of the deplasticizing effect brings about migration of glycerol to the surface of the samples. From that result, glycerol cannot reduce internal hydrogen bonding between starch molecules. Therefore, the intermolecular and intramolecular reactions between starch molecules were rebuilt and a novel crystalline structure was immediately obtained after the samples were compression molded. This is referred to as retrogradation. The sample with a ratio of GS:CS of 0:100 showed a similar behavior but had a longer delay before significant crystallization could be observed. There were weak peaks in the XRD pattern, when the ratio of GS:CS was 0:100 within 24 h. This is because glycerol formed the strong hydrogen bonds with the starch molecules (Ma et al., 2006; Yang et al., 2006). Therefore, the interaction of starch molecules and the re-crystallization (retrogradation) occurred with difficulty. However, when it was stored for 4 weeks obvious peaks due to the retrogradation of cassava starch were observed.

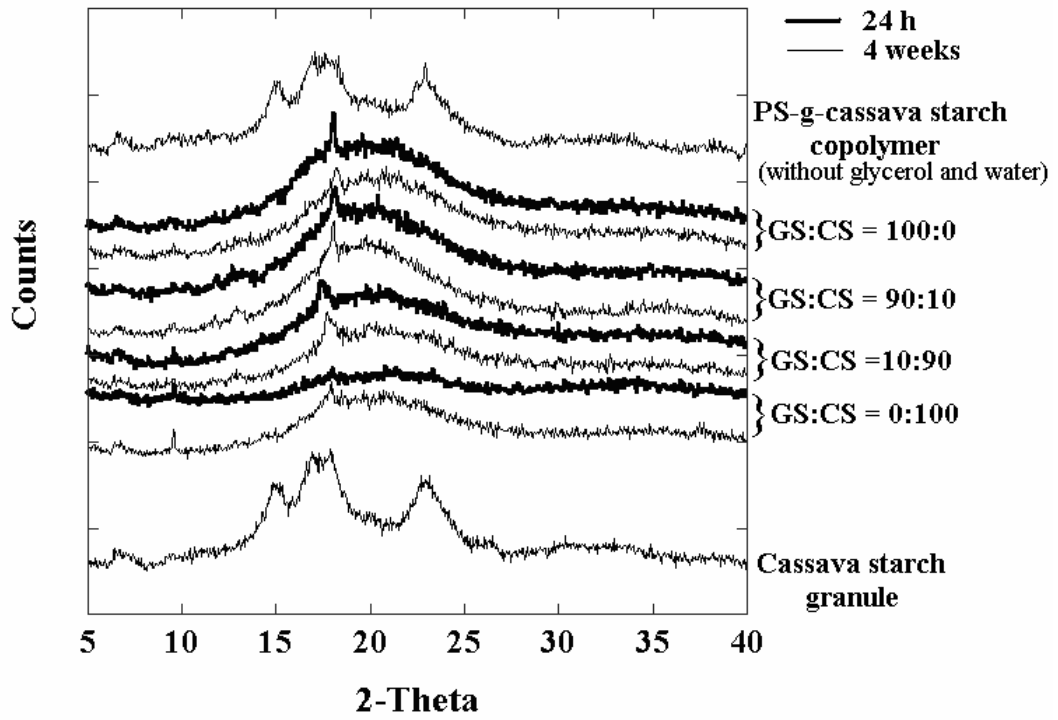


Figure 4.23 XRD patterns of the cassava starch, PS-g-cassava starch copolymer and the PS-g-cassava starch/cassava starch blend.

## CHAPTER 5

### CONCLUSIONS

The preparation of polystyrene (PS) was successfully prepared via suspension polymerization using potassium persulfate (PPS) as an initiator. The PS spherical microbeads that were smaller than 200  $\mu\text{m}$  were occurred under suspension polymerization in an aqueous medium. Thermogravimetric analysis (TGA) was used to determine the glass transition temperature ( $T_g$ ) of the PS spherical microbeads. The  $T_g$  of those PS spherical microbeads was 107.5  $^{\circ}\text{C}$ .

The synthesis of cassava starch grafted with PS (PS-g-starch copolymer) was carried out via suspension polymerization using potassium persulfate (PPS) as an initiator. The effect of the amounts of cassava starch, styrene monomer, PPS, reaction time and reaction temperature were investigated. The homopolystyrene was extracted by using the Soxhlet extraction process. The optimum G (%) (31.47%) and GE (%) (10.49%) were obtained when using 2.5 g of cassava starch, 7.5 g of styrene monomer, 0.4 g of PPS, a reaction time of 2 h and reaction temperature of 50  $^{\circ}\text{C}$ .

The chemical structures, morphology, degree of crystallinity, thermal decomposition temperatures and thermal behavior of cassava starch, PS and PS-g-starch copolymer were investigated by using Fourier Transform Infrared Spectroscopy (FTIR), scanning electron microscopy (SEM), X-ray diffraction (XRD), TGA and differential scanning calorimetry (DSC), respectively. These results indicated that the preparations of PS and PS-g-starch copolymer via suspension polymerization using PPS as an initiator were successful.

The PS-g-starch copolymer with a G (%) = 21.80% was mixed with cassava starch in order to prepare PS-g-starch/cassava starch blends using glycerol (45 phr) and water (10 phr) as plasticizers. When the amount of PS-g-starch increased the blends were very brittle and their surfaces were very sticky. From that result, it was difficult to measure the tensile testing. This can be attributed to the deplasticizing effect and the retrogradation of cassava starch.



## CHAPTER 6

### INTRODUCTION

#### 6.1 Background and rationale

Nowadays, research and development on bioplastics is attractive because of the increase in fossil energy costs and the environmental pollution by synthetic plastics which are now regarded as being a worldwide environmental problem. Renewable bioplastic materials such as starch and proteins have a huge advantage because of their abundant resources, low cost, good biodegradability and suitable properties for usage. Therefore, this thesis focused on the development of the bioplastics that made from starch and protein (wheat gluten) which is the by-product of the wheat starch fabrication and the food processing industry. A starch-based polymer which was cassava starch grafted with polystyrene (PS-g-cassava starch copolymer) was explained in part 1 (Chapter 1 – 5). This part (Chapter 6 – 10) explained about the bioplastic that made from protein. Proteins derived from plants such as wheat gluten, soya and zein are classical renewable materials. Wheat gluten is unique among plant proteins, because of its low cost, availability in large quantities, good biodegradability and unique viscoelastic properties. Wheat gluten is a mixture of the (monomeric) gliadin and (polymeric) glutenin (about 52/48, w/w, respectively) (Auvergne et al., 2008). Gliadin provides the viscous component of gluten while glutenin contributes to the elastic properties (Jerez et al., 2005). Wheat gluten is composed of many types of amino acids. Cystine is the amino acid that plays an important role in the wheat gluten-based bioplastics. Although, cystine is a minor amino acid of wheat gluten but it consists of SH group which can form disulfide (SS) bonds between protein chains. The SS bonds influences the quality of the bioplastics made. Wheat gluten can be processed into a bioplastic through extrusion or compression molding (Pommet et al., 2003). The addition of a plasticizer can overcome the brittleness of the wheat gluten-based materials and facilitates its processability. Small polar molecules such as glycerol, water, sorbitol, sugars and fatty acid can be used as plasticizer but according to the literature glycerol is the most commonly used (Pouplin et al., 1999; Pommet et al., 2003; Pommet et al., 2005).

Mechanical mixing and thermal treatment play an important role in wheat gluten-based bioplastics because they cause wheat gluten aggregation (crosslinking) through SS bonds. Gluten crosslinking occurs through both radical and nucleophilic mechanisms (Auvergne et al., 2008). The origin point of forming radical species occurs during mixing (Auvergne et al., 2008). During the thermal treatment, proteins unfold at temperatures above 75°C and this facilitates crosslinking (Schofield et al., 1983). The structure and properties of wheat gluten are strongly modified by crosslinking. A loss of solubility in sodium dodecyl sulfate (SDS) buffer provides good evidence of the extent of crosslinking (Schofield et al., 1983; Hayta and Schofield., 2004; Rosell and Foegeding., 2007). It is necessary to control the extent of protein crosslinking that occurs during the mechanical mixing and thermal treatment because protein crosslinking plays a key role in the properties of wheat gluten-based bioplastic. The protein crosslinking of gluten film was controlled by using gamma-irradiation (Lee et al., 2005). Sun and coworkers (2008) also have studied control of protein crosslinking for wheat gluten-based bioplastic by varying the molding temperature from 25°C to 125°C.

Polyphenolic structures such as tannin and lignin interact readily with proteins, leading to the formation of protein-polyphenol complexes. Tannin can precipitate salivary proteins via hydrophobic forces and hydrogen bonding (Sarni-Manchado et al., 1999). Zahedifar and coworkers (2002) have shown that lignin can precipitate protein and protect protein from degradation in the rumen. Keaft lignin (KL) and liginosulfonate can form a crosslinking network with soy proteins (Huang et al, 2003 (a); Hung et al., 2003 (b)). The addition of KL was able to control the crosslinking of a wheat gluten-based bioplastic (Kunanopparat, 2008). KL can impair the free radicals that cause crosslinking during the mixing and thermal treatment, of wheat gluten leading to an increase of the soluble protein content. In this study two possible mechanisms were described. The first involves the formation of a complex between KL and wheat gluten during processing that modifies the 3D structure of the wheat gluten protein, and modifies its reactivity. The second involves a direct influence of some functional chemical groups found in KL on the wheat gluten crosslinking mechanism.

Lignin is a complex phenolic polymer obtained from trees and agricultural crops (Pouteau et al., 2003; Boeriu et al., 2004). KL is a by-product of the alkaline (Kraft) pulping process, and is the main type of industrial lignin produced in the world. Kraft lignin exhibits complex structures, resulting from the alkaline modification of the native lignin found in the woods. Its structure, generally speaking has been poorly characterized, and is dependent on the properties of the native lignin (wood species, agricultural conditions of growth) and on the intensity of the Kraft process. Native lignin is basically formed by the combination of three monomers, namely p-coumaryl, coniferyl and sinapyl alcohols. The resulting structure is a polyphenolic compound, of very high molecular weight (Ralph et al., 2004). The most important chemical functional groups in KL are composed of the hydroxyl (phenolic or alkyl), methoxyl, carbonyl and carboxyl groups. The phenolic structures are known for their radical scavenging properties and the conjugation of the aromatic nucleus can induce the resonance stabilization of the phenoxy radicals (Graf., 1992; Zang et al., 2000; Butterfield et al., 2002).

Some research groups have studied modifying lignin through various methods such as acid treatment (Pouteau et al., 2005), laccase and laccase-mediated with methyl syringate treatment (Liu et al., 2009), ozone treatment (Severtson and Guo, 2002) and oxidation (Crestini et al., 2006). Moreover, the available reactive hydroxyl groups in lignin can be chemically reacted by esterification and etherification (Lora and Glasser, 2002).

In this part of this thesis, the effect of KL on the crosslinking of wheat gluten, in terms of providing a chemical interpretation was investigated. Two routes were followed. The first one was to compare the effect of KL with an Esterified lignin (EL) in order to clarify the influence of hydroxyl groups on the reactivity with the 3D structure of the wheat gluten protein. The second one was to evaluate independently the effect of different simple aromatics structures (guaiacol, ferulic acid, coumaric acid, cinnamaldehyde, cinnamyl alcohol, trans anethole and vanillin) commercially available in order to check for the effects of their different functions on the wheat gluten reactivity. All the chemical functions can be found in KL itself (or in its degradation products obtained by oxidation, vanillin). Moreover, the effect of hydroxyl and conjugated double bonds (in which the nucleophilic reactivity has been

reinforced by addition of carboxylic or aldehydes groups), all of them located on an aromatic structure. The effects of those compounds on protein plasticization and crosslinking were separately investigated.

## **6.2 Objectives of the research**

1. To synthesize the esterified lignin via the esterification reaction of hydroxyl groups in Kraft lignin.
2. To investigate the plasticizing properties of Kraft lignin, esterified lignin and other additives on wheat gluten-based bioplastic.
3. To investigate the effect of Kraft lignin, esterified lignin and different simple aromatics structures on wheat gluten-based bioplastic.

## **6.3 Benefits**

The addition of Kraft lignin, esterified lignin and other additives appears as a new promising and environmentally-friendly way to control gluten crosslinking during processing which is useful to develop the properties of bioplastic that made from wheat gluten for various applications. Moreover, the environmental pollution problems caused by the use of synthetic polymers based on petrochemicals can be decreased and the value of agriculture products increased.

## CHAPTER 7

### LITERATURE REVIEW

#### 7.1 Gluten

Gluten is a special protein commonly found in rye, wheat, corn and barley. There are some types of grain do not contain gluten e.g. wild rice, buckwheat, millet, amaranth, quinoa, teff and oats. Gluten from wheat flour has the capability to form strong and cohesive dough. Proteins from other cereal flours do not have dough forming properties except rye can form the weak dough. Wheat gluten is often the protein by-product of the wheat starch fabrication and the food processing industry (Hoseney, 1998; Domenek et al., 2004; Jerez et al., 2005). During the production of wheat starch, dough is first formed by mixing water and flour together. Wheat gluten is easy to isolate from wheat starch because gluten is insoluble in water. Wheat flour is rinsed and kneaded until all of the wheat starch is removed from the dough (Hoseney, 1998).

Normally, there are four types of proteins present in wheat flour. The major proteins are gliadin and glutenin and the minor proteins are albumin and globulins. Glutenin and gliadin are the two proteins that can form gluten and are responsible for the unique viscoelastic properties of gluten (Walsh, 2002). Wheat gluten contains about 75-85% of the proteins with 40-50% gliadin and 35-45% glutenin (Sun et al., 2007).

Gluten is composed of many large protein components present as either monomers or linked by interchain disulfide (SS) bonds, such as oligomers and polymers. They consist of many amino acid components including a high content of glutamine and proline. The structures of glutamine and proline are presented in Figure 7.1. The amino acid composition of glutenine and gliadine in the gluten are shown in Table 7.1.

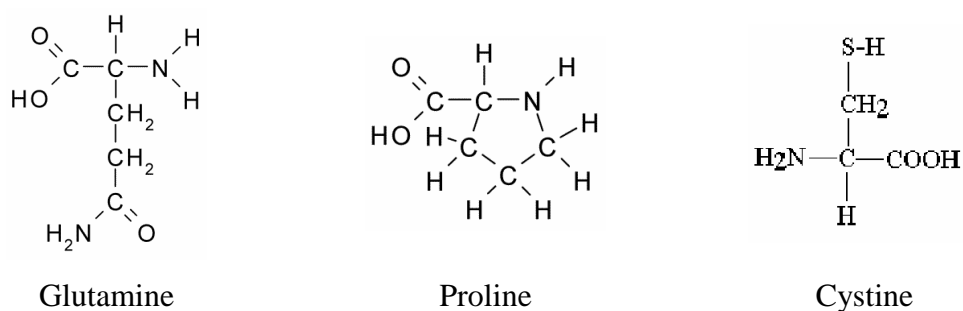


Figure 7.1 The structures of glutamine, proline and cystine (Walsh, 2002).

Table 7.1 Amino acid units of gliadine and glutenine in gluten (Kunanopparat, 2008)

Amino acid	Gliadine (%)	Glutenine (%)
Arginine	2.7	4.1
Lysine	0.6	2.3
Asparagine	2.9	3.7
Cystine	3.0	2.4
Glutamine	38.9	33.1
Histidine	2.2	2.3
Serine	4.7	5.4
Threonine	2.2	3.1
Tyrosine	2.6	3.6
Alanine	2.0	2.8
Glycine	1.5	3.8
Isoleucine	4.3	3.7
Leucine	6.9	6.6
Methionine	1.4	1.7
Phenylalanine	5.5	4.8
Proline	13.8	10.3
Tryptophane	0.7	2.1
Valine	4.1	4.2

Although, cystine is a minor amino acid of gluten protein it has a huge influence on the structure and function of gluten. Cystine has a SH group in its structure (Figure 7.1). Therefore, cystines can form both intrachain SS bonds within a molecular and interchain SS bonds between proteins (Wieser, 2007). It is difficult to identify the gluten structure because the SS bonds in the gluten structure are cleaved and reformed according to the disulfide interchange theory (Tilley et al., 2001). SH groups and SS bonds have a significant role in determining gluten properties and SS bond formation within gluten are important in the formation of protein networks that affects the quality of the final product (Hayta and Schofield, 2004).

### **7.1.1 Gliadin**

Gliadin is a glycoprotein present in wheat and several other cereals. The molecular weights of gliadin range from 30,000 to 74,000 (Walsh, 2002). Gliadin presents viscous flow properties on the gluten (Redl et al., 2003; Jerez et al., 2005; Rosell and Foegeding, 2007). The gliadins are divided into four groups e.g. alpha- ( $\alpha$ -), beta- ( $\beta$ -), gamma- ( $\gamma$ -) and omega- ( $\omega$ -) gliadins which are separated on the basis of their electrophoretic mobility at low pH and isoelectric focusing. The amino acid compositions of the  $\alpha$ -,  $\beta$ -,  $\gamma$ - and  $\omega$ - gliadins are similar to each other. The  $\alpha$ - and  $\beta$ - gliadins are closely related and thereby they are often referred to as  $\alpha$ -type gliadins. All cysteine in  $\alpha$ - and  $\gamma$ - gliadins are involved in intrachain SS bonds. In contrast, the  $\omega$ -gliadins contain little or no cysteine (Lagrain et al., 2008).

### **7.1.2 Glutenin**

Glutenin is one of the largest natural molecules. The glutenin fraction consists of a mixture of 20% high-molecular weight glutenin subunits (HMW-GS) and 80% low-molecular-weight glutenin subunits (LMW-GS) (Lagrain et al., 2008). The HMW-GS have molecular weights that range from 80-160,000 and LMW-GS have molecular weights range from 30-51,000. Glutenin has a wide range of molecular sizes (Redl et al., 2003). Glutenin provides the elasticity properties of the gluten (Redl et al., 2003; Rosell and Foegeding, 2007). Both HMW-GS and LMW-GS play important roles in the elasticity properties of wheat flour.

There are two mechanisms used to explain the SH groups and SS bonds exchange a method involving radicals and the other a nucleophilic exchange mechanism (Figure 7.2). Their mechanisms depend on the thermal and mechanical conditions (Auvergne et al., 2008; Kunanopparat, 2008).

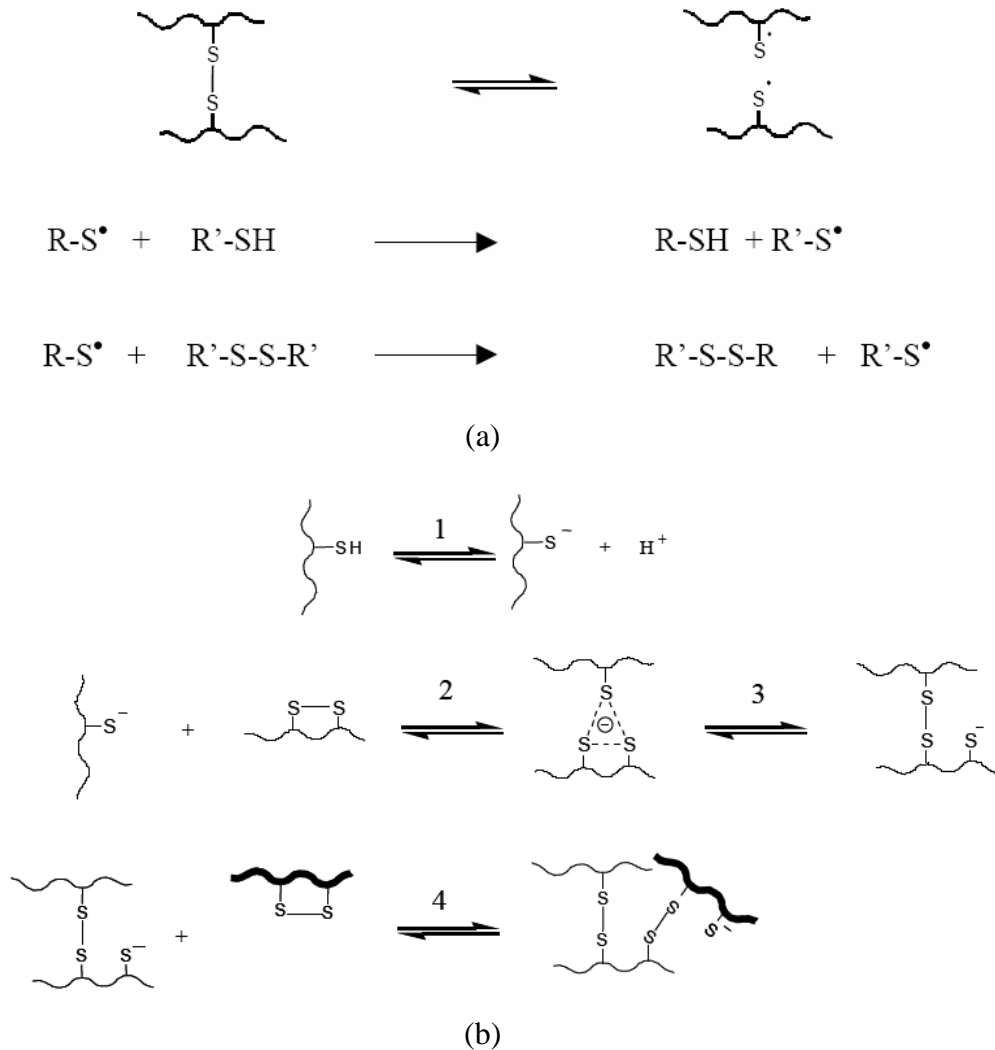


Figure 7.2 Radical (a) and (b) nucleophilic exchange mechanisms between a thiol and a disulfide bond (Walsh, 2002; Auvergne et al., 2008; Kunanopparat, 2008).

Heat treatment and mechanical processing causes the gluten protein to aggregate (crosslinking). This occurs through SH-SS interchange reactions (Micard et al., 2001; Hayta et al., 2004; Sun et al., 2007; Kunanopparat et al., 2008; Lagrain et al., 2008). The extractability of proteins by sodium dodecyl sulfate (SDS) solution



gives a good indication of the degree of crosslinking. As aggregation progresses, the SDS extractable fraction decreases and the SDS unextractable fraction increases (Hayta and Schofield, 2004; Lagrain et al., 2008). Weegels and coworker (1994a,b) investigated the SH-SS interchange reaction of gluten during thermal treatment. They found that free SH groups decreased and SS bonds increased.

### **7.1.3 Wheat gluten based materials**

Wheat gluten has been produced either edible or non-edible film, biodegradable and packaging materials (Pommet et al., 2003; Jerez et al., 2005). Wheat gluten has many advantages for preparing bioplastics because it is inexpensive, renewable, an abundant raw material, readily available in large quantities, fully biodegradable does not release toxic products and has properties suitable for usage as films and plastics (Irission-Mangata et al., 2001; Domenek et al., 2004; Sun et al., 2007; Kunanopparat et al., 2008; Zuo et al., 2008; Zuo et al., 2009). However, gluten based materials are brittle so are difficult to handle. A plasticizer is a major component of gluten based materials because it can reduce the intermolecular forces and increases the mobility of polymeric chains. Therefore, the flexibility and the extensibility of gluten based materials are improved. Water and glycerol are very common plasticizers of gluten based bioplastics. Polyols, sugars ethylene glycol, lipids and fatty acids can also be used as plasticizers for gluten based bioplastics (Irission-Mangata et al., 2001; Pommet et al., 2003; Pommet et al., 2005; Zuo et al., 2008). Recently, two technological processes have been used to prepare gluten based materials. They are a wet and a dry process. The wet process uses a casting method, based on dispersion or solubilization of the gluten. The dry process uses a common thermoplastic processing (e.g. extrusion and compression molding) which consists of mixing gluten and plasticizer to obtain a dough-like material (Micard et al., 2001; Jerez et al., 2005; Pommet et al., 2005; Kunanopparat et al., 2008). The mechanical properties of wheat gluten based materials are lower than synthetic polymers resulting in limited applications. Several research workers have attempted to improve the performance of wheat gluten based materials.

(i) Films made from wheat gluten

Films of wheat gluten can be processed through casting, thermoforming and extrusion (Domenek et al., 2004; Hochstetter et al., 2006; Min et al., 2008). Films made from gluten have a good quality such as being effective barriers against oxygen, carbon dioxide and have a low polarity (Domenek et al., 2004; Hernandez-Munoz et al., 2004; Zuo et al., 2009). However, they are a poor barrier against humidity due to the hydrophilic nature (Zuo et al., 2009). The factors that influence the gluten films properties include plasticizer, pH, relative humidity, kind of solvent, concentration of solvent and thermal treatment (Sun et al., 2007). Chitosan (Park and Bae, 2006), cellulose acetate phthalate (Fakhouri et al., 2004), diethanolamine, triethanolamine (Irission-Mangata et al., 2001) and methylcellulose (Zuo et al., 2009) have been used to mix with wheat gluten to prepare blended films with improved mechanical properties and water vapor permeability. The effect of the glycerol content on the water barrier and mechanical properties of wheat gluten have been studied (Park and Chinnan, 1995; Hochstetter et al., 2006). They found that glycerol improved the flexibility of gluten film but its tensile properties, puncture strengths and water barrier property were decreased. Water vapor permeability reduced after increasing the treatment temperature (Ali et al., 1997). Films obtained from casting suspensions followed by evaporation of solvent at pH 11 were stronger than the films prepared at pH 4 and 6. This indicated the formation of irreversible intermolecular crosslinks upon forming films at pH 11 (Kayseriliolu et al., 2001).

(ii) Other bioplastics made from wheat gluten

The degree of protein crosslinking decreased when acid plasticizers (e.g. citric, lactic and octanoic acid) were added into wheat gluten based bioplastics and this provided properties that were suitable for agricultural applications (Pommet et al., 2005; Gomez-Martinez et al., 2009). The properties of gluten based bioplastics were also improved by using saturated fatty acids as plasticizer (Pommet et al., 2003). A combination of hydrophilic plasticizer (glycerol) and hydrophobic liquids (castor oil, silicone oil or polydimethylsiloxane (PDMS)) were an effective method to improve the mechanical and moisture barrier properties of wheat gluten based bioplastics (Song and Zheng, 2008). Hemp and wood fiber were used as

reinforcement for wheat gluten/glycerol based materials. It was found that the tensile strength and Young's modulus increased but elongation at break decreased. However, the deplasticizing effect occurred at high fiber contents (Kunanopparat et al., 2008). The crosslinking density of protein increased when the molding temperature was increased from 25 to 125 °C (Sun et al., 2008). Zuo and coworker (2008) prepared wheat gluten based bioplastics by using calcium carbonate as a filler and glycerol as a plasticizer followed by compression molding the mixture at 120 °C to crosslink the wheat gluten matrix. Aldehyde increased both the degree of crosslinking and the tensile strength of thermomolded glycerol-plasticized wheat gluten based biodegradable plastics (Sun et al., 2007).

## 7.2 Lignocellulosic materials of plant cell walls

Lignocellulosic materials of plant cell walls consist of cellulose, hemicellulose and lignin (Figure 7.3). The hemicellulose and lignin are located between the cellulose microfibrils and inter-laminar spaces. The ratio of these three components depends on the kind of plant and their growth conditions (Table 7.2) (Lewin and Goldstein, 1991).

Table 7.2 Cellulose, hemicellulose and lignin content of various plant (McGinnis and Shafizaden, 1991)

Plant	Cellulose (%)	Hemicellulose (%)	Lignin (%)
Hardwoods	40-45	24-40	18-25
Softwoods	45-50	25-35	25-35
Monocotyledons(e.g. grasses such as palms, bamboo, wheat rice and sugar	25-40	25-50	10-30
Parenchyma cells of most leaves	15-20	80-85	-
Fiber (e.g. seed hairs of cotton)	80-95	5-20	-

### 7.2.1 Cellulose

Cellulose is one of the many polymers found in nature which is an excellent fiber. Wood, paper, and cotton are all made of fibrous cellulose. Cellulose is a structural polysaccharide that provides strength and rigidity to plants. It is a linear homopolymer consisting of glucose subunits linked by  $\beta$ -(1,4) glucosidic bonds (Figure 7.4) that can contain 5,000 or more than 20,000 glucose units (Allcock and Lampe, 1990; Bettelheim and March, 1990; Rehm and Reed, 1996; Walsh, 2002).

The linkage of cellulose is  $\beta$ -(1,4) makes it different from starch. There are no branch chains in cellulose as there are in starch. The different configurations of cellulose and starch cause the different properties. Humans cannot digest cellulose because the hydrolytic enzymes needed to degrade  $\beta$ -(1,4) glucosidic bonds do not present in the human digestive tracts. However, ruminant animals (such as cows) and other herbivores have bacterias that can degrade cellulose are exist in their gut. Therefore, they can digest cellulose as a food via the action of symbiotic bacteria that exist in the gut (Allcock and Lampe, 1990).

### 7.2.2 Hemicellulose

Hemicelluloses are covalently connected to lignin in wood cell walls but are structurally more closely related to cellulose than to lignin. Hemicelluloses are generally lower molecular mass polysaccharides. They are heteropolymers of D-galactose, D-mannose, D-glucose, D-xylose, L-arabinose, 4-*O*-methyl-D-glucuronic acid and various other sugars as well as their uronic acids (Rehm and Reed, 1996; Walsh, 2002).

### 7.2.3 Lignin

Lignin is a natural amorphous crosslinked resin that has an aromatic three-dimensional polymer structure containing a number of functionl groups such as phenolic, hydroxyl, carboxyl, benzyl alcohol, methoxyl and aldehyde groups. Lignin is a component of plant cell walls that provides rigidity to the plants by acting as the glue between the cellulose fibers. Lignin creates a barrier against microbial destruction and protects the readily degradable carbohydrates (cellulose and hemicellulose) (Rehm and Reed, 1996; Guo et al., 2008). Lignin consists in the main

of three primary monolignols: *p*-coumaryl alcohol, coniferyl alcohol and sinapyl alcohol (Figure 7.6). As a result, the lignin structure is a complex macromolecule with over 10 different types of linkages; for example, the linkage between benzylic carbon of lignin and the carbohydrates by ether bonds; the linkage between the benzylic of lignin and uronic acid residues by ester bonds and ligninglycosidic bonds (Figure 7.7) (Jittima, 2002; Walsh, 2002; Kubo and Kadla, 2005; Tejado et al., 2007; Holmgren et al., 2009). The lignin structure and properties depend on its original sources, environmental conditions of plant growth and extraction methods (Boeriu et al., 2004; Tejado et al., 2007).

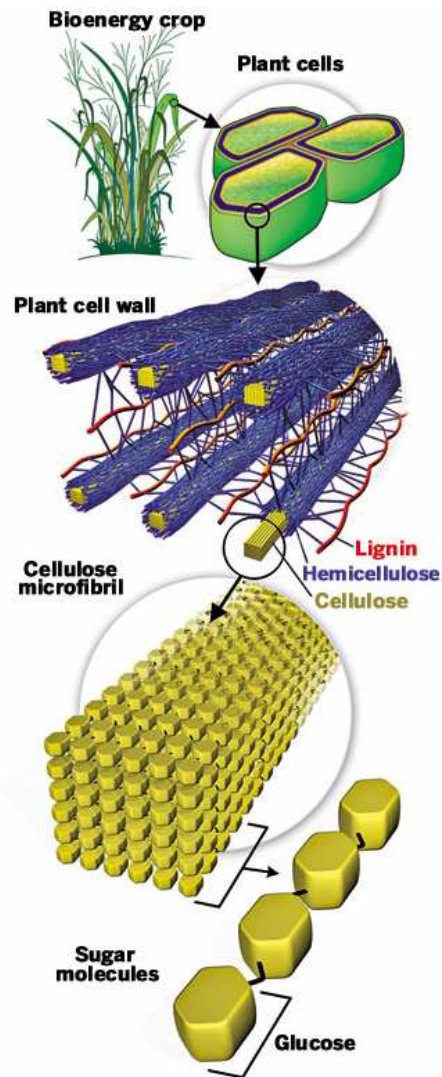


Figure 7.3 Cellulose, hemicellulose and lignin in cell walls (Charles and Bin, 2009).

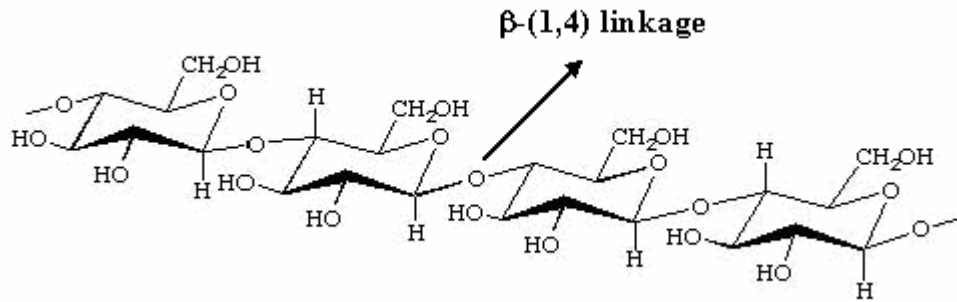


Figure 7.4 Cellulose structure (Ouellette, 1998).

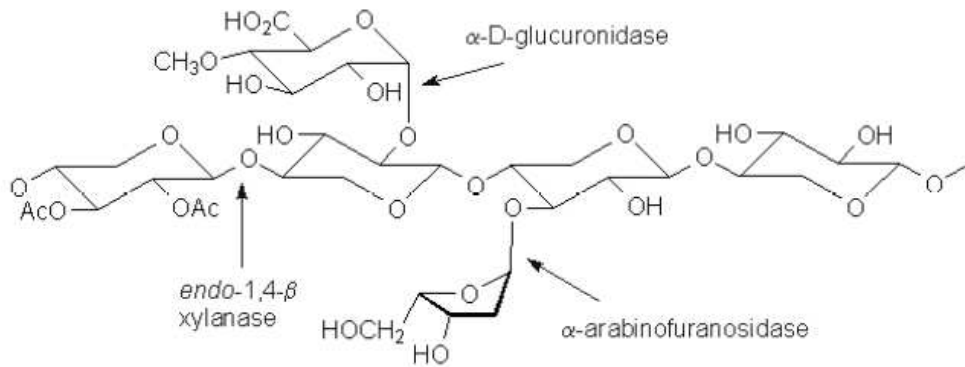


Figure 7.5 Hemicellulose structure (Kunanopparat, 2008).

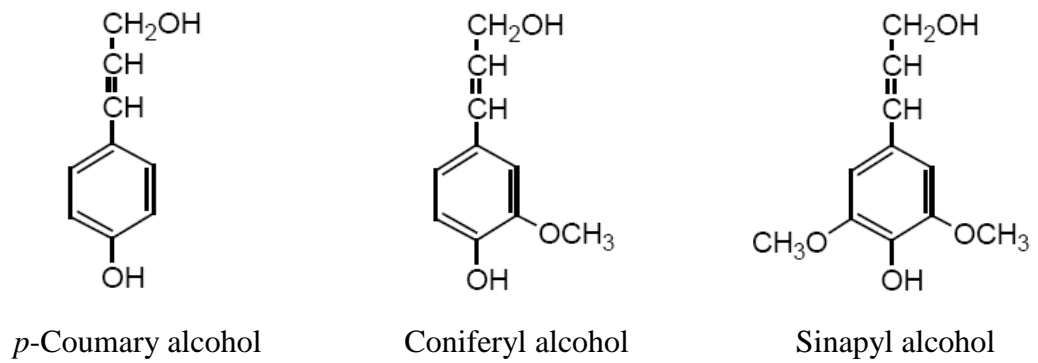


Figure 7.6 The main primary monolignols of lignin (Kunanopparat, 2008).

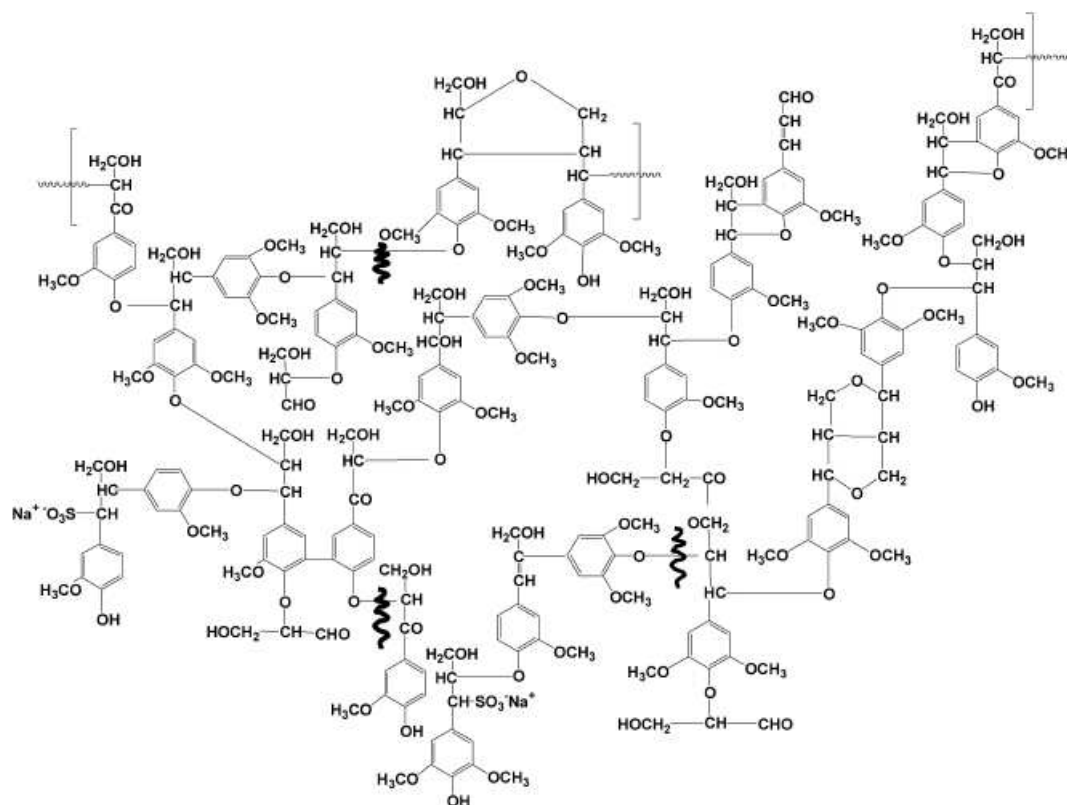



Figure 7.7 Lignin structure (Nimz, 1974). Sulfonate sites are introduced and many β-O-4 linkages are cleaved during Kraft pulping. Cleavage locations are shown by  line (Mohan et al., 2006).

Native lignin is difficult to obtain from plant cell walls (Boeriu et al., 2004). However, commercial lignins are a by-product mainly obtained from the pulp and paper industry (Kraft lignins and liginosulfonate) (Boeriu et al., 2004; Pouteau et al., 2004; Vinardell et al., 2008). Kraft lignin (also called sulfate lignin) is a by-product of the alkaline (Kraft) pulping process which is the main lignin type produced in the world. It can be soluble in alkaline solution. Liginosulfonate (also called lignin sulfonates and sulfite lignins) is a product of the acid (sulfite) pulping process. It can be soluble in acid and also in water because of its sulfonic groups (Kunanopparat, 2008; Ugartondo et al., 2008).

### 7.2.3.1 Lignin properties and applications

Lignin has some good properties such as being an antioxidant, flame retardant, heavy metal absorbent and nucleating agent (de Chirico et al., 2003; Boeriu et al., 2004; Guo et al., 2008). The antioxidant property of lignin has been especially important in recent research activities. The antioxidant activity is a result of the phenolic hydroxyl groups in the lignin structure. Figure 7.8 provides an example of the trapping and stabilization of radicals by lignin that has been suggested by Barclay and coworkers (1997).

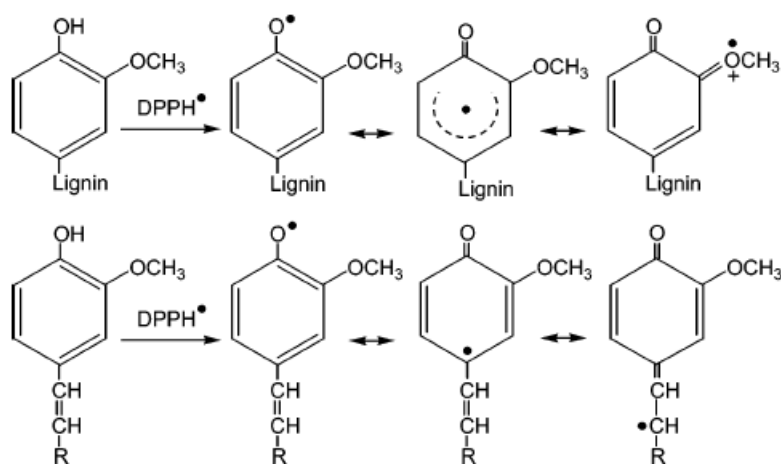


Figure 7.8 Trapping and stabilization of radicals by lignin (Barclay et al., 1997).

The 1,1-diphenyl-2-picrylhydrazyl (DPPH•) was used as a reactive free radical in order to identify the structures in the lignin macromolecular that were the most important for its antiradical efficiency (Dizhbite et al., 2004). The non-etherified OH phenolic groups, ortho-methoxy groups, hydroxyl groups and the double bonds between the outermost carbon atoms in the side chain supported the radical scavenging properties of lignin. On the other hand, the  $\alpha$ -carbonyl substitution in the side chain displayed the negative effect.

The properties of lignin are interesting. Presently, many papers have described the efficiency of lignin blend with various synthetic polymers such as isotactic propylene (Canetti et al., 2006), polypropylene, recycled polypropylene (Gregorova et al., 2005), polystyrene, low-density polyethylene and linear low-



density polyethylene (Pucciariello et al., 2004). They found that lignin could act as the stabilizer against thermal and UV radiation for these polymers. Lignin also had a stabilizing effect in carbon black filled natural rubber (Gregorova et al., 2006). A mixture of lignin and the commercial rubber antioxidant *N*-phenyl-*N*-isopropyl-*p*-phenylene diamine (IPPD) had the highest antioxidant efficiency in the examined vulcanisates. Lignin could be used as an antioxidant for cellulose (Schmidt et al., 1995) and edible oils such as arachide oil (Kasprzycka-Guttman and Odzeniak, 1994). Lignins from different sources such as Bagasse, Lignosulfonate, Kraft lignin and steam explosion have shown good antioxidant properties (Ugartondo et al 2008; Vinardell et al 2008) especially from Bagasse that had the best antioxidant properties. Moreover, it was found that these lignins were safety when applied to the eyes and skin. Soda lignin (SL), dioxane lignin (DL) and milled lignin (ML) were isolated from Alfa grass (*Stipa tenacissima L.*) (Nadji et al., 2009). SL was a by-product from industrial. DL and ML were isolated under laboratory conditions. It was found that SL, DL and ML exhibited antioxidant activity comparable to that of Butylated Hydroxytoluene (BHT) and Irganox 1010<sup>®</sup> that are commonly used in the thermoplastic industries. Lignin can act as the flame retardant for isotactic polypropylene due to lignin presents the high char yield during the thermal degradation (de Chirico et al., 2003). Therefore, the combustion rate of materials decreased. Lignin has a potential as the biosorbent for the heavy metal ions (Pb(II), Cu(II), Cd(II), Zn(II) and Ni(II)) from the waste water (Guo et al., 2008). The mechanisms of metal sorption by lignin included several processes such as ion exchange, surface adsorption and complexation. Lignin affected the kinetics of crystallization of isotactic polypropylene (Canetti et al., 2004) and poly(ethylene terephthalate) (Canetti and Bertini, 2007). It can act as a nucleating agent that induced an increase of the lamellar thickness and a reduction of the amorphous interlamellar phase.

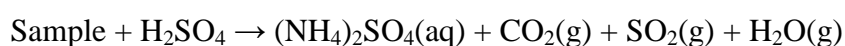
### 7.3 Kjeldahl method

There are two standard methods used to determine the nitrogen contents: Kjeldahl and Dumas methods. Both methods provide a quantitative determination of the total nitrogen content in samples and the protein contents were then calculated

using different multiplying factors suitable for different kinds of samples. The Kjeldahl method seems to be simpler, less expensive and more sensible than the Dumas method (Pontes et al., 2009). The Kjeldahl method is the worldwide standard method for determining the nitrogen contents in a wide variety of materials (e.g. pharmaceutical, agricultural, food products, biological sediments and waste water matrices). The Kjeldahl method involves three main steps: digestion, distillation and titration (Holme and Peck, 1993; Junsomboon and Jakmune, 2008; Gruner et al., 2009).

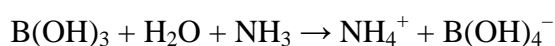
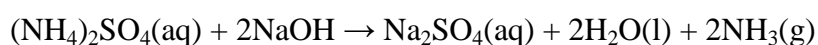
#### (i) Digestion

The nitrogen-containing samples are oxidized to ammonia ions by heating the sample with concentrated sulfuric acid for several hours in the presence of a catalyst (mercury oxide or copper sulfate) which helps in the conversion of the nitrogen to ammonium sulfate. In the initially digestion step the colour of the solution is very dark. The reaction is complete when the solution has become clear and colorless. The end result is an ammonium sulfate solution. The general equation for the digestion of an organic sample is given below.



#### (ii) Distillation

The digestion solution is distilled with sodium hydroxide. This converts the ammonium ions into ammonia gas. The ammonia gas is trapped in a boric acid solution where it dissolves and becomes an ammonium ion once again.



## (iii) Titration

The amount of the ammonium ions are determined by titration with a standard acid solution. The amount of nitrogen in a sample can be calculated from the amount of ammonia ions in the receiving solution. The total nitrogen (%) and crude protein (%) can be determined based on equations (1) and (2), respectively (Merrill and Watt, 1973):

$$\text{Total nitrogen (\%), (\%N)} = [(A-B) \times C \times 0.0014 \times 100] / D \quad (1)$$

Where;        A = Volume of standard acid used in sample (ml)  
                   B = Volume of standard acid used in blank (ml)  
                   C = Concentration of standard acid (N)  
                   D = Sample weight (g)

$$\text{Crude protein (\%)} = \%N \times \text{Kjeldahl factor} \quad (2)$$

Table 7.3 Kjeldahl factor for various proteins (Merrill and Watt, 1973)

Source of protein	Kjeldahl factor
Wheat gluten	5.70
Meat	6.25
Milk	6.38
Blood plasma	6.54
Egg	6.25
Peanuts	5.46

## CHAPTER 8

### EXPERIMENTAL

#### 8.1 Materials

The commercial wheat gluten was obtained from Amylum Group (Aalst, Belgium). Its moisture content was about 11%. Kraft lignin (KL) was provided by Westvaco (Charleston SC, USA). Dioxan, acetic anhydride, pyridine, ether and sodium dodecyl sulfate (SDS) were purchased from Sigma-Aldrich. Glycerol was purchased from Fluka and all the commercially available additives were purchased from Sigma-Aldrich, except for cinnamaldehyde (from SAEC). The structures and molecular weights of those additives are given in Table 1. The number average molecular weight  $M_n$  of KL was estimated by gel permeation chromatography to be 850 g/mol (Pouteau et al., 2003). However, the value reported in the table is an estimation of the molecular weight of one aromatic unit, assuming that the structure of KL is basically constituted by an assembly of the three monomers. This value was used to allow a comparison between simple additives (containing only one aromatic group) and the KL and esterified lignin (EL) structure.

#### 8.2 Esterification on Kraft lignin

50 g of KL was mixed with 250 ml dioxane, 45 g acetic anhydride and 36 g pyridine in a one-neck flask and was stirred at room temperature over night. This mixture was dropped into ether and the precipitate was filtered. The reagent was separated from the precipitate by mixing the precipitate with water (1 L), stirred (30 min) and filtered. To ensure the complete removal of the reagent, the above separation was carried out 6 times. Finally, the precipitate was dried in an oven at 40°C until constant weight.

#### 8.3 Sample preparation

The controlled wheat gluten products were prepared by mixing 35 g of un-plasticized wheat gluten and 15 g of glycerol. The controlled wheat gluten was mixed with 1, 5 or 10% additives by wt (KL, EL, additive-glycerol, guaiacol, *trans*-anethole,

cinnamaldehyde vanillin, cinnamyl alcohol, ferulic acid and coumaric acid). The plasticizer (glycerol) content was constant at 30% in all of the products. The products were mixed in a two blade counter-rotating batch mixer turning at a 3:2 differential speed (Plasti-corder W50, Brabender, Duisburg, Germany). The temperature of the mixing chamber was regulated at 30°C by using a regulation temperature unit (Julabo F34, Seelbach, Germany). Mixing speed was 100 rpm and the mixing time was kept constant at 10 min (after reaching the maximum torque). Torque and temperature were continuously recorded during the mixing process.

Compounds like glycerol, guaiacol, *trans*-anethole and cinnamaldehyde, which are liquid at ambient temperature, were added directly into the mixer. The solid additives such as vanillin, cinnamyl alcohol, ferulic acid and coumaric acid were first dissolved in 15 g of glycerol before mixing. Wheat gluten, KL and EL were added directly into the mixer.

#### **8.4 Thermal treatment**

The thermal treatment was performed using compression molding (PLM 10 T, Techmo, Nazelles, France). 5 g of sample was compressed at 100°C for 10 min and a pressure of 4 MPa was directly applied to the sample.

#### **8.5 Gluten protein extraction**

The gluten protein solubility measurement is a common way to determine the extent of the crosslinking between proteins. The soluble proteins were first extracted in a 1% SDS solution, and their amounts were determined using the Kjeldahl method.

0.8 g of the sample and 4.0 g of the starch were ground in the presence of liquid nitrogen using a laboratory ball mill. 0.75 g of the mixture of ground sample and starch was shaken in 30 ml of a 1% SDS solution at 60°C for 1 h 20 min. Next, the SDS-soluble protein was centrifuged (12,000 rpm, 20°C for 30 min). The solution of SDS-soluble protein extract was recovered.

## 8.6 Characterization

### 8.6.1 Kjeldahl method

#### (i) Digestion

26 ml of the SDS-soluble protein extract was mixed with 15 ml of H<sub>2</sub>SO<sub>4</sub> (95%) and 2 pellets of catalyst for Kjeldahl (composed of 3.5 g of K<sub>2</sub>SO<sub>4</sub> and 3.5 mg of selenium) during 2 h at 400°C. The chemical decomposition of the sample was completed when the medium became clear and colorless. This step consisted of heating a substance with H<sub>2</sub>SO<sub>4</sub> which decomposed the organic substance by oxidation to liberate the reduced nitrogen as ammonium sulfate.

#### (ii) Distillation

50 ml of deionized water was added in the solution that obtained from the digestion step and the solution was distilled with sodium hydroxide (32%) for 10 min to convert the ammonium salt to ammonia.

#### (iii) Titration

The amount of ammonia was determined by titration with 0.05 N H<sub>2</sub>SO<sub>4</sub>. The SDS-soluble protein (%) content was calculated following the equations below,

#### 1. Determination of protein concentration (Pc (mg/ml))

It refers to the concentration of protein in each sample that was extracted by using 30 ml of 1% SDS solution and it can then be determined based on equation (8.1):

$$Pc \text{ (mg/ml)} = \frac{(V_1 - V_2)}{26} \times 14.01 \times 0.05 \times 5.7 \quad (8.1)$$

where  $P_c$  (mg/ml) was the protein concentration,  $V_1$  was the volume of 0.005 N  $H_2SO_4$  that was titrated with the sample,  $V_2$  was the volume of 0.005 N  $H_2SO_4$  that was titrated with blank, 14.01 is the atomic mass of nitrogen, 0.05 was the concentration of standard  $H_2SO_4$  and 5.7 was a correction factor for the wheat protein.

## 2. Determination of the total protein weight (TPW(g))

It is used to indicate the weight of total protein in each sample that includes all of the SDS-soluble protein content and SDS-dissoluble protein content and it can be determined based on equation (8.2):

$$TPW (g) = \frac{0.8 \times 0.75 \times W_G}{50 \times 4.8} \quad (8.2)$$

where TPW (g) was the total protein weight (soluble protein and dissoluble protein),  $W_G$  was the weight of wheat gluten that mixing in internal mixer (g), 0.8 was the weight of sample in the mixer of sample and starch (g) that was prepared in section 8.5, 0.75 was amount of the mixture of wheat gluten with additive and starch that was dissolved in 30 ml of 1% SDS solution (g), 50 was the total weight of the sample that mixing in internal mixer (g) and 4.8 was the total weight of the mixture between wheat gluten with additive (0.8 g) and starch (4.0 g) (g).

## 3. Determination of the SDS-soluble protein weight (SPW (g))

This is used to indicate the weight of soluble protein in each sample and it can be determined based on equation (8.3):

$$SPW (g) = \frac{P_c \times 30}{1000} \quad (8.3)$$

where SPW (g) was the SDS-soluble protein weight,  $P_c$  (mg/ml) was the protein concentration and 30 was the volume of 1% SDS solution that was used to extract the protein (ml).

#### 4. Determination of the percentage of SDS-soluble protein content (SP (%))

This is used to describe the soluble protein as a percentage that was extracted by using 30 ml of 1 % SDS solution and it was determined based on equation (8.4):

$$SP (\%) = \frac{SPW(g)}{TPW(g)} \times 100 \quad (8.4)$$

where SP (%) was the percentage of SDS-soluble protein content, TPW (g) was the total protein weight and SPW (g) was the soluble protein weight.

#### 8.6.2 Morphological analysis

A scanning electron microscope (JEOL<sup>®</sup> JSM-5800LV) was used to study the surface morphology of Kraft lignin and Esterified lignin. The samples were first mounted on the brass stub with double sticky tape. Then the samples were coated with a thin evaporated layer of gold in order to improve conductivity and prevent electron charging on the surface. The scanning electron microscopy was operated at 10 kV.

#### 8.6.3 Fourier transform infrared analysis

The Fourier Transform Infrared Spectroscopy (FTIR) technique used a BRUKER<sup>®</sup> EQUINOX 55 to characterize the chemical structure of the Kraft lignin and the Esterified lignin. The samples were dried at 100 °C for 6 h in an oven prior to the test. The dried powder samples were mixed with KBr and pressed into the disc form by hydraulic compression. The samples were scanned at a frequency range of 4000-400 cm<sup>-1</sup> with 128 consecutive scans in a 4 cm<sup>-1</sup> resolution.



Table 8.1 Structure and molecular weight of all additives

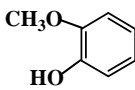
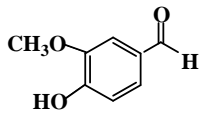
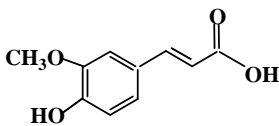
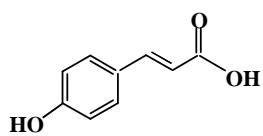
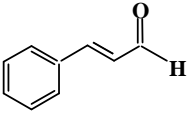
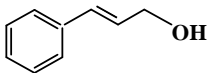
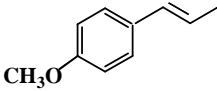
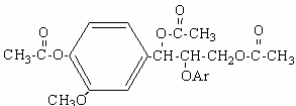
Additive	Structure	Additive content in %wt	Additive content in mmol/g of gluten
Guaiacol (MW = 124) Clear red solution		1	0.0815
		5	0.4244
		10	0.8961
Vanillin (MW = 152) Clear crystal Melting point = 80°C		1	0.0665
		5	0.3463
		10	0.7310
Ferulic acid (MW = 194) Light yellow powder Melting point = 170°C		1	0.0521
		5	0.2713
		10	0.5727
Coumaric acid (MW = 164) White powder Melting point = 214°C		1	0.06160
		5	0.3209
		10	0.6775
Cinnamaldehyde (MW = 132) Clear yellow solution		1	0.0765
		5	0.3987
		10	0.8418

Table 8.1 (cont.)

Additive	Structure	Additive content in %wt	Additive content in mmol/g of gluten
Cinnamyl alcohol (MW = 134) Clear crystal Melting point = 33°C		1	0.0754
		5	0.3928
		10	0.8292
<i>trans</i> -Anethole Clear solution (MW = 148)		1	0.0683
		5	0.3556
		10	0.7508
Glycerol (MW = 92) Clear solution	$\begin{array}{c} \text{H}_2\text{C-OH} \\   \\ \text{HC-OH} \\   \\ \text{H}_2\text{C-OH} \end{array}$	1	0.1098
		5	0.5721
		10	1.2077
Kraft lignin (MW <sub>eq</sub> = 180*) Dark brown powder	Figure 7.6 and Figure 7.7	1	0.0561
		5	0.2924
		10	0.6173
Esterified lignin (MW <sub>eq</sub> = 273 *) Light brown powder		1	0.0383
		5	0.1994
		10	0.4209

\* An estimated equivalent molecular weight (MW<sub>eq</sub>) per aromatic unit which was explained in chapter 9.

## CHAPTER 9

## RESULTS AND DISCUSSION

## 9.1 Kraft lignin (KL) esterification

Phenolic and aliphatic hydroxyl groups have been detected in KL structure (Pouteat et al., 2003; Guo and Rockstraw, 2006) (Figures 7.6 and 7.7). Those functional groups can act as a plasticizer (through hydrogen bonding) (Bouajila et al., 2005). Moreover, the radical scavenging properties of KL were derived from the scavenging action of their phenolic structures that have an impact on the gluten crosslinking (Kunanopparat, 2008). In order to show the effect (or absence of effect) of those structure, we conducted the esterification of the hydroxyl groups (Figure 9.1).

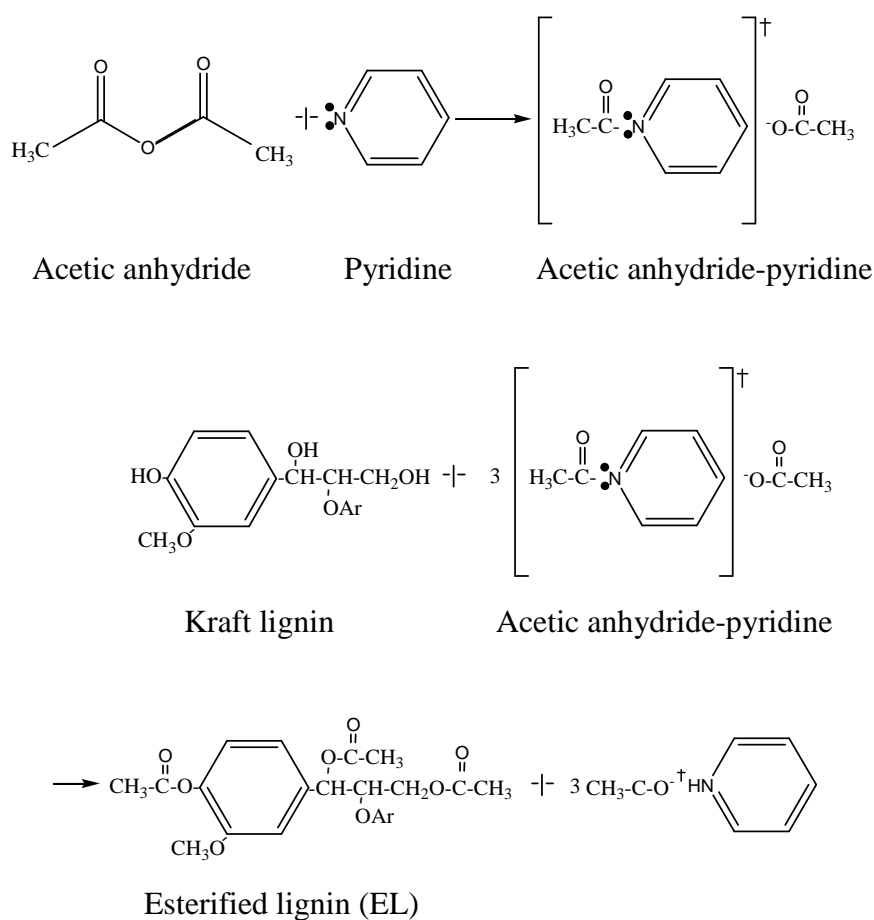


Figure 9.1 Mechanism of Kraft lignin esterification.

After modification, the color of the KL changed from dark brown to light brown and the smooth surface of KL changed to a rough surface (Figure 9.2). Therefore, it was believed that the esterification reaction in KL had been achieved.

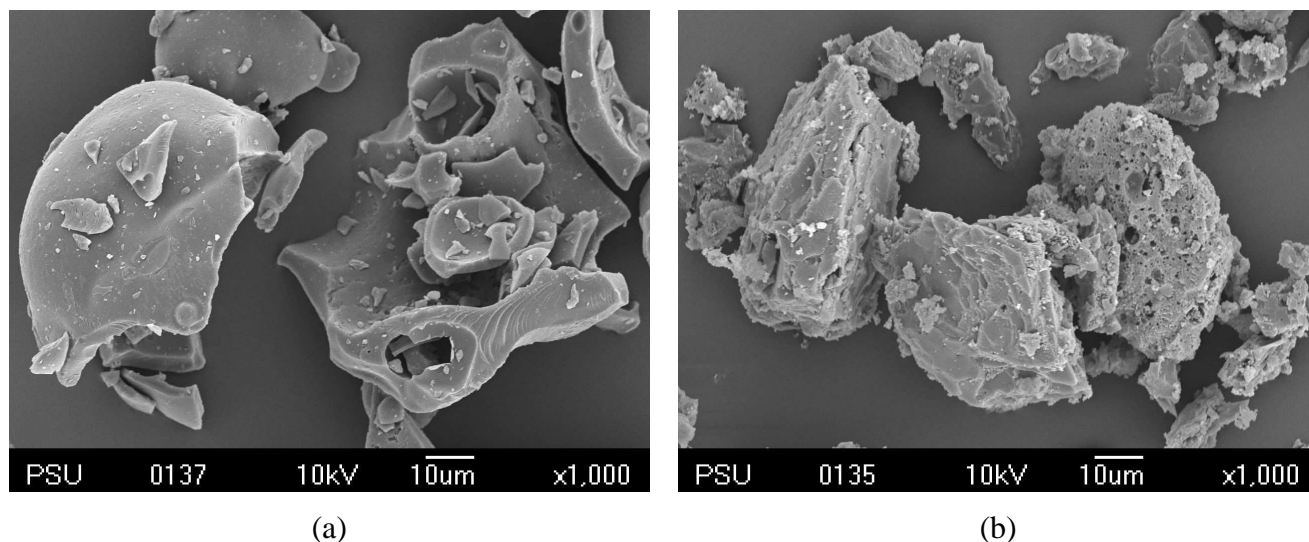


Figure 9.2 SEM micrographs of (a) Kraft lignin and (b) Esterified lignin (EL).

The FTIR spectra of the KL is shown in Figure 9.3. The broad peak at  $3407\text{ cm}^{-1}$  was dominated by the stretching vibrations of aromatic and aliphatic OH groups (Guo et al., 2006; Tejado et al., 2007; Guo et al., 2008). The peaks at  $2845$  and  $2931\text{ cm}^{-1}$  relate to the C-H stretching in  $\text{CH}_2$  and  $\text{CH}_3$  of the side chains and aromatic methoxyl groups. Three peaks at  $1424$ ,  $1513$  and  $1600\text{ cm}^{-1}$  depicted the vibration of the aromatic skeleton (Tejado et al., 2007; Guo et al., 2008). Moreover, the FTIR spectrum of EL exhibited two new peaks at  $1743$  and  $1762\text{ cm}^{-1}$ , that correspond to the C=O stretching in the ester groups. It has been shown that in the presence of imidazole, a basic catalyst, this reaction is complete (Thielemans and Wool, 2005). We therefore chose to use pyridine, another basic compound (Morck and Kringstad, 1985). The OH groups still present in the structure are thus likely to be mainly ones associated with acidic functions initially presents in the product. Lignin modification has been extensively study, either for the characterization of its structure, or for the modification of its properties, in order to test its use for various specific purposes. It has been shown that the chemical modification usually result in a modification to its solubility (Thielemans and Wool, 2005). However, we did not observe the formation

of any residual solid during the evaporation of the ether phase after modification. From this we concluded that the lignin modification that occurred was not associated with a fractionation. The molecular weight of EL was estimated by assuming each aromatic group has two OH functions (Figure 7.6) (one aromatic and one aliphatic) that had been completely modified. Even if this assumption was not completely satisfactory, especially because the total OH group number was not well-known, it will be sufficient for the analysis that will follow.

The estimated equivalent molecular weight ( $MW_{eq}$ ) of KL was 180, obtained by using the simple calculation, reported in terms of an average value derived from the MW of the representation units in the KL structure (Figure 7.6). From Figure 7.6, the average value of OH groups per KL monomers was 2 groups which were changed to  $OCOCH_3$  groups after esterification reaction. It also indicated that the  $MW_{eq}$  of EL was 264.

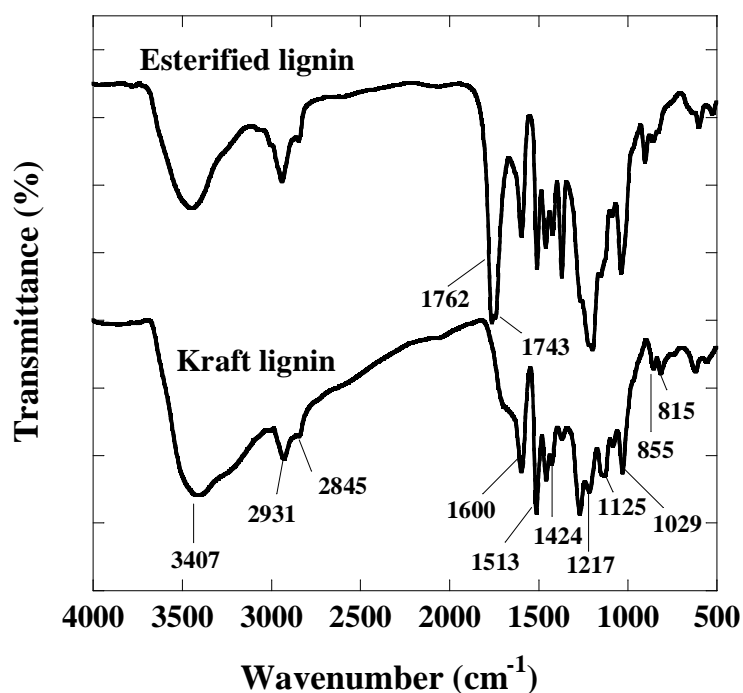


Figure 9.3 The FTIR spectrum of the Kraft lignin and Esterified lignin.

## **9.2 Materials processing**

Figures 9.4 – 9.16 shows the torque and temperature evolution in the batch mixer for wheat gluten with different additives. The torque and temperature curves depended strongly on the types and amount of additives. The peak characteristics (time to peak, intensity of the maximum torque and temperature at peak) were good parameters to study the gluten plasticization in the presence of the different functional groups of the additives.

### **(i) The controlled wheat gluten**

The controlled wheat gluten processing was repeated for six samples and each gave the same result with a torque value of about 42 N.m (Figure 9.4). This indicated that the important parameters were the torque and temperature values and these were reproducible and could be accurately detected. The initial torque rapidly increased up to a maximum value, then gradually decreased and stabilized when homogeneous samples were obtained. The temperature increased and stabilized after the torque reached its maximum value which was accompanied by an increase in the viscosity (Micard et al., 2001; Pommet et al., 2005; Kunanopparat et al., 2008). Moreover, the shear stress applied by the internal mixer during mixing and the reaction between wheat gluten and glycerol could cause the increase of temperature.

### **(ii) Effect of glycerol**

Figure 9.5 shows that the torque and temperature evolution of wheat gluten was highly sensitive to the glycerol content. Glycerol is generally used as a protein plasticizer (Pommet et al., 2003). Glycerol is a small molecule able to interact through hydrogen bonding with the protein, thus reducing direct protein-protein interactions (Pommet et al., 2005; Song and Zheng, 2008). As the glycerol content increased in the sample, the torque increase became more delayed, while the maximum torque, stabilization torque and stabilization temperature obtained during the processing were decreased. The lag-time before the torque started to increase may be related to the homogenization of the samples because of the shear force that was produced by the internal mixer during mixing and the viscosity of the mixture decreased when the glycerol content increased.

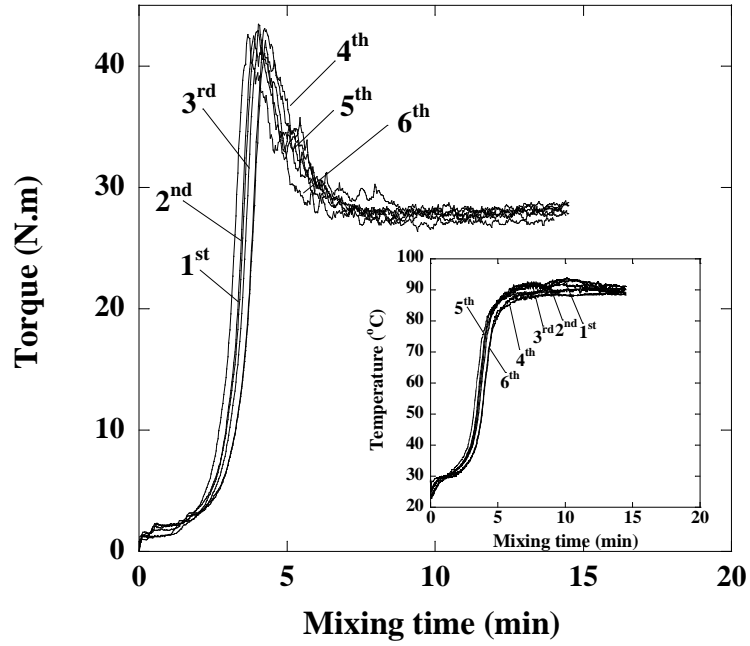


Figure 9.4 Torque and temperature evolution of controlled wheat gluten (glycerol 30%).

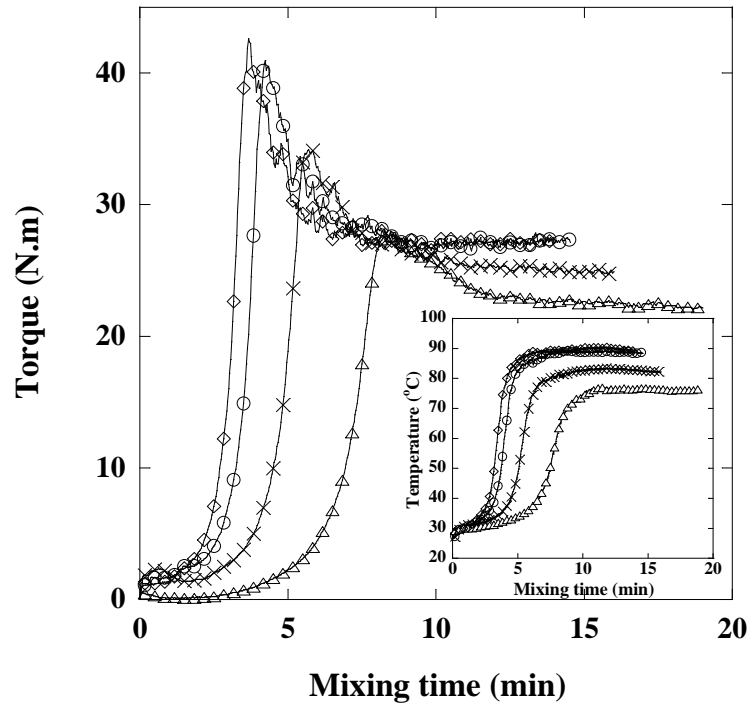


Figure 9.5 Effect of glycerol content on torque and temperature evolution of wheat gluten; controlled wheat gluten (glycerol 30%) ( $\diamond$ ), 31% ( $\circ$ ), 35% ( $\times$ ) and 40% ( $\triangle$ ).

### **(iii) Effect of KL and EL**

KL addition resulted in an increase of the stabilization torque, whereas the stabilization temperature decreased (Figure 9.6). This uncommon effect could be associated with both the presence of hydroxyl groups and the large size of the molecule when compared to a common plasticizer. During processing, wheat gluten and KL can form a crosslinking network through covalent bonds, hydrogen bonds and hydrophobic interactions (Kunanoparrat et al., 2009). The influence of the hydroxyl groups was evidenced by the finding that their suppression after esterification in EL resulted in a different evolution during the processing. Figure 9.7 shows the effect of the EL content on the torque and temperature evolution of the wheat gluten. The EL addition abolished any effect on the processing parameters of plasticized wheat gluten.

### **(iv) Effect of other additives**

Torque curves were strongly dependent on the types of additives and additive content. Three different behaviors can be identified from the curves. Vanillin, ferulic acid and coumaric acid gave the evolution very similar to the evolution of glycerol (Figures 9.8 – 9.10). This indicated that these additives acted as plasticizers of the wheat gluten. Guaiacol (Figure 9.11) and cinnamyl alcohol (Figure 9.12) also produced similar characteristics of the torque curve to those when a plasticizer was added, except that the increasing torque was not delayed. Cinnamaldehyde and *trans*-anethole exhibited a different specific behavior, as it can be observed in Figures 9.13 and 9.14. Their pattern of torque change had an irregular trend with significant oscillations that could be attributed to a wall-slip effect. Those experiments were repeated twice in order to be sure that they really corresponded to a specific behavior and not to an artifact (Figures 9.15 and 9.16). These two additives have in common the absence of hydroxyl groups, and this indicates that they did not plasticize the wheat gluten proteins.



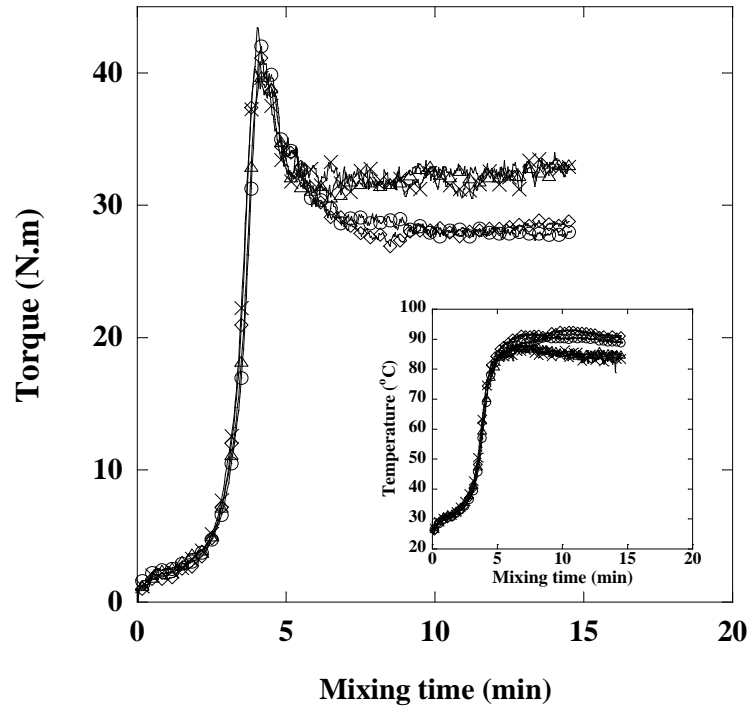


Figure 9.6 Effect of KL content on torque and temperature evolution of wheat gluten; controlled wheat gluten ( $\diamond$ ), 1% ( $\circ$ ), 5% ( $\times$ ) and 10% ( $\triangle$ ).

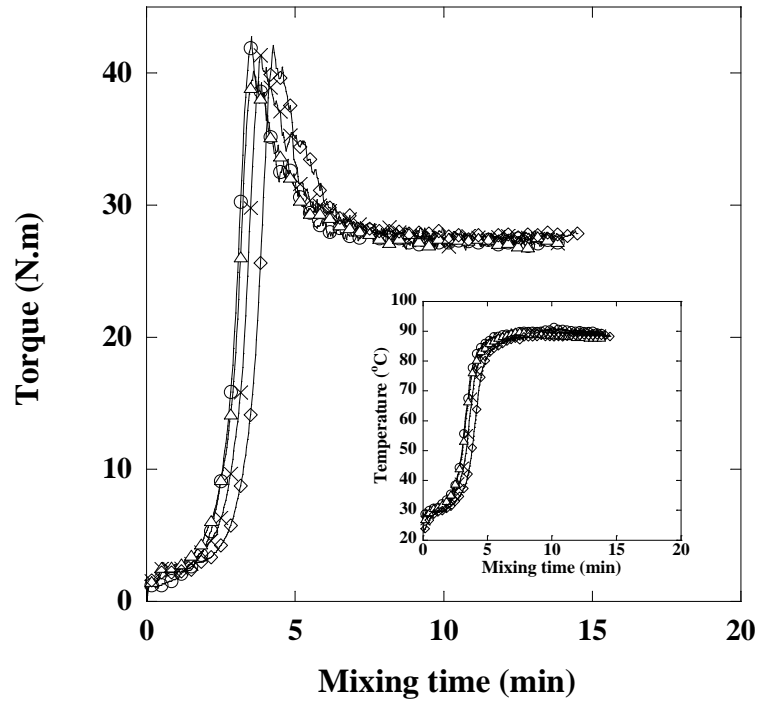


Figure 9.7 Effect of EL content on torque and temperature evolution of wheat gluten; controlled wheat gluten ( $\diamond$ ), 1% ( $\circ$ ), 5% ( $\times$ ) and 10% ( $\triangle$ ).

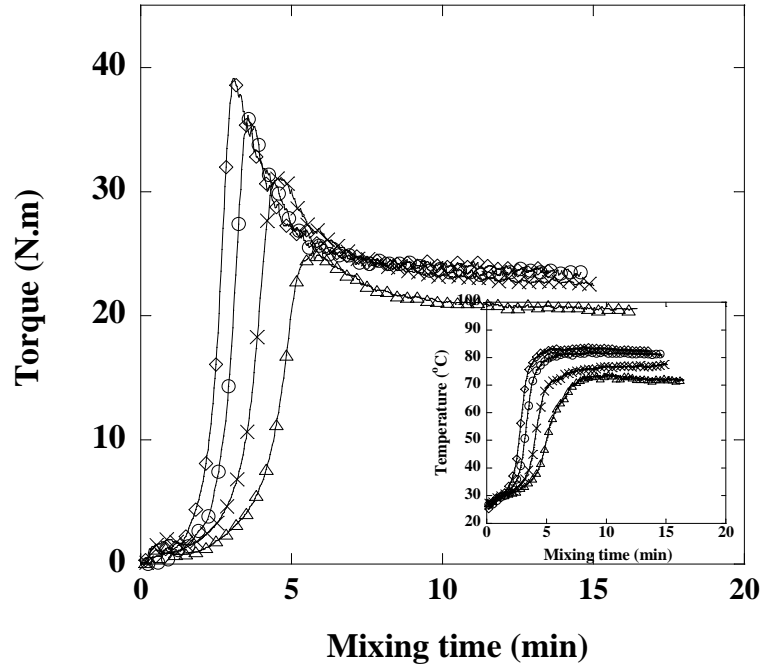


Figure 9.8 Effect of vanillin content on torque and temperature evolution of wheat gluten; controlled wheat gluten ( $\diamond$ ), 1% ( $\circ$ ), 5% ( $\times$ ) and 10% ( $\triangle$ ).

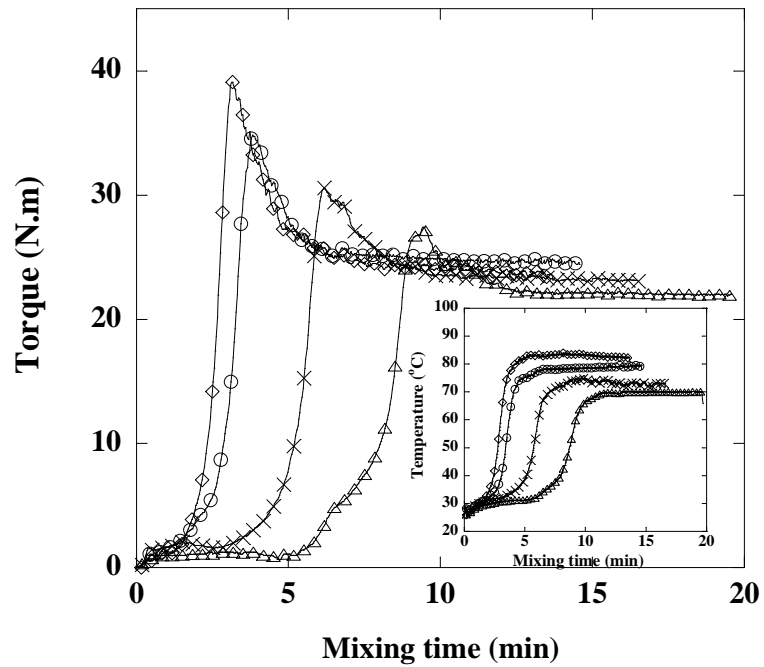


Figure 9.9 Effect of ferulic acid content on torque and temperature evolution of wheat gluten; controlled wheat gluten ( $\diamond$ ), 1% ( $\circ$ ), 5% ( $\times$ ) and 10% ( $\triangle$ ).

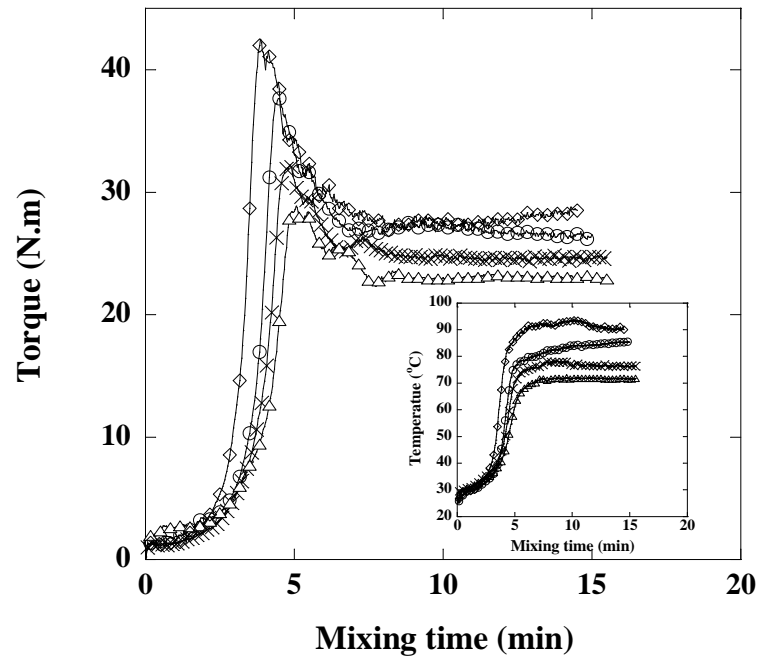


Figure 9.10 Effect of coumaric acid content on torque and temperature evolution of wheat gluten; controlled wheat gluten ( $\diamond$ ), 1% ( $\circ$ ), 5% ( $\times$ ) and 10% ( $\triangle$ ).

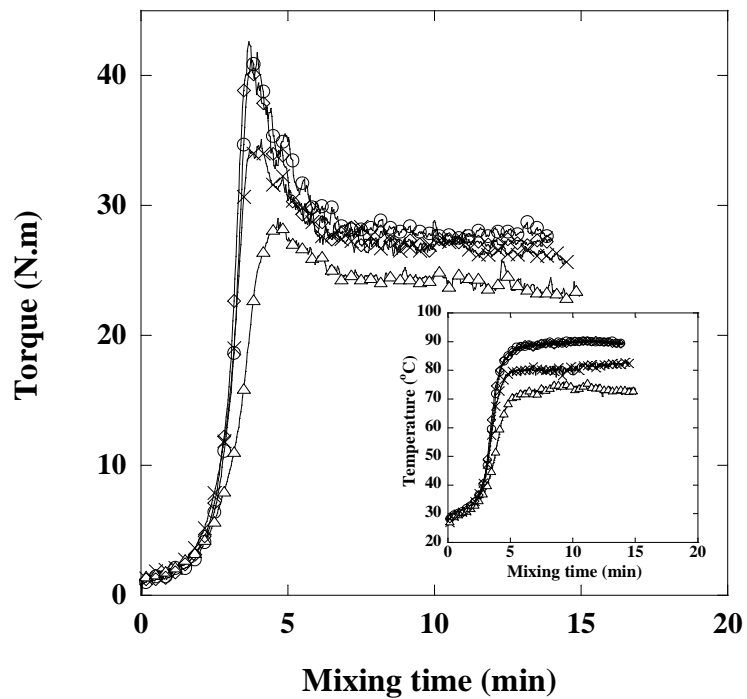


Figure 9.11 Effect of guaiacol content on torque and temperature evolution of wheat gluten; controlled wheat gluten ( $\diamond$ ), 1% ( $\circ$ ), 5% ( $\times$ ) and 10% ( $\triangle$ ).

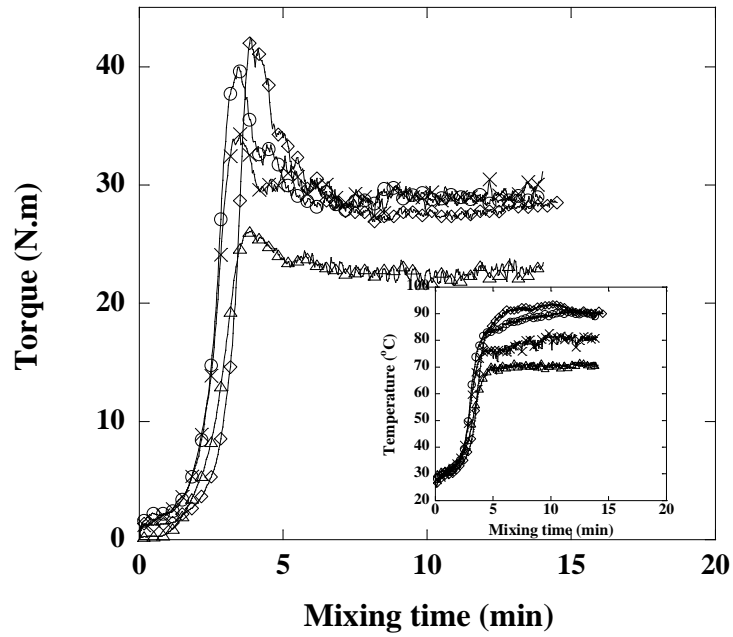


Figure 9.12 Effect of cinnamyl alcohol content on torque and temperature evolution of wheat gluten; controlled wheat gluten ( $\diamond$ ), 1% ( $\circ$ ), 5% ( $\times$ ) and 10% ( $\triangle$ ).

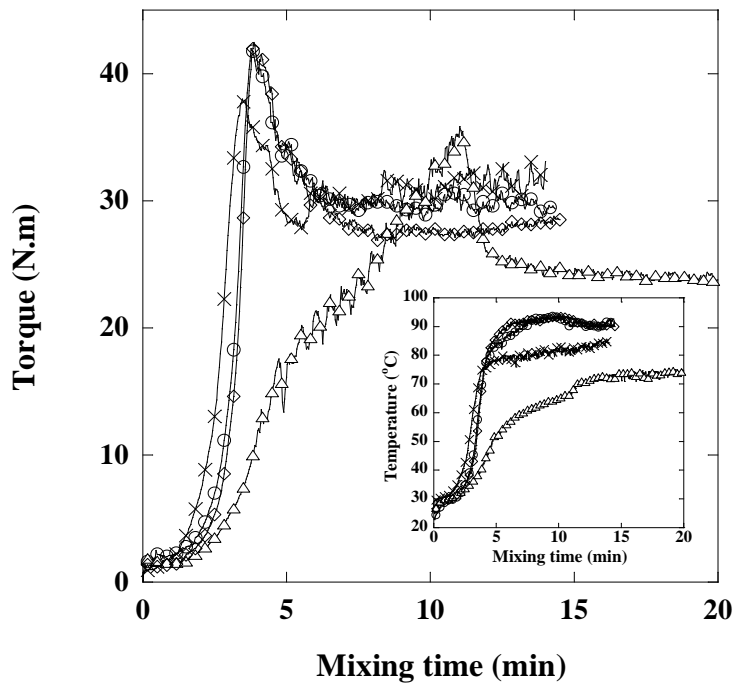


Figure 9.13 Effect of cinnamaldehyde content on torque and temperature evolution of wheat gluten; controlled wheat gluten ( $\diamond$ ), 1% ( $\circ$ ), 5% ( $\times$ ) and 10% ( $\triangle$ ).

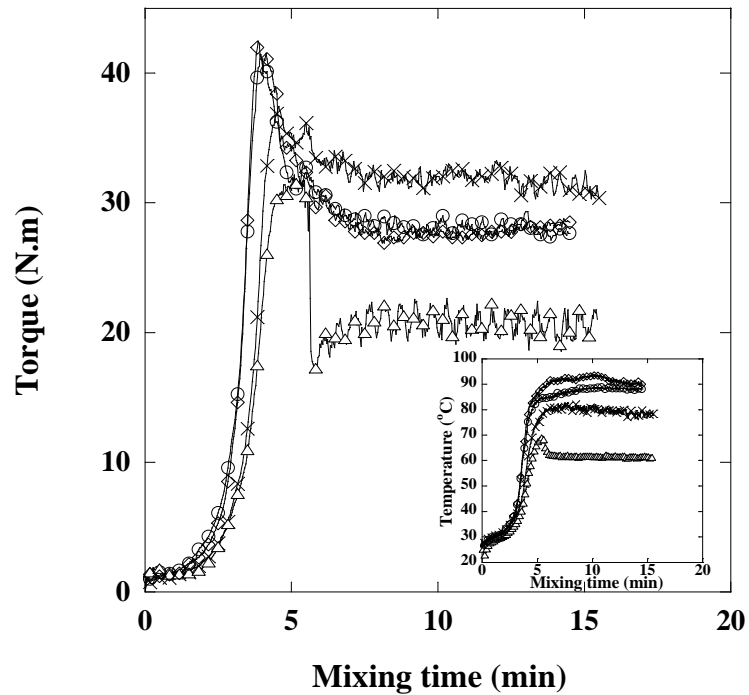


Figure 9.14 Effect of *trans*-anethole content on torque and temperature evolution of wheat gluten; controlled wheat gluten ( $\diamond$ ), 1% ( $\circ$ ), 5% ( $\times$ ) and 10% ( $\triangle$ ).

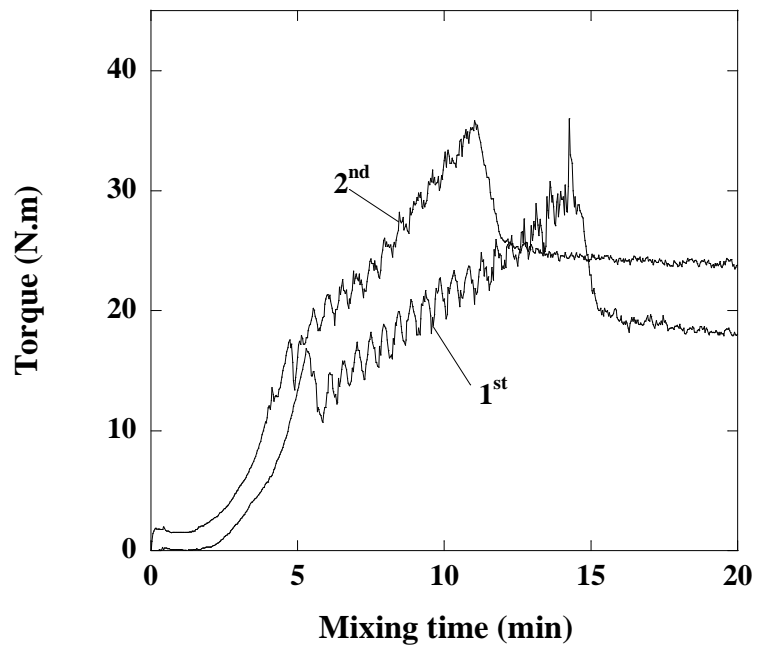


Figure 9.15 The repetition of torque evolution of wheat gluten with cinnamaldehyde 10%.

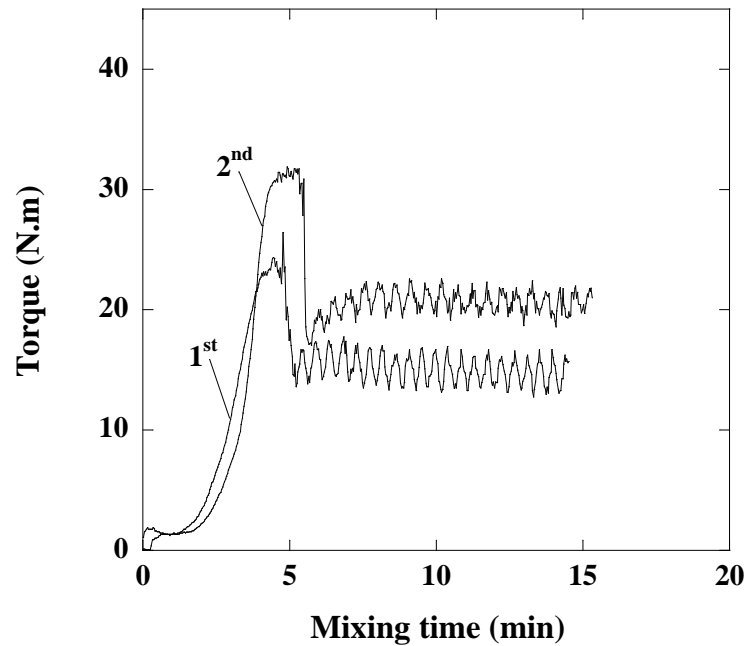


Figure 9.16 The repetition of torque evolution of wheat gluten with *trans*-anethole 10%.

### 9.3 Protein solubility during processing

During mixing, the mechanical energy transferred to the system results in the strong shear and the viscous dissipation (i.e. an increasing temperature). Both phenomena can cause the formation of intermolecular disulfide (SS) bonds between protein chains, a crosslinking which affected in a loss of their solubility in SDS solution (Micard et al., 2001; Redl et al., 2003). The measurement of the protein solubility in SDS was a simple and direct method that quantified the extent of the crosslinking. Usually, this determination was done by using a spectrophotometer that measured the absorbance in the UV spectra. However, specific interactions between additives and wheat gluten can modify the absorbance of the protein, thus making it an unsatisfactory method for this determination. In this study, the SDS-soluble protein content in the SDS solution was determined by using the Kjeldahl method that measured the quantification of the total nitrogen content.

The effect of the different types of additives and amounts of additives on the SDS-soluble protein content for the wheat gluten (without thermal treatment) is

shown in Figure 9.17. The SDS-soluble protein content of un-plasticize wheat gluten (the unprocessed and unplastitized powder) is close to 76%. After the processing in plasticized conditions of the controlled wheat gluten (glycerol 30%) resulted in the decrease of the SDS-soluble protein content up to  $56 \pm 2.50\%$ , due to protein crosslinking during mixing. The addition of 0.2 Mmol/g (or more) of KL, EL or any other additives used in this study promoted an increase in the protein extractability, in comparison with the controlled wheat gluten. Those results obviously presented the effects of those compounds on protein crosslinking formed by specific chemical interaction or by the possible protein plasticization caused by the additives.

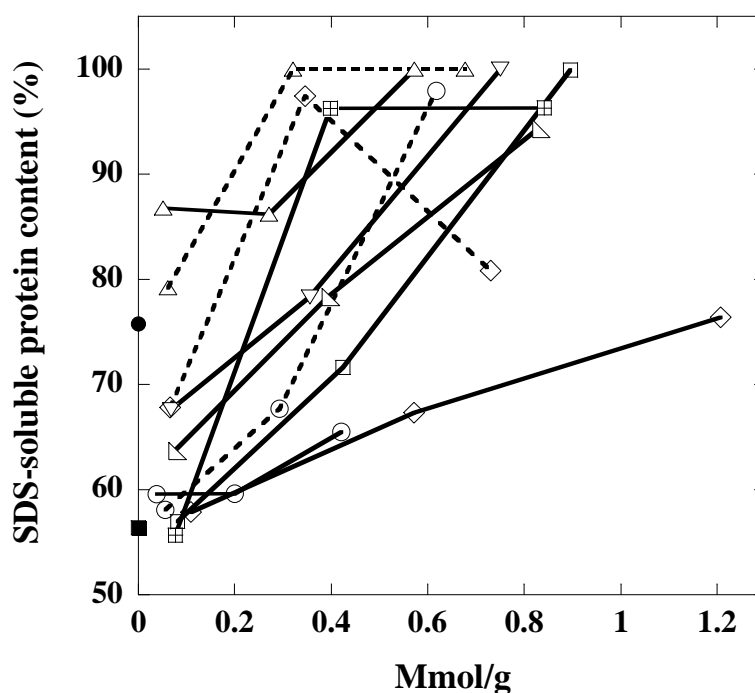


Figure 9.17 Effect of additives on the SDS-soluble protein content of wheat gluten after mixing (without thermal treatment): glycerol ( $\diamond$ , —), KL ( $\circ$ , ---), EL ( $\circ$ , —), guaiacol ( $\square$ , —), vanillin ( $\diamond$ , ---), *trans*-anethole ( $\nabla$ , —), ferulic acid ( $\triangle$ , - - -), coumaric acid ( $\triangle$ , —), cinnamaldehyde ( $\boxplus$ , —), cinnamyl alcohol ( $\blacktriangleleft$ , —); controlled wheat gluten (glycerol 30%) ( $\blacksquare$ ) and un-plasticize wheat gluten ( $\bullet$ ).

As previously observed, the addition of those additives resulted in a decrease of the temperature during mixing and this did affect the crosslinking. It could be assumed that the lower Brownian energy disfavors the disulfide bond formation in those samples. Although the evidence shows that the gluten solubility appeared to be sensitive to the glycerol content. In fact glycerol did not supposed to participate in any way in the chemical mechanisms involve in the crosslinking. This “plasticizing” or “thermal” effect necessarily affects the protein crosslinking when additives with a plasticizing effect are added. In order to eliminate this effect, all the samples were thermomolded at 100°C for 10 min, so that their thermal history can be considered to be being the same.

#### **9.4 Protein solubility after mixing and thermomolding**

The thermal treatment was carried on all the samples after mixing. Figures 9.18-9.20 show the insoluble protein content of the different samples after thermalmolding. The insoluble protein content (ISP) was simply calculated by using the equation 9.1.

$$\text{ISP} = 100 - \text{the SDS-soluble protein content} \quad (9.1)$$

The insoluble protein content is directly proportional to the extent of the protein crosslinking. It is expressed as a function of the additive concentrations expressed in Mmol/g of gluten to allow a direct comparison with the wheat gluten composition in terms of amino acids (cysteine content is assumed to be about 130  $\mu\text{mol/g}$ ).

As observed in a previous study (Kunanopparat, 2008), KL had a strong effect on protein aggregation, and inhibited the wheat gluten crosslinking and even produced a decrease in the insoluble protein content. Interestingly, KL amount was higher than the cysteine that still affected the protein solubility. It might be that some parts of the reactive groups in the Kraft lignin did not react. This was probably due to the densely interconnected structure of KL that limited their ability to interact with the protein groups. The addition of EL had only a slight effect on the protein crosslinking. The insoluble protein content of EL was very similar to that of the controlled wheat gluten



(Figure 9.18). It demonstrates that the formation of a complex between KL and wheat gluten during processing which by modifying the 3D structure of the protein was not the main reaction that influenced the protein crosslinking but the effect of KL with wheat gluten occurred through the phenol groups on the crosslinking kinetics was the main reaction. This hypothesis was confirmed by the fact that the addition of guaiacol resulted in an effect very similar to the one of the KL (Figure 9.18).

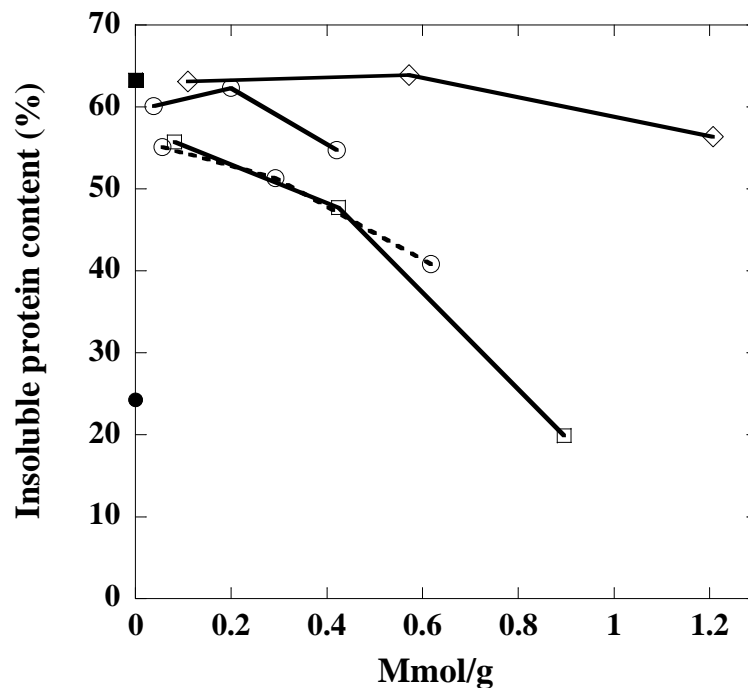


Figure 9.18 Effect of KL (○, - - -), EL (○, —), guaiacol (□, —) and glycerol (◇, —) on the insoluble protein content of wheat gluten after thermal molding; controlled wheat gluten (■) and un-plasticize wheat gluten (●).

Figure 9.19 shows the effect of guaiacol, vanillin and ferulic acid. This indicates that the effect of an aldehyde and a double bond (conjugate with acid function) on the reactivity of a phenolic additive. The protein crosslinking decreased together with an increase of the guaiacol content. The behaviour of this compound corresponds to that of KL. Guaiacol acts as a simple phenol but the ortho-methoxyl substitution increases its radical scavenging efficiency (Brand-Williams et al., 1995).

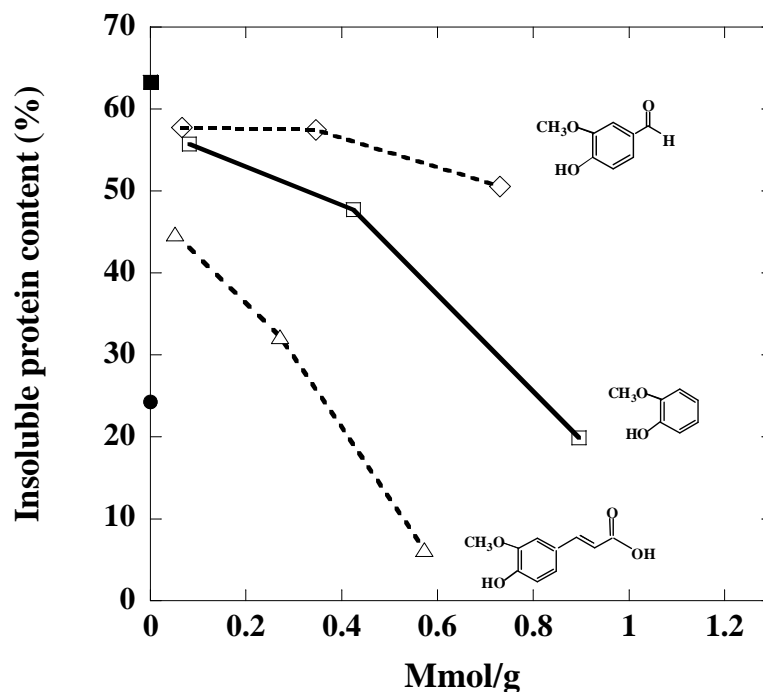


Figure 9.19 Effect of phenolic compounds on the insoluble protein content of wheat gluten after thermalmolding; controlled wheat gluten (■), un-plasticize wheat gluten (●), guaiacol (□, —), vanillin (◇, - - -) and ferulic acid (△, - · -).

It has been suggested that the ortho-methoxyl function can form intramolecular hydrogen bonds with phenolic hydrogen by making it easier to abstract the hydrogen atom from the ortho-methoxyphenols (Figure 9.20) (de Heer et al., 2000; Zhou et al., 2007). Phenoxide ion initiation occurs by abstraction of a hydroxyl hydrogen atom (Butterfield et al., 2002). Phenoxide ion is more stable to resonance than phenol because there is no charge separation in the structure of the phenoxide ion (Figures 9.21) (Brown and Foote, 2002; Cheng et al., 2007) whereas the presence of an ortho-methoxyl substitution on the benzene ring can support the radical scavenging properties of guaiacol.

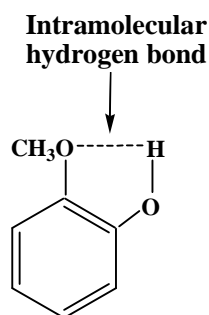


Figure 9.20 The structure of intramolecular hydrogen bond in guaiacol.

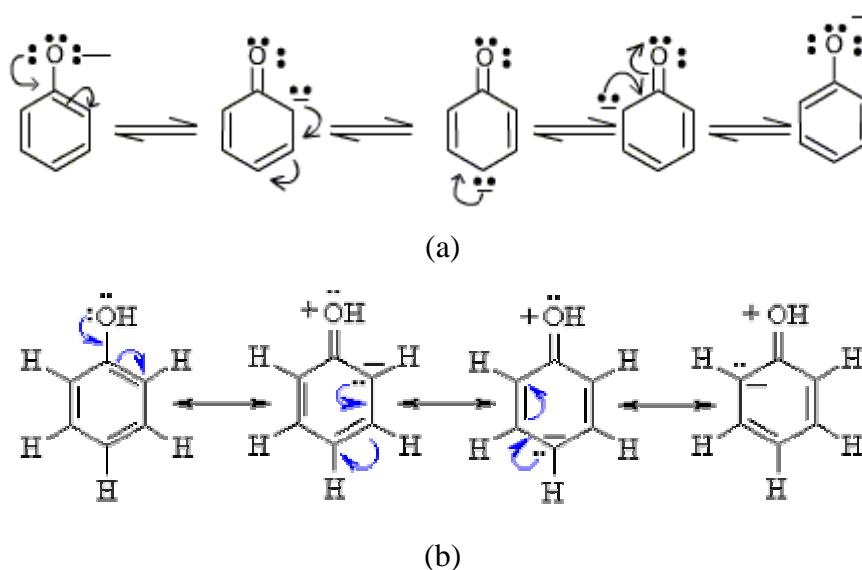


Figure 9.21 The resonance structures of phenoxide ion (a) and phenol (b) (Brown and Foote, 2002).

The addition of an aldehyde group on the phenolic structure (vanillin) inhibits the radical scavenging efficiency (Brand-Williams et al., 1995). Although, vanillin has a structure similar to the structures of guaiacol and ferulic acid, the aldehyde group in the vanillin structure caused the properties of vanillin differently from guaiacol and ferulic acid. The insoluble protein content of vanillin was higher than the insoluble protein content of guaiacol and ferulic acid because of the presence of an electron withdrawing aldehyde group in the vanillin structure (Dizhbite et al., 2004). The addition of ferulic acid strongly reduced the gluten crosslinking during processing because ferulic acid is able to react by two reactions, a radical reaction (Figure 9.22) or a nucleophilic addition reaction (Michael reaction) (Figure 9.23).

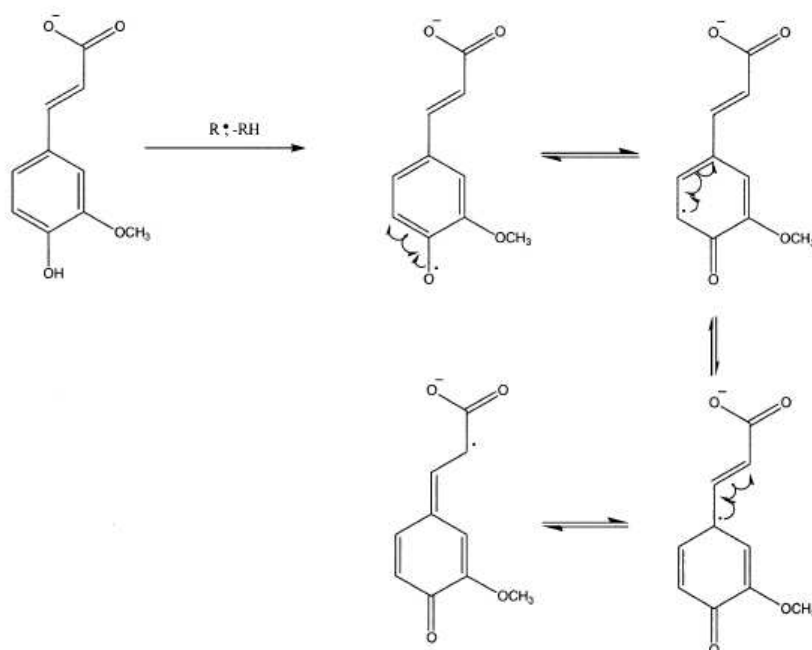


Figure 9.22 Possible resonance structures of ferulic acid phenoxyl radical (Butterfield et al., 2002).

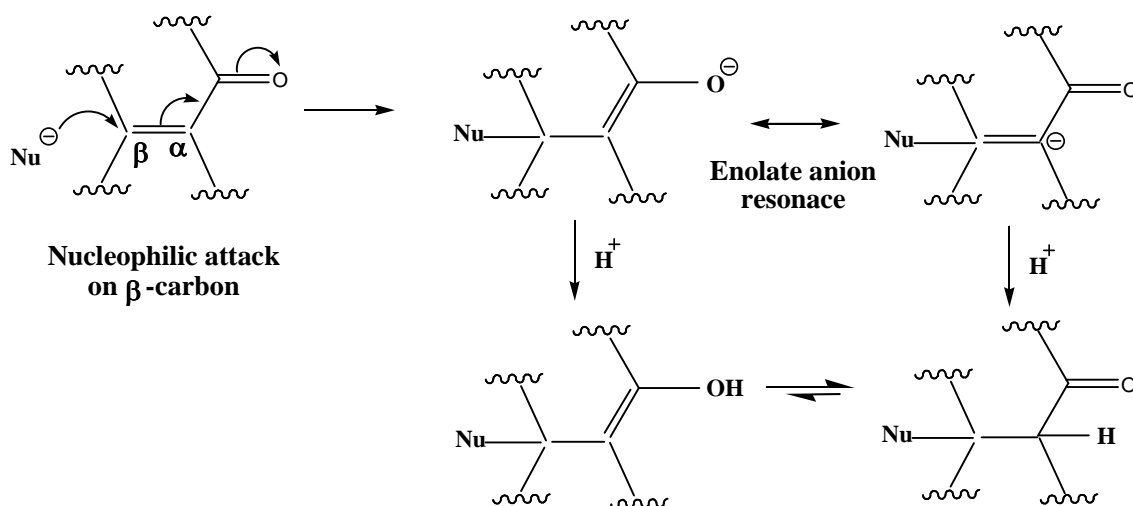


Figure 9.23 Nucleophilic addition reaction (Michael reaction) (Dewick, 2006).

The presence of electron donating groups on the benzene ring (3-methoxy and more importantly 4-hydroxyl) of ferulic acid provides an additional resonance structure of the resulting phenoxyl radical (Figure 9.22) (Butterfield et al., 2002). Conjugation of the carbonyl with a double bond of ferulic acid transfers the electronic characteristics  $\delta^+/\delta^-$  of the carbonyl group along the carbon chain, termed the Michael reaction (Figure 9.23) (Dewick, 2006). The alkene would normally be nucleophilic and react with electrophiles. When conjugated with a carbonyl, it now becomes electrophilic and reacts with nucleophiles. A typical nucleophilic attack on the  $\beta$ -position (Figure 9.23), resulting in transfer of negative charge onto the oxygen atom. The product is a resonance form of an enolate anion with a charge on the oxygen. Both the radical reaction and nucleophilic addition reaction support ferulic acid ability to react with thiyl radical ( $S^\bullet$ ) and nucleophilic species, like the thiolate anion ( $S^-$ ) which acts as a catalyst for the mechanism of protein crosslinking. Figure 9.24 provides an example of a radical reaction and a nucleophilic addition reaction of ferulic acid with a cysteine function. A similar result was observed with coumaric acid which has a very similar structure (Figure 9.25).

The effect of ferulic acid and coumaric acid was significantly more important than for guaiacol. The radical scavenging activity of polyphenolic depended not only on the rate of hydrogen atom abstraction from the phenol molecule by free radicals but also on the stability of the radical formed. The latter is increased if the phenolic structures with substituents can stabilize the free radicals. For example, ortho substituents such as methoxyl groups stabilize phenoxyl radicals by resonance as well as by hindering them from propagation. Conjugated double bonds can provide additional stabilization of the phenoxyl radicals through extended delocalization. The effect of the presence of double bonds on an aromatic structure was investigated and compared with the results previously shown for the addition of ferulic acid in order to demonstrate the effect of the conjugated double bonds on protein crosslinking (Figure 9.25). Those compounds were likely to interact with thiyls groups formed during processing. *Trans*-anethole and cinnamyl alcohol have only a slight effect on the gluten crosslinking, this effect was clearly stronger when cinamaldehyde, ferulic acid and coumaric acid were used. Cinamaldehyde produce a the stronger effect on the gluten crosslinking than *trans*-anethole and cinnamyl alcohol because cinamaldehyde

can react with thiolate anion through a nucleophilic addition reaction. This observation is strongly supported through an interaction of the conjugated double bonds and its ability to interact with thiolate anion that hindered protein crosslinking. Indeed, a nucleophilic addition reaction favored the ability of the additives that contained a double bond in their structures to react with the thiolate anion.

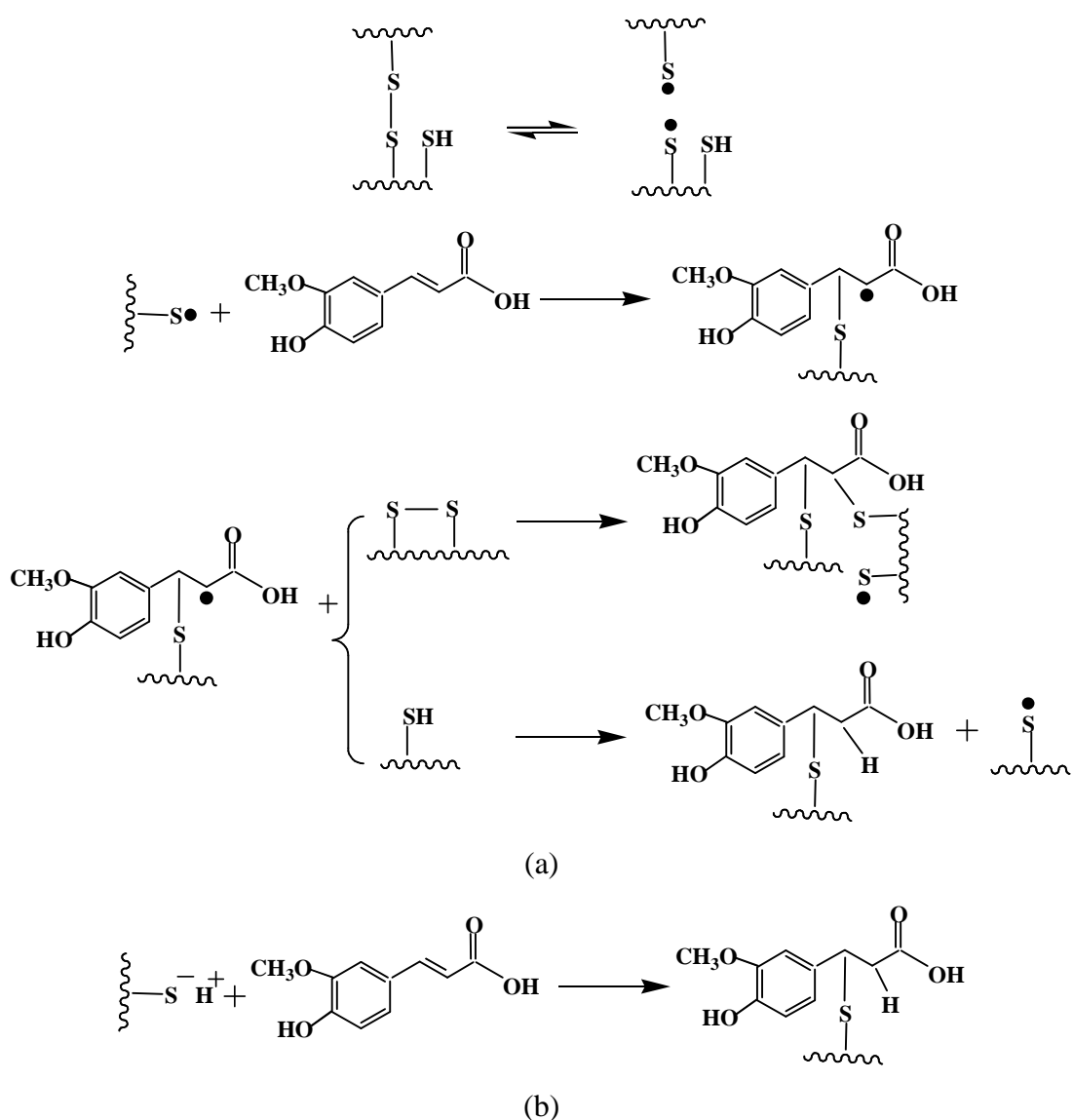


Figure 9.24 Example of radical reaction (a) and nucleophilic addition reaction (b) of ferulic acid with cysteine functions.

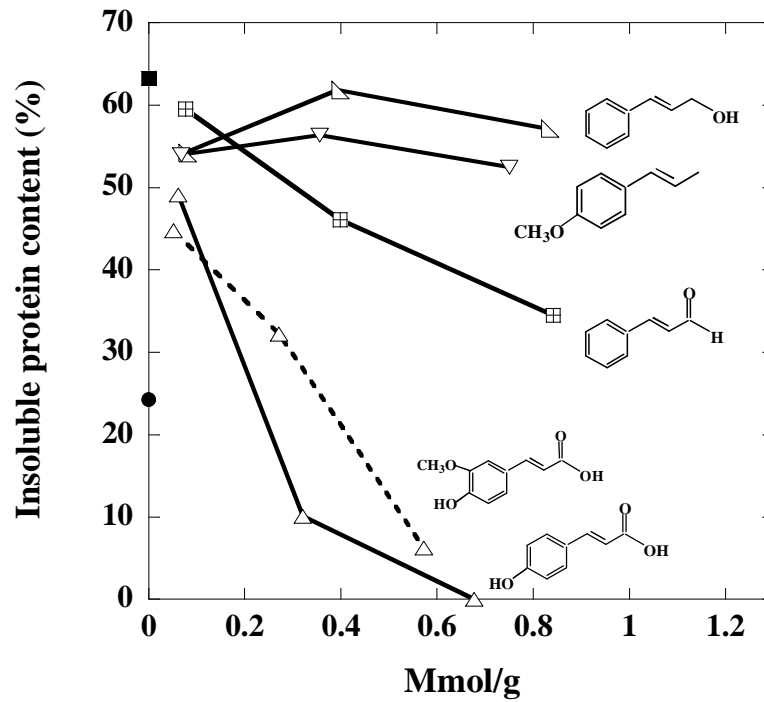


Figure 9.25 Effect of aromatics compounds containing conjugated double bonds on the insoluble protein content of wheat gluten after thermal molding; controlled wheat gluten (■), un-plasticized wheat gluten (●), ferulic acid (△, - - -), coumaric acid (△, —), cinnamaldehyde (⊠, —), cinnamyl alcohol (◄, —) and *trans*-anethole (▽, —).

## CHAPTER 10

### CONCLUSIONS

In Part II, the effects of Kraft lignin (KL), Esterified lignin (EL) and other additives on wheat gluten crosslinking and plasticization that influenced the properties of wheat gluten-based bioplastics were investigated. KL, EL and other additives presented different functional groups (i.e. conjugated double bond, hydroxyl, ester, aldehyde, carboxyl and ortho-methoxy groups). EL was produced via an esterification reaction on the KL hydroxyl groups. The chemical structures and morphology of EL were investigated by using Fourier Transform Infrared Spectroscopy (FTIR) and scanning electron microscopy (SEM), respectively. These results indicated that the hydroxyl groups in KL were changed to ester groups via the esterification reaction.

Based on torque and temperature curves, it was found that the additives that contained hydroxyl groups in their structures exhibited plasticizing properties. Both KL and EL did not act as plasticizers because they have large structures and less polarity. Mechanical mixing and thermal treatment produced wheat gluten free radicals, leading to the crosslinking of wheat gluten. Therefore, the properties of wheat gluten-based bioplastics were controlled from crosslinking and plasticization. The soluble protein content was determined by using the Kjeldahl method to identify the extent of crosslinking. The addition of more simple compounds, based on aromatic structures with additional functions, allowed for clarification of the potential role of the complex structures found in KL. The analysis mainly demonstrated the effect the phenol structures and of the conjugated double bonds. The first one was to interact with the wheat gluten crosslinking pathway through an ability to catch the radicals formed under shearing (and heating) on cysteine groups. The second one was more likely to interact with the thiolate anions formed during processing. Evidence of a similar behavior between guaiacol and KL indicated that the main interaction occurred through the aromatic hydroxyde antiradical activity. Obviously, those results demonstrated that an approach based only on the chemical interactions is sufficient to describe the effect of KL on protein crosslinking, even if it does not exclude a complementary complexation between agropolymers. This constitutes a new step in



understanding the polyphenol-protein interactions that are involved in the production and properties of new bioplastics from wheat gluten.

## References

- Ali, Y., Ghorpade, V. M. and Hanna, M. A. (1997). Properties of thermally-treated wheat gluten films. *Industrial Crops and Products*, 6, 177-184.
- Allcock, H. R. and Lampe, F. W. (1990). *Contemporary Polymer Chemistry*. Second edition. Prentice Hall. USA.
- Athawale, V. D. and Lele, V. D. (1998). Grafting copolymerization onto starch. II. Grafting of acrylic acid and preparation of its hydrogels. *Carbohydrate Polymers*, 35, 21-27.
- Athawale, V. D. and Lele, V. D. (2000). Syntheses and characterization of graft copolymers of maize starch and methacrylonitrile. *Carbohydrate Polymers*, 41, 407-416.
- Athawale, V. D. and Lele, V. D. (2000). Thermal studies on granular maize starch and its graft copolymers with vinyl monomers. *Starch/Starke*, 52, 205-213.
- Auvergne, R., Morel, M. -H., Menut, P., GianI, O., Guilbert, S. and Robin, J. -J. (2008). Reactivity of wheat gluten protein during mechanical mixing: Radical and Nucleophilic reactions for the addition of molecules on sulfur. *Biomacromolecules*, 9, 664-671.
- Averous, L. and Boquillon, N. (2004). Biocomposites based on plasticized starch: thermal and mechanical behaviours. *Carbohydrate Polymers*, 56, 111-122.
- Averous, L., Fauconnier, N., Moro, L. and Fringant, C. (2000). Blends of thermoplastic starch and polyesteramide: Processing and properties. *Journal of Applied Polymer Science*, 76, 1117-1128.

- Averous, L. and Fringant, C. (2001). Association between plasticized starch and polyesters: processing and performances of injected biodegradable systems. *Polymer Engineering and Science*, 41, 727-734.
- Averous, L., Fringant, C. and Moro, L. (2001). Plasticized starch-cellulose interactions in polysaccharide composites. *Polymer*, 42, 6565-6572.
- Barclay, L. R. C., Xi, F. and Norris, J. Q. (1997). Antioxidant properties of phenolic lignin model compounds. *Journal of Wood Chemical Technology*, 17, 73-90.
- Bettelheim, F. A. and March, J. (1990). *Introduction to Organic & Biochemistry*. Saunders College. USA.
- Bhattacharya, A. and Misra, B. N. (2004). Grafting: a versatile means to modify polymers Techniques, factors and applications. *Progress in polymer science*, 29, 767-814.
- Boeriu, C. G., Bravo, D., Gosselink, R. J. A., van Dam, J. E. G. (2004). Characterisation of structure-dependent functional properties of lignin with infrared spectroscopy. *Industrial Crops and Products*, 20, 205-218.
- Bouajila, J., Limare, A. Joly, C. and Dole, P. (2005). Lignin plasticization to improve binderless fiberboard mechanical properties. *Polymer Engineering and Science*, 45, 809-816.
- Brand-Williams, W., Cuvelier, M. E. and Berset, C. (1995). Use of a free radical method to evaluate antioxidant activity. *LWT-Food Science and Technology*, 28(1), 25-30.
- Brockway, C. E. and Moser, K. B. (2003). Grafting of poly (methyl methacrylate) to granular corn starch. *Journal of Polymer Science Part A: General Papers*, 1, 1025-1039.

- Brockway, C. E. and Seaberg, P. A. (2003). Grafting of polyacrylonitrile to granular corn starch. *Journal of Polymer Science Part A-1: Polymer Chemistry*, 5, 1313-1326.
- Brown, W. H. and Foote, C. S. (2002). *Organic Chemistry*. Third edition. Thomson Learning, Inc. USA.
- Bucio, E., Titau, G. A. and Contreras-Garcia, A. (2009). Surface modification by  $\gamma$ -ray induced grafting of PDMAEMA/PEGMEMA onto PE films. *Radiation Physics and Chemistry*, 78, 485-488.
- Bulemon, A., Colonna, P., Planchot, V., and Ball, S. (1998). Starch granules: structure and biosynthesis. *International Journal of Biological Macromolecules* 23, 85–112.
- Burton, S. G., Chigorimbo-Murefu, N. T. L. and Riva, S. (2009). Lipase-catalysed synthesis of esters of ferulic acid with natural compounds and evaluation of their antioxidant properties. *Journal of Molecular Catalysis B: Enzymatic*, 56, 277-282.
- Butterfield, D. A., Kanski, J., Aksenova, M. and Stoyanova, A. (2002). Ferulic acid antioxidant protection against hydroxyl and peroxy radical oxidation in synaptosomal and neuronal cell culture systems in vitro: structure-activity studies. *Journal of Nutritional Biochemistry*, 13, 273-281.
- Cao, Y., Qing, X., Sun, J., Zhou, F. and Lin, S. (2002). Graft copolymerization of acrylamide onto carboxymethyl starch. *European Polymer Journal*, 38, 1921-1924.
- Campbell, D., Pethrick, R. A. and White, J. R. (1989). *Polymer Characterization; Physical Techniques*. 2<sup>nd</sup> edition. Chapman and Hall. United Kingdom.

- Campbell, I. M. (1994). *Introduction Synthetic Polymers*. 1<sup>st</sup> edition. Oxford Science. New York. USA.
- Canetti, M. and Bertini, F. (2007). Supermolecular structure and thermal properties of poly(ethylene terephthalate)/lignin composites. *Composites Science and Technology*, 67, 3131-3157.
- Canatti, M., Bertini, F., de Chiric, A. and Audisio, G. (2006). Thermal degradation behaviour of isotactic polypropylene blended with lignin. *Polymer Degradation and Stability*, 91, 494-488.
- Canetti, M., De Chirico, A. and Audisio, G. (2004). Morphology, crystallization and melting properties of isotactic polypropylene blended with lignin. *Journal of Applied Polymer Science*, 91, 1435-1442.
- Charles, E. and Bin, Y. (2009). Cellulosic biomass could help meet California's transportation fuel needs. *California Agriculture*, 63, 185-190.
- Cheetham, N. W. H. and Tao, L. (1998). Variation in crystalline type with amylase content in maize starch granules: an X-ray powder diffraction study. *Carbohydrate Polymers*, 35, 277-284.
- Chen, L., Ni, Y., Bian, X., Qiu, X., Zhuang, X., Chen, X. and Jing, X. (2005). A novel approach to grafting polymerization of  $\epsilon$ -caprolactone onto starch granules. *Carbohydrate Polymers*, 60, 103-109.
- Chen, L., Qiu, X., Deng, M., Hong, Z., Luo, R., Chen, X. and Jing, X. (2005). The starch grafted poly(L-lactide) and the physical properties of its blending composites. *Polymer*, 46, 5723-5729.
- Cho, C. G. and Lee, K. (2002). Preparation of starch-g-polystyrene copolymer by emulsion polymerization. *Carbohydrate Polymers*, 48, 125-130.

- Copeland, L., Blazek, J., Salman, H. and Tang, M. C. (2009). Form and functionality starch. *Food Hydrocolloids*, 23, 1527-1534.
- Corradini, E., de Carvalho, A. J. F., de Silva Curvelo, A. A., Agenelli, J. A. M. and Mattoso, L. H. C. (2007). Preparation and Characterization of Thermoplastic Starch/Zein Blends. *Materials Research*, 10, 227-231.
- Crestini, C., Caponi, M., C., Argyropoulos, D., S. and Saladino, R. (2006). Immobilized methyltrioxo rhenium (MTO)/H<sub>2</sub>O<sub>2</sub> systems for the oxidation of lignin and lignin model compounds. *Bioorganic and Medicinal Chemistry*, 14, 5292-5302.
- de Chirico, A., Armanini, M., Chini, P., Cioccolo, G., Provasoli, F. and Audisio, G. (2003). Flame retardants for polypropylene based on lignin. *Polymer Degradation and Stability*, 79, 139-145.
- de Geaaf, R. A., Karman, A. P. and Janssen, L. P. B. M. (2003). Material properties and glass transition temperature of different thermoplastic starches after extrusion processing. *Starch/Starke*, 55, 80-86.
- de Heer, M. I., Mulder, P., Korth, H. G., Ingold, K. U. and Luszyk, J. (2000). Hydrogen atom abstraction kinetics from intramolecularly hydrogen bonded ubiquinol-10 and other (poly)methoxy phenols. *Journal of the American Chemical Society*, 122, 2355-2360.
- Dewick, P. M. (2006). *Essentials of Organic Chemistry for students of pharmacy, medicinal chemistry and biological chemistry*. John Wiley & Sons. USA.
- Dizhbite, T., Telysheva, G., Jurkjane, V. and Viesturs, U. (2004). Characterization of the radical scavenging activity of lignin-natural antioxidants. *Bioresource Technology*, 95, 309-317.

- Domenek, S., Feuilloley, P., Gratraud, J., Morel, M. –H. and Guilbert, S. (2004). Biodegradability of wheat gluten based bioplastics. *Chemosphere*, 54, 551-559.
- Don, T. –M., Lai, S. –M., Liu, Y. –H. and Chiu, W. –Y. (2006). Graft polymerization of vinyl acetate onto granular starch: Comparison on the potassium persulfate and ceric ammonium nitrate initiated system. *Journal of Applied Polymer Science*, 102, 3017-3027.
- Donald, A. M., Waigh, T. A., Jenkins, P. J., Gidley, M. J., Debet, M. and Smith, A. (1997). Internal structure in: *Starch Structure and Functionality*. Cambridge: The Royal Society of Chemistry, 172-179.
- Eliasson, A. C. (2000). *Starch in food*. CRC . USA.
- Ezekiel, R., Rana, G., Singh, N., and Singh, S. (2007). Physicochemical, thermal and pasting properties of starch separated from c-irradiated and stored potatoes. *Food Chemistry*, 105, 1420-1429.
- Fakhouri, F. M., Tanada-Palmu, P. S. and Grosso, C. R. F. (2004). Characterization of composite biofilms of wheat gluten and cellulose acetate phthalate. *Brazilian Journal of Chemical Engineering*, 21, 261-264.
- Fang, J. M. Fowler, P. A. and Hill, C. A. S. (2005). Studies on the grafting of acryloylated potato starch with styrene. *Journal of Applied Polymer Science*, 96, 452-459.
- Fang, Y., Chen, P., Zhang W. and Luo, W. (2004). Synthesis of superabsorbent polymers by irradiation and their applications in agriculture. *Journal of Applied Polymer Science*, 93, 1748-1755.

- Fang, Y., Chen, P., Zhang W. and Luo, W. (2005). Synthesis and properties of starch grafted poly[acrylamide-co-(acrylic acid)]/montmorillonite nanosuperabsorbent via  $\gamma$ -ray radiation technique. *Journal of Applied Polymer Science*, 96, 1341-1346.
- Fanta, G. F., Burr, R. C., Doane, W. M. and Russell, C. R. (1975). Graft polymerization of styrene onto starch by simultaneous cobalt-60 irradiation. *Journal of Applied Polymer Science*, 21, 425-433.
- Fried, J. R. (2003). *Polymer and Technology*. 2<sup>nd</sup> edition. Prentice Hall Professional Technical Reference. USA.
- Geresh, S., Gilboa, Y., Peisahov-Korol, J., Gdalevsky, G., Voorspoels, J., Remon, J. P. and Kost, J. (2002). Preparation and characterization of bioadhesive grafted starch copolymers as platforms for controlled drug delivery. *Journal of Applied Polymer Science*, 86, 1157-1162.
- Gomez-Martinez, D., Partal, P., Martinez, I. and Gallegos, C. (2009). Rheological behaviour and physical properties of controlled-release gluten-based bioplastics. *Bioresource Technology*, 100, 1828-1832.
- Graf, E. (1992). Antioxidant potential of ferulic acid. *Free Radical Biology and Medicine*, 13, 435-448.
- Gregorova, A., Cibulkova, Z., Kosikova, B. and Simon, P. (2005). Stabilization effect of lignin in polypropylene and recycled polypropylene. *Polymer Degradation and Stability*, 89, 553-558
- Gregorova, A., Kosikova, B. and Moravcik, R. (2006). Stabilization effect of lignin in natural rubber. *Polymer Degradation and Stability*, 91, 229-233.



- Gruner, W., Halber, J., Barth, P., Behm, J. and Sunderkotter, L. (2009). The precise determination of nitrogen in boron nitride. *Journal of the European Ceramic Society*, 29, 2029-2035.
- Guo, X., Zhang, S. and Shan, X. -Q. (2008). Adsorption of metal ions on lignin. *Journal of Hazardous Materials*, 151, 134-142.
- Guo, Y. and Rockstraw, D. A. (2006). Physical and chemical properties of carbons synthesized from xylan, cellulose and Kraft lignin by H<sub>3</sub>PO<sub>4</sub> activation. *Carbon*, 44, 1464-1475.
- Hamdam, S., Hashim, D. M. A., Ahmad, M. and Embong, S. (2000). Compatibility studies of polypropylene (PP)-sago starch (SS) blends using DMTA. *Journal of Polymer Research*, 7, 237-244.
- Hayta, M. and Schofield, J. D. (2004). Heat and additive induced biochemical transitions in gluten from good and poor breadmaking quality wheats. *Journal of Cereal Science*, 40, 245-256.
- Hebeish, A., Beliakova, M. K. and Bayazeed, A. (1998). Improved synthesis of poly(MAA)-starch graft copolymers. *Journal of Applied Polymer Science*, 68, 1709-1715.
- Henderson, A. M. and Rudin, A. (1981). Effects of water, methanol, and ethanol on the production of starch-g-polystyrene copolymers by cobalt-60 irradiation. *Journal of Polymer Science: Polymer Chemistry Edition*, 19, 1707-1719.
- Hernandez-Munoz, P., Villalobos, R. and Chiralt, A. (2004). Effect of thermal treatments on functional properties of edible films made from wheat gluten fractions. *Food Hydrocolloids*, 18, 647-654.

- Hochstetter, A., Talja, R. A., Helen, H. J., Hyvonen, L. and Jouppila, K. (2006). Preparation of gluten-based sheet produced by twin-screw extruder. *LWT-Food Science and Technology*, 39, 893-901.
- Holme, D. J. and Peck, H. (1993). *Analytical Biochemistry*. Longman Singapore Publishers. 2<sup>nd</sup> edition. Singapore.
- Holmgren, A., Norgren, M., Zhang, L. and Henriksson G. (2009). On the role of the monolignol  $\gamma$ -carbon functionality in lignin biopolymerization. *Phytochemistry*, 70, 147-155.
- Hoseney, R. C. (1998). *Principles of cereal science and technology*. 2<sup>nd</sup> edition. The American Association of Cereal Chemists, Inc. USA.
- Huang, J., Zhang, L. and Chen, F. (2003) Effects of lignin as a filler on properties of soy protein plastics. I. Lignosulfonate. *Journal of Applied Polymer Science*, 88, 3284–3290 (a).
- Huang, J., Zhang, L. and Chen, F. (2003) Effects of lignin as a filler on properties of soy protein plastics. II. Alkaline lignin. *Journal of Applied Polymer Science*, 88, 3291–3297 (b).
- Ikan, R. (1991). *Natural Products*. 2<sup>nd</sup> edition. Academic Press, Inc. USA.
- Irission-Mangata, J., Bauduin, G., Boutevin, B. and Gontard, N. (2001). New plasticizers for wheat gluten films. *European Polymer Journal*, 37, 1533-1541.
- Janarthanan, P., Yunus, W. M. Z. W. and Ahmad, M. B. (2003). Thermal behavior and surface morphology studies on polystyrene grafted sago starch. *Journal of Applied Polymer Science*, 90, 2053–2058.

- Jerez, A., Partal, P., Martinez, I., Gallegos, C. and Guerrero, A. (2005). Rheology and processing of gluten based bioplastics. *Biochemical Engineering Journal*, 26, 131-138.
- Jiang, W., Qiao, X. and Sun, K. (2006). Mechanical and thermal properties of thermoplastic acetylated starch/poly(ethylene-co-vinyl alcohol) blends. *Carbohydrate Polymers*, 65, 139-143.
- Jittima, I. (2002). Screening of lignocellulosic-degrading enzymes from basidiomycetes isolated from forests in Thailand. Thesis. School of bioresources and technology, King Monkut's University of Technology Thonburi.
- Jiugao, Y., Ning, W. and Xiaofei, M. (2005). The effect of citric acid on the properties of thermoplastic starch plasticized by glycerol. *Starch/Starke*, 57, 494-504.
- Junsomboon, J. and Jakmune, J. (2008). Flow injection conductometric system with gas diffusion separation for the determination of Kjeldahl nitrogen in milk and chicken meat. *Analytica Chimica Acta*, 627, 232-238.
- Kasprzycka-Guttman, T. and Odzeniak, D. (1994). Antioxidant properties of lignin and its fractions. *Thermochimica Acta*, 231, 161-168.
- Kayseriliolu, B., Stevels, W. M., Mulder, W. J. and Akka, N. (2001). Mechanical and biochemical characterisation of wheat gluten films as a function of pH and co-solvent. *Starch-Starke*, 53, 381-386.
- Khalil, M. I., Mostafa, Kh. M. and Hebeish, A. (1993). Graft polymerization of acrylamide onto maize starch using potassium persulfate as initiator. *Macromolecular Material and Engineering*, 213, 43-54.

- Kiatkamjornwong, S., Sonsuk, M. and Chomsaksakul, W. (2000). Radiation modification of water absorption of cassava starch by acrylic acid/acrylamide. *Radiation Physics and Chemistry*, 59, 413-427.
- Kiatkamjornwong, S., Sonsuk, M., Wittayapichet, S., Prasassarakich, P. and Vejjanukroh, P. (1999). Degradation of styrene-g-cassava starch filled polystyrene plastics. *Polymer Degradation and Stability*, 66, 323-335.
- Kiatkamjornwong, S., Lanthong, P. and Nuisin, R. (2006). Graft copolymerization, characterization and degradation of cassava starch-g-acrylamide, itaconic acid superabsorbents. *Carbohydrate Polymers*, 66, 229-245.
- Kubo, S. and Kadla, J. F. (2005). Kraft lignin/poly(ethylene oxide) blends: Effect of lignin structure on miscibility and hydrogen bonding. *Journal of Applied Polymer Science*, 98, 1437-1444.
- Kumar, A. and Gupta, R. K. (1998). *Fundamentals of Polymers*. International edition. McGraw-Hill. Singapore.
- Kunanopparat, T. (2008). Reactivity of Kraft lignin/wheat gluten blends upon biomaterials processing. Thesis. SupAgro, Montpellier, France.
- Kunanopparat, T., Menut, P., Morel, M. –H. and Guilbert, S. (2008). Reinforcement of plasticized wheat gluten with natural fibers: From mechanical improvement to deplasticizing effect. *Composites: Part A*, 39, 777-785.
- Lagrain, B., Thewissen, B. G., Brijs, K. and Delcour, J. A. (2008). Mechanism of gliadin-glutenin cross-linking during hydrothermal treatment. *Food Chemistry*, 107, 753-760.
- Laohakunijit, N. and Noomhorm, A. (2004). Effect of plasticizers on mechanical and barrier properties of rice starch film. *Starch/Starke*, 56, 348-356.

- Lee, E. J., Kweon, D. K., Koh, B. K. and Lim, S. T. (2004). Physical characteristics of sweet potato pulp/polycaprolactone blends. *Journal of Applied Polymer Science*, 92, 862-866.
- Lee, S. L., Lee, M. S. and Song, K. B. (2005). Effect of gamma-irradiation on the physicochemical properties of gluten films. *Food Chemistry*, 92, 621-625.
- Lewin, M. and Goldstein, I. (1991). *Wood structure and composition*. Marcel Dekker Inc, New York.
- Lindeboom, N., Chang, P. R. and Tyler, R. T. (2004). Analytical, biochemical and physicochemical aspects of starch granule size with emphasis on small granule starches: a review. *Starch*, 56, 89-99.
- Liao, H. T. and Wu, C. S. (2009). Preparation and characterization of ternary blends composed of polylactide, poly( $\epsilon$ -caprolactone) and starch. *Materials Science and Engineering A*, 515, 207-214.
- Liu, N., Shi, S., Gao, Y. and Qin, M. (2009). Fiber modification of Kraft pulp with laccase in presence of methyl syringate. *Enzyme and Microbial Technology*, 44, 89-95.
- Lora, J. H. and Glasser, W. G. (2002). Recent industrial applications of lignin: A sustainable alternative to nonrenewable materials. *Journal of Polymers and the Environment*, 10, 39-48.
- Lyer, V., Varadarajan, P. V., Sawakhande, K. H. and Nachane, N. D. (1990). Preparation of superabsorbents by gamma-ray radiation. *Journal of Applied Polymer Science*, 39, 2259-2265.
- Ma, X. F., Yu, J. G. and Wan, J. J. (2006). Urea and ethanolamine as a mixed plasticizer for thermoplastic starch. *Carbohydrate Polymer*, 64, 267-273.

- Manners, D. J. (1989). Recent developments in our understanding of amylopectin structure. *Carbohydrate Polymers*, 11, 87-112.
- Mano, J. F., Koniarova, D. and Reis, R. L. (2003). Thermal properties of thermoplastic starch/synthetic polymer blends with potential biomedical applicability. *Journal of Materials Science: Materials in Medicine*, 14, 127-135.
- McGinnic and Shafizadec. (1991). Cellulose in wood structure and composition, In: wood structure and composition. Marcel Dekker, Inc. USA.
- Meng, Y. Z., Ge, X. C. and Li, R. K. Y. (2005). Thermal and mechanical properties of biodegradable composites of poly(propylene carbonate) and starch-poly(methyl acrylate) graft copolymer. *Composites Science and Technology*, 65, 2219-2225.
- Merrill, A. L. and Watt, B. K. (1973). Energy value of foods: basis and derivation; Agriculture Handbook No 74. ARS. Washington. USA.
- Micard, V., Morel, M. –H. Bonicel, J. and Guilbert, S. (2001). Thermal properties of raw and processed wheat gluten in relation with protein aggregation. *Polymer*, 42, 477-485.
- Min, Z., Song, Y. and Zheng, Q. (2008). Influence of reducing agents on properties of thermo-molded wheat gluten bioplastics. *Journal of Cereal Science*, 48, 794-799.
- Mohan, D., Pittman, C. U. J. and Steele, P. H. (2006). Single, binary and multi-component adsorption of copper and cadmium from aqueous solutions on Kraft lignin-a biosorbent. *Journal of Colloid and Interface Science*, 297, 489-504.

- Morck, R.; Kringstad, K. P. (1985).  $^{13}\text{C}$ -NMR Spectra of Kraft Lignins - II. Kraft Lignin Acetates. *Holzforschung*, 39(2), 109-119.
- Nadji, H., Diouf, P. N., Benaboura, A., Bedard, Y., Riedl, B. and Stevanovic, T. (2009). Comparative study of lignin isolated from Alfa grass (*Stipa tenacissima L.*). *Bioresource Technology*, 100, 3585-3592.
- Nimz, H. (1974). Beech lignin—Proposal of a constitutional scheme. *Angewandte Chemie-International Edition*, 13, 313-321.
- Noda, T., Isono, N., Krivandin, A. V., Shatalova, O. V., Blaszcak, W. and Yuryev, V. P. (2009). Origin of defects in assembled supramolecular structures of sweet potato starches with different amylopectin chain-length distribution. *Carbohydrate Polymers*, 76, 400-409.
- Odian, G. 1991. *Principles of Polymerization*. 3<sup>rd</sup> edition. John Wiley & Sons. USA.
- Orts, W. J., Nobes, G. A. R., Glenn, G. M., Gray, G. M., Imam, S. and Chiou, B. -S. (2007). Blends of starch with ethylene vinyl alcohol copolymers: effect of water, glycerol and amino acids as plasticizers. *Polymer for advanced technologies*, 18, 629-635.
- Ouellette, R. J. (1998). *Organic Chemistry; A brief introduction*. Prentice-Hall, Inc. New Jersey, USA.
- Park, H. J. and Chinnan, M. S. (1995). Gas and water vapour barrier properties of edible films from protein and cellulosic materials. *Journal of Food Engineering*, 25, 497-507.

- Park, S. K. and Bae, D. H. (2006). Antimicrobial properties of wheat gluten-chitosan composite film in intermediate-moisture food systems. *Food Science and Biotechnology*, 15, 133-137.
- Patil, D. R. and Fanta, G. F. (1995). Synthesis and processing of graft copolymers prepared from cereal flour and methyl acrylate. *Starch/Starke*, 47, 110-115.
- Patra, C. M. and Singh, B. C. (1994). Influence of N-acetylglycine on the kinetics of the ceric-initiated graft copolymerization of acrylonitrile and methyl methacrylate onto jute fibers. *Journal of Applied Polymer Science*, 52, 1557-1568.
- Pimpan, V. and Thothong, P. (2006). Synthesis of Cassava Starch-g-Poly(methyl methacrylate) Copolymers with Benzoyl Peroxide as an Initiator. *Journal of Applied Polymer Science*, 101, 4083-4089.
- Pommet, M., Redl, A., Morel, M. –H. and Guilbert, S. (2003). Study of wheat gluten plasticization with fatty acids. *Polymer*, 44, 115-122.
- Pommet, M., Redl, A., Morel, M. –H. and Guilbert, S. (2005). Intrinsic influence of various plasticizers on functional properties and reactivity of wheat gluten thermoplastic materials. *Journal of Cereal Science*, 42, 81-91.
- Pontes, F. V. M., Carneiro, M. C., Vaitsman, D. S., da Rocha, G. P., da Silva, L. I. D., Neto, A. A. and Monteiro, M. I. C. (2009). A simplified version of the total kjeldahl nitrogen method using an ammonia extraction ultrasound-assisted purge-and-trap system and ion chromatography for analyses of geological samples. *Analytica Chimica Acta*, 632, 284-288.
- Pouplin, M., Redl, A. and Gontard N. (1999). Glass transition of wheat gluten plasticized with water, glycerol, or sorbitol. *Journal of Agricultural and Food Chemistry*, 47(2), 538-543.



- Pouteau, C., Baumberger, S., Cathala, B. and Dole, P. (2004). Lignin-polymer blends: evaluation of compatibility by image analysis. *Comptes Rendus Biologies*, 327, 935-943.
- Pouteau, C., Cathala, B., Dole, P., Kurek, B. and Monties, B. (2005). Structure modification of Kraft lignin after acid treatment : characterisation of the apolar extracts and influence on the antioxidant properties in polypropylene. *Industrial Crops and Products*, 21, 101-108.
- Pouteau, C., Dole, P., Cathala, B., Averous, L. and Boquillon, N. (2003). Antioxidant properties of lignin in polypropylene. *Polymer Degradation and Stability*, 81, 9-18.
- Pucciariello, R., Villani, V., Bonini, C., Auria, M. D. and Vetere, T. (2004). Physical properties of straw lignin-based polymer blends. *Polymer*, 45, 4159-4169.
- Qudsieh, I. Y. M., Fakhral-Razi, A., Muyibi, S. A., Ahmad, M. B., Rahman, M. Z. A. and Yunus, W. M. Z. W. (2004). Preparation and characterization of poly(methyl methacrylate) grafted sago starch using potassium persulfate as redox initiator. *Journal of Applied Polymer Science*, 94, 1891-1897.
- Qudsieh, I. Y. M., Fakhurul-Razi, A., Yunus, W. M. Z. W., Ahmad, M. B. and Rahman, M. Z. A. (2001). Graft copolymerization of methyl methacrylate onto sago starch using ceric ammonium nitrate and potassium persulfate as redox initiator systems. *Journal of Applied Polymer Science*, 82, 1375-1381.
- Redl, A., Guilbert, S. and Morel, M. -H. (2003). Heat and shear mediated polymerisation of plasticized wheat gluten protein upon mixing. *Journal of Cereal Science*, 38, 105-114.
- Rehm, H. -J. and Reed, G. (1996). *Biotechnology. Second, Completely revised edition. Volume 6. Products of Primary Metabolism.* VCH. New York. USA.

- Rosell, C. M. and Foegeding, A. (2007). Interaction of hydroxypropylmethylcellulose with gluten properties: Small deformation properties during thermal treatment. *Food Hydrocolloids*, 21, 1092-1100.
- Roz, A. L. D., Carvalho, A. J. F., Gandini, A. and Curvelo, A. A. A. S. (2006). The effect of plasticizers on thermoplastic starch compositions obtained by melt processing. *Carbohydrate Polymers*, 63, 417-424.
- Rudnik, E., Matuschek, G., Milanov, N. and Kettrup, A. (2005). Thermal properties of starch succinates. *Thermochimica acta*, 427, 163-166.
- Sacak, M. and Celik, M. (2002). Synthesis and characterization of starch-poly(methyl methacrylate) graft copolymers. *Journal of Applied Polymer Science*, 86, 53-57.
- Sangramsingh, N. M., Patra B. N., Singh, B. C. and Patra, C. M. (2004). Graft copolymerization of Methyl Methacrylate onto starch using a Ce(IV)-Glucose initiator system. *Journal of Applied Polymer Science*, 91, 981-990.
- Sarni-Manchado, P., Cheynier, V. and Moutounet, M. (1999). Interactions of grape seed tannins with salivary proteins. *Journal of Agricultural and Food Chemistry*, 47, 42-47.
- Schmidt, J. A., Rye, C. S. and Gurnagul, N. (1995). Lignin inhibits autoxidative degradation of cellulose. *Polymer Degradation and Stability*, 49, 291-297.
- Schofield, J. D., Bottomley, R. C., Timms, M. F. (1983). The effect of heat on wheat gluten and the involvement of sulphhydryl-disulphide interchange reaction. *Journal of Cereal Science*, 1, 241-253.

- Severtson, S. and Guo, J. (2002). Influence of ozonized Kraft lignin on the crystallization of CaCO<sub>3</sub>. *Journal of Colloid and Interface Science*, 249, 423-431.
- Shi, R., Liu, Q., Ding, T., Han, Y., Zhang, L., Chen, D. and Tian, W. (2007). Ageing of soft thermoplastic starch with high glycerol content. *Journal of Applied Polymer Science*, 103, 574-586.
- Shujun, W., Jinglin, Y. and Wenyuan, G. (2005). Use of X-ray diffractometer (XRD) for identification of *Fritillaria* according to geographical origin. *American Journal of Biochemistry and Biotechnology*, 1 (4), 207-211.
- Silong, S., Rahman, L., Zin, W. M., Rahman, M. Z. A., Ahmad, M. and Haron, J. (2000). Graft copolymerization of methyl acrylate onto sago starch using ceric ammonium nitrate as an initiator. *Journal of Applied Polymer Science*, 76, 516-523.
- Sing, R. P., Pal, S. and Mal, D. (2005). Cationic starch: an effective flocculating agent. *Carbohydrate Polymers*, 59, 417-423.
- Singh, V., Tiwari, A., Pandey, S. and Singh, S. K. (2006). Microwave-accelerated synthesis and characterization of potato starch-g-poly(acylamine). *Starch/Starke*, 58, 536-543.
- Soest, J. J. G. and Borger, D. B. (1996). Structure and properties of compression-molded thermoplastic starch materials from normal and high-amylose maize starches. *Journal of Applied Polymer Science*, 64, 631-644.
- Soest, J. J. G., Wit, D. D. and Vliegthart, J. F. G. (1996). Mechanical properties of thermoplastic waxy maize starch. *Journal of Applied Polymer Science*, 61, 1927-1937.

- Song, Y. and Zheng, Q. (2008). Improved tensile strength of glycerol-plasticized gluten bioplastic containing hydrophobic liquids. *Bioresource Technology*, 99, 7665-7671.
- Souza, R. C. R. and Andrade, C. T. (2002). Investigation of the gelatinization and extrusion processes of corn starch. *Advances in polymer technology*, 21, 17-24.
- Steinbuchel, A. and Rhee, S. K. (2005). *Polysaccharides and Polyamides in the Food Industry*. Volume 1. The Federal Republic of Germany.
- Suat, K. (2001). Grafting of 1-Vinyl 2-Pyrrolidone into starch using azobisisobutyronitrile initiator. Thesis. Fen Edebiyat Fakültesi, Kimya Bölümü, Teknikokullar, Ankara, Gazi University, Turkey.
- Sun, S., Song, Y. and Zheng, Q. (2007). Morphologies and properties of thermo-molded biodegradable plastics based on glycerol-plasticized wheat gluten. *Food Hydrocolloids*, 21, 1005-1013.
- Sun, S., Song, Y. and Zheng, Q. (2008). Thermo-molded wheat gluten plastics plasticized with glycerol: Effect of molding temperature. *Food Hydrocolloids*, 22, 1006-1013.
- Taghizadeh, M. T. and Mafakhery, S. (2001). Kinetics and mechanism of graft polymerization of acrylonitrile onto starch initiator with potassium persulfate. *Iranian International Journal Science*, 12, 333-338.
- Tejado, A., Pena, C., Labidi L., Echeverria, J. M. and Mondragon, I. (2007). Physico-chemical characterization of lignins from different sources for use in phenol-formaldehyde resin synthesis. *Bioresource technology*, 98, 1655-1663.

- Telysheva, G., Dizhbite, T., Jurkjane, V. and Viesturs, U. (2004). Characterization of the radical scavenging activity of lignins-natural antioxidants. *Bioresource Technology*, 95, 309-317.
- Thielemans, W; Wool, R. P. (2005). Lignin esters for use in unsaturated thermosets: Lignin modification and solubility modeling. *Biomacromolecules*, 6, 1895-1905.
- Thomas, D. J. and Atwell, W. A. (1999). *Starches*. American Association of Cereal Chemists. USA.
- Tilley, K. A., Benjamin, R. E., Bagorogoza, K. E., Okot-Kotber, M. B., Prakash, O. and Kwen, H. (2001). Tyrosine cross-links: Molecular basis of gluten structure and function. *Journal of Agricultural and Food Chemistry*, 49, 2627-2632.
- Trimnell, D., Stout, E. I., Doane, W. M. and Russell, C. R. (2003). Graft copolymers from thiolated starch and vinyl monomers. *Journal of Applied Polymer Science*, 21, 655-663.
- Ugartondo, V., Mitjans, M. and Vinardell, M. P. (2008). Comparative antioxidant and cytotoxic effects of lignins from different sources. *Bioresource Technology*, 99, 6683-6687.
- Uttapap, D., Punch-arnon, S., Pathipanwat, W., Puttanlek, C. and Rungsardthonh, V. (2008). Effects of relative granule size and gelatinization temperature on paste and gel properties of starch blends. *Food Research International*. 14. 552-561.
- Vinardell, M. P., Ugartondo, V. and Mitjans, M. (2008). Potential applications of antioxidant lignins from different sources. *Industrial Crops and Products*, 27, 220-223.

- Walsh, G. (2002). *Proteins biochemistry and biotechnology*. John Wiley & Sons Ltd, England.
- Wang, H. -Y. and Hung, M. -F. (2007). Preparation, characterization and performances of biodegradable thermoplastic starch. *Polymers and advanced technologies*, 18, 910-915.
- Wang, Z. F., Peng, Z., Li, S. D., Lin, H., Zhang, K. X., She, X. D. and Fu, X. (2009). The impact of esterification on the properties of starch/natural rubber composite. *Composites Science and Technology*, 69, 1797-1803.
- Weegels, P. L., Verhoek, J. A., de Groot., A. M. G. and Hamer, R. J. (1994a). Effects on gluten of heating at different moisture contents. I. Changes in functional properties. *Journal of Cereal Science*, 19, 31-38.
- Weegels, P. L., de Groot., A. M. G., Verhoek, J. A. and Hamer, R. J. (1994b). Effects on gluten of heating at different moisture contents. I. Changes in physico-chemical properties and secondary structure. *Journal of Cereal Science*, 19, 39-47.
- Whistler, R. L., BeMiller, J. N. and Paschall, E. F. (1984). *Starch: Chemistry and Technology*. 2<sup>nd</sup> edition. Harcourt Brace Jovanovich. USA.
- Wieser, H. (2007). Chemistry of gluten proteins. *Food Microbiology*, 24, 115-119.
- Willett, J. L. (2008). Humidity-Responsive Starch-Poly(methyl acrylate) Films. *Macromolecular Chemistry and Physics*, 209, 764-772.
- Wurzburg, O. B. (1987). *Modified starch: Properties and uses*. National Starch and Chemical Corp. CRC. New Jersey. USA.

- Yang, J. -H., Yu, J. -G. and Ma, X. -F. (2006). Study on the properties of ethylenebisformamide and sorbitol plasticized corn starch (ESPTPS). *Carbohydrate Polymer*, 66, 110-116.
- Yin, Y., Yin, Q., Dong, A. and Wang, J. (2008). Rheological and thermal behavior of starch/LDPE blends containing ESS. *Polymer Composites*, 1-5.
- Young, R. J. and Lovell, P. A. (1991). *Introduction to polymers*. 2<sup>nd</sup> edition. Chapman and Hall. New York. USA.
- Yu, L., Liu, X., Liu, H., Chen, L. and Li, L. (2008). In situ thermal decomposition of starch with constant moisture in a sealed system. *Polymer Degradation and Stability*, 93, 260-262.
- Zahedifar, M., Castro, F. B. and Orskov, E. R. (2002) Effect of hydrolytic lignin on formation of protein-lignin complexes and protein degradation by rumen microbes. *Animal Feed Science and Technology*, 95, 83-92.
- Zang, L. Y., Cosma, G., Gardner, H., Shi, X., Castranova, V. and Vallyathan, V. (2000). Effect of antioxidant protection by p-coumaric acid on low-density lipoprotein cholesterol oxidation. *American journal of physiology. Cell physiology*, 279, c954-c960.
- Zaragoza-Contreras, E.A., Lozano-Rodriguez, E.D., Roman-Aguirre, M., Antunez-Flores, W., Hernandez-Escobar, C.A., Flores-Gallardo, S. G. and Aguilar-Elguezabal, A. (2009). Evidence of multi-walled carbon nanotube fragmentation induced by sonication during nanotube encapsulation via bulk-suspension polymerization. *Micron*, 40, 621-627.
- Zhou, B., Cheng, J. -C., Dai, F., Yang, L. and Liu, Z. -L. (2007). Antioxidant activity of hydroxycinnamic acid monomers in human low density lipoprotein: Mechanism and structure-activity relationship. *Food Chemistry*, 104, 132-139.

Zuo, M., Lai, Z. Z., Song, Y. H. and Zheng, Q. (2008). Preparation and properties of gluten/calcium carbonate composites. *Chinese Chemical Letters*, 19, 992-995.

Zuo, M., Song, Y. and Zheng, Q. (2009). Preparation and properties of wheat gluten/methylcellulose binary blend film casting from aqueous ammonia: A comparison with compression molded composites. *Journal of Food Engineering*, 91, 415-422.



## **Appendices**

## **Appendix A**

### **Rheology of native cassava starch, ester starch and oxidized starch**

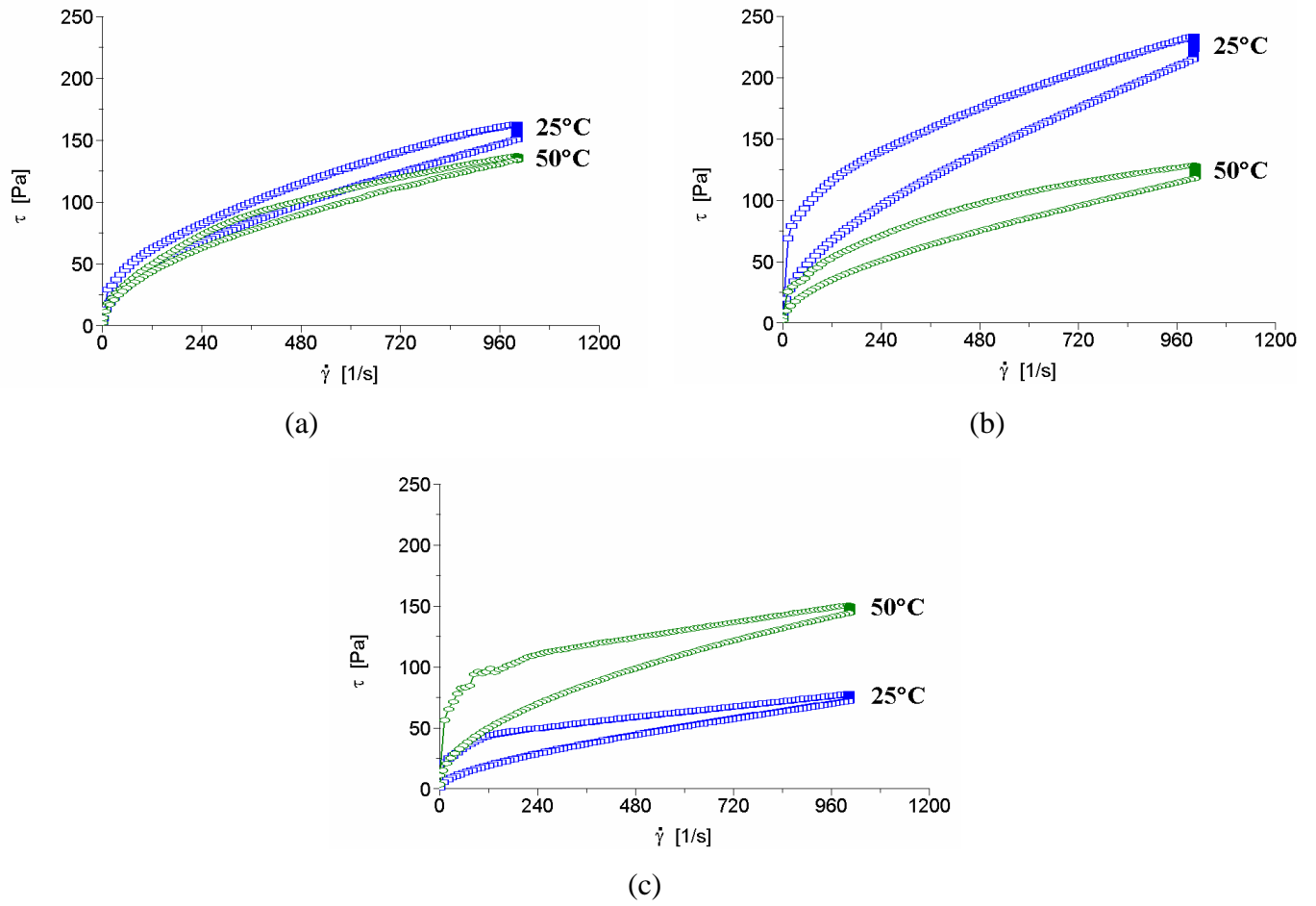


Figure 1 (A) Flow curves of 5% w/w native cassava starch pastes at different storage time; (a) 0 day, (b) 1 day and(c) 7 days.

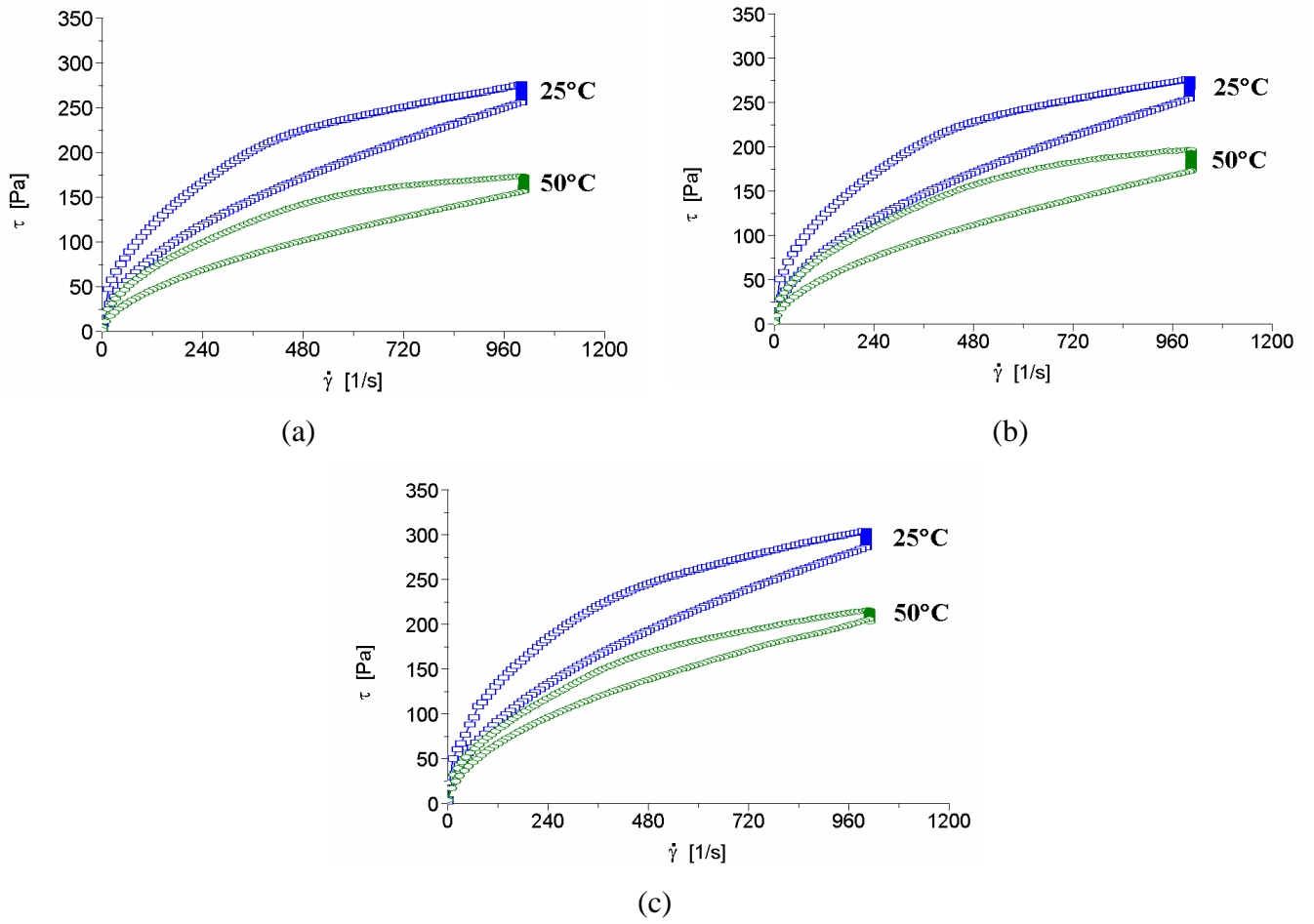


Figure 2 (A) Flow curves of 5% w/w ester starch pastes at different storage time; (a) 0 day, (b) 1 day and (c) 7 days.

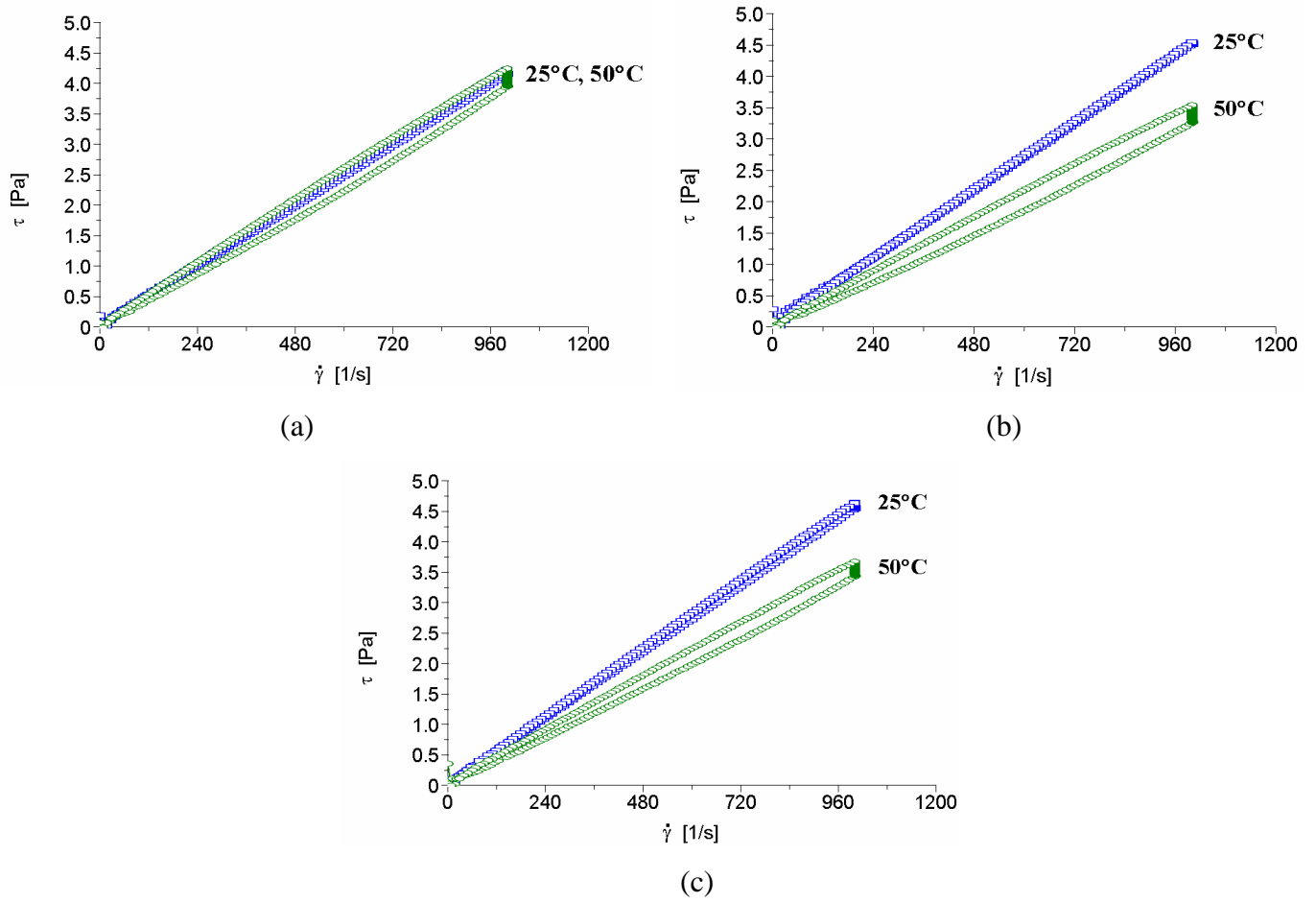


Figure 3 (A) Flow curves of 5% w/w oxidized starch pastes at different storage time;

(a) 0 day, (b) 1 day and(c) 7 days.

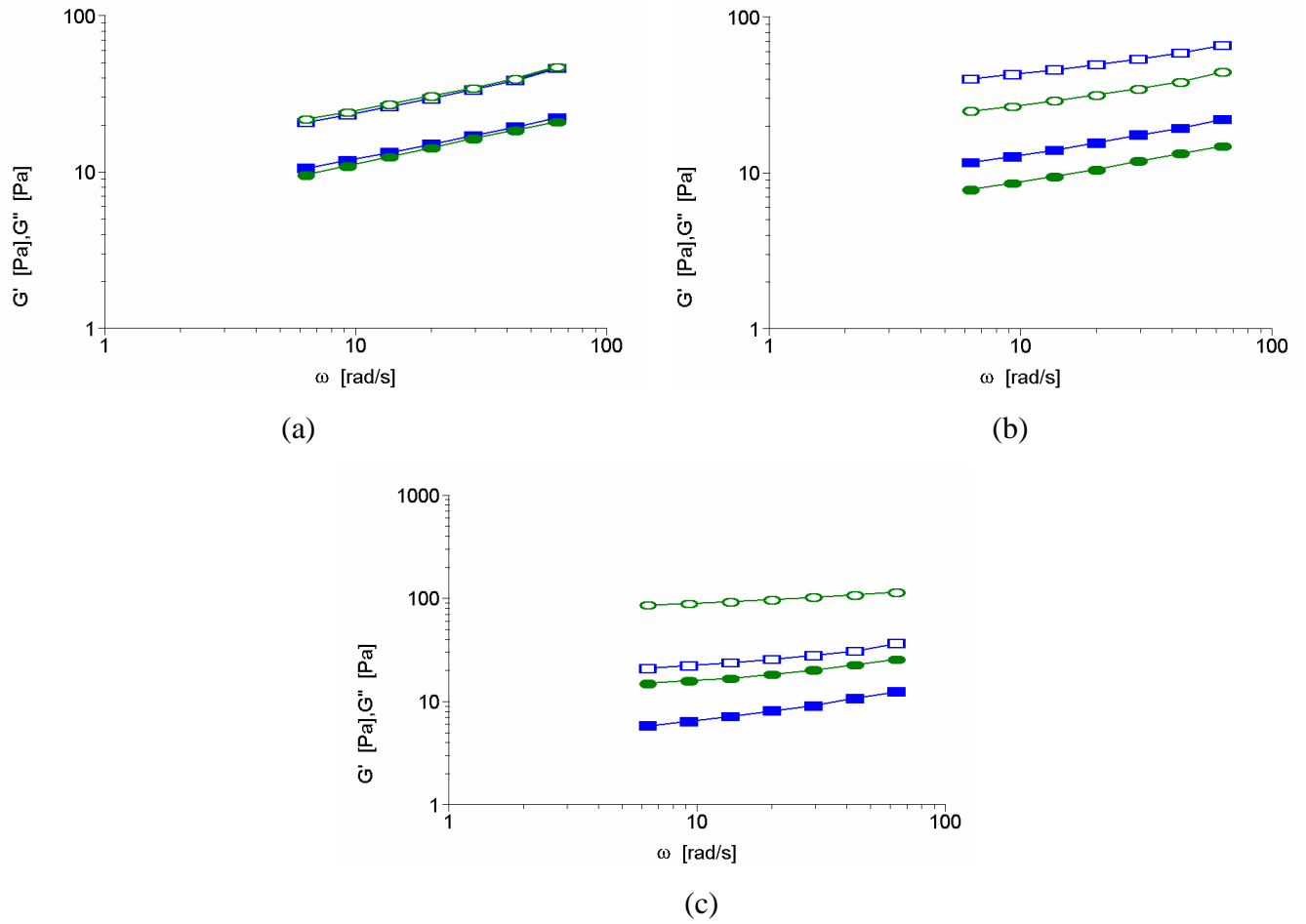


Figure 4 (A) Dynamic mechanical spectra of 5% w/w native cassava starch pastes at different storage time; (a) 0 day, (b) 1 day and (c) 7 days; ( $\square$ )25 $^{\circ}$  and ( $\circ$ ) 50 $^{\circ}$ C. Opened symbols, storage modulus( $G'$ ); closed symbols, loss modulus( $G''$ ).

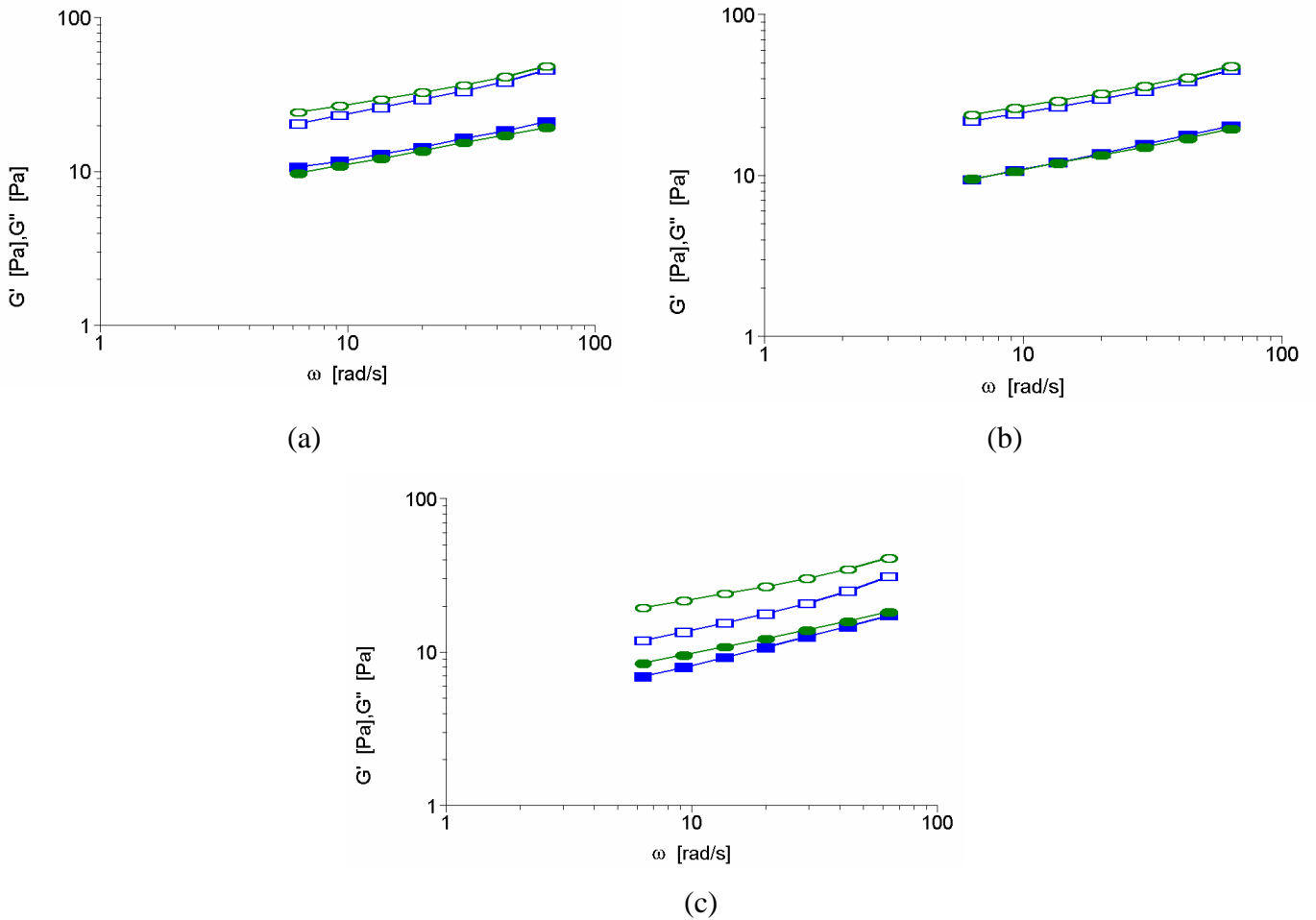


Figure 5 (A) Dynamic mechanical spectra of 5% w/w ester starch pastes at different storage time; (a) 0 day, (b) 1 day and (c) 7 days; ( $\square$ )25° and (O) 50°C. Opened symbols, storage modulus( $G'$ ); closed symbols, loss modulus( $G''$ ).

## **Appendix B**

**Surface morphology of native cassava starch, ester starch and oxidized starch**



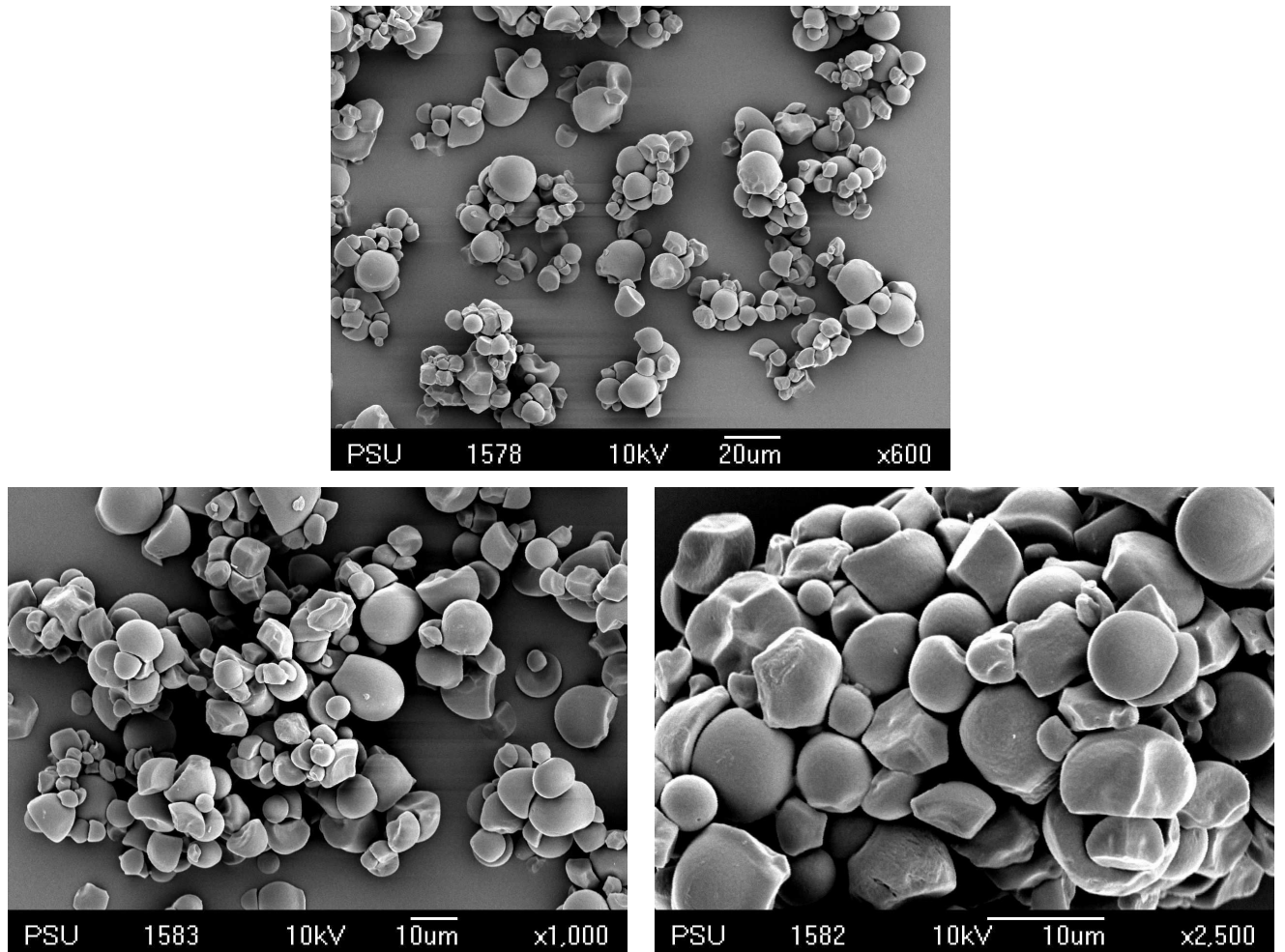


Figure 1 (B) Surface morphology of native cassava starch.

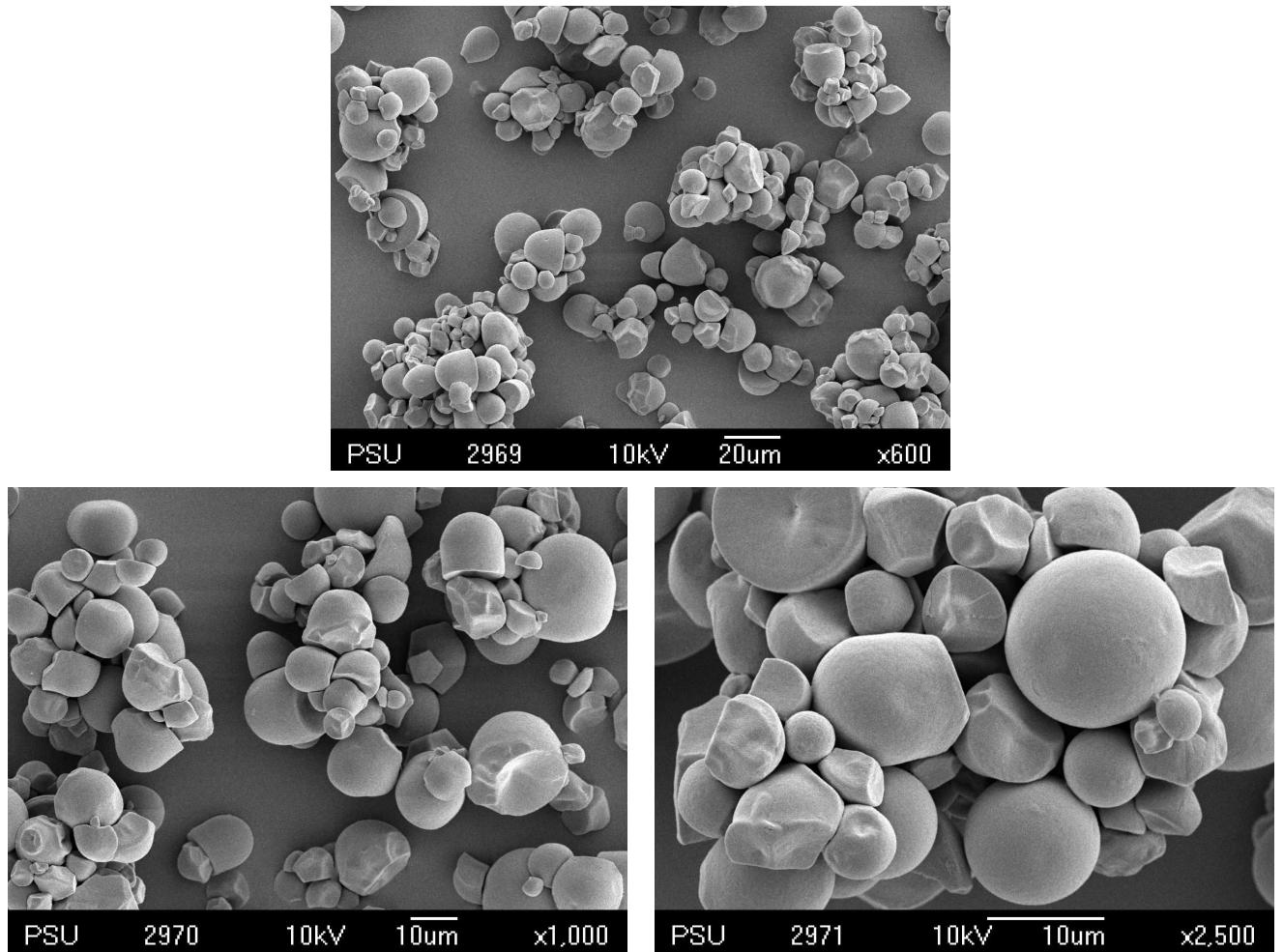


Figure 2 (B) Surface morphology of ester starch.

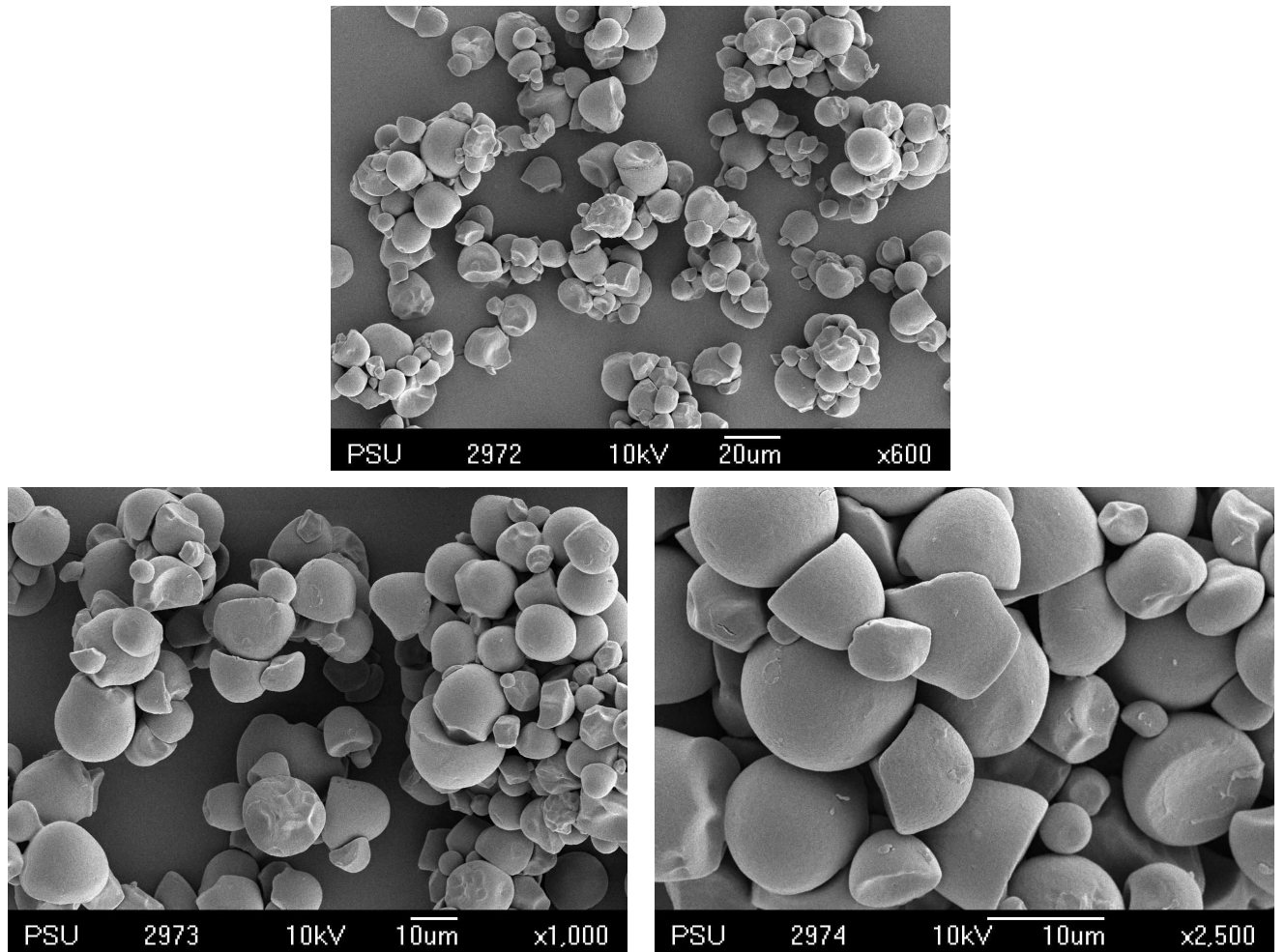


Figure 3 (B) Surface morphology of oxidized starch.

### **Appendix C**

**Effect of glycerol content on storage modulus, loss modulus and tan delta of wheat gluten**

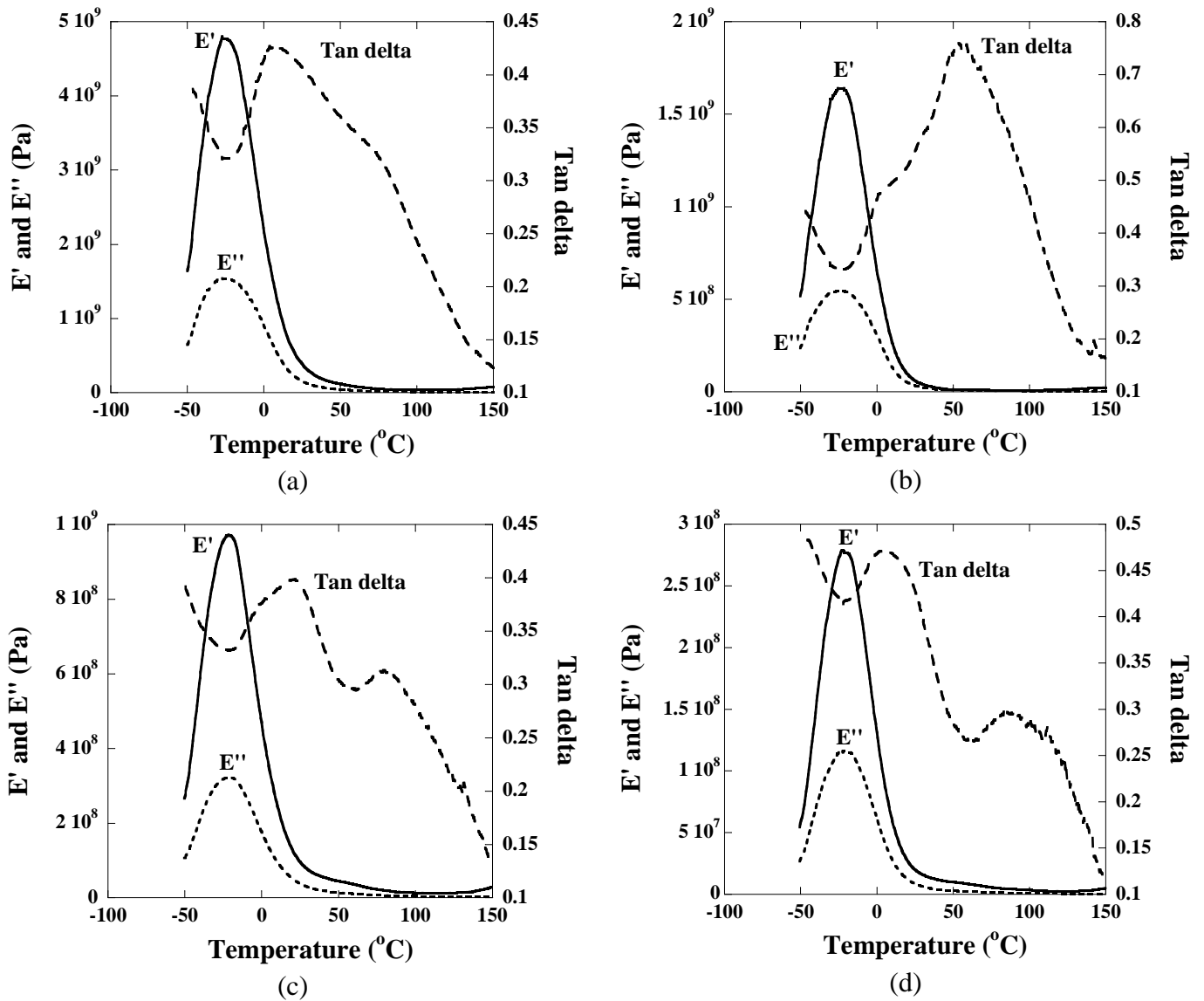


Figure 1 (C) Effect of glycerol content on storage modulus, loss modulus and tan delta of wheat gluten (without thermal treatment); controlled wheat gluten (glycerol 30%) (a), 31% (b), 35% (c) and 40% (d).

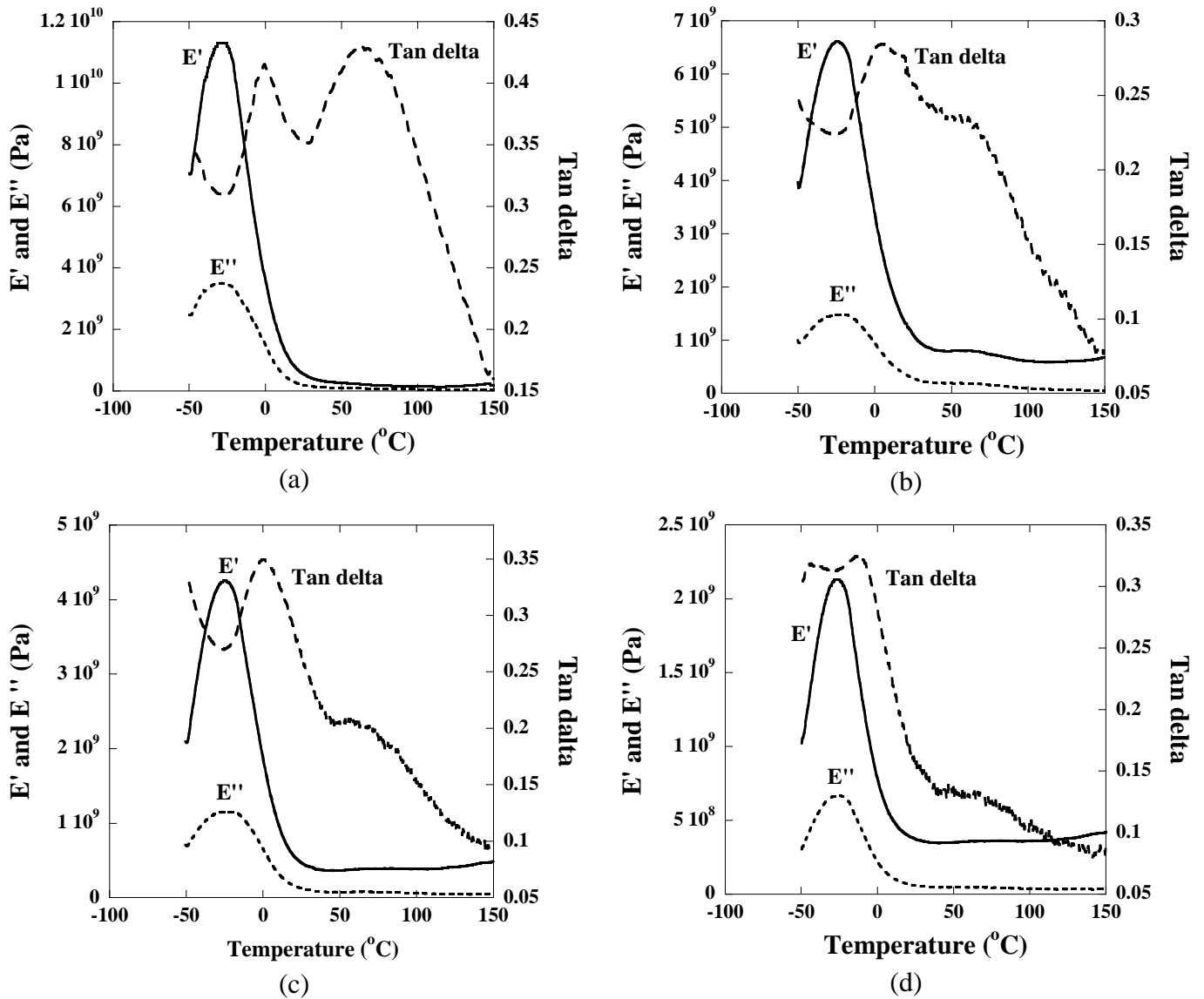


Figure 2 (C) Effect of glycerol content on storage modulus, loss modulus and tan delta of wheat gluten after thermalmolding; controlled wheat gluten (glycerol 30%) (a), 31% (b), 35% (c) and 40% (d).

**Appendix D**  
**Publication**

Available online at [www.sciencedirect.com](http://www.sciencedirect.com)

Carbohydrate Polymers 73 (2008) 647–655

---

**Carbohydrate  
Polymers**


---

[www.elsevier.com/locate/carbpol](http://www.elsevier.com/locate/carbpol)

## Preparation of cassava starch grafted with polystyrene by suspension polymerization

Kaewta Kaewtatip<sup>a</sup>, Varaporn Tanrattanakul<sup>a,b,\*</sup><sup>a</sup> *Polymer Science Program, Faculty of Science, Prince of Songkla University, Hatyai, Songkla 90112, Thailand*<sup>b</sup> *Bioplastic Research Unit, Faculty of Science, Prince of Songkla University, Hatyai, Songkla 90112, Thailand*

Received 12 September 2007; received in revised form 25 December 2007; accepted 4 January 2008

Available online 16 January 2008

---

### Abstract

Cassava starch grafted with polystyrene (PS-g-starch) copolymer was synthesized via free-radical polymerization of styrene by using suspension polymerization technique. Potassium persulfate (PPS) was used as an initiator and water was used as a medium. The graft copolymer was characterized by Fourier transform infrared spectroscopy, differential scanning calorimetry, thermal gravimetric analysis, X-ray diffraction and scanning electron microscopy. The sub-micron spherical beads of PS were observed on the surface of starch granules. SEM micrographs showed porous patches of PS adhering on the starch granules after Soxhlet extraction. FTIR spectra also indicated the presence of PS-g-starch copolymer. XRD analysis exhibited insignificant changes in crystalline structure and degree of crystallinity. The effects of starch:styrene weight ratio, amount of PPS, reaction time and reaction temperature on the percentage of grafting – G (%), were investigated. G (%) increased with increasing starch content. Other variables showed their own individual optimal values. The optimum condition yielding 31.47% of G (%) was derived when the component ratio was 1:3 and reaction temperature and time were 50 °C and 2 h, respectively. Graft copolymerization did not change granular shape and crystallinity of starch. This study demonstrated the capability of polymerization of styrene monomer on the granular starch without emulsifier and the synthesis of graft copolymer without gelatinization of starch.

© 2008 Elsevier Ltd. All rights reserved.

**Keywords:** Cassava starch; Polystyrene; Biodegradable polymer; Graft copolymer; Bioplastic

---

### 1. Introduction

In the last three decades, there has been tremendous interest in bioplastic and biodegradable polymers. In the beginning, there were many attempts to use starch as a bio-filler in thermoplastic polymers. Starch is used as a filler because it is a natural polymer, abundant, inexpensive and a renewable resource. Starch is degraded by microorganisms and is suitable for blending with bioplastics and biodegradable polymers. Unfortunately, the mechanical properties of thermoplastic polymer/starch blends are very poor due to the incompatibility and hydrophilic nature of

starch. As a result, graft copolymerization of thermoplastic polymer onto starch has been widely studied.

Graft copolymerization can be performed by irradiation or free-radical graft copolymerization. Graft copolymerization of polystyrene onto starch has been previously reported. Bagley, Fanta, Burr, Doane, and Russell (1977) prepared starch graft copolymers with styrene, methyl methacrylate, methyl acrylate, and butyl acrylate. Preparation of starch grafted with polystyrene (PS-g-starch copolymer) using <sup>60</sup>Co irradiation has been reported (Fanta, Burr, Doane, & Russell, 2003; Henderson & Rudin, 1981; Henderson & Rudin, 2003a; Kiatkamjornwong, Sonsuk, Wittayapichet, Prasassarakich, & Vejjanukroh, 1999).

It is well established that potassium persulfate (PPS), ceric ammonium nitrate, manganic pyrophosphate, potassium permanganate, benzoyl peroxide and redox couples such as ferrous ammonium sulfate – hydrogen peroxide

---

\* Corresponding author. Address: Polymer Science Program, Faculty of Science, Prince of Songkla University, Hatyai, Songkla 90112, Thailand. Tel.: +66 8973 54720; fax: +66 7444 6925.

E-mail address: [varaporn.t@psu.ac.th](mailto:varaporn.t@psu.ac.th) (V. Tanrattanakul).



are effective for grafting vinyl monomers onto starch via free-radical graft copolymerization (Graaf & Janssen, 2000; Pimpan & Thothong, 2006). Graaf and Janssen (2000) prepared PS-g-starch copolymer by reactive extrusion. They used benzoyl peroxide and PPS as the thermal initiators. Cho and Lee (2002) prepared PS-g-starch copolymer by emulsion polymerization. The aqueous solution consisted of corn starch, styrene monomer, PPS, emulsifier and chain transfer agent. The gelatinized sago starch grafted with PS was prepared by using ceric ammonium nitrate in aqueous solution (Janarthanan, Yunus, & Ahmad, 2003). Although both ceric ammonium nitrate (cerium (IV)) and PPS could be used for preparation of PS-g-starch copolymer, PPS may be better because it can initiate homopolymerization of styrene directly but cerium (IV) cannot.

Trimnell, Stout, Doane, and Russell (2003) used hydrogen peroxide as the initiator for grafting PS onto the thiolated starch. The acryloylated potato starch was grafted with PS using PPS in aqueous solution (Fang, Fowler, & Hill, 2005). They employed a two-step process where the starch was modified by acryloyl chloride prior to graft copolymerization. Ammonium persulfate has been used as the initiator for grafting PS onto starch (Singh & Sharma, 2007). Recently, ozone was used to synthesize starch grafted with poly(styrene-*co*-*n*-butyl acrylate) latexes (De Bruyn et al., 2006). PS-g-starch copolymers have been used for different applications. For example it was used as a compatibilizer of PS/starch blend (Graaf & Janssen, 2004), a filler of PS (Graaf & Janssen, 2004, and Kiatkamjornwong et al., 1999), or used directly as a thermoplastic starch and processed by extrusion (Henderson & Rudin, 2003b).

To the best of our knowledge, there is no report of cassava starch grafted with PS via suspension polymerization using PPS as the initiator. One research group has used gamma radiation (Kiatkamjornwong et al., 1999) and another PPS under emulsion polymerization (Cho & Lee, 2002) to make grafted starch. The latter group reported that no PS was obtained when no emulsifier was used and the redox initiation system failed unless the starch was gelatinized. The utilization of PPS as the initiator in other systems has been reported. For instance, poly(methyl methacrylate) grafted sago starch (Qudsieh et al., 2004; Razi, Qudsieh, Yunus, Ahmad, & Rahman, 2001), and poly(acrylamide) grafted with potato starch (Singh, Tiwari, Pandey, & Singh, 2006) have been reported. Cho & Lee, 2002 stated that although PS-g-starch copolymer has been prepared by persulfate initiation in the slurry state it is difficult to prepare styrene graft copolymer with granular starch by free-radical polymerization. Simple solution grafting polymerization did not yield graft copolymer. This may be due to the different reaction conditions. It is difficult to polymerize styrene with the water-soluble initiator. However, it is necessary to employ the water-soluble initiator for starch graft copolymerization because water is the medium used in making a starch slurry.

The objective of this study was to synthesize PS-g-starch copolymer by using PPS as the initiator. This study showed the success of graft copolymerization between granular cassava starch and polystyrene via the suspension polymerization. The PS-g-starch copolymer derived from this study will be used as a thermoplastic starch and compatibilizer for PS/starch blends. Based on these applications, it was not necessary to extract or digest ungrafted starch from the graft copolymer.

## 2. Experimental

### 2.1. Materials

Cassava starch was kindly supplied by GSL General Starch Ltd., Thailand. It is a native, granular starch and had standard specification as follows: maximum moisture content = 12.2%, maximum ash = 0.07%, fiber content = 0.10%, pH 5.6, SO<sub>2</sub> content = 21.59 ppm, maximum viscosity = 630 Brabender units, and sieve test = 99.61% after passing through 100 mesh. The starch was dried at 100 °C for 48 h in an oven and kept in a desiccator prior to using. Styrene monomer (from Fluka) was used after inhibitor was extracted with 5% sodium hydroxide aqueous solution and distilled water sequentially. The inhibitor-free styrene was dried with anhydrous calcium chloride and stored at 4 °C. Potassium persulfate, toluene and methanol (from Fisher chemicals) were used as received.

### 2.2. Preparation of PS-g-starch copolymer

Dried starch and distilled water were mixed in a three-neck flask under nitrogen atmosphere and stirred at reaction temperature for 30 min to obtain homogeneous slurry. After adding PPS for 10 min, styrene monomer was added. Water was 100 ml while the total amount of starch and styrene monomer was 10 g. Graft copolymerization was carried out at various conditions. The graft copolymerization parameters included starch:styrene ratios (1:3, 1:1 and 3:1 by weight), PPS content (0.2–1.2 g), reaction time (1–5 h) and reaction temperature (30–60 °C). The nitrogen atmosphere and agitation at 420 rpm of slurry were maintained throughout the experiment. After the reaction time was over, the slurry was dropped into methanol. The precipitate was filtered, washed with methanol, dried in an oven at 50 °C until a constant weight was achieved and kept in a desiccator. The “controlled starch” was prepared under identical experimental condition as described earlier except the addition of styrene monomer. In order to test reproducibility of graft copolymerization, three runs of polymerization were carried out for all samples.

Soxhlet extraction with toluene was applied to the precipitate for removing polystyrene homopolymer. The extraction was done at 120 °C for 10 h. The extracted solution was dropped into methanol which is a non-solvent of PS, if no precipitation was observed, complete extraction was confirmed. The PS-g-starch copolymer was dried in a

vacuum oven at 60 °C until a constant weight and kept in the desiccator. To substantiate the validity of Soxhlet extraction technique, the same extraction technique was applied to a polymer blend of starch and polystyrene homopolymer. The product prior to Soxhlet extraction was called as “non-extracted product”, and the product after extraction was called as “un-extractable product”.

In order to verify the polymerization of styrene monomer with PPS by the suspension polymerization technique, the reaction was carried out under identical reaction condition except the presence of starch. Styrene monomer (7.5 g), PPS (0.4 g) and distilled water (100 g) were mixed together and stirred at 420 rpm. Reaction time and temperature were 2 h and 50 °C, respectively. The mixture was precipitated in methanol. The precipitate was filtered and dried before characterizing similar to the PS-g-starch copolymer.

### 2.3. Characterization of PS-g-starch copolymer

The products before and after Soxhlet extraction were weighed and characterized by various techniques. The percentage of grafting,  $G$  (%), and yield of graft copolymerization,  $Y$  (%), were calculated from Eqs. (1) and (2), respectively:

$$G(\%) = \frac{w_2 - w_1}{w_1} \times 100 \quad (1)$$

$$Y(\%) = \frac{w_2 - w_1}{w_3} \times 100 \quad (2)$$

where  $w_1$  was the original weight of cassava starch,  $w_2$  was the weight of un-extractable products (after Soxhlet extraction), and  $w_3$  was weight of styrene monomer. Because  $w_2$  represented to the weight of starch and PS grafted on starch; therefore, the differences in  $w_2$  and  $w_1$  could be equal to the weight of PS grafted on starch granules. The calculation of  $G$  (%) and  $Y$  (%) was similar to that reported by Singh et al. (2006) and Fang et al. (2005). The  $G$  (%) and  $Y$  (%) were reported in terms of an average value and standard deviation derived from triplicated polymerization.

The Fourier Transform Infrared Spectrometer BRUKER® EQUINOX 55 was used to determine the presence of PS in the graft copolymer. The dried powder samples were mixed with potassium bromide and pressed into disc shape. The samples were scanned at a frequency range of 4000–400  $\text{cm}^{-1}$  with 128 consecutive scans in a 4  $\text{cm}^{-1}$  resolution. A scanning electron microscope (JEOL® JSM-5800LV) was used to observe the presence of PS on starch granules. The samples were coated with gold prior to observation. Thermal properties were evaluated by thermogravimetric analysis (PerkinElmer® TGA 7) and differential scanning calorimetry (PerkinElmer® DSC 7). TGA analysis was operated at a heating rate of 10 °C/min from 50 to 950 °C under nitrogen atmosphere. DSC analysis of starch and graft copolymers was conducted on the second heating of a heating-cooling-heating cycle with a heating rate of 5 °C/min. The first and the second heating scans were operated from 25 to 180 °C and 25–500 °C, respectively, under nitrogen atmosphere in order to ensure that there was no influence of the thermal history and moisture. Semi-crystalline structure of starch granules was detected by using a wide angle X-ray diffractometer (Phillips® PW1830).

## 3. Results and discussion

### 3.1. Suspension polymerization of polystyrene

The mixture became turbid after reaction time was over. This was due to very fine particles of PS were dispersed in the water. These particles were filtered and dried at 100 °C for 24 h. SEM micrographs of PS micro-particles are shown in Fig. 1a and b. Fig. 1a shows agglomerates of very fine PS particles which smaller than 200  $\mu\text{m}$ . At higher magnification (Fig. 1b) a number of sub-micron spherical PS particles are observed. Practically, it is difficult to polymerize styrene monomer with water-soluble initiator under suspension polymerization. Comparing to another work (Pimpan & Thothong, 2006), benzoyl peroxide, monomer

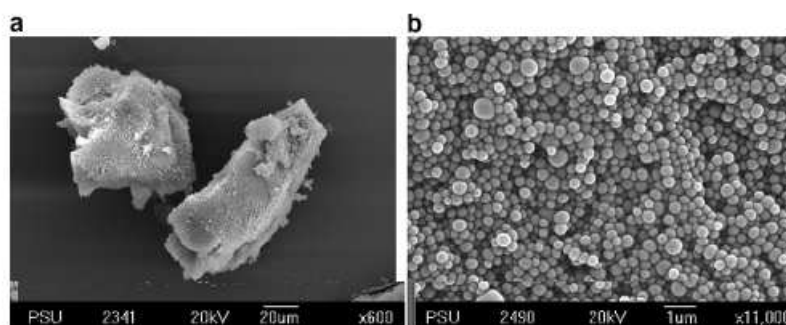


Fig. 1. SEM micrographs of PS polymerized by suspension polymerization using PPS as the initiator. (a) agglomerates of PS; (b) sub-micron spherical particles of PS.

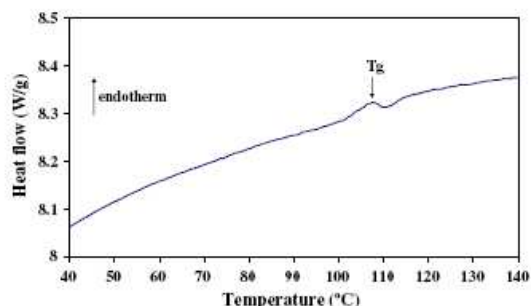


Fig. 2. DSC thermogram of PS polymerized by suspension polymerization using PPS as the initiator showing  $T_g$  at 107.5 °C.

soluble initiator, was employed to polymerize poly(methyl methacrylate) (PMMA). The PMMA particles obtained were about 50  $\mu\text{m}$  in diameter whereas the PS particles in the present study were  $<0.5 \mu\text{m}$ . The glass transition temperature of these PS particles was 107.5 °C (Fig. 2). This experiment confirmed that suspension polymerization of styrene monomer with PPS was successful. As a result, graft copolymerization between PS and starch could be carried out in the present system. The present result is contrast to the previous result which was unable to polymerize PS without emulsifier (Cho & Lee, 2002).

### 3.2. Graft copolymerization on native starch granules

It is well established that the free-radical water-soluble initiators, including PPS, are dissociated in water and attract the OH group of starch causing free-radicals on the starch molecules and these free-radicals will attract the double bonds of vinyl monomers resulting in graft copolymer. Based on the results described in Section 3.1, PPS was able to initiate free-radicals on styrene monomer without the presence of surfactant and starch. Therefore, it is believed that synthesis of PS-g-starch copolymer under the present system is capable. Although PPS is water-soluble, radical formation on a starch chain and styrene monomer were simultaneously occurred due to sulfate ions ( $\text{S}_2\text{O}_8^{2-}$ ) and finally the starch radicals reacted with a growing PS chain. The graft copolymerization occurred only at the interface between starch granule and PS phase. The evidence of this phenomenon was proved by SEM analysis and will discuss later. In practice the starch graft copolymer was performed in a slurry reactor with gelatinized starch or granular starch including the present study. Therefore, factors studied always include initiator concentration, monomer concentration, reaction time and temperature. In the present study, various conditions were chosen for graft copolymerization and compared grafting efficiency in terms of the percentage of grafting – G (%), and yield of graft copolymerization – Y (%). Table 1 represents G (%) and Y (%) of various samples polymerized in 0.2 g of PPS and 100 g of water for 2 h. The G (%) indicates the

Table 1

Effect of starch:styrene ratio and reaction temperature on the percentage of grafting, G (%), and yield of graft copolymerization, Y (%), of samples polymerized for 2 h with 100 g of water and 0.2 g of PPS

Starch (g)	Styrene (g)	Temperature (°C)	G (%)	Y (%)
2.5	7.5	30	1.07 ± 0.23	0.36 ± 0.08
2.5	7.5	40	9.33 ± 1.01	3.11 ± 0.34
2.5	7.5	50	15.07 ± 1.01	5.02 ± 0.33
2.5	7.5	60	2.67 ± 0.61	0.89 ± 0.20
5.0	5.0	30	2.60 ± 0.40	2.60 ± 0.40
5.0	5.0	40	5.40 ± 0.40	5.40 ± 0.40
5.0	5.0	50	8.80 ± 0.92	8.80 ± 0.92
5.0	5.0	60	4.67 ± 0.99	4.67 ± 0.99
7.5	2.5	30	5.07 ± 0.48	15.20 ± 1.44
7.5	2.5	40	5.96 ± 0.87	17.87 ± 2.60
7.5	2.5	50	7.20 ± 0.87	21.60 ± 2.62
7.5	2.5	60	2.40 ± 0.27	7.20 ± 0.80

amount of polystyrene grafted on starch granules and the Y (%) indicates yielding of polymerization of PS grafted on starch granules. In the starch-rich and styrene-rich systems both values show similar tendency, higher G (%) value showed higher Y (%) value. In the system containing 50:50 starch:styrene, both values were identical. Undoubtedly, the values of G (%) and Y (%) are not the same number due to different meaning. In the present study, G (%) was a criterion of grafting reaction. As evident from Table 1, the results indicate that the amount of cassava starch and styrene monomer showed significant effects on G (%), the styrene-rich system was preferable. The highest styrene content (7.5 g) offered the highest G (%). The G (%) increasing with monomer concentration and the optimal condition obtained from the monomer-rich system were reported by others (Fang et al., 2005; Pimpan & Thothong, 2006). The more styrene monomer the more polymerization; therefore, there was more opportunity for graft copolymerization. In general, there will be an optimum monomer concentration for each system. The too low concentration leads to decrease in active sites on the growing chains and the too high concentration leads to more homopolymerization (Qudsieh et al., 2004; Singh & Sharma, 2007).

Reaction temperature also played an important role on graft copolymerization. The G (%) increased with increasing reaction temperature up to 50 °C then decreased at 60 °C. The maximum G (%), 15.07%, was achieved when the reaction temperature was 50 °C. Undoubtedly, every polymerization system has its own optimum reaction temperature. Similar result was reported, the maximum grafting efficiency in graft copolymerization of starch and PMMA with PPS was at 50 °C (Qudsieh et al., 2004). Singh and Sharma (2007) also showed the optimum temperature in preparation of PS-g-starch copolymer. It is well established that the rate of decomposition of initiator increased with increasing reaction temperature, leading to more free-radicals. Increase in temperature also increased the molecular mobility and rate of diffusion of monomer. Conse-

quently grafting reaction was promoted. Decrease in grafting after the optimum temperature was attributed to premature termination of growing chains and grafted chains as well as chain transfer reactions. It should be noted that the present study used very low reaction temperature. The gelatinization temperature of cassava starch is 62–73 °C (Taggare, 2004). For that reason, the crystallinity and starch granules of PS-g-starch should be similar to the native starch. These were proved by XRD and SEM analysis as discussed later.

To optimize PPS content, the 1:3 weight ratio of starch:styrene was polymerized at 50 °C for 2 h by using PPS in the range of 0.2–1.2 g. The experimental results are listed in Table 2. The G (%) and Y (%) increased after increasing PPS content from 0.2 to 0.4 g. Further increases in PPS content ( $\geq 0.6$  g), both values decreased. The maximum G (%), 31.47%, and Y (%), 10.49%, were obtained from the system containing 0.4 g of PPS. More PPS content may promote homopolymerization of styrene. The incidence of an optimum PPS content in polymerization has been reported (Qudsieh et al., 2004; Singh et al., 2006). The former group stated that the decrease of G (%) after the optimum may be due to an increase in the number of starch radicals terminated prior to monomer addition and an increase in homopolymer formation. The latter group mentioned that the decrease of G (%) may be due to accumulation of a large number of free-radicals resulting into premature termination of the growing chains and the grafting.

The reaction time was determined in the range of 1–5 h by using the reaction conditions giving G (%) = 31.47% in Table 2. The results were tabulated in Table 3. It was found that the reaction temperature of 2 h yielded the highest G

(%). All conditions used in Table 3, except the reaction time of 5 h, provided high grafting reaction, and both values of G (%) and Y (%) were higher than those listed in Tables 1 and 2. In the present study longer reaction time was favorable to homopolymerization of styrene. Because graft copolymerization performed only on the surface of the starch granules; consequently, the rate of graft copolymerization was controlled by the surface of starch granules covering with PS growing chains. Once the starch surface was fully covered with PS, no more new PS could attach on the starch. As a result, longer reaction time generated more PS homopolymer. This optimum reaction time was in the same range as reported by Qudsieh et al. (2004) but Pimpan and Thothong (2006) reported slight effect of reaction time on grafting efficiency. The latter group used 80 °C for grafting reaction whereas the former group and the present study used 50 °C. The former group stated that the decrease of G (%) after the maximum was due to the solution viscosity increased with reaction time resulting in the reduction of reactive sites exposed to the vinyl monomer.

To determine validation of graft copolymerization technique, the experiments were performed three replicates for each value. The standard deviations of G (%) and Y (%) shown in Tables 1–3 were in the acceptable range. Most of the standard deviations were less than 1%. The experimental results substantiated the reliability of grafting reaction in the present study.

### 3.3. Characterization of PS-g-starch copolymer

FTIR spectra of virgin materials and graft copolymer are represented in Fig. 3, and FTIR assignment of cassava starch and PS are listed in Table 4. FTIR assignment of starch had been reported by many research groups (Athawale & Lele, 2000; Ezekiel, Rana, Singh, & Singh, 2007; Mano, Koniarova, & Reis, 2003; Park, Im, Kim, & Kim, 2000). The cassava starch (Fig. 3a) and PS (Fig. 3b) showed the characteristic peaks as described in Table 4.

**Table 2**  
Effect of PPS content on the percentage of grafting, G (%), and yield of graft copolymerization, Y (%), of samples polymerized at 50 °C for 2 h with 100 g of water, 2.5 g of starch and 7.5 g of styrene

PPS (g)	G (%)	Y (%)
0.2	15.07 ± 1.01	5.02 ± 0.33
0.4	31.47 ± 1.40	10.49 ± 0.47
0.6	12.53 ± 1.22	4.18 ± 0.41
0.8	6.93 ± 0.83	2.31 ± 0.28
1.0	8.00 ± 0.80	2.67 ± 0.27
1.2	13.07 ± 0.61	4.53 ± 0.20

**Table 3**  
Effect of reaction time on the percentage of grafting, G (%), and yield of graft copolymerization, Y (%), of samples polymerized at 50 °C with 100 g of water, 2.5 g of starch, 7.5 g of styrene, and 0.4 g of PPS

Reaction time (h)	G (%)	Y (%)
1	21.07 ± 1.80	7.02 ± 0.60
2	31.47 ± 1.40	10.49 ± 0.47
3	17.60 ± 0.80	5.87 ± 0.27
4	20.40 ± 1.20	6.80 ± 0.40
5	7.07 ± 0.83	2.36 ± 0.28

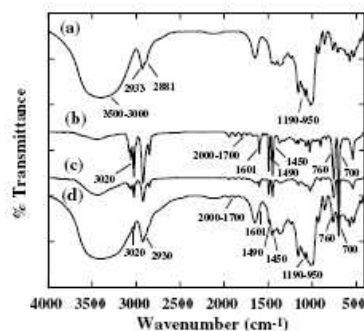


**Fig. 3.** FTIR spectrum of cassava starch (a), PS (b), PS-g-starch before Soxhlet extraction (c) and PS-g-starch after Soxhlet extraction with G (%) = 22.80% (d).

Table 4

FTIR assignment of cassava starch and polystyrene

Wavenumber (cm <sup>-1</sup> )	Assignment
<b>Cassava starch</b>	
3600–3000	O–H stretching
2933 and 2881	C–H stretching of CH <sub>2</sub>
1190–950	C–O stretching
<b>Polystyrene</b>	
3020, 1601, 1490, 760 and 700	C–H stretching of aromatic ring
2920 and 2850	C–H stretching of CH <sub>2</sub>
2000–1660	C=C in aromatic ring

The peak of starch at 1640–1650 cm<sup>-1</sup> is controversial as had been reported in many articles. Ezekiel et al. (2007) mentioned bending mode of water at 1800–1600 cm<sup>-1</sup>, while the  $\delta$  (OH) bend of adsorbed water was assigned at the wave number at 1640 cm<sup>-1</sup> (Athawale & Lele, 2000; Mano et al., 2003; Park et al., 2000) and at 1650 cm<sup>-1</sup> (Athawale & Lele, 2000). The wavenumber at 1653 cm<sup>-1</sup> was assigned as a peak of the first overtone of OH bending (Pal, Mal, & Singh, 2005). On the other hand, 1650 cm<sup>-1</sup> was assigned as COC stretching (Lee, Kweon, Koh, & Lim, 2004). Nevertheless, this peak was not the main characteristic of starch; therefore, discussion of this peak was beyond the scope of this study. The little peak at 3444 cm<sup>-1</sup> appeared in PS spectrum may be due to the moisture content in the PS. The FTIR spectrum of the product obtained from grafting reaction (non-extracted product) is shown in Fig. 3c. It showed a combination of both PS's and cassava starch's characteristics. The peaks of CH stretching (2933 and 2881 cm<sup>-1</sup>) and CO stretching (1190–950 cm<sup>-1</sup>) of starch were not observed; only a broad peak of OH stretching at 3444 cm<sup>-1</sup> was detected. In contrast, all characteristics of PS were remarkably shown in this spectrum. After Soxhlet extraction, the precipitate (un-extractable product) exhibited the spectrum similar to that of starch and also showed the characteristic peaks of PS: CH stretching of aromatic ring (1601, 1490, 760 and 700 cm<sup>-1</sup>) and C=C in aromatic ring (2000–1700 cm<sup>-1</sup>) as shown in Fig. 3d. Both starch and PS showed CH stretching in CH<sub>2</sub> within the same range of wavenumber; therefore, this assignment was not in consideration. The main characteristics of the precipitate arose from the starch manner due to the non-reacted starch was not extracted. The result indicates that PS-g-starch copolymer was derived in the present system.

TGA thermograms of polymers are shown in Fig. 4. PS showed higher thermal stability than starch; degradation temperature of PS and starch was in the range of 360–465 °C and 275–360 °C respectively. Furthermore, PS showed very little ash (~0%) after thermal degradation, whereas starch showed 20% of ash. The weight loss from 50 to 110 °C of starch could be the result of water evaporation and has been reported by others (Janarthanan et al., 2003; Kiatkamjornwong et al., 1999). The product without extraction of PS homopolymer (the non-extracted product) showed two-step degradation process including

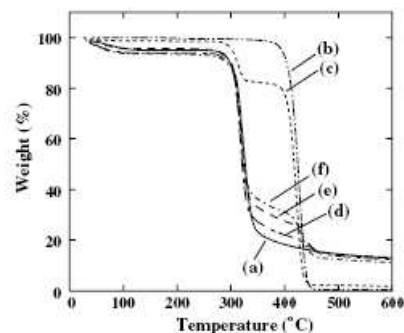


Fig. 4. TGA thermogram of cassava starch (a), PS (b), the non-extracted product with G (%) = 22.80% (c), the un-extractable product with G (%) = 14% (d), 22.80% (e) and 32.8% (f).

the characteristics of both PS and starch (Fig. 4c). The first step was higher than the degradation temperature of starch but lower than that of PS. The second step was in the degradation temperature of PS. Remarkably, the major percentage of weight loss derived mainly from PS homopolymer. After Soxhlet extraction, TGA thermograms of the graft copolymers (the un-extractable product) also showed the two-step degradation process (Fig. 4d–f); however, the starch characteristics played a major role in the thermograms. This was because the PS homopolymer was completely extracted and the starch remains became the major component of the graft copolymer. The evidence of PS-g-starch copolymer was only exhibited at the temperature range of 320–450 °C similarly to the non-extracted product. The degree of weight loss at this temperature range increased with increasing G (%). The TGA results confirmed the achievement of graft copolymerization in the present study and also indicated the increase in thermal stability of starch with PS-g-starch copolymer.

DSC traces of starch, PS and graft copolymers are demonstrated in Fig. 5. In general DSC thermograms of starch

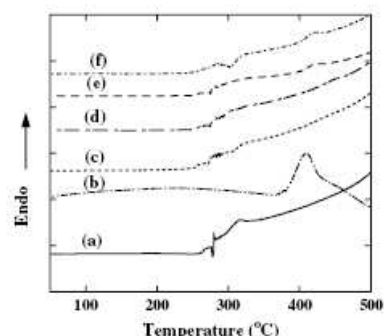


Fig. 5. DSC thermogram of cassava starch (a), PS (b), the non-extracted product with G (%) = 22.80% (c), the un-extractable product with G (%) = 14% (d), 22.80% (e), and 32.8% (f).

obtained from the first heating scan will show a broad endothermic peak at 100 °C. Some researchers reported the crystalline melting temperature in native starch. Hamdan, Hashim, Ahmad, and Embong (2000) mentioned that the peak between 50 and 150 °C was due to the melting of the amylopectin fraction in sago starch, while Ge, Xu, Meng, and Li (2005) believed that the endothermic peak at 126.9 °C was due to the crystalline melting which was formed between residue water and molecular chains of starch via hydrogen bondings. Mano et al. (2003) assumed that it may be due to water adsorption occurring above room temperature during heating scan. There is no conclusion for these explanations at this moment although all native starch shows this peak. However, this broad peak will not be observed on the second heating scan as shown in Fig. 5a. A sharp exothermic peak at 275 °C on DSC thermogram of starch agreed with its TGA thermogram, the starting decomposition temperature. PS showed thermal oxidation at 400 °C (Fig. 5b) correspondingly to TGA result. DSC trace of the product before and after Soxhlet extraction (Fig. 5c–f) looked similar to that of starch. Thermal oxidation of the starch phase in the graft copolymer occurred at higher temperature (>275 °C) as increasing G (%).

SEM micrographs of the non-extracted product or the product before Soxhlet extraction are shown in Fig. 6a and b. Sub-micron spherical particles of PS covering the starch granules were observed. The PS particles adhered both on the surface of the starch granules and on themselves. The fibrils between PS particles and starch granules are shown in Fig. 6b indicating PS-g-starch copolymer. After Soxhlet extraction, PS patches covering on the starch granules were obtained as demonstrated in Fig. 6c. The number of holes on the patchy PS were the homopolymer particles ("Free PS") dissolved by toluene during Soxhlet extraction. Similar feature has been observed by others (Chen et al., 2005; Cho & Lee, 2002). SEM micrographs of other un-extractable products are shown in Fig. 7. At low G (%), PS patches still showed many holes (Fig. 7a and b). The hole free patchy PS was obtained from the product with the highest G (%) (Fig. 7c). The morphology of graft copolymer correlated to the value of G (%). The highest G (%) showed denser graft copolymer.

Based on the above characterization, it was shown that PS-g-starch copolymer could be prepared by using suspension polymerization technique. The graft copolymerization was carried out at temperature lower than gelatinized temperature; as such, there was no change in granular shape of starch as determined by SEM. However, the semi-crystalline structure of the starch granules may or may not change after grafting reaction. In order to identify changes in crystallinity, XRD technique was utilized. XRD pattern of the un-extractable product with G (%) = 22.80% looked similar to that of the virgin starch (Fig. 8). Degree of crystallinity obtained from area under the peaks was in the same range, 37% and 39% for the native starch and the un-extractable product with G (%) = 22.80%, respectively.

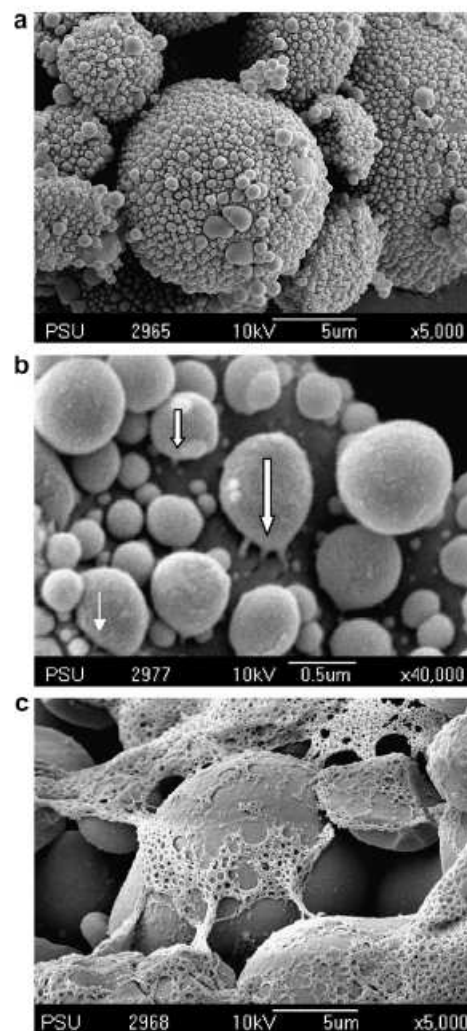


Fig. 6. SEM micrographs of product with G (%) = 22.80% (a) and (b) the non-extracted product (before Soxhlet extraction); (c) the un-extractable product (after Soxhlet extraction).

This indicated that the reaction condition did not impact the crystalline phase. Undoubtedly, this is due to the low reaction temperature. If the system employed gelatinized starch, the crystallinity should be lower than the native one.

#### 3.4. Soxhlet extraction validation

The Soxhlet extraction was the key process to identify the PS-g-starch copolymer. For that reason, it is very important to validate this process. Every extraction was checked with precipitation in the non-solvent as described

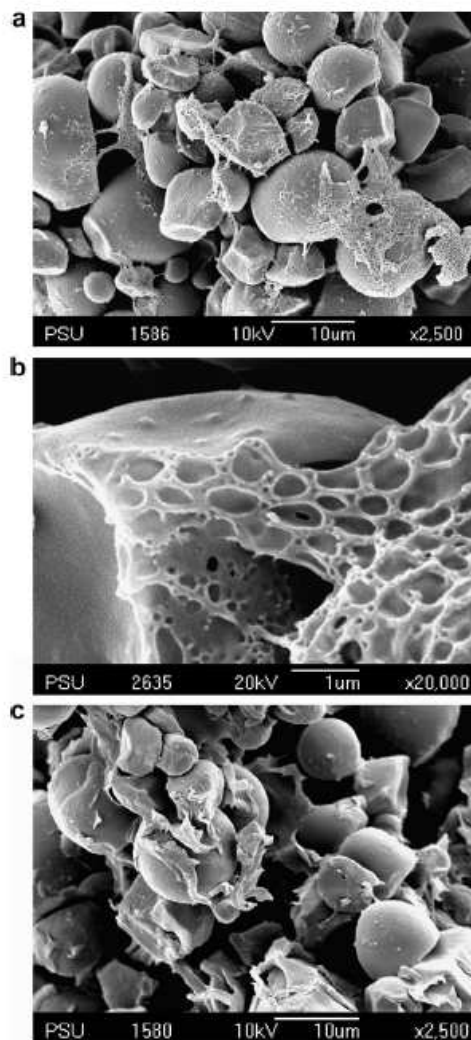


Fig. 7. SEM micrographs of the un-extractable product (after Soxhlet extraction). (a and b)  $G(\%) = 14.00\%$ ; (c)  $G(\%) = 32.80\%$ .

in Section 2.2. Nonetheless, to confirm this process, blend of starch and PS was prepared and was extracted under the same procedure. The FTIR spectrum of the un-extractable product from the polymer blend was the same as that of virgin starch (Fig. 9). As a result, the process of Soxhlet extraction in the present study was valid.

#### 4. Conclusions

The synthesis of polystyrene grafted cassava starch was carried out from styrene monomer and cassava starch using potassium persulfate as an initiator. The optimum

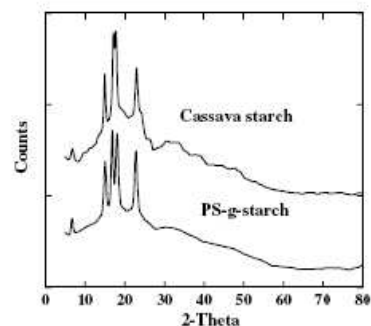


Fig. 8. XRD pattern of the cassava starch and the un-extractable product (after Soxhlet extraction) with  $G(\%) = 22.80\%$ .

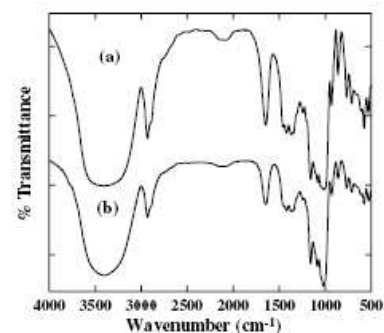


Fig. 9. FTIR spectrum of the virgin cassava starch (a) and the un-extractable product (after Soxhlet extraction) of the starch/PS blend (b).

condition giving the maximum percentage of grafting (31.47%) was derived when 2.5 g of cassava starch, 7.5 g of styrene monomer, reaction time of 2 h and reaction temperature of 50 °C were used. The formation of the polystyrene grafted on cassava starch was investigated by FTIR technique. The results obtained from SEM, TGA and DSC confirmed the presence of polystyrene grafted on cassava starch. Morphology of starch granules did not change after grafting reaction as determined by SEM and XRD. The present study shows that PS-g-starch copolymer could be prepared by suspension polymerization of styrene monomer on the starch granules.

#### Acknowledgements

We thank the Prince of Songkla University, the Faculty of Science and the Graduate School for their financial support and GSL General Starch Ltd., Thailand, for their cassava starch support.

#### References

- Athawale, V. D., & Lek, V. (2000). Thermal studies on granular maize starch and its graft copolymers with vinyl monomers. *Starch/Stärke*, 52, 205–213.

- Bagley, E. B., Fanta, G. F., Burr, R. C., Doane, W. M., & Russell, C. R. (1977). Graft copolymers of polysaccharides with thermoplastic polymers. A new type of filled plastic. *Polymer Engineering and Science*, 17(5), 311–316.
- Chen, L., Ni, Y., Bian, X., Qiu, X., Zhuang, X., & Chen, X. et al. (2005). A novel approach to grafting polymerization of  $\epsilon$ -caprolactone onto starch granules. *Carbohydrate Polymers*, 60, 103–109.
- Cho, C. G., & Lee, K. (2002). Preparation of starch-g-polystyrene copolymer by emulsion polymerization. *Carbohydrate Polymers*, 48, 125–130.
- De Bruyn, H., Sprong, E., Gaborieau, M., David, G., Roper, J. A., & Gilbert, R. G. (2006). Starch-graft-copolymer latexes initiated and stabilized by ozonolyzed amylopectin. *Journal Polymer Science Part A: Polymer Chemistry*, 44, 5832–5845.
- Ezekiel, R., Rana, G., Singh, N., & Singh, S. (2007). Physicochemical, thermal and pasting properties of starch separated from  $\gamma$ -irradiated and stored potatoes. *Food Chemistry*, 105, 1420–1429.
- Fang, J. M., Fowler, P. A., & Hill, C. A. S. (2005). Studies on the grafting of acryloylated potato starch with styrene. *Journal of Applied Polymer Science*, 96, 452–459.
- Fanta, G. F., Burr, R. C., Doane, W. M., & Russell, C. R. (2003). Graft polymerization of styrene onto starch by simultaneous cobalt-60 irradiation. *Journal of Applied Polymer Science*, 21(2), 425–433.
- Ge, X. C., Xu, Y., Meng, Y. Z., & Li, R. K. Y. (2005). Thermal and mechanical properties of biodegradable composites of poly(propylene carbonate) and starch-poly(methyl acrylate) graft copolymer. *Composites Science and Technology*, 65, 2219–2225.
- Graaf, R. A. D., & Janssen, L. P. B. M. (2000). The production of a new partially biodegradable starch plastic by reactive extrusion. *Polymer Engineering and Science*, 40(9), 2086–2094.
- Graaf, R. A. D., & Janssen, L. P. B. M. (2004). Properties and manufacturing of a new starch plastic. *Polymer Engineering and Science*, 41(3), 584–594.
- Hamdan, S., Hashim, D. M. A., Ahmad, M., & Embong, S. (2000). Compatibility studies of polypropylene (PP) sago starch (SS) blends using DMTA. *Journal of Polymer Research*, 7(4), 237–244.
- Henderson, A. M., & Rudin, A. (1981). Effects of water, methanol, and ethanol on the production of starch-g-polystyrene copolymers by cobalt-60-irradiation. *Journal of Applied Polymer Science*, 19, 1707–1719.
- Henderson, A. M., & Rudin, A. (2003a). Effects of water on starch-g-polystyrene and starch-g-poly(methyl acrylate) extrudates. *Journal of Applied Polymer Science*, 27(11), 4115–4135.
- Henderson, A. M., & Rudin, A. (2003b). Extrusion behavior of starch graft copolymers: starch-g-polystyrene and starch-g-poly(methyl acrylate). *Angewandte Makromolekulare Chemie*, 194(1), 23–33.
- Janarthanan, P., Yunus, W. M. Z. W., & Ahmad, M. B. (2003). Thermal behavior and surface morphology studies on polystyrene grafted sago starch. *Journal of Applied Polymer Science*, 90, 2053–2058.
- Kiatkamjornwong, S., Sonsuk, M., Wittayapichet, S., Prasassarakich, P., & Vejjanukroh, P. (1999). Degradation of styrene-g-cassava starch filled polystyrene plastics. *Polymer Degradation and Stability*, 66, 323–335.
- Lee, E. J., Kweon, D. K., Koh, B. K., & Lim, S. T. (2004). Physical characteristics of sweet potato pulp/polycaprolactone blends. *Journal of Applied Polymer Science*, 92, 861–866.
- Mano, J. F., Koniarova, D., & Reis, R. L. (2003). Thermal properties of thermoplastic starch/synthetic polymer blends with potential biomedical applicability. *Journal of Materials Science: Materials in Medicine*, 14, 127–135.
- Pal, S., Mal, D., & Singh, R. P. (2005). Cationic starch: An effective flocculating agent. *Carbohydrate Polymers*, 59, 417–423.
- Park, J. W., Im, S. S., Kim, S. H., & Kim, Y. H. (2000). Biodegradable polymer blends of poly(L-lactic acid) and gelatinized starch. *Polymer Engineering and Science*, 40(12), 2539–2550.
- Pimpan, V., & Thothong, P. (2006). Synthesis of cassava starch-g-poly(methyl methacrylate) copolymers with benzoyl peroxide as an initiator. *Journal of Applied Polymer Science*, 101, 4083–4089.
- Qudsieh, I. Y. M., Razi, A. F., Muiyibi, S. A., Ahmad, M. B., Rahman, M. Z. A., & Yunus, W. M. Z. W. (2004). Preparation and characterization of poly(methyl methacrylate) grafted sago starch using potassium persulfate as redox initiator. *Journal of Applied Polymer Science*, 94, 1891–1897.
- Razi, A. F., Qudsieh, I. Y. M., Yunus, W. M. Z. W., Ahmad, M. B., & Rahman, M. Z. A. (2001). Graft copolymerization of methyl methacrylate onto sago starch using ceric ammonium nitrate and potassium persulfate as redox initiation systems. *Journal of Applied Polymer Science*, 82, 1375–1381.
- Singh, B., & Sharma, N. (2007). Optimized synthesis and characterization of polystyrene graft copolymers and preliminary assessment of their biodegradability and application in water pollution alleviation technologies. *Polymer Degradation and Stability*, 92, 876–885.
- Singh, V., Tiwari, A., Pandey, S., & Singh, S. K. (2006). Microwave-accelerated synthesis and characterization of potato starch-g-poly(acrylamide). *Starch/Stärke*, 58, 536–543.
- Taggare, P. (2004). Starch as an ingredient: Manufacture and applications. In A. C. Eliasson (Ed.), *Starch in food* (pp. 369). Boca Raton, FL: CRC Press.
- Trimnell, D., Stout, E. I., Doane, W. M., & Russell, C. R. (2003). Graft copolymers from thiolated starch and vinyl monomers. *Journal of Applied Polymer Science*, 21(3), 655–663.



**Appendix E**  
**Manuscript 2**

# Interactions of Kraft Lignin and Wheat-Gluten during Biomaterial Processing : Evidence for The Role of Phenolic Groups.

*KAEWTA KAEWTATIP<sup>†,‡</sup>, PAUL MENUT<sup>‡,\*</sup>, REMI AUVERGNE<sup>‡</sup>,  
VARAPORN TANRATTANAKUL<sup>†</sup>, MARIE-HELENE MOREL<sup>‡</sup> AND STEPHANE  
GUILBERT<sup>‡</sup>*

<sup>†</sup> Bioplastic Research Unit, Department of Materials Science and Technology, Faculty of Science, Prince of Songkla University, Hatyai, Songkhla, 90112 Thailand

<sup>‡</sup> UMR IATE, Montpellier SupAgro, INRA, CIRAD, UMII, 2 Place Viala, 34060, Montpellier Cedex 1, France

\*Corresponding author (Tel: (33) 499613018; Fax: (33) 499613076; E-mail : [paul.menut@supagro.inra.fr](mailto:paul.menut@supagro.inra.fr))

**Abstract**

The chemical interactions between Kraft lignin and wheat gluten under processing conditions were investigated by determining the extent of the protein network formation. To clarify the role of different chemical functions found in lignin, the effect of Kraft lignin was compared with that of an esterified lignin, in which hydroxyl groups were suppressed by esterification, and with a series of simple aromatics and phenolic structures with different functionalities (conjugated double bonds, hydroxyl, carboxylic acid and aldehyde). The protein solubility was determined by using the Kjeldahl method. The role of the hydroxylic function was assessed by the significantly lower effect of esterified lignin. The importance of the phenolic radical scavenging structure is evidenced by the effect of guaiacol, which results in a behavior similar to the Kraft lignin. In addition, the significant effect of conjugated double bond on gluten reactivity, through nucleophilic addition, was demonstrated.

Keyword: polyphenol, protein, mixing, wheat gluten, Kraft lignin, esterification, cross-linking

## Introduction

Plastic waste is now regarded as a worldwide environmental problem. Biodegradable materials from renewable agricultural resources such as carbohydrates, starches and proteins have attracted much attention for sustainable development and environmental concern. Between those resources, wheat gluten appears as an interesting raw material because of its low cost and availability in large quantities. Wheat gluten is a by-product of the wheat starch industry (1). It is a mixture of (monomeric) gliadin and (polymeric) glutenin (about 65/45, w/w, respectively). In native gluten, the cysteine groups of gliadin polypeptides are all involved in intrachain covalent disulfide bonds. Due to its monomeric structure, gliadin is mainly responsible for the viscous behavior of gluten. Glutenin, which provides the elastic properties of gluten, consists of a polymeric assembly of different sub-units connected by disulfide bonds. Gluten-based materials are amorphous and can be prepared using common thermoplastic processing such as extrusion or thermomolding (2-4). The addition of a plasticizer overcomes the final product brittleness and provides a better processability. Small polar molecules such as water, sorbitol and fatty acids can be used for that purpose, but glycerol is the most commonly used (5-7).

During processing, the wheat gluten structure is strongly modified by protein aggregation through interchain disulfide bonds (8). This type of covalent cross-link confers to cysteine a key role in the product structure formation. A loss of solubility in sodium dodecyl sulfate (SDS) buffer is usually used as an evidence and a measure of the cross-linking extent (2, 9). The first step of the cross-linking reaction is the rupture of existing intra-molecular disulfide bonds, so that the final material structure is highly dependent to mechanical and thermal inputs, both controllable during processing. Both radical and nucleophilic reaction pathways are involved in gluten aggregation (10). It is thus possible to control the extent of gluten reactivity by the addition of some compounds able to interact with some of those pathways. A recent study conducted in our group has demonstrated that Kraft lignin can impair the gluten cross-linking during mixing and thermal treatment, leading to an increase of the soluble protein content (11). Two mechanisms were hypothesized. The first one is the complexation through interactions forces (as hydrogen bonding, dipole-dipole interactions or interactions forces) between Kraft lignin and wheat gluten during

processing, which by modifying the 3D structure of the protein, might have modified its reactivity. The second is a direct chemical interaction of some of the functional chemical groups found in Kraft lignin with the gluten cross-linking mechanism, which mainly implies thiol radicals and thiolate anions.

Kraft lignin is the by-product of the alkaline (Kraft) pulping process. Its structure, resulting from the alkaline modification of the native lignin of wood, is rather complex. Native lignin is basically formed by the combination of three monomers, namely *p*-coumaryl, coniferyl and sinapyl alcohols, resulting in a three-dimensional polymeric structure (12). As its characterization implies its partial degradation, the real molecular weight of lignin in plants is still unknown (12). The chemical structure of Kraft lignin depends both on the properties of the native lignin (wood species, agricultural conditions of growth) and on the intensity of the Kraft process, which causes the cleavage of native lignin aryl–ether linkages (13-15).

Kraft lignin is thus basically a polyphenolic compound, with a high thermal decomposition temperature (13), containing mainly aromatic groups (16) with different functions ranging from hydroxyl (phenolic or alkyl), conjugated double bond, methoxyl, sulfonate, etc. Such phenolic structures are known for their radical scavenging properties: the conjugation of the aromatic nucleus in their structure induces the resonance stabilization of the phenoxy radical (17-19). The radical scavenging properties of various phenolic structures have been characterized, showing a significant dependence on the functions presents on the side-chains of the aromatic ring (20). As a result, Kraft lignin antioxydant properties have been investigated for the prevention of polypropylene degradation (21) or as an additive for cosmetics products (22, 23). Kraft lignin oxidation, likely to occur in the presence of radicals formed during gluten processing, give rise to the formation of various kinds of aldehydes (24). This complex structure makes difficult the analysis of its interactions with the wheat gluten protein blend, itself very complex. However, understanding these interactions is a main goal for the production of low cost materials made from natural polymers.

The objectives of this work are to investigate wheat gluten cross-linking in the presence of lignin with an emphasis on the potential chemical interactions. Two routes were followed : the first one was to compare the effect of Kraft lignin with an

esterified lignin, in which we have suppressed hydroxylic groups, in order to clarify their influence on the reactivity. The second one was to evaluate independently the effect of different commercially available simple aromatic structures, in order to check precisely the effect of their different functions on gluten reactivity. Between all the chemical functions that can be found in Kraft lignin itself (or in its degradation products obtained by oxidation), we have focused our research on four kinds of functions, more likely to interact with the gluten cross-linking, through nucleophilic or radical pathway. We have evaluated the effect of hydroxyl and conjugated double bonds (in which the nucleophilic reactivity has been reinforced by addition of carboxylic or aldehydes groups), all of them located on an aromatic structure. The effects of those compounds on protein plasticization and cross-linking were separately investigated.

## **MATERIALS AND METHODS**

### **Materials**

Wheat gluten was obtained from Amylum Group (Aalst, Belgium). Its moisture content was about 11%. Kraft lignin was provided by Westvaco (Charleston SC, USA). 1,4-dioxane, acetic anhydride and pyridine were purchased from Sigma-Aldrich. Glycerol was purchased from Fluka and all the commercially available additives were purchased from Sigma-Aldrich, except for cinnamaldehyde (SAEC). The number average molecular weight  $M_n$  of Kraft lignin was estimated by gel permeation chromatography to be 850 g/mol (25). As in this study, we focus on the reactivity of aromatics units, we deduced from the lignin structure an estimated equivalent molecular weight ( $MW_{eq}$ ) per aromatic units. We used for Kraft lignin the value of 180 g.mol<sup>-1</sup>, assuming that its structure is basically constitute with an assembly of the three main precursors. A value of 273 g.mol<sup>-1</sup> was used for the esterified lignin, as explain below.

### **Esterification on Kraft lignin**

50 g of Kraft lignin was mixed with 250 mL dioxane, 45 g acetic anhydride and 36 g pyridine in a one-neck flask and was stirred at room temperature over night. After that, the mixture was dropped into ether and the precipitate was filtered. The

reagent was separated from the precipitate by mixing the precipitate with water (1 L), stirring (30 min) and filtering. To ensure the complete removal of the reagent, the above separation was carried out six times. Finally, the precipitate was dried in an oven at 40 °C until constant weight.

### **Preparation of wheat gluten materials**

A sample was prepared by mixing 35 g of native wheat gluten and 15 g of glycerol. This composition was referred as a “reference”. The others samples were prepared by substituting 1, 5 or 10%wt of the 35 g of wheat gluten with Kraft lignin, esterified lignin or additives, while maintaining the glycerol content at 15 g. The products were mixed in a two blade counter-rotating batch mixer turning at a 3:2 differential speed (Plasti-corder W50, Brabender, Duisburg, Germany). The mixing chamber included a water circulation system which allow the control of its inner wall temperature. This circulating water was regulated at 30 °C by using a regulation temperature unit (Julabo F34, Seelbach, Germany). Mixing speed was 100 rpm and the mixing time was kept constant at 10 min after reaching the maximum torque. This apparatus allowed the electronical measure of the torque on the main axis, and of the product temperature in the chamber, which were continuously recorded during mixing. The standard deviation of this measure, determined from five repetitions of the same experiment on a wheat gluten-glycerol mixture, was estimate to be less than 1%.

The compounds like glycerol, guaiacol, *trans*-anethole and cinnamaldehyde, which are liquid at ambient temperature, were added directly into the mixer. The solid additives such as vanillin, cinnamyl alcohol, ferulic acid and coumaric acid were first dissolved in 15 g of glycerol before mixing. Wheat gluten, Kraft lignin and esterified lignin were added directly into the mixer.

### **Thermal treatment of the wheat gluten materials**

The thermal treatment was performed by using a thermal molding press (PLM 10 T, Techmo, Nazelles, France). 5 g of the product was compressed at 100 °C for 10 min, at a pressure of 4 MPa, directly applied to the sample. We experimentally

checked that this thermal treatment does not modify lignin solubility (11), which is consistent with its high thermal stability (26).

#### Wheat gluten protein solubility

The wheat gluten protein solubility measurement is a common way to determine the extent of the cross-linking between proteins. The soluble proteins were first extracted in a sodium dodecyl sulfate (SDS) solution. Then their content was determined by the Kjeldahl method, which consisted in the precise measurement of the nitrogen content (27). The soluble protein content was then expressed as a percentage of the protein content originally present in the sample.

#### Morphological analysis

A scanning electron microscope (JEOL JSM-5800LV) was used to study the surface morphology of Kraft lignin and esterified lignin. The samples were first mounted on the brass stub with double sticky tape. Then the samples were coated with a thin evaporated layer of gold in order to improve conductivity and prevent electron charging on the surface. The scanning electron microscopy was operating at 10 kV.

#### Fourier transform infrared analysis

Fourier Transform Infrared Spectroscopy (FTIR) was performed (BRUKER EQUINOX 55) to characterize the chemical structure of Kraft lignin and esterified lignin. The samples were dried at 100 °C for 6 h in an oven prior to test. The dried powder samples were mixed with KBr and pressed into the disc form by the hydraulic compression. The samples were scanned at a frequency range of 4000-400  $\text{cm}^{-1}$  with 128 consecutive scans in a 4  $\text{cm}^{-1}$  resolution.

## RESULTS AND DISCUSSION

### Esterification on Kraft lignin

Phenolic and aliphatic hydroxyl groups are found in the Kraft lignin structure (28, 29), which derive from the natural lignin structure (**Figure 1**). Those functions are usually known for their plasticizing action (through hydrogen bonding) on wheat gluten protein. Moreover, phenol is well-known for its radical scavenging properties,



which impact the wheat gluten cross-linking that implies the formation and transfer of radical species. In order to show the effect, or absence of effect, of those structures, we conducted the esterification of the hydroxyl groups, which have been extensively documented (30-34). After esterification, the color of lignin changed from dark brown to light brown. The powder surface evolved from a smooth one in Kraft lignin to a rough one in the modified sample (**Figure 2**). The FTIR analysis conducted on esterified lignin and Kraft lignin shows a significant decrease in the hydroxyl peak (at  $3407\text{ cm}^{-1}$ ) after the esterification, and the appearance of two new bands at  $1743$  and  $1762\text{ cm}^{-1}$ , corresponding to the C=O stretching in the ester group (**Figure 3**). It has been shown that in presence of imidazole, a basic catalyst, this reaction is complete (35), which drive our choice to use pyridine, another basic compound (36). The OH group still presents in the structure are thus likely to be mainly the ones of acidic functions initially presents in the product. Lignin modification has been extensively study, either for the characterization of its structure, or for the modification of its properties, in view of specific applications. It has been shown that the modification usually results in a modification of its solubility (35). However, we did not observed the formation of any residual solids during the evaporation of the ether phase after modification, which conduct us to assume that the lignin modification conduct here have not been associate with a fractionation. The molecular weight of esterified lignin was estimated assuming that each aromatic group has two OH functions (one aromatic and one aliphatic carried by a side chain) that were completely modified. This calculation has been done with the aim to give a rough estimation of the molar content of aromatics groups in the mixture, in order to compare it with the effect of more simple additives. In this study, the additives and lignin molar concentration are varied by one order of magnitude (from 1 to 10%wt), which is much more important than the uncertainty on the molar concentration that result from this calculation (less than 30%). This approximation is thus sufficient to allow a comparison with the protein cystein content, or with the others additives used.

## Materials processing

### (a) Effect of glycerol content

Glycerol is a well-known plasticizer of wheat gluten. The sample evolution during processing, from a wheat gluten/glycerol mixture to a homogeneous sample, was assessed by the torque and internal temperature changes. **Figure 4A** presents the torque and temperature evolution of wheat gluten processed with various glycerol content : the reference contained 30%wt glycerol, while the others samples contained additional amounts of glycerol. The amount of this additional glycerol was the same, on a weight basis, as used for the different additives in the subsequent experiments. The initial torque rapidly increased up to a maximum value, then gradually decreased and stabilized when a homogeneous mixture was obtained. The lag-time before the torque increase is mainly function of the wettability of the wheat gluten powder by the plasticizer, and is thus associated to the dynamics of the system during mixing. The torque enhancement reflected an increase in the viscosity (6, 37), so that the plasticizing efficiency is assessed by the torque level at the plateau. Despite the use of a recirculating water bath, the mixing chamber temperature increased, which is commonly attributed to an important viscous dissipation of the mechanical energy transmitted to the medium, which cannot be compensate by a sufficiently fast calories extraction. The temperature increased and stabilized after the torque reached the maximum value. **Figure 4A** shows that this evolution is highly sensitive to the glycerol content, which acted as a plasticizer. In protein-based materials, a plasticizer is a small molecule able to interact through hydrogen bonding with the protein, thus reducing the direct protein-protein interaction (6, 38). As its content increased in the sample, the torque increase is delayed, while the maximum torque, stabilization torque and stabilization temperature reach during processing decreased, which reflected the lower viscosity of the mixture.

### (b) Effect of Kraft lignin and esterified lignin

Kraft lignin addition resulted in an increase of the stabilization torque, whereas the stabilization temperature decreased (**Figure 4B**). This effect is uncommon as usually, added compound results in an increase (or a decrease) in both parameters, as shown previously with glycerol. At a macroscopic level, either Kraft or

esterified lignin might form agglomerates in the medium. In that case, lignin acts as a filler, which explains the torque increase, previously observed with fibers in similar conditions (37). At a molecular level, numbers of interactions between protein and Kraft lignin can be envisaged (11):  $\pi$ - $\pi$  interaction between aromatic structures, hydrophobic interactions, hydrogen bonding, and covalent linkages. Among these, hydrogen bonding is supposed to have a strong influence, as primarily responsible for protein plasticization, which usually results in a viscosity decrease (6). The presence of hydroxyl groups in Kraft lignin structure might favor interactions between wheat gluten and Kraft lignin, giving rise to a strong reinforcing effect. The influence of the hydroxyl groups was evidenced by the fact that their suppression resulted in a different evolution during processing: when esterified lignin was added, it did not modify in any way the processing parameters of plasticized wheat gluten, as indicated in **Figure 4C**.

### (c) Effect of the additives

Investigation of the effect of various functional groups was done by adding commercially available aromatic additives exhibiting various functions. Whereas the maximum torque reached during the processing of the reference was about 43 N.m, the one measured with additives ranges between 25 N.m and 43 N.m (**Table 1**). Torque curves strongly depended on the added additive, and different behaviors have been identified. Vanillin and ferulic acid gave evolutions very similar to the ones observed with increasing glycerol contents (**Figure 4A**), thereby demonstrating their plasticizing action on the wheat gluten (data not shown). Basically, guaiacol and cinnamyl alcohol gave the same evolution, except that the torque increase was not delayed. Thus, it can be considered that those compounds also efficiently plasticized wheat gluten. Finally, cinnamaldehyde and *trans*-anethole both exhibited a specific behavior, as it can be observed in **Figures 5A** and **5B**, respectively. Their torque evolution presented an irregular trend, with significant oscillations (especially at 10%) that could be attributed to a wall-slip effect. Those experiments were repeated two times in order to check their reproducibility, which was very good. These two additives have in common the absence of hydroxyl groups, suggesting that they

cannot plasticize the wheat gluten proteins. From a physical point of view, they were more likely to act as lubricant rather than plasticizer.

### **Protein solubility after mixing**

During mixing, the mechanical energy transferred to the system resulted in a strong shear and a viscous dissipation (i.e. a temperature increase). Both phenomena have been identified to promote the formation of intermolecular disulfide bonds between proteins, resulting in a loss of their solubility in SDS (2, 39). The measure of the protein solubility is a simple and direct method to quantify the cross-linking extent. This determination can be done by a measure of the protein absorbance at 214 nm in the UV spectra. However, it has been shown (11) that the specific interaction between lignin and wheat gluten can change the absorbance of the protein, thus making this determination inappropriate. In this study, the protein content in the SDS solution was thus determined by the quantification of the total nitrogen content, using the Kjeldahl method.

Guaiacol is basically a phenol, with a reactivity only slightly modified by the addition of the methoxyl group in *para*-position on the aromatic ring. It has a slightly higher radical-scavenging activity than a simple phenol (40). Thus, if this behavior is involved in the interaction with gluten, it should give rise to a more significant effect, making it easier to observe. The comparison between guaiacol and vanillin, a residue of Kraft lignin oxidation (24), allowed us to evaluate the effect of the presence of an aldehyde on the aromatic ring. The effect of a double bond conjugated with the aromatic ring was assessed by using ferulic acid, cinnamyl alcohol, cinnamaldehyde and *trans*-anethole. Those compounds differ by the presence of others groups like aldehyde, hydroxyl (phenolic or aliphatic), and carboxylic acid.

The effect of the various additives on protein solubility is present in **Figure 6**. While the protein solubility of native wheat gluten (the unprocessed and unplasticized powder) is close to 76%, the processing in plasticized conditions of the reference sample resulted in the decrease of the solubility up to  $56 \pm 2.50\%$ , due to protein cross-linking. The addition of 0.2 Mmol/g (or more) of Kraft lignin, esterified lignin or any other additives used in this study promoted an increase in the protein extractability, in comparison with the reference. Those results obviously showed an

effect of those compounds on protein cross-linking, which can take its origin in a specific chemical interaction, but also in the possible protein plasticization by the additive. Indeed, protein cross-linking increased with the processing temperature. The plasticization of the protein, which resulted as previously shown in a lower plateau temperature when additives are added, can then be responsible for a lower cross-linking. In those samples, the lower Brownian energy disfavored the disulfide bond formation. This was shown by the fact that in **Figure 6**, glycerol addition appeared to modify the final wheat gluten solubility, whereas it was not supposed to participate in any way in the chemical mechanism involved in cross-linking. This “plasticizing” or “thermal” effect necessarily affects the protein cross-linking when additives with a plasticizing effect are added. In this study, we mainly wanted to focus on the chemical interactions between wheat gluten and Kraft lignin. Thus, in order to eliminate this effect, all the samples were thermomolded at 100 °C for 10 min, so that their thermal history can be considered as being the same.

#### Protein solubility after mixing and thermomolding

On **Figures 7**, we present the protein insoluble content of the different samples after thermomolding. The protein insoluble content (expressed in percentage, and defined as one hundred minus the protein soluble content) is directly proportional to the extent of the protein cross-linking. It is expressed as a function of the additives concentration expressed in Mmol/g of wheat gluten, which allows a direct comparison with the wheat gluten composition in amino-acids (cysteine content is assumed to be about 130  $\mu\text{mol/g}$ ). The “reference” wheat gluten/glycerol sample insoluble protein content is given in each graph. A previous study (11) showed that Kraft lignin strongly affects protein aggregation, inhibiting the wheat gluten cross-linking and even resulting in an increase in the soluble protein content.

It can be seen in **Figure 7A** that the Kraft lignin amount (expressed in aromatic units) needed to inhibit the wheat gluten cross-linking was clearly higher than the cysteine one. If the inhibition of the cross-linking was due to the reaction of the added compounds with the cysteine groups (then preventing them from forming disulfide bonds), it suggests that the mechanism does not have a one-to-one stoichiometry, or that Kraft lignin reactive groups reactivity is weak. This is probably due to the fact that the densely interconnected structure of Kraft lignin limited their

ability to interact with the protein groups. The addition of esterified lignin had only a slight effect on protein solubility, which demonstrated the effect of the phenol group on the cross-linking kinetics. This hypothesis is moreover confirmed by the fact that the addition of guaiacol resulted in an effect very similar to the one of the Kraft lignin.

From the effect of additives, it is possible to identify the influence of the various functionalities used in this study. The effect of on **Figure 7B**, the comparison of the effect of guaiacol, vanillin and ferulic acid allows the evaluation of the effect of an aldehyde and of a double bond (conjugated with an acid function) on the reactivity of a phenolic additive in presence of wheat gluten. The protein cross-linking in wheat gluten/guaiacol sample decreased as long as guaiacol content increased in the investigated range of concentration. In that sense, this compound presented the closest behavior with Kraft lignin. Guaiacol acts as a simple phenol, but the *ortho*-methoxyl substitution increase its radical scavenging efficiency (40). It has been suggested that the *ortho*-methoxyl function can form an intramolecular hydrogen bond with the phenolic hydrogen, making the hydrogen atom abstraction from the *ortho*-methoxyphenols more easy (41, 42). The evidence of a strong effect of a simple phenolic structure on wheat gluten cross-linking significantly reinforce the hypothesis that Kraft lignin can interact with wheat gluten protein by trapping the radicals formed during processing, and not only by a complexation involving interactions forces (11). The addition of an aldehyde group on the phenolic structure (vanillin) seems to inhibit partially its action. This observation is already consistent with some results demonstrating that the presence of an aldehyde on the aromatic ring in vanillin reduces the radical scavenging efficiency (40). The addition of ferulic acid strongly reduced the wheat gluten cross-linking during processing. A similar result (not shown) was observed with coumaric acid, which have a very similar structure. As this effect is, on a molar basis, significantly more important than for guaiacol, it can be attributed to the presence of a double bond. Both the presence of an aromatic structure and of a carboxylic function, on both side of this double bond, significantly favored its ability to react with nucleophilic species, like the thiolate anion, which are implied in the mechanism of wheat gluten cross-linking. It could be hypothesized that in the case of ferulic acid, both the presence of a phenol group, which are well known

as radical scavengers, and of reactive delocalised double bond, contributed to inhibit the wheat gluten cross-linking that occur during processing, even resulting in a protein depolymerization in comparison to the native state.

In order to demonstrate the effect of the conjugated double bond, we have checked the effect of different aromatic but non phenolic structure which possess this structure. In **Figure 7C**, the effect of the presence of double bond on an aromatic structure is investigated independently of the presence of a phenol, and compared with the results previously shown for the addition of ferulic acid. Those compounds are likely to interact with thiol groups formed during processing, especially by radical addition on the double bond, or by nucleophilic addition of a thiolate anion (10). While *trans*-anethole and cinnamyl alcohol have a slight, but measurable, effect on the wheat gluten cross-linking, this effect was clearly stronger when cinamaldehyde and ferulic acid were used. This observation strongly supports an interaction of the conjugated double bond through its ability to interact with thiolate anion, implied in the nucleophilic step of wheat gluten cross-linking. Indeed, aldehyde and acids functions favored the ability of the double bond to react with an anion. This observation demonstrate that the presence of double bonds, conjugated with an aromatic group, can interact with the wheat gluten cross-linking, and that the most probable mechanism of this action is a nucleophilic attack on this group.

Kraft lignin and wheat gluten are both renewable resources exhibiting promising potential as new raw materials for bioplastic production. Their blending allows the monitoring of some of the materials key properties, especially because it reduced the wheat gluten cross-linking during processing. However, due to their complex structure, the description of their interaction is not easy. In this study, the suppression of the hydroxyl groups present in the lignin structure, by esterification, appeared to suppress the plasticizing effect of Kraft lignin (assessed by its effect on the torque/temperature curves recorded during mixing) and to significantly reduce its interference with wheat gluten cross-linking.

The addition of more simple compounds, based on an aromatic structure with additional functions, allowed clarifying the potential role of the complex structure find in Kraft lignin. Mainly, the analysis demonstrated the effect of the phenol structures and of the conjugated double bond. The first one was interacting with the

wheat gluten cross-linking pathway through their ability to trap the radicals formed under shearing (and heating) on cysteine groups. The second one was more likely to interact with the thiolate anions formed during processing. Evidence of a similar behavior between guaiacol and Kraft lignin suggested that the main interaction was occurring through the aromatic hydroxyl antiradical activity. Those results demonstrated that the Kraft lignin structure chemical reactivity can explain the protein depolymerisation. This constitutes a new step in understanding the polyphenol-protein interaction in view of the production of bioplastics.

### **Acknowledgements**

We would like to thank Graduate School and Faculty of Science in Prince of Songkla University, the French embassy in Thailand and Montpellier SupAgro - INRA for their financial support. We thanks Joelle Bonicel and Therese-Marie Lasserre for valuable help for protein solubility determination, and Bernard Kurek for supplying Kraft lignin.



**Literature cited**

- (1) Hosney, R. C. *Principles of cereal science and technology*. 2<sup>nd</sup> edition. **1998**. The American Association of Cereal Chemists, Inc. USA.
- (2) Redl, A.; Guilbert, S.; Morel, M. –H. Heat and shear mediated polymerisation of plasticized wheat gluten protein upon mixing. *J. Cereal Sci.* **2003**, 38, 105-114.
- (3) Redl, A.; Morel, M. –H.; Bonjcel, J.; Vergnes. B.; Guilbert, S. Extrusion of wheat gluten plasticized with glycerol influence of process condition on flow behavior, rheological properties, and molecular size distribution. *Cereal Chem.* **1999**, 76, 361-370.
- (4) Jerez, A.; Partal, P.; Martinez, I.; Gallegos, C.; Guerrero, A. Rheology and processing of gluten based bioplastics. *Biochem. Eng. J.* **2005**, 26, 131-138.
- (5) Pouplin, M.; Redl, A.; Gontard N. Glass transition of wheat gluten plasticized with water, glycerol, or sorbitol. *J. Agric. Food. Chem.* **1999**, 47(2), 538-543.
- (6) Pommet, M.; Redl, A.; Guilbert, S.; Morel, M. –H. Intrinsic influence of various plasticizers on functional properties and reactivity of wheat gluten thermoplastic materials. *J. Cereal Sci.* **2005**, 42(1), 81-91.
- (7) Pommet, M.; Redl, A.; Morel, M. –H.; Domenek, S.; Guilbert, S. Thermoplastic processing of protein-based bioplastic: chemical engineering aspects of mixing, extrusion and hot molding. *Macromol. Symp.* **2003**, 197(1), 207-218.
- (8) Cuq, B; Gontard, N; Guilbert, S. Proteins as agricultural polymers for packaging production. *Cereal Chem.* **1998**, 75(1), 1-9.

- (9) Schofield, J. D.; Bottomley, R. C.; Timms, M. F.; Booth, M. R. The effect of heat on wheat gluten and the involvement of sulphhydryl-disulphide interchange reaction. *J. Cereal Sci.* **1983**, *1*, 241-253.
- (10) Auvergne, R.; Morel, M. -H.; Menut, P.; Giani, O.; Guilbert, S.; Robin, J. -J. Reactivity of wheat gluten protein during mechanical mixing: Radical and nucleophilic reactions for the addition of molecules on sulfur. *Biomacromolecules.* **2008**, *9*, 664-671.
- (11) Kunanopparat, T.; Menut, P.; Morel, M. -H.; Guilbert, S. Modification of the wheat gluten network by Kraft lignin addition. *J. Agric. Food. Chem.* **2009**, *57* (18), 8526-8533.
- (12) Ralph, J.; Lundquist, K.; Brunow, G.; Lu, F.; Kim, H.; Schatz, P. F.; Marita, J. M.; Hatfield, R. D.; Ralph, S. A.; Christensen, J. H.; Boerjan, W. Lignins : natural polymers from oxidative coupling of 4-hydroxyphenyl-propanoids. *Phytochem. Rev.* **2004**, *3*, 29-60.
- (13) Tejada, A.; Pena, C.; Labidi, J.; Echeverria, J. M.; Mondragon, I. Physico-chemical characterization of lignins from different sources for use in phenol-formaldehyde resin synthesis. *Bioresour. Technol.* **2007**, *98*, 1655-1663.
- (15) Chakar, F. S.; Ragauskas, A. J. Review of current and future softwood Kraft lignin process chemistry. *Ind. Crops Prod.* **2004**, *20*(2), 131-141.
- (15) Pan, X.; Kadla, J. F.; Ehara, K.; Gilkes, N.; Saddler, J. N. Organosolv Ethanol Lignin from Hybrid Poplar as a Radical Scavenger: Relationship between Lignin Structure, Extraction Conditions, and Antioxidant Activity. *J. Agric. Food. Chem.* **2006**, *54*, 5806-5813.

- (16) Balakshin, M. Y.; Capanema, E. A.; Chen, C. -L.; Gracz, H. S. Elucidation of the structures of residual and dissolved pine Kraft lignins using an HMQC NMR technique. *J. Agric. Food. Chem.* **2003**, *51*, 6116-6127.
- (17) Graf, E. Antioxidant potential of ferulic acid. *Free Radical Biol. Med.* **1992**, *13*, 435-448.
- (18) Zang, L. Y.; Cosma, G.; Gardner, H.; Shi, X.; Castranova, V.; Vallyathan, V. Effect of antioxidant protection by p-coumaric acid on low-density lipoprotein cholesterol oxidation. *Am. J. Physiol. Cell Physiol.* **2000**, *279*, c954-c960.
- (19) Butterfield, D. A.; Kanski, J.; Aksenova, M.; Stoyanova, A. Ferulic acid antioxidant protection against hydroxyl and peroxy radical oxidation in synaptosomal and neuronal cell culture systems in vitro: structure-activity studies. *J. Nutr. Biochem.* **2002**, *13*, 273-281.
- (20) Dizhbite, T.; Telysheva, G.; Jurkjane, V.; Viesturs, U. Characterization of the radical scavenging activity of lignins—natural antioxidants. *Bioresour. Technol.* **2004**, *95*, 309-317.
- (21) Gregorova, A.; Kosikova, B.; Stasko, A. Radical scavenging capacity of lignin and its effect on processing stabilization of virgin and recycled polypropylene. *J. Appl. Polym. Sci.* **2007**, *106*, 1626-1631.
- (22) Vinardell, M. P.; Ugartondo, V.; Mitjans, M. Potential applications of antioxidant lignins from different sources. *Ind. Crops Prod.* **2008**, *27*, 220-223.
- (23) Vinardell, M. P.; Ugartondo, V.; Mitjans, M. Comparative antioxidant and cytotoxic effects of lignins from different sources. *Bioresour. Technol.* **2008**, *99*, 6683-6687.

- (24) Villar, J. C.; Caperos, A.; GarciaOchoa, F. Oxidation of hardwood kraft-lignin to phenolic derivatives. Nitrobenzene and copper oxide as oxidants. *J. Wood Chem. Technol.* **1997**, *17* (3), 259-285.
- (25) Pouteau, C.; Dole, P.; Cathala, B.; Averous, L.; Boquillon, N. Antioxidant properties of lignin in polypropylene. *Polym. Degrad. Stab.* **2003**, *81*, 9-18.
- (26) Brodin, I.; Sjöholm, E.; Gellerstedt, G. The behavior of Kraft lignin during thermal treatment. *J. Anal. Appl. Pyrolysis.* **2010**, *87*, 70-77.
- (27) Norm NF EN ISO 20483, BIPEA
- (28) Mansouri, N. -E. E.; Salvado, J. Structural characterization of technical lignins for the production of adhesives: Application to lignosulfonate, kraft, soda-anthraquinone, organosolv and ethanol process lignins. *Ind. Crops Prod.* **2006**, *24*, 8-16.
- (29) Baptista, C.; Robert, D.; Duarte, A. P. Effect of pulping conditions on lignin structure from maritime pine Kraft pulps. *Chem. Eng. J.* **2006**, *121*, 153-158.
- (30) Chen, C. L.; Lin, S. Y.; Dence, C. W. *Methods in Lignin Chemistry.* **1992**. Springer, Berlin.
- (31) Lewis, H. F.; Brauns, F. E.; Buchanan, M. A.; Brookbank, E. B. Lignin Esters of Mono- and Dibasic Aliphatic Acids. *Ind. Eng. Chem.* **1943**, *35*(10), 1113-1117.
- (32) Brauns, F. E.; Lewis, H. F.; Brookbank, E. B. Lignin Ethers and Esters - Preparation from Lead and Other Metallic Derivatives of Lignin. *Ind. Eng. Chem.* **1945**, *37*(1), 70-73.

- (33) Mansson, P. Quantitative determination of phenolic and total hydroxyl groups in lignins. *Holzforschung*. **1983**, *37*, 143-146.
- (34) Glasser, W. G.; Jain, R. K. Lignin derivatives. *Holzforschung*. **1993**, *47*, 225-233.
- (35) Thielemans, W; Wool, R. P. Lignin esters for use in unsaturated thermosets: Lignin modification and solubility modeling. *Biomacromolecules*. **2005**, *6*, 1895-1905.
- (36) Morck, R.; Kringstad, K. P. <sup>13</sup>C-NMR Spectra of Kraft Lignins - II. Kraft Lignin Acetates. *Holzforschung*. **1985**, *39*(2), 109-119.
- (37) Kunanopparat, T.; Menut, P.; Morel, M. -H.; Guilbert, S. Reinforcement of plasticized wheat gluten with natural fibers : from mechanical improvement to deplasticizing effect. *Composites Part A*. **2008**, *39*, 777-785.
- (38) Song, Y.; Zheng, Q. Improved tensile strength of glycerol-plasticized gluten bioplastic containing hydrophobic liquids. *Bioresour. Technol.* **2008**, *99*, 7665-7671.
- (39) Micard, V.; Morel, M. -H.; Bonicel, J.; Guilbert, S. Thermal properties of raw and processed wheat gluten in relation with protein aggregation. *Polymer*. **2001**, *42*, 477-485.
- (40) Brand-Williams, W.; Cuvelier, M. E.; Berset, C. Use of a free radical method to evaluate antioxidant activity. *LWT Food Sci. Technol.* **1995**, *28*(1), 25-30.

- (41) de Heer, M. I.; Mulder, P.; Korth, H. G.; Ingold, K. U.; Lusztyk, J. Hydrogen atom abstraction kinetics from intramolecularly hydrogen bonded ubiquinol-10 and other (poly)methoxy phenols. *J. Am. Chem. Soc.* **2000**, *122*, 2355-2360.
- (42) Zhou, B.; Cheng, J. -C.; Dai, F.; Yang, L.; Liu, Z. -L. Antioxidant activity of hydroxycinnamic acid monomers in human low density lipoprotein: Mechanism and structure-activity relationship. *Food Chem.* **2007**, *104*, 132-139.

## FIGURE LEGENDS

**Figure 1.** Representation of the main primary monolignols of lignin (**A**) and of a lignin polymer structure (**B**).

**Figure 2.** SEM micrographs of Kraft lignin (**A**) and esterified lignin (**B**).

**Figure 3.** FTIR spectrum of Kraft lignin and esterified lignin.

**Figure 4.** Effect of glycerol (**A**), Kraft lignin (**B**) and esterified lignin (**C**) contents on torque and temperature evolution of wheat gluten; wheat gluten reference ( $\diamond$ ), 1% ( $\circ$ ), 5% ( $\times$ ) and 10% ( $\triangle$ ).

**Figure 5.** Effect of cinnamaldehyde (**A**) and *trans*-anethole (**B**) contents on torque and temperature evolution of wheat gluten; wheat gluten reference ( $\diamond$ ), 1% ( $\circ$ ), 5% ( $\times$ ) and 10% ( $\triangle$ ).

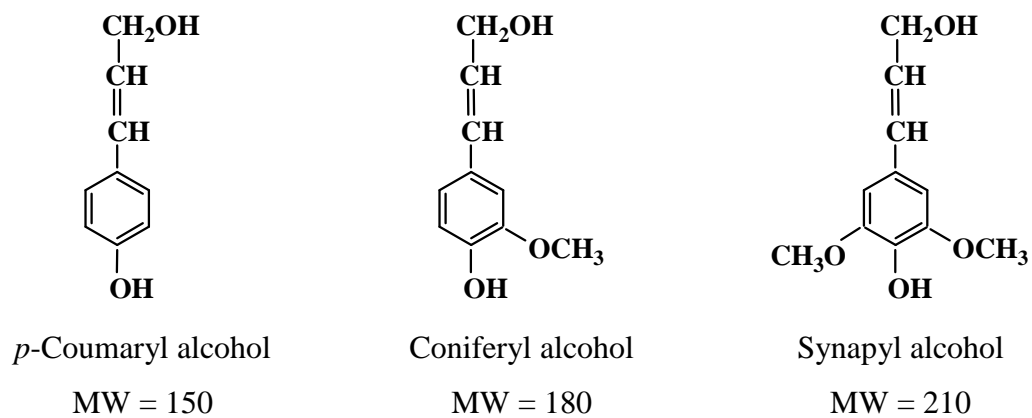
**Figure 6.** Effect of additives on the SDS-soluble protein content of wheat gluten after mixing (without thermal treatment): glycerol ( $\diamond$ , —), Kraft lignin ( $\circ$ , - - -), esterified lignin ( $\circ$ , —), guaiacol ( $\square$ , —), vanillin ( $\diamond$ , - - -), *trans*-anethole ( $\nabla$ , —), ferulic acid ( $\triangle$ , - - -), cinnamaldehyde ( $\boxplus$ , —), cinnamyl alcohol ( $\blacktriangleleft$ , —); wheat gluten reference ( $\blacksquare$ ) and native wheat gluten ( $\bullet$ ).

**Figure 7.** Effect of additives on the insoluble protein content of wheat gluten after thermal treatment; Kraft lignin, esterified lignin, guaiacol and glycerol (**A**), phenolic compounds (**B**) and aromatics compounds containing conjugated double bond (**C**); glycerol (◇, —), Kraft lignin (○, - - -), esterified lignin (○, —), guaiacol (□, —), vanillin (◇, - - -), *trans*-anethole (▽, —), ferulic acid (△, - - -), cinnamaldehyde (⊞, —), cinnamyl alcohol (⊞, —), wheat gluten reference (■) and native wheat gluten (●).

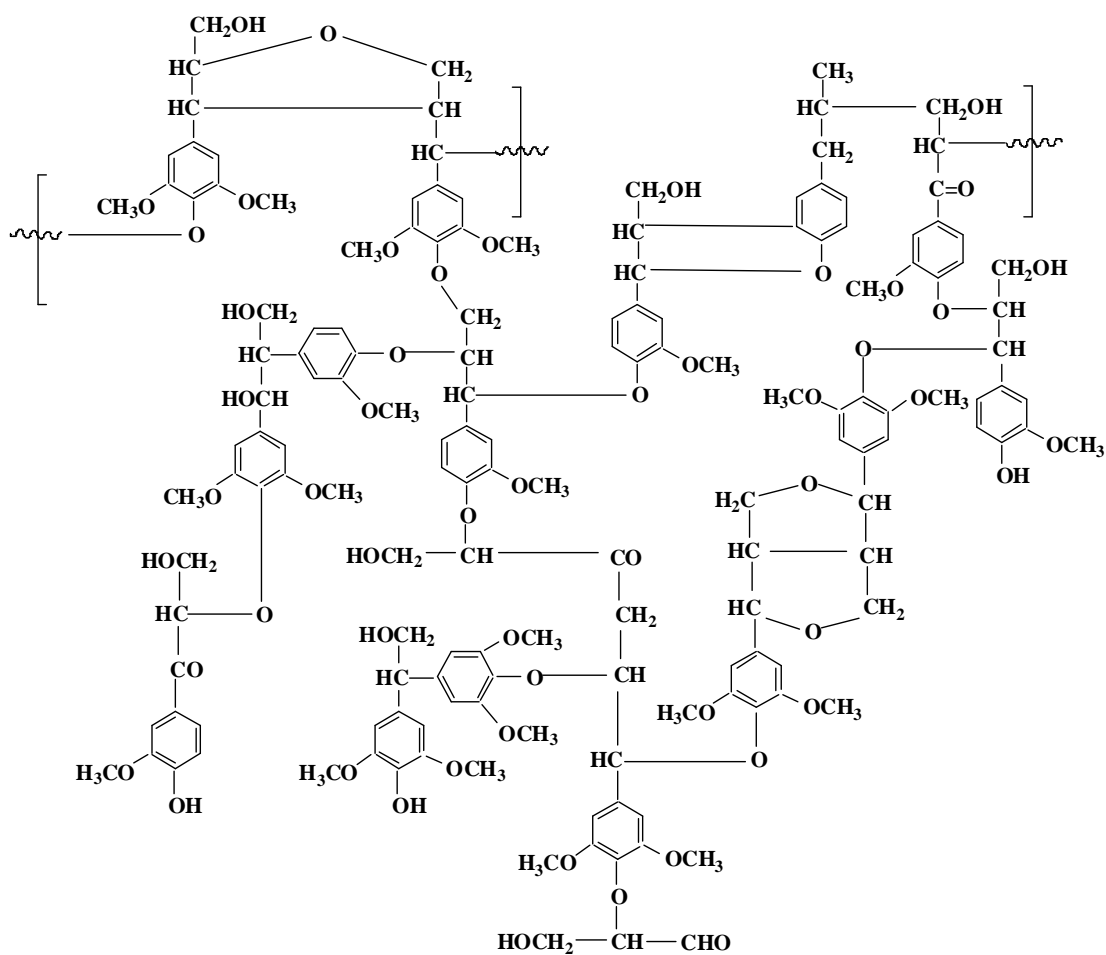


**Table 1.** Maximum torque and stabilization temperature of the samples

Additive	Maximum torque (N.m)			Stabilization temperature (°C)		
	1% wt	5%wt	10%wt	1% wt	5%wt	10%wt
Glycerol	41	34	28	89	83	76
Kraft lignin	42	40	41	90	84	86
Esterified lignin	43	41	40	90	89	88
Guaiacol	42	35	29	89	82	75
Vanillin	36	31	25	81	77	72
<i>trans</i> -Anethole	41	37	32	88	80	61
Ferulic acid	35	31	27	79	73	70
Coumaric acid	38	32	29	85	76	72
Cinnamaldehyde	42	38	36	92	84	74
Cinnamyl alcohol	40	34	26	90	82	71

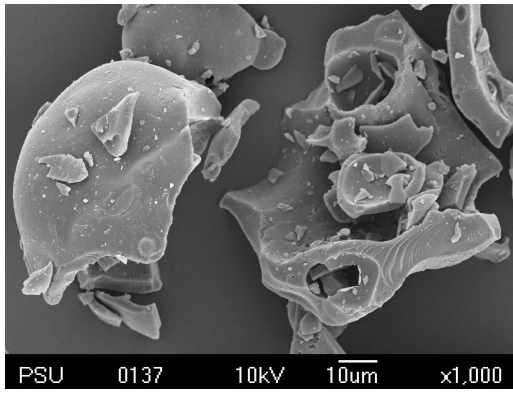


A

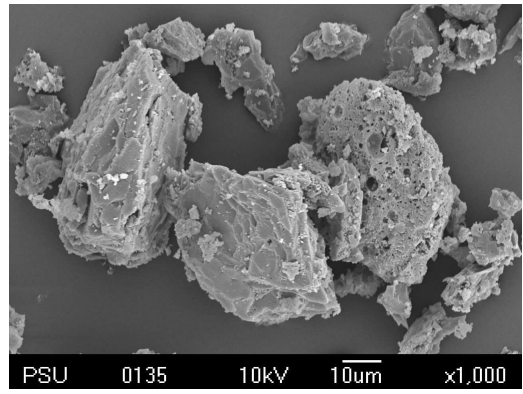


B

Figure 1



**A**



**B**

**Figure 2**

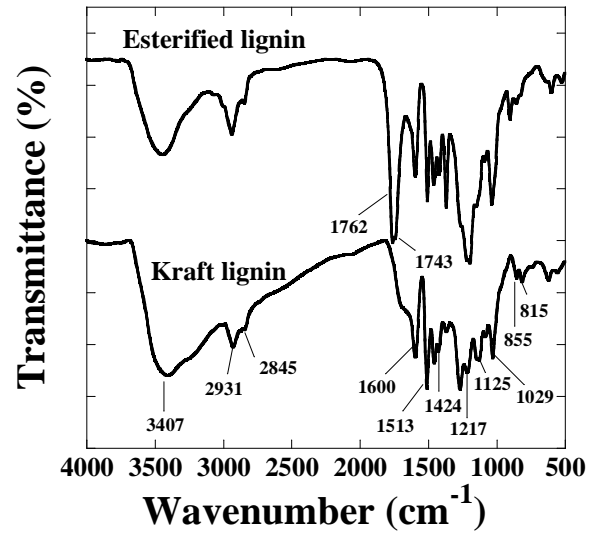


Figure 3

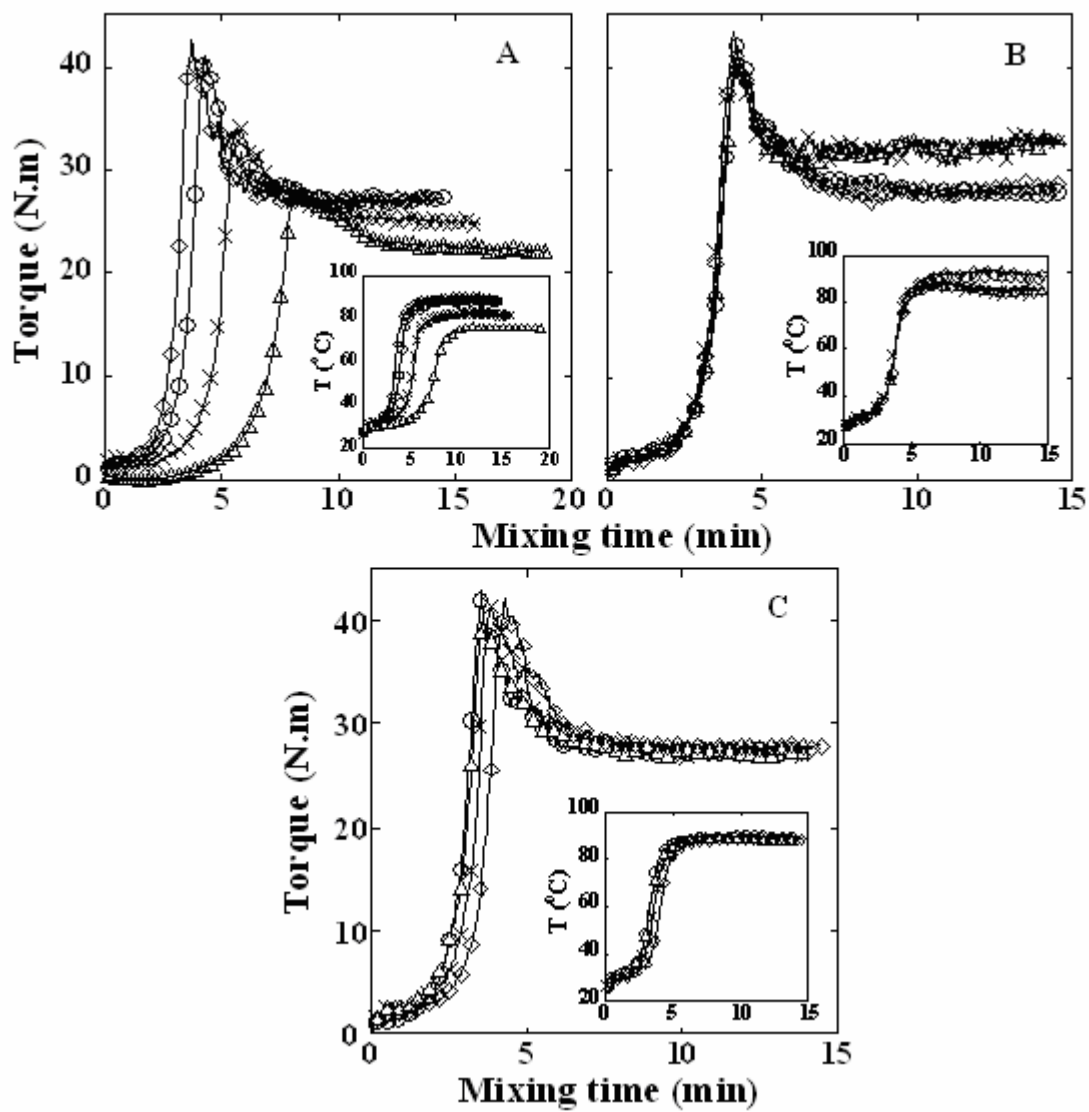


Figure 4

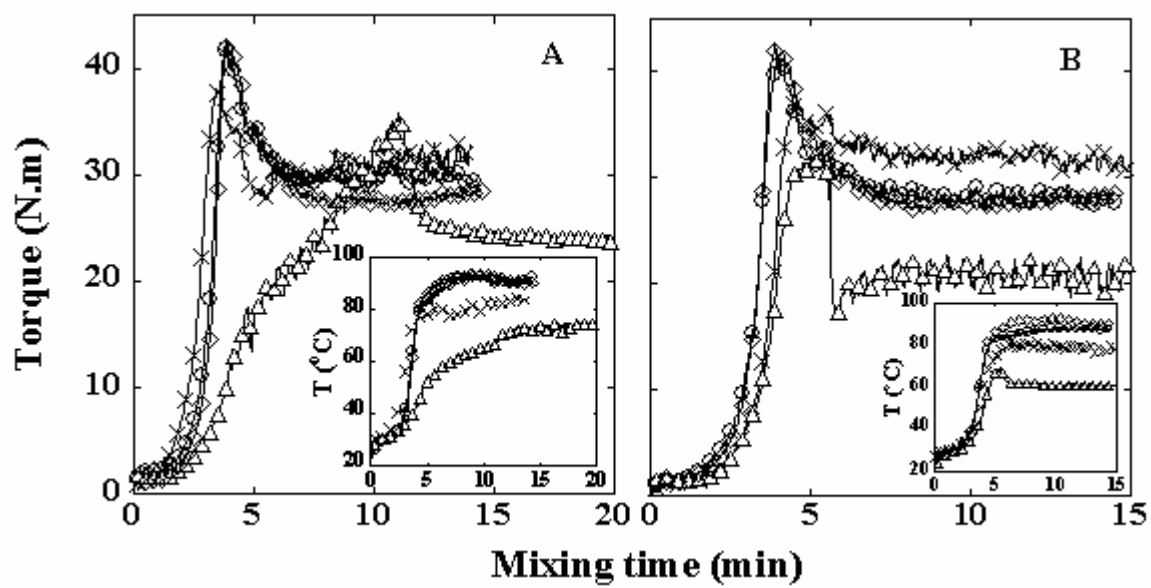


Figure 5

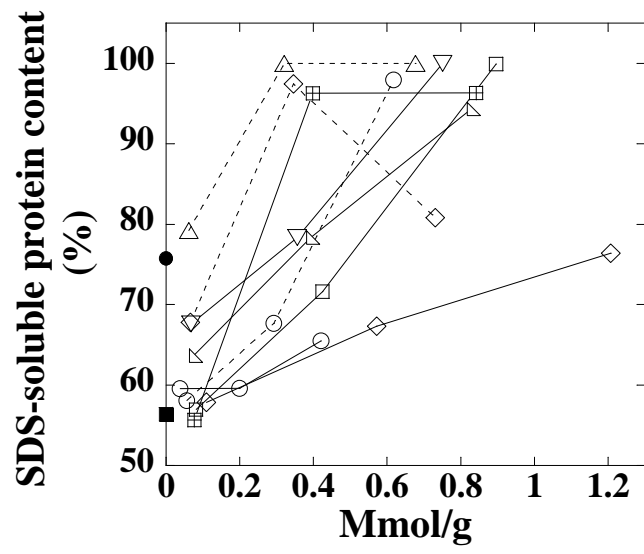


Figure 6

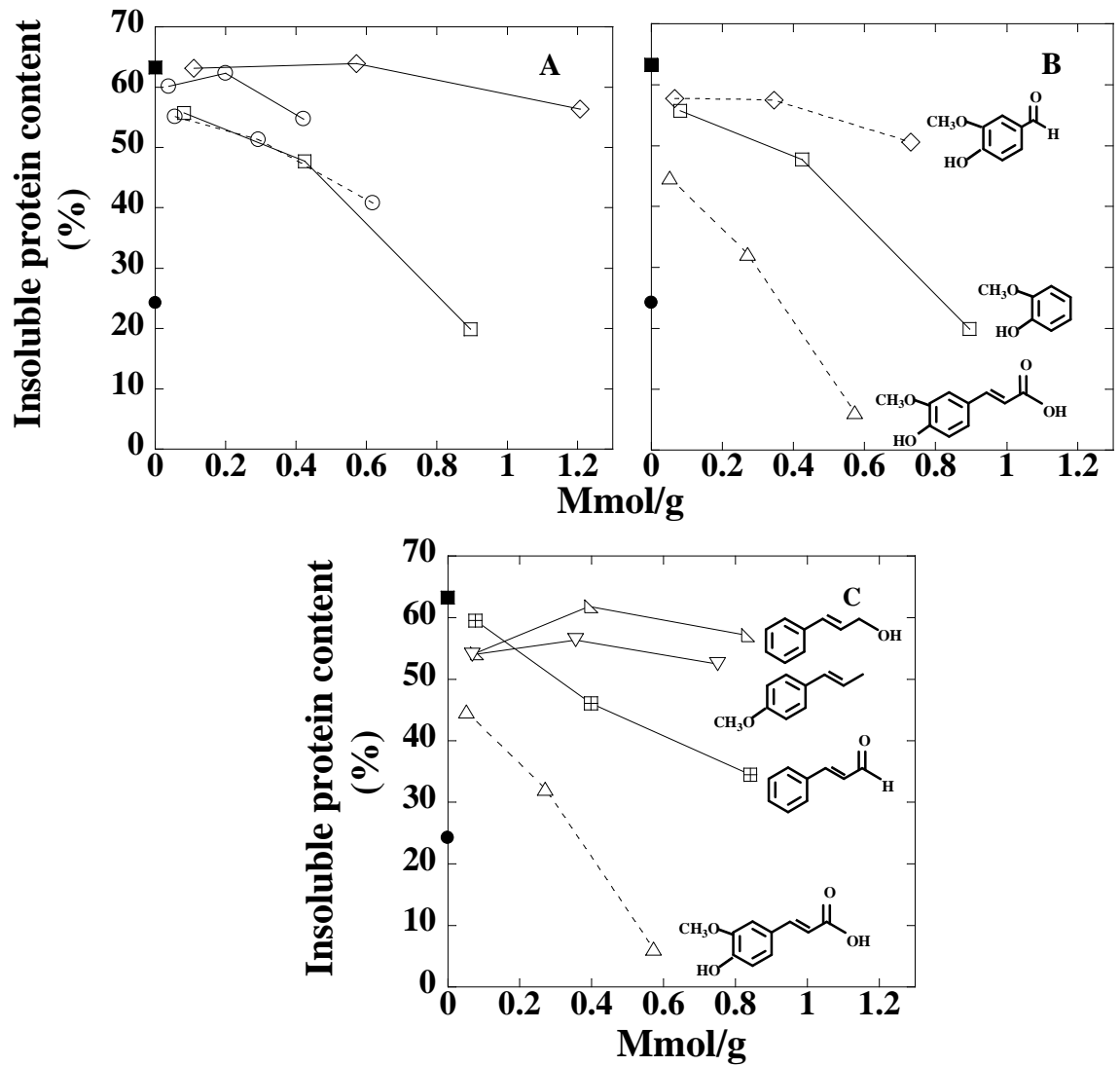


Figure 7



## Vitae

**Name** Miss Kaewta Kaewtatip

**Student ID** 4910230018

### **Educational Attainment**

Degree	Name of Institution	Year of Graduation
Bachelor of Science (Chemistry)	Prince of Songkla University	2002
Master of Science (Polymer Science and Technology)	Prince of Songkla University	2005

### **Scholarship Awards during Enrolment**

Prince of Songkla University graduate studies grant

### **List of Publication and Proceeding**

#### **Publication**

Kaewtatip, K. and Tanrattanakul, V. (2008). Preparation of cassava starch grafted with polystyrene by suspension polymerization. *Carbohydrate Polymer*, 73, 647-655.

#### **Presentation**

##### **Poster Presentation**

Kaewta Kaewtatip, Paul Menut, Varaporn Tanrattanakul, Remi Auvergne, Marie-Helene Morel, Stephane Guilbert. (2009). The effect of Kraft lignin on plasticization and de-polymerization of wheat gluten biomaterials during processing. ICMAT 2009; IUMARS-ICA 2009, Suntec Singapore International Convention and Exhibition Centre, Singapore. 28 June – 3 July 2009.